
Geological Survey of Canada
Commission géologique du Canada

PAPER/ÉTUDE
89-1D

This document was produced
by scanning the original publication.

Ce document est le produit d'une
numérisation par balayage
de la publication originale.

CURRENT RESEARCH PART D
INTERIOR PLAINS AND ARCTIC CANADA

RECHERCHES EN COURS PARTIE D
PLAINES INTÉRIEURES ET RÉGION ARCTIQUE DU CANADA



NOTICE TO LIBRARIANS AND INDEXERS

The Geological Survey's Current Research series contains many reports comparable in scope and subject matter to those appearing in scientific journals and other serials. Most contributions to Current Research include an abstract and bibliographic citation. It is hoped that these will assist you in cataloguing and indexing these reports and that this will result in a still wider dissemination of the results of the Geological Survey's research activities.

AVIS AUX BIBLIOTHÉCAIRES ET PRÉPARATEURS D'INDEX

La série Recherches en cours de la Commission géologique paraît une fois par année; elle contient plusieurs rapports dont la portée et la nature sont comparables à ceux qui paraissent dans les revues scientifiques et autres périodiques. La plupart des articles publiés dans Recherches en cours sont accompagnés d'un résumé et d'une bibliographie, ce qui vous permettra, nous l'espérons, de cataloguer et d'indexer ces rapports, d'où une meilleure diffusion des résultats de recherche de la Commission géologique.

GEOLOGICAL SURVEY OF CANADA
COMMISSION GÉOLOGIQUE DU CANADA
PAPER/ÉTUDE 89-1D

**CURRENT RESEARCH, PART D
INTERIOR PLAINS AND ARCTIC CANADA**

**RECHERCHES EN COURS, PARTIE D
PLAINES INTÉRIEURES ET RÉGION
ARCTIQUE DU CANADA**

1989



Energy, Mines and
Resources Canada

Énergie, Mines et
Ressources Canada

© Minister of Supply and Services Canada 1989

Available in Canada through

authorized bookstore agents and other bookstores

or by mail from

Canadian Government Publishing Centre
Supply and Services Canada
Ottawa, Canada K1A 0S9

and from

Geological Survey of Canada offices:

601 Booth Street
Ottawa, Canada K1A 0E8

3303-33rd Street N.W
Calgary, Alberta T2L 2A7

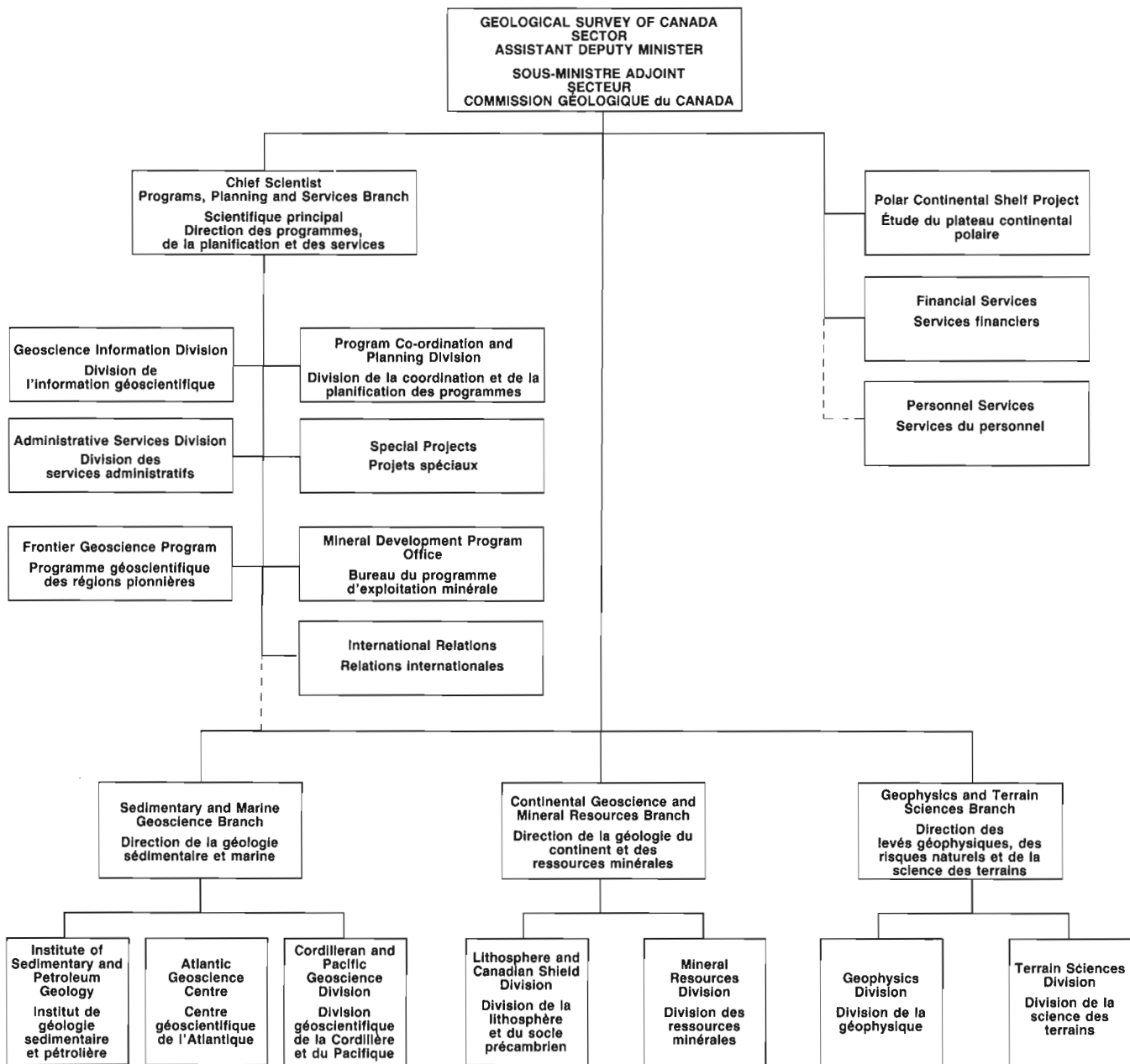
100 West Pender Street
Vancouver, British Columbia V6B 1R8

A deposit copy of this publication is also available
for reference in public libraries across Canada

Cat. No. M44-89/1D
ISBN 0-660-54777-5

Cover description

Ordovician cherts (ridge) and Cambrian maroon
shales, Barn Mountains, Yukon Territory.
ISPG 3135-2



Separates

A limited number of separates of the papers that appear in this volume are available by direct request to the individual authors. The addresses of the Geological Survey of Canada offices follow:

601 Booth Street,
OTTAWA, Ontario
K1A 0E8

Institute of Sedimentary and Petroleum Geology,
3303-33rd Street N.W.,
CALGARY, Alberta
T2L 2A7

Cordilleran and Pacific Geoscience Division,
100 West Pender Street,
VANCOUVER, B.C.
V6B 1R8

Pacific Geoscience Centre
P.O. Box 6000,
9860 Saanich Road
SIDNEY, B.C.
V8L 4B2

Atlantic Geoscience Centre
Bedford Institute of Oceanography,
P.O. Box 1006,
DARTMOUTH, N.S.
B2Y 4A2

Geological Survey of Canada
National Scientific Research Institute
Complexe scientifique
2700, rue Einstein
C.P. 7500
STE-FOY, Quebec
G1V 4C7

When no location accompanies an author's name in the title of a paper, the Ottawa address should be used.

Tirés à part

On peut obtenir un nombre limité de «tirés à part» des articles qui paraissent dans cette publication en s'adressant directement à chaque auteur. Les adresses des différents bureaux de la Commission géologique du Canada sont les suivantes:

601, rue Booth
OTTAWA, Ontario
K1A 0E8

Institut de géologie sédimentaire et pétrolière
3303-33rd St. N.W.,
CALGARY, Alberta
T2L 2A7

Division géoscientifique de la Cordillère et du Pacifique
100 West Pender Street,
VANCOUVER, Colombie-Britannique
V6B 1R8

Centre géoscientifique du Pacifique
B.P. 6000,
9860 Saanich Road
SIDNEY, Colombie-Britannique
V8L 4B2

Centre géoscientifique de l'Atlantique
Institut océanographique de Bedford
B.P. 1006
DARTMOUTH, Nouvelle-Écosse
B2Y 4A2

Commission géologique du Canada
Institut national de la recherche scientifique
Complexe scientifique
2700, rue Einstein
C.P. 7500
STE-FOY, Québec
G1V 4C7

Lorsque l'adresse de l'auteur ne figure pas sous le titre d'un document, on doit alors utiliser l'adresse d'Ottawa.

CONTENTS

- 1 C.J. MWENIFUMBO
The symmetrical lateral resistivity log in coal seam mapping, Highvale mine, Alberta
- 9 I. BANERJEE
Petrography of the Upper Albian Basal Colorado Sandstone in the Cessford Field, southern Alberta
- 19 M.G. FOWLER, P.W. BROOKS and R.W. MACQUEEN
A comparison between the biomarker geochemistry of some samples from the Lower Jurassic Nordegg Member and western Canada Basin oil sands and heavy oils
- 25 A.H. MAJID
Regional geology and hydrocarbon occurrences in the Wabamun Group, west-central Alberta
- 35 K.G. OSADETZ, L.R. SNOWDON and L.D. STASIUK
Association of enhanced hydrocarbon generation and crustal structure in the Canadian Williston Basin
- 49 J.S. BELL and P.F. LLOYD
Modelling of stress refraction in sediments around the Peace River Arch, western Canada
- 55 L.P. GAL, E.D. GHENT and P.S. SIMONY
Geology of the northern Solitude Range, Western Rocky Mountains, British Columbia
- 61 W.D. STEWART
A preliminary report on stratigraphy and sedimentology of the lower and middle Chancellor Formation (Middle to Upper Cambrian) in the zone of facies transition, Rocky Mountain Main Ranges, southeastern British Columbia
- 69 M.M. BURGESS and D.W. RISEBOROUGH
Measurement frequency requirements for permafrost ground temperature monitoring: analysis of Norman Wells pipeline data, Northwest Territories and Alberta
- 77 D.E. KERR
Late Quaternary marine record of the Cape Parry - Clinton Point region, District of Mackenzie, N.W.T.
- 85 C.R. BURN
Frost heave of subaqueous lake-bottom sediments, Mackenzie Delta, Northwest Territories
- 95 D.A. ST-ONGE, I. McMARTIN and R. AVERY
Rock blisters and other frost-heaved landforms in the Bernard Harbour area, District of Mackenzie, N.W.T.
- 101 J.G. FYLES
High terrace sediments, probably of Neogene age, west-central Ellesmere Island, Northwest Territories
- 105 J.V. MATTHEWS, Jr.
New information on the flora and age of the Beaufort Formation, Arctic Archipelago, and related Tertiary deposits in Alaska
- 113 M.B. POTSCHIN
Drumlin fields of the Bernard Harbour area, Northwest Territories
- 119 A. TAYLOR, A. JUDGE and V. ALLEN
Recovery of precise offshore permafrost temperatures from a deep geotechnical hole, Canadian Beaufort Sea
- 125 S.A. EDLUND, B. T. ALT and K.L. YOUNG
Interaction of climate, vegetation, and soil hydrology at Hot Weather Creek, Fosheim Peninsula, Ellesmere Island, Northwest Territories

The symmetrical lateral resistivity log in coal seam mapping, Highvale mine, Alberta

C.J. Mwenifumbo
Mineral Resources Division

Mwenifumbo, C.J., *The symmetrical lateral resistivity log in coal seam mapping, Highvale mine, Alberta*; in *Current Research, Part D, Geological Survey of Canada, Paper 89-1D*, p. 1-8, 1989.

Abstract

Symmetrical lateral array resistivity measurements were carried out at the Highvale coal mine in Alberta to compare their performance with the standard electrical logs; self potential, single point resistance, normal and lateral resistivity logs. The symmetrical lateral logs provide better coal bed thickness and boundary definition with thin beds being clearly resolved. Compared to the conventional lateral array, the symmetrical lateral array gives resistivity logs across resistive coal seams which are symmetrical, clearer and hence easier to interpret. The resistivities are not as severely affected by the finite bed thicknesses of the coal seams. The resistivity variations within the coal seams are clearly resolved, whereas the standard electrical logs tend to produce smoothed logs with less detail. The array is definitely superior to the single point resistance, normal resistivity and the asymmetrical lateral arrays. Bed-boundary resolution of this array is comparable to the high resolution density logs.

Résumé

Des mesures de résistivité en réseau latéral symétrique ont été effectuées à la mine de charbon Highvale en Alberta pour comparer leur qualité avec celle des enregistrements électriques standard, de la polarisation spontanée, de la résistance ponctuelle, des résistivités normale et latérale. Les enregistrements latéraux symétriques permettent une meilleure définition de l'épaisseur et des limites des couches de charbon, notamment des couches minces. Contrairement au réseau latéral classique, le réseau latéral symétrique produit des enregistrements de résistivité en travers des couches de charbon qui sont symétriques, plus nets et plus faciles à interpréter. Les résistivité ne dépendent pas autant de l'épaisseur finie des couches de charbon. Les variations de résistivité dans les couches de charbon sont nettement définies, tandis que les enregistrements électriques standard tendent à produire des enregistrements lissés moins détaillés. Le réseau est définitivement supérieur aux mesures de résistance ponctuelles, aux mesures de la résistivité normale et aux réseaux latéraux asymétriques. La résolution des limites des couches dans ce réseau se compare à celle des enregistrements de densité à haute résolution.

INTRODUCTION

Single and multiple electrode arrays for electrical resistivity logging are frequently used in coal exploration to determine the depth and thickness of coal seams. The most commonly used arrays are the single point resistance, normal and lateral arrays. Bed boundary definition is not as precise as often required with these arrays. The normal array can not resolve beds whose thicknesses are smaller than the electrode spacing. The lateral array was developed in an attempt to improve the bed-boundary resolution for thin beds. The response characteristic of this array is, however, quite complicated and asymmetrical. The results are difficult to interpret. When precise bed boundary resolution and accurate formation resistivity estimates are required, special focused resistivity arrays are currently used. The design of these focused resistivity logging devices is also complicated. We chose to build the symmetrical lateral array because its resistivity response is symmetrical as opposed to the asymmetrical lateral arrays. This electrode configuration is similar to the Schlumberger Limestone Sonde (Schlumberger Document 8, 1958) and was also suggested by Dakhnov (1959). It is essentially a superposition of the lateral and the inverted lateral arrays. It is not an improvement over the special focussed resistivity arrays but provides better bed-boundary resolution than either the asymmetrical lateral or normal arrays. No focussing is used on this configuration. Field results using this array, acquired in summer 1988 at the Highvale open pit mine in Alberta, are presented in this paper and are compared with the standard electrode arrays.

ELECTRODE ARRAYS.

Figures 1a, 1b and 1d show the common electrode configurations used in electrical borehole logging applications to coal exploration. The downhole and surface current electrodes are labelled A and B, respectively and the potential electrodes M and N. The single point resistance array is the simplest of the arrays and consists of one downhole electrode which is used both as a current electrode, A, and potential electrode, M. The return current electrode, B, and the reference potential electrode, N are also the same but fixed at the surface near the drill hole collar. Resistances are measured with this array which reflect changes in the formation resistivities along the drill hole. These measurements have been successfully used for the identification of coal seams and for stratigraphic correlation. Even though the single point resistance measurements are simple and inexpensive to run, apparent resistivities cannot be determined from them and therefore no quantitative interpretations can be made. A 10-cm-long cylindrical lead electrode was used as the downhole current/potential electrode for the data presented in this paper.

The normal array shown in Figure 1b, is the so called inverted normal. The conventional normal array commonly used in the industry has the N electrode above the current electrode A. An 'ideal' normal array has 2 electrodes, A and M, downhole with the return current electrode and the reference potential electrode placed effectively at infinity on the surface. The normal arrays commonly used are

3-electrode arrays, AMN, with the reference potential electrode, N, placed at a distance large enough for its contribution to the overall measured potentials to be minimal. The different arrays are identified by their various AM separations. The conventional normal arrays currently used in coal, oil and gas industry are the 16-inch short normal and the 64-inch long normal. The normal array frequently used with the GSC logging system is a 40-cm normal array (AM = 40 cm, AN = 260 cm). The normal array resistivity data presented in this paper were acquired with the Dakhnov micronormal array (Dakhnov, 1959). This array is a high-resolution, 10-cm normal array mainly used to improve the resolution of induced polarization measurements. The potential measurement electrode, M, is placed between two closely spaced current electrodes of the same polarity. Figure 1c shows the electrode setup of the Dakhnov micronormal.

Figures 1d, 1e and 1f show the lateral arrays. The conventional lateral array consists of a current electrode, A, and a potential dipole, MN. The common electrode setup for the lateral is shown in Figure 1d with a trailing current electrode. The array is called an inverted lateral if it has a leading current electrode downhole (Figure 1e). The MN spacing for the lateral and inverted lateral used in acquiring the present data was 10 cm with an AM-spacing of 20 cm (AO=L=15 cm, Figure 1e). These dimensions are not the standard arrays used in the coal, oil and gas industry where an 18' 8" lateral is commonly used (AO = 18' 8"). The resistivity response for the lateral arrays is asymmetrical and complicated to interpret. Figure 1f shows the newly constructed symmetrical lateral array. This array consists of a single current electrode A, and a potential dipole consisting of two measurement electrodes M'M and N'N, spaced at equal distances above and below the current electrode. This array was constructed because of its symmetrical resistivity response, and delineates the boundaries between beds more precisely than the asymmetrical three-electrode lateral array. The apparent resistivities determined from this array provide better approximations of the true formation resistivities.

APPARENT RESISTIVITIES

In a homogeneous medium of resistivity, ρ , the potential difference, ΔV_{MN} between M and N for a 3-electrode array is

$$\Delta V_{MN} = \frac{\rho I}{4\pi} \left(\frac{1}{AM} - \frac{1}{AN} \right)$$

Where I is the point source current. The resistivity is therefore computed as follows

$$\rho = K \frac{\Delta V_{MN}}{I}$$

and the geometric factor, K, is given as

$$K = 4\pi \left(\frac{AM \cdot AN}{AN - AM} \right)$$

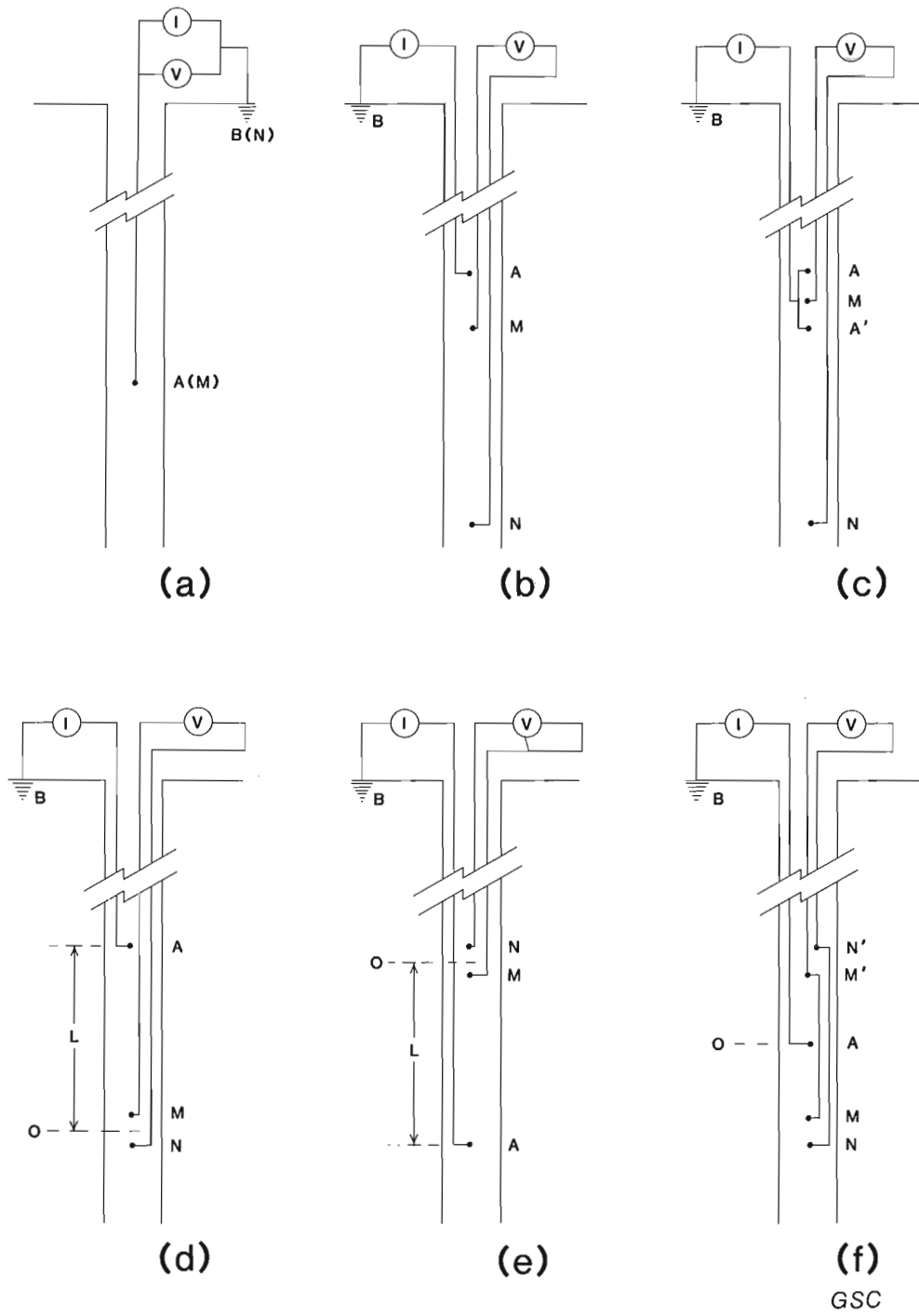


Figure 1. Electrode arrays. 1a Single point resistance, 1b Inverted Normal, 1c Dakhnov microneutral, 1d Lateral, 1e Inverted Lateral and 1f Symmetrical lateral.

Since we are not dealing with a homogeneous medium in the borehole, the measured resistivities are apparent resistivities. The normal, lateral and symmetrical lateral are essentially 3-electrode arrays and the geometric factor for all of them is as given in the equation above. The 10-cm micronormal has $AM \ll AN$ ($AN = 28 \cdot AM$) and the geometric factor in this case approaches that of an 'ideal' normal array.

LOGGING EQUIPMENT

The measurements presented in this study were carried out with the GSC R&D, slim-hole, time domain IP/Resistivity logging system. It consists of a minicomputer-based data acquisition system and downhole components which comprise the probe electronics and the electrode arrays. The electrode arrays are designed in a modular fashion so that changes in array type can be made easily. The voltage signal is measured in the probe and the signal is transmitted uphole digitally as a frequency as opposed to analogue signal transmission commonly used by standard industry logging systems. The transmitter used in single hole logging operations is a constant current 40-watt transmitter. The period of the time domain wave form for resistivity measurements is usually set at 1 second (ie. a transmit/receive time of 0.25 seconds) and data are sampled every second. All measurements are made in a continuous mode at logging speeds varying from 6.0 to 1.0 m/minute depending on the sample depth resolution required. The data acquired in this study were recorded at either 1.0 or 3.0 m/minute logging speeds. A full description of the logging system is given by Bristow (1986).

COMPARISON OF ARRAYS

A number of vertical holes were drilled for geotechnical logging studies at the Highvale Coal Mine in Alberta in summer 1988. These holes were 15 cm in diameter and filled with fresh water. Electrical logging with a variety of arrays was carried out in these holes to evaluate their resistivity response characteristics and their performance. The single point resistance, 10-cm micronormal, lateral, inverted lateral and the symmetrical lateral resistivity logs are presented and compared to each other. Corrections for the effects of borehole fluid, invasion zone and borehole diameter on the response characteristics of the resistivity logs have not been made to any of these data. The objective here is to compare the resistivity data in their raw form. The parameters investigated are coal seam recognition, bed-boundary resolution and the effect of finite bed thickness on the magnitude of the apparent resistivities.

SYMMETRICAL LATERAL VERSUS LATERAL ARRAY

Figure 2 shows the lateral, inverted lateral and symmetrical lateral apparent resistivity logs acquired in hole HV88-414. These logs were acquired at a logging speed of 1 m/minute with a measurement approximately every 2 cm. The asymmetrical response of the lateral and inverted lateral arrays is clearly indicated in Figure 2a and 2b. Maximum apparent resistivities are observed at the lower contacts of the coal

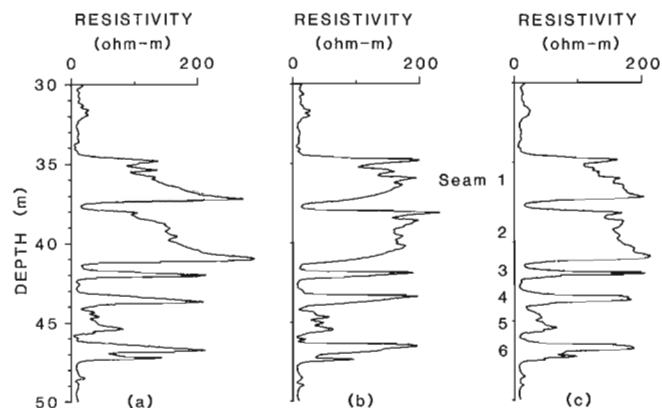


Figure 2. Conventional lateral (2a), inverted lateral (2b) and symmetrical lateral (2c) apparent resistivity logs acquired in hole HV88-414. The asymmetrical resistivity response of the lateral and inverted lateral is clearly shown across coal seam numbers 1 and 2. The conventional lateral array with a trailing current electrode indicates higher resistivities on the upper boundary of the coal seams whereas the inverted lateral with a leading current electrode downhole shows the reverse response. The symmetrical lateral array response is symmetrical across a bed of finite thickness and hence the variations in resistivities within the coal seams reflect true changes in resistivities.

seams for the conventional lateral array. The inverted lateral array resistivity log shows the opposite response; maximum resistivities on the upper contacts. Theoretical model results show that the lateral log resistivities are higher than the true resistivities near the contact of resistive beds (Dakhnov, 1959). Since the resistivities vary within the coal seams, the variations in apparent resistivities are difficult to interpret for these asymmetric arrays. The symmetrical lateral resistivity log in Figure 2c shows apparent resistivities within the coal seams, especially in seams 1 and 2, that should reflect true resistivity variations that may be interpreted to indicate changes in the quality of coal. The lower parts of the coal seams exhibit higher resistivities implying better coal at the bottom with decreasing resistivities towards the top indicating increasing ash content upwards. This interpretation is confirmed by the natural gamma ray and density logs which are discussed in a later section. Good bed-boundary definition is achieved by all of the three arrays, however, the resistivity variations within the coal seams are misleading for the lateral and inverted lateral logs and therefore quantitative interpretation based on the magnitude of the resistivities would be difficult with these data.

Figure 3 shows a more detailed response of the lateral, inverted lateral and symmetrical lateral logs across coal seam number 4 in the same hole. The asymmetrical resistivity responses of the lateral and inverted lateral are clearly indicated in these logs. The symmetrical lateral log shows a symmetrical resistivity response across the coal seam and bed-boundaries are more clearly defined. The resistivity response of the symmetrical lateral array is essentially the sum of the lateral and inverted lateral responses with the indicated resistivity being lower at the centre of the coal seam. This is a characteristic response for resistive beds whose thickness is less than the electrode spacing and it is also seen for example with the normal resistivity log (Dakhnov, 1959).

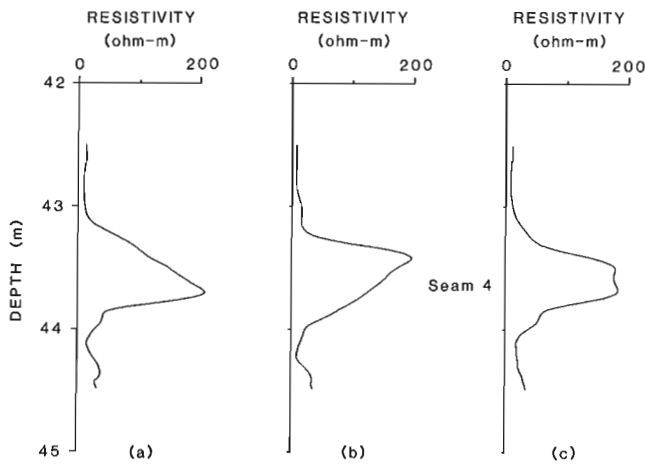


Figure 3. Expanded section of figure 2 showing a more detailed lateral (3a), inverted lateral (3b) and symmetrical lateral (3c) resistivity responses across coal seam number 4.

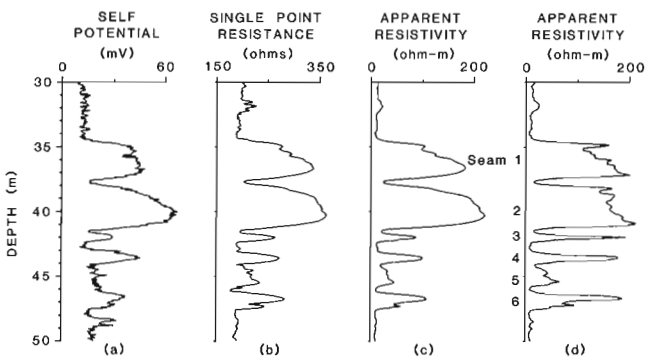
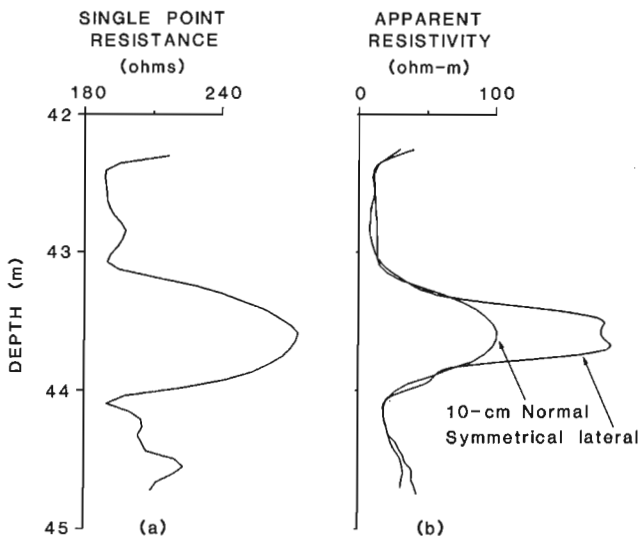


Figure 4. Symmetrical lateral resistivity log compared with the standard electrical logs; self potential (4a), single point resistance (4b) and 10-cm normal resistivity (4c) logs. Better boundary definition is clearly indicated on the symmetrical lateral resistivity log (4d). Apparent resistivities of the thin coal seams 3, 4 and 6 are comparable to those observed in thicker coal seams 1 and 2. Finite bed thickness effects are not as severe for the symmetrical lateral as for either the single point resistance or normal arrays.



SINGLE POINT, NORMAL AND SYMMETRICAL LATERAL ARRAYS

Figure 4 compares the symmetrical lateral resistivity logs with the standard electrical logs; self potential, single point resistance and 10-cm normal resistivity logs. All logs clearly indicate the resistive coal seams and resolve the coal bed-boundaries fairly well. The single point resistance and normal resistivity logs show smooth variations in resistivities within the coal seams especially seams numbers 1 and 2 with increasing resistivities towards the lower contact. The resistivity response of the symmetrical lateral array is sharper at the contacts and hence provides better bed-boundaries definition. The fine details in the resistivity variations within the coal seams (seam numbers 1 and 2) are better defined with the symmetrical lateral logs than with the other electrical logs. These variations reflect changes in the quality of coal (ash content) within the seam. It is interesting to note that both the single point resistance and the normal resistivity logs show reduced amplitudes in seams 3, 4 and 6. This does not necessarily imply that the resistivities of these seams are lower than those of seam numbers 1 and 2 but rather this is a characteristic response of these logs to thin beds in these large diameter holes. The symmetrical lateral resistivity log, however, shows the magnitude of the resistivities of seams 3, 4 and 6 to be equivalent to those of the thicker seams 1 and 2.

Figure 5 shows an expanded section of Figure 4 showing the single point resistance, normal resistivity and symmetrical lateral log across seam number 4. It is clear that the symmetrical lateral log has better resolution and that the measured apparent resistivities are a better estimate of the true resistivities of these thin coal seams. The apparent resistivity values reach a maximum at the centre of a bed of finite thickness for both the normal and the symmetrical lateral logs. This value is usually less than the true resistivity of an infinitely thick bed. As the bed thickness decreases, the maximum apparent response decreases as well. The symmetrical lateral resistivity values of the thin coal seams are not severely affected by the finite bed thickness and therefore, can be used in quantitative assessment of the coal (relating coal quality to the resistivity values) thus obviating the need for special focused resistivity logging devices.

COMPARISON OF GAMMA RAY AND ELECTRICAL LOGS

Figure 6 compares the natural gamma ray log with the three electrical logs; single point resistance, 10-cm normal and symmetrical lateral resistivity logs. This data was obtained in hole HV88-428. All the electrical logs show an excellent negative correlation with the gamma ray log. Figure 7 is plot of the conductivities in Siemens/m (reciprocal of resistivity

Figure 5. Expanded section of Figure 4 illustrating the improved bed boundary resolution of the symmetrical lateral over the normal resistivity and single point resistance logs. Apparent resistivities observed with the symmetrical lateral array provide a better approximation to the true resistivities of the coal seams.

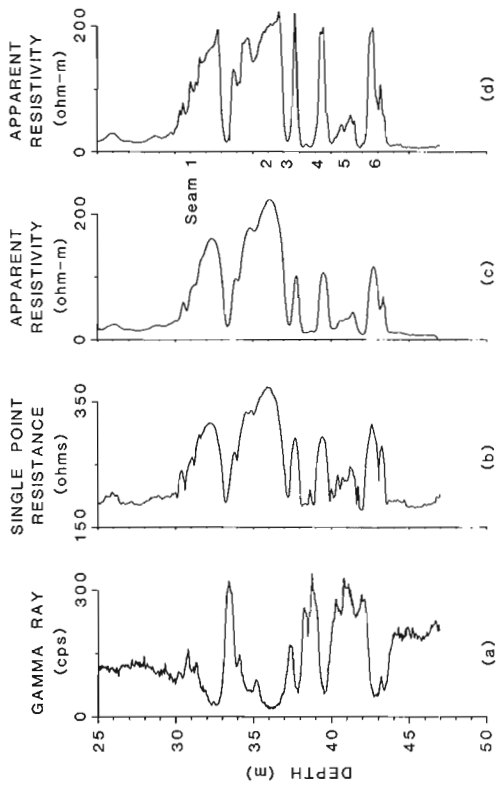


Figure 6. Natural gamma ray (6a), single point resistance (6b), 10-cm normal resistivity (6c) and the symmetrical lateral resistivity (6d) logs obtained in hole HV88-428. The electrical logs show a negative correlation with the gamma ray log.

Figure 8. The symmetrical lateral resistivity log (8a) compared with the high resolution gamma density log (8b) and the 10-cm normal resistivity log (8c). Data was acquired in hole HV88-414.

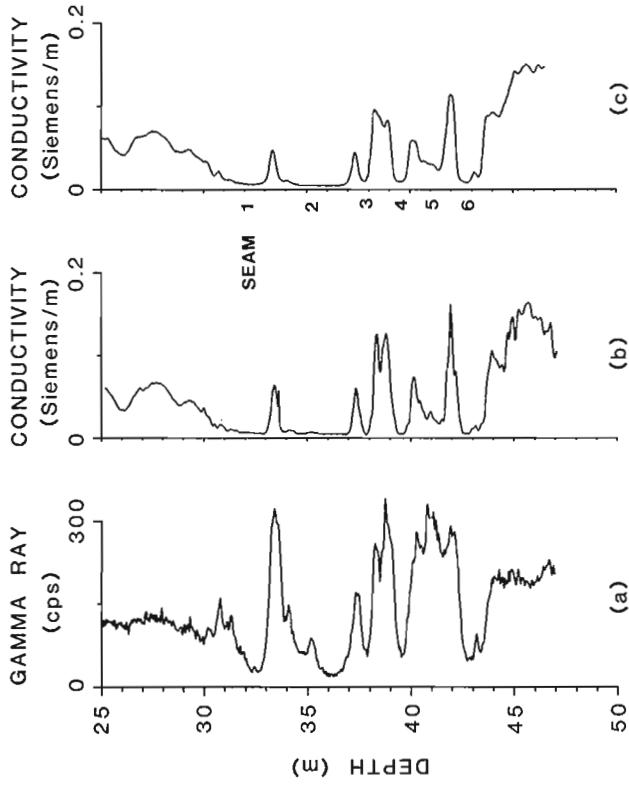


Figure 7. Conductivity logs derived from the symmetrical lateral (7b) and 10-cm normal resistivity (7c) logs of figure 6 are compared with the gamma ray log (7a). Both the conductivity logs show a good positive correlation with the gamma ray log. The symmetrical lateral conductivity log shows better fine detail correlation especially between 38 and 40 metres.

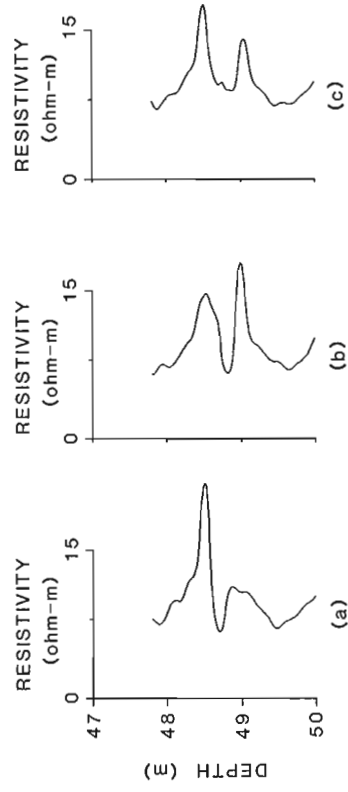


Figure 9. Expanded section of Figure 4 showing detailed characteristics of the lateral, inverted lateral and symmetrical lateral arrays across two narrow resistive calcareous sandstone layers. The symmetrical lateral resistivity log clearly resolves the two layers and establishes which one of the two is more resistive.

in ohm-m, presented in Figure 6) for the normal and symmetrical arrays compared with the total count gamma ray log. The presentation of the conductivities emphasizes the relationship between the in seam mudstone/bentonite layers and the natural gamma radiation. The positive correlation between the electrical conductivity and gamma radioactivity indicates that the major constituents of these in seam layers are conductive clays. The symmetrical lateral conductivity log defines these in seam layers better than the normal conductivity log especially the layer between seams number 3 and 4. The interesting thing to note in the amplitude relationship between the radioactivity and conductivity is that layers with the highest radioactivity are not necessarily the most conductive layers. The explanation is clear when one looks at the natural spectrometry data (not presented here). These data show that uranium is present in higher concentrations within these layers. Enrichment in uranium is not necessarily related to increases in conductive clays. The high gamma radioactivity layer between 40 and 42.5 m shows that the lower and upper zones are more conductive than the middle zone. The conductive zones consist of bentonitic mudstone whereas the resistive, high radioactivity, centre zone consists of carbonaceous mudstone with the poorly defined seam 5.

GAMMA GAMMA DENSITY VERSUS SYMMETRICAL LATERAL LOGS

Figure 8 compares the symmetrical lateral resistivity, gamma gamma density and the 10-cm micronormal resistivity logs. The high resolution gamma gamma density measurements (source-detector spacing of 15 cm) are frequently used for defining boundaries and coal bed thicknesses. The density measurements presented in Figure 8 were acquired with the GSC high resolution spectral density tool consisting of a source-detector spacing of 17 cm. The data are presented in arbitrary density units. It is clear that the coal bed-boundary definition provided by the symmetrical resistivity log is equivalent to that observed from the density data. There is an excellent negative correlation between these two logs. Subtle increases in density between 35 and 36 m within coal seam number 1 are clearly delineated as lower resistivity zones. Even the spike type, high resistivity anomaly at the top of the coal seam is indicated as having lower density implying better coal quality at this depth. The normal resistivity log does not provide good bed-boundary resolution.

RESOLUTION OF THIN MULTIPLE LAYERS

Figure 9 shows an expanded section of Figure 2 across two narrow, resistive calcareous sandstone layers between 48 and 50 metres. The conventional lateral resistivity log shows a pronounced resistivity high across the upper layer. The lower layer resistivity is suppressed to such an extent that it is virtually nonexistent. Both layers are clearly resolved on the inverted lateral resistivity log. However, the lower layer is indicated as a more resistive layer than the upper layer on the inverted lateral log whereas the upper layer is indicated as the more resistive one on the conventional lateral log. The symmetrical resistivity log clearly resolves the two layers and properly defines the relative amplitudes of the resistivities of the two layers.

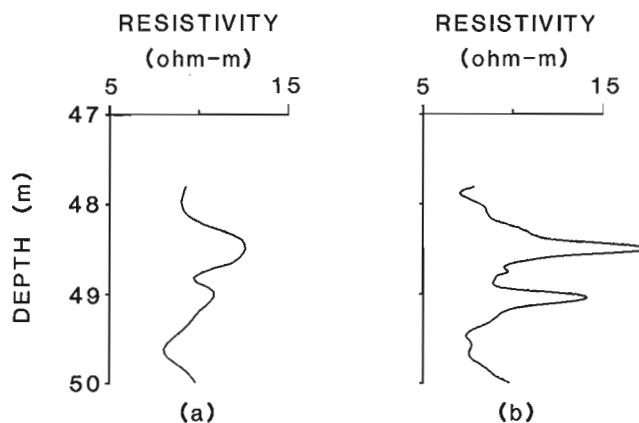


Figure 10. Symmetrical lateral resistivity log across the two narrow resistive calcareous sandstone layer of figure 9, compared with the 10-cm normal resistivity log.

Figure 10 shows how the symmetrical lateral array compares with the normal resistivity log. Both the normal and symmetrical lateral resistivity logs clearly show the two layers and indicate that the upper layer is more resistive than the lower layer. The anomalies on the normal resistivity log are broader and the resistivities are lower than those observed on the symmetrical lateral log. These data demonstrate the superiority of the symmetrical lateral resistivity log over either the normal or the lateral resistivity logs. The asymmetrical resistivity response of the lateral array makes interpretation of the resistivity anomalies difficult. Multiple layers may be resolved but the significance of the amplitudes is ambiguous whether one uses the lateral or inverted lateral array. It is therefore recommended that the symmetrical lateral array be used instead of the lateral or inverted lateral array.

CONCLUSIONS

Even though the lateral resistivity logs are still being widely used to improve bed resolution, their resistivity response characteristics are asymmetrical and complicated to interpret. The symmetrical lateral resistivity log provides better bed-boundary definition than either the single point resistance, lateral or high resolution 10-cm micronormal resistivity logs. The departure of the measured apparent resistivities from the true resistivities of thin beds is not as drastic as for the other electrical resistivity logs. The apparent resistivities provide a better approximation to the true resistivities even in thin beds. The symmetrical lateral is non focusing and simple to implement. The bed-boundary resolution provided by the symmetrical array resistivity log is comparable to that from the high resolution density log.

ACKNOWLEDGMENTS

The author is indebted to TransAlta Utilities Corporation for the permission to carry out these experiments in their holes at the Highvale coal mine, Alberta. Thanks to Bill Hyatt and Steven Birk for the help in the data acquisition and Barbara Elliot for the help rendered in the processing of the data.

REFERENCES

Bristow, Q.

1986: A system for digital transmission and recording of induced polarization measurements in boreholes; in Borehole Geophysics for Mining and Geotechnical Applications, ed. P.G. Killeen, Geological Survey of Canada, Paper 85-27, p.127-143.

Dakhnov, V.N.

1959: The application of geophysical methods: electrical well logging, Moscow Petroleum Institute; translated by G.V. Keller (1962), Colorado School of Mines quarterly, v. 57, no. 2, 445 p.

Schlumberger Document 8.

1958: Introduction to Schlumberger Well Logging. Schlumberger, Houston.

Petrography of the Upper Albian Basal Colorado Sandstone in the Cessford Field, southern Alberta

I. Banerjee

Institute of Sedimentary and Petroleum Geology, Calgary

Banerjee, I., *Petrography of the Upper Albian Basal Colorado Sandstone in the Cessford Field, southern Alberta*; in *Current Research, Part D, Geological Survey of Canada, Paper 89-1D*, p. 9-18.

Abstract

Studies of the Basal Colorado Sandstone in the Cessford Field, southern Alberta, show that petrographic characteristics are related to facies subdivisions.

The sandstone has been interpreted as a tidal sand sheet, and comprises five facies: black shale (Facies 1), tidal sand with small sand waves (Facies 2), tidal sand with gravel waves (Facies 3), storm-generated graded sand (Facies 4), and bioturbated tidal sand (Facies 5). The sandstone becomes finer grained and better sorted in Facies order 4, 3, 2, 5. The coarser facies (Facies 4, 3) are chert-grain rich, and the finer ones (Facies 2, 5) are feldspar-rich. Glauconite is concentrated in Facies 4 and 5. Heavy minerals in the sandstone indicate plutonic (apatite), high grade metamorphic (garnet, kyanite, chloritoid), and sedimentary (well rounded zircon) sources.

The cements show a paragenetic sequence of early quartz and cone-in-cone calcite → siderite → barite → calcite → replacement pyrite. Clay material was derived from two sources. Alteration of feldspar grains produced a kaolinitic and illitic clay matrix, and redistribution of slack-water mud drapes within the sand by burrowing also produced a kaolinitic matrix with associated 2:1 interstratified mixed layer phyllosilicates, presumably of primary detrital origin.

Résumé

Des études du grès basal de Colorado dans le champ Cessford dans le sud de l'Alberta montrent que les caractéristiques pétrographiques sont liées aux subdivisions des faciès.

Le grès serait constitué de couches de sable de marée et comporte cinq faciès: de l'ampélite (faciès 1), du sable de marée avec de petites dunes sousmarines (faciès 2), du sable de marée avec des dunes de gravier (faciès 3), du sable classé par des tempêtes (faciès 4) et du sable de marée bioturbé (faciès 5). Le grès devient plus fin et mieux classé dans l'ordre des faciès 4, 3, 2, 5. Les faciès à grains plus gros (faciès 4, 3) sont riches en grains de chert, et les faciès à grains plus fins (faciès 2, 5) sont riches en feldspath. La glauconite est concentrée dans les faciès 4 et 5. Les minéraux lourds dans le grès proviendraient de sources plutoniques (apatite), métamorphiques à teneur élevée (grenat, kyanite, chloritoïde) et sédimentaires (zircon bien arrondi).

Les ciments présentent une série paragénétique de quartz ancien et de calcite — sidérite — barytine — calcite — pyrite de substitution en cônes emboîtés. Le matériau argileux provient de deux sources. L'altération des grains de feldspath a produit une matrice d'argile kaolinitique et illitique, et la redistribution de rideaux de boue qui s'étale dans le sable par fouissage a aussi produit une matrice kaolinitique à laquelle sont associés des phyllosilicates à couches alternées dans un rapport de 2 à 1, qui seraient d'origine détritique primaire.

INTRODUCTION

The Basal Colorado Sandstone (BCS) is a thin (<15 m), narrow (<26 km wide), transgressive sheet sandstone of Late Albian age that overlies a sequence of coal-shale-sandstone of lagoon-coastal swamp origin belonging to the Mannville Group (Aptian-Albian), and underlies offshore marine shales of the Joli Fou Formation (Late Albian) (Fig. 1). In the Cessford Field (Fig. 1a) of southern Alberta, this sandstone has been interpreted as a tidal sand sheet (Banerjee, 1986, in press; Belderson, 1986) and subdivided into five facies: 1. black shale, 2. medium grained, crossbedded (tidal) sandstone, 3. gravelly, crossbedded, coarse grained (tidal) sandstone, 4. gravelly, coarse grained, graded (storm) sandstone, and 5. fine grained, crosslaminated, bioturbated sandstone (tidal). A facies map and two cross-sections (Fig. 2) illustrate the facies relationships of the BCS.

The present study is a report on the thin section petrography of the sandstones of the BCS. The data presented here include mechanical analyses of 10 thin sections, 33 modal analyses, 27 heavy mineral analyses, and diagenetic studies of the cement from 58 thin sections. The results are presented under the following headings: grain size, mineralogy of grains (the light fraction), heavy minerals, clay matrix, compaction, and cement.

GRAIN SIZE

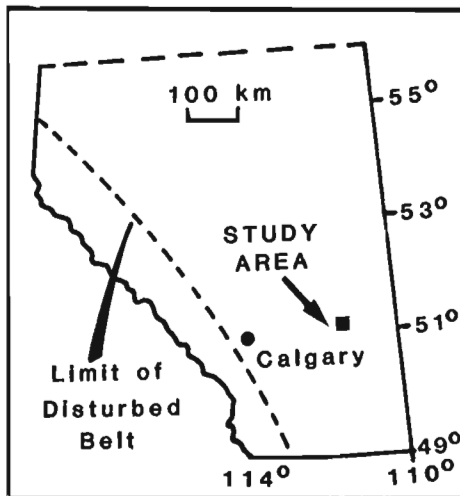
Ten thin sections of standard size (24 x 40 mm), representing all four sandstone facies of the BCS, were chosen for the study. In each thin section the minor axes of 300 to 350 grains, along ten, equally spaced traverses, were measured using an eyepiece micrometer with appropriate magnification. The results were plotted on arithmetic probability paper using a phi scale (Fig. 3) and Inclusive Graphic measures of grain size were calculated (Folk, 1974).

Before thin section grain size analysis was undertaken, a trial run on one sample showed that measuring the intermediate axes of loose grains (obtained from disaggregating the carbonate-cemented sample) yielded very similar results to measuring minor axes of sectioned grains (Fig. 3a). In other words, the "sectioning effect" for the grains in these samples seems to be within reasonable limits.

However, microscopic measurement appears to produce a truncated log-normal distribution in most samples (Fig. 3b), reflecting the limits of resolution of the microscope (maximum magnification used was 450x).

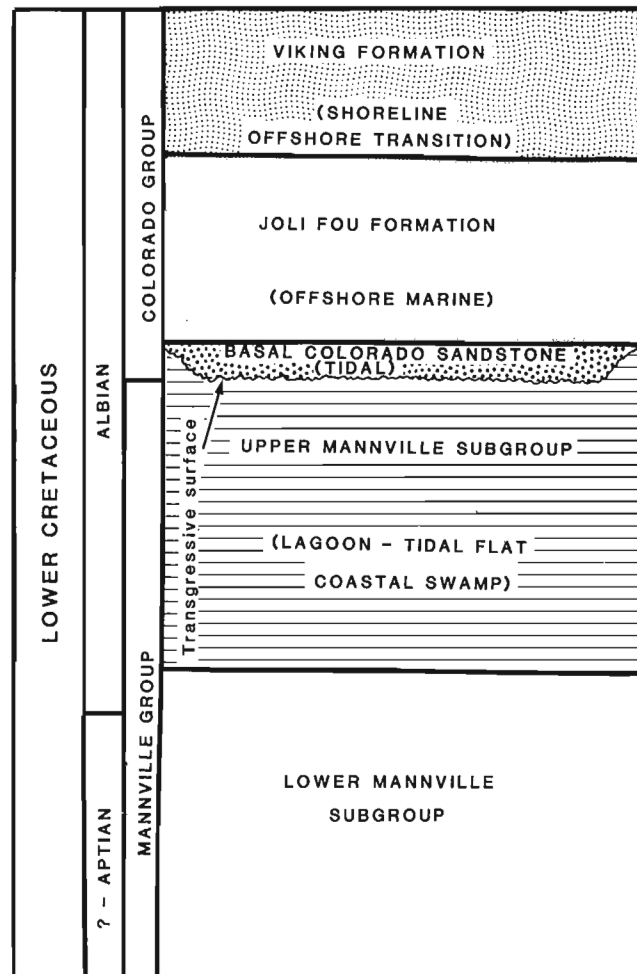
Several facts emerge from this study:

1. Three straight-line segments signifying ideal lognormal distributions (Fig. 3c) indicate three basic populations.

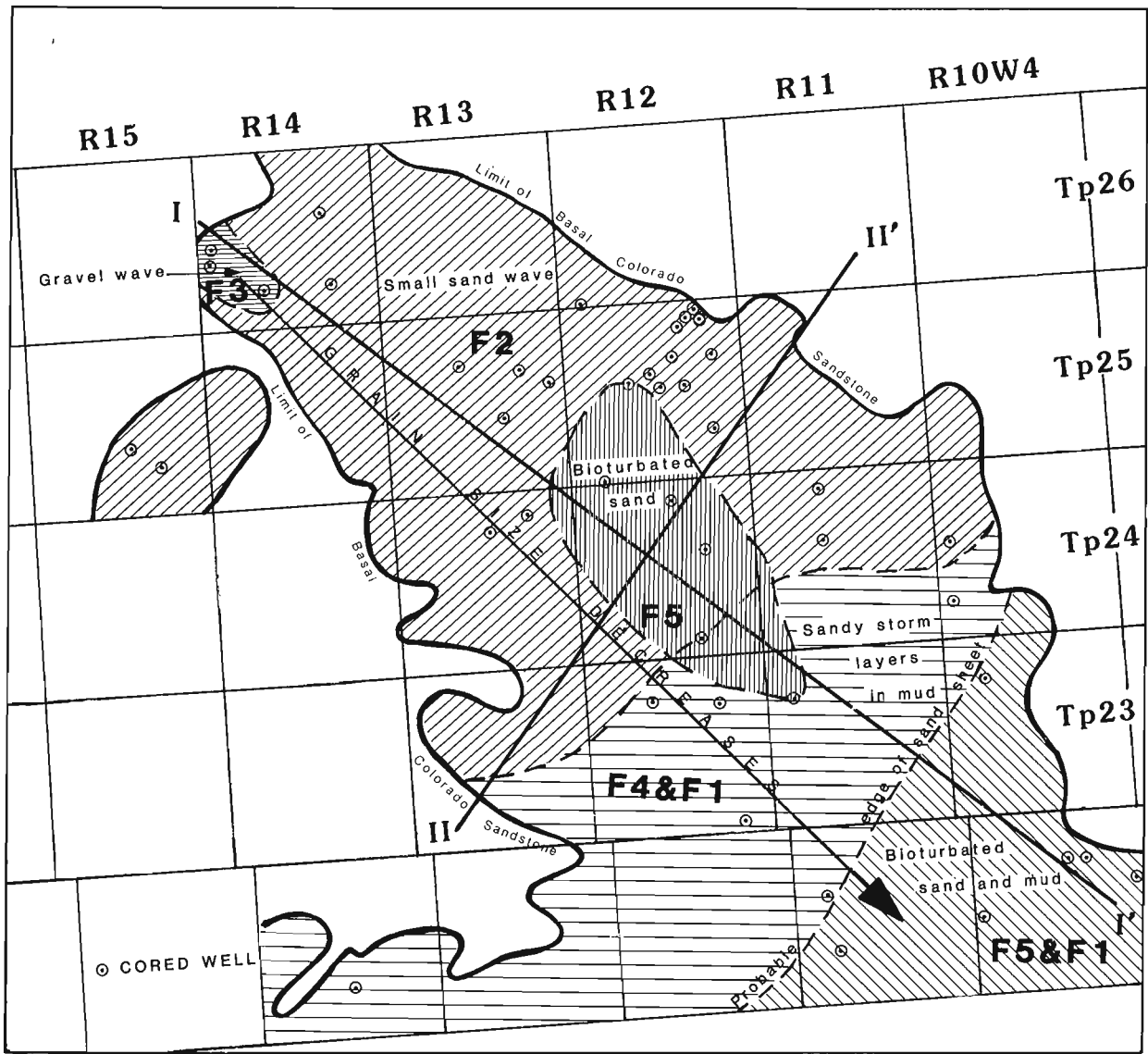


a

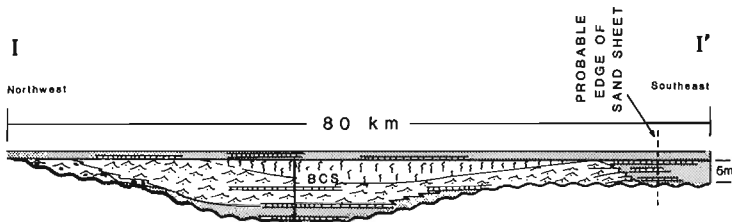
Figure 1. a. Location map showing the Cessford Field study area. b. General stratigraphy of the Cessford area showing position of the Basal Colorado Sandstone.



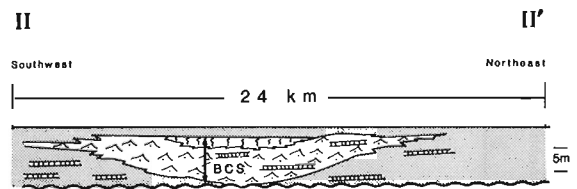
b



a



b



c



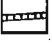



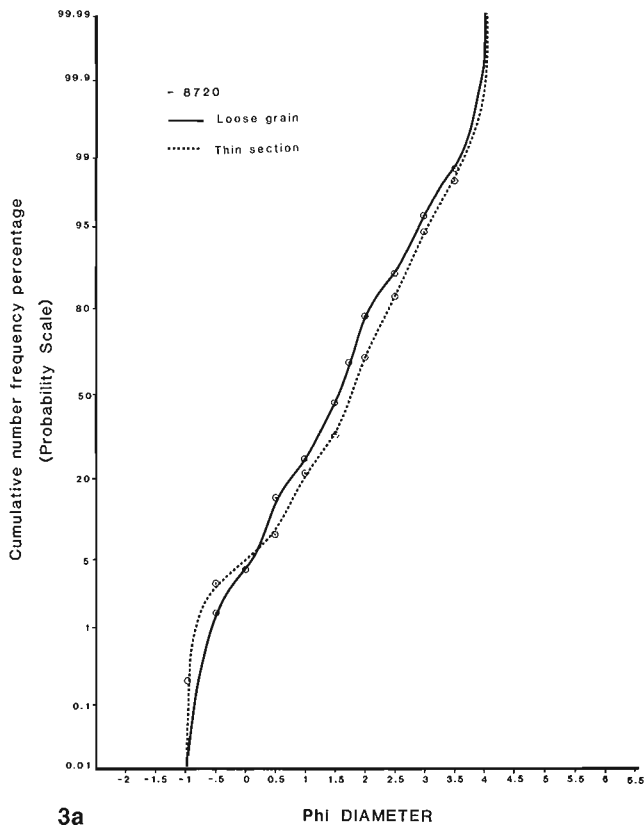
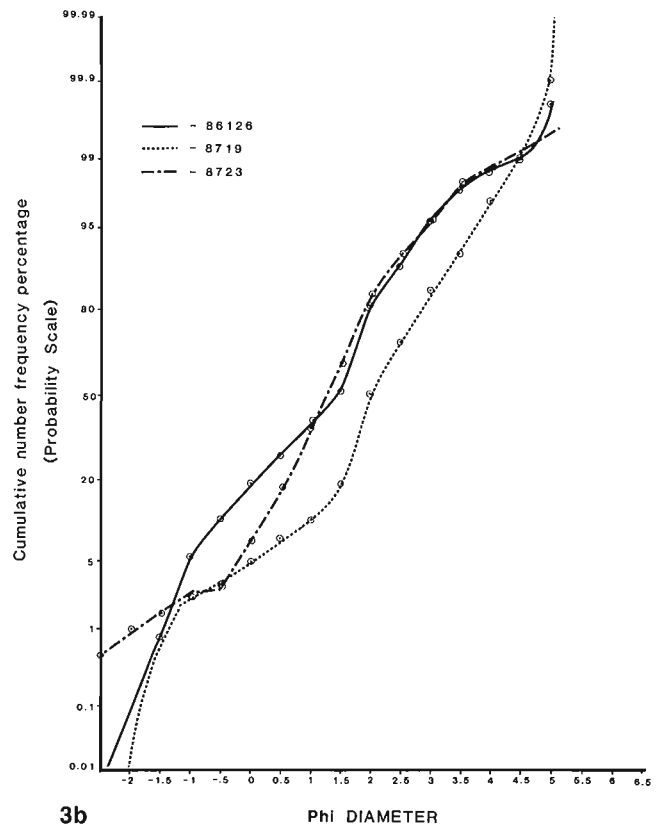
- BCS - Basal Colorado Sandstone
-  GRAVEL WAVE (Facies 3 - F3)
 -  SMALL SAND WAVE (Facies 2 - F2)
 -  STORM LAYER (Facies 4 - F4)
 -  BIOTURBATION (Facies 5 - F5)
 -  SHALE/MUDSTONE (Facies 1 - F1)
 -  SURFACE OF TRANSGRESSION

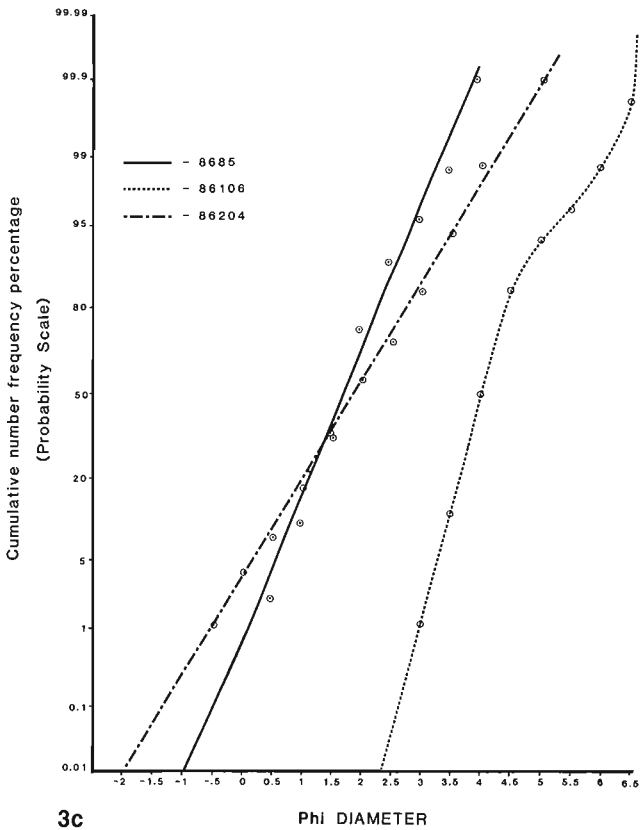
Figure 2. Facies map (2a) and cross-sections (2b, c) of the Basal Colorado Sandstone in the Cessford Field.



3a



3b



3c

Figure 3. a. Grain size curves for the same sample, obtained by two methods of grain measurements: axes of loose grain mounts and axes of sectioned grains. The grain size curves are very similar, and size parameters are close. **b.** Grain size curves of samples showing bimodality and truncation at finer end. **c.** Straight line curves of three samples showing existence of three basic lognormal populations.

Table 1. Summary of grain size parameters for the Basal Colorado Sandstone.

Sample no.	Facies	Mean (M_2)		Sorting (σ_1)		Skewness (SK_1)	
		Phi	mm	Phi	Verbal	Phi	Verbal
8685	2	1.70	0.31	0.69	Moderate-well	+0.002	Symmetrical
86198	2	2.75	0.15	0.74	Moderate	+0.007	Symmetrical
8720	3	1.55	0.34	0.83	Moderate	-0.328	Strongly coarse-skewed
8719	3	2.16	0.22	0.93	Moderate	-0.060	Symmetrical
86167	4	1.00	0.50	1.24	Poor	-0.040	Symmetrical
8723	4	1.17	0.44	0.85	Moderate	0.000	Symmetrical
86126	4	1.18	0.44	1.15	Poor	-0.070	Symmetrical
86151	4	1.53	0.35	1.30	Poor	+0.230	Fine-skewed
86204	4	1.83	0.28	1.03	Poor	0.000	Symmetrical
86106	5	4.05	0.06	0.52	Moderate-well	+0.190	Fine-skewed

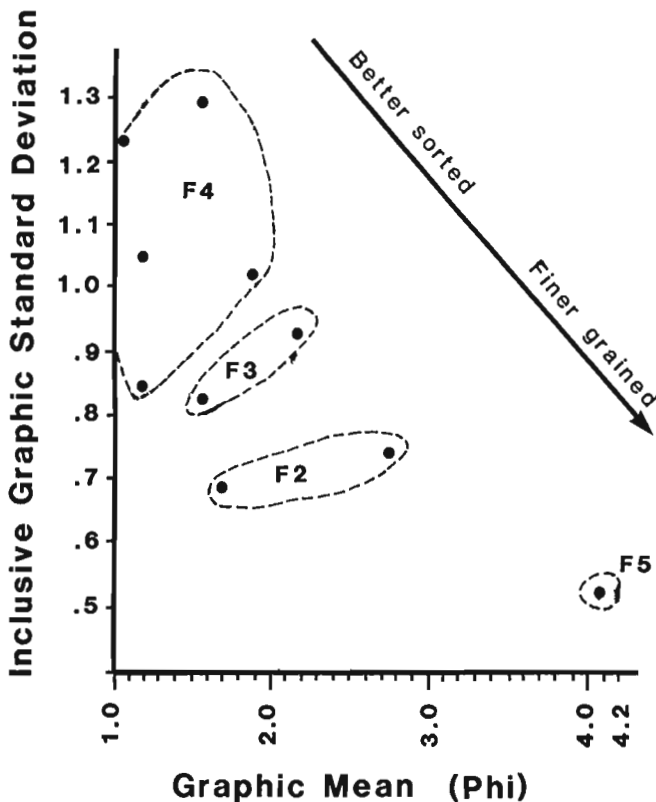


Figure 4. Graphic Mean Size (M_z) vs. Inclusive Graphic Standard Deviation (σ_1) of ten samples. Samples define distinct fields for the four facies and a sequential arrangement from coarser and more poorly sorted, to finer and better sorted.

- Two curves (Fig. 3b) are bimodal, reflecting the presence of a small (<5%) granule - gravel population (-5ϕ to -1ϕ) and a sand population (0ϕ to 4ϕ).
- The size-sorting diagram (Fig. 4) shows that four facies occupy distinct fields in a sequence where they become progressively finer grained and better sorted. This change takes place along the assumed path of the tidal current flowing parallel to the long axis of the BCS sheet (Fig. 2).

A summary of the size parameters of the samples is given in Table 1.

MINERALOGY OF GRAINS (the light fraction)

The major constituent grains that make up the framework material of the BCS are: quartz, lithic grains (mainly chert) and feldspar (Fig. 5).

Quartz: The majority of the sandstones are chert-arenites; quartz content never exceeds 55 per cent of total grains. Both mono- and polycrystalline grains are present. Monocrystalline grains are dominant. Some polycrystalline grains are of hydrothermal quartz-vein origin, and some with elongated shape and sutured contacts must be of metamorphic origin. Quartz content, directly controlled by grain size, is maximum in the medium grained sandstones of tidal origin (Facies 2) and minimum in the gravelly, storm-laden sandstones (Facies 4).

Chert: Chert is volumetrically the dominant constituent of the sandstones in the BCS units. The three main types of chert grains are: 1. Sponge spiculite (Fig. 6a), 2. non-diagnostic microcrystalline chert (Fig. 6b), and 3. chalcedonic chert. Spiculite grains dominate over the other two varieties, especially in the coarser size range. The provenance of the spiculites was probably the underlying Mississippian carbonate rocks (Schultheis and Mountjoy, 1978; Rapson, 1965; Mellon, 1967). Chalcedonic chert may indicate an evaporitic source, possibly the Triassic Charlie Lake Formation of the Rocky Mountains (Leckie, 1986). Most chert grains are well rounded, indicating their greater (than quartz) susceptibility to abrasion.

Sideritic clasts: These clasts, which measure up to 6 mm in diameter, are intrabasally derived rip-up clasts from sideritic nodules and bands deposited within the sandstones.

Phosphatized grains: Some dark brown or yellowish brown, semi-opaque grains are thought to be phosphatized shale clasts or other similar grains.

Shale clasts: Rounded clasts of shale, up to 10 mm in diameter, presumed to be of rip-up origin, occur throughout the BCS, but their proportion is always less than 10 per cent.

Shells: At a few places, thick pelecypod valves, gastropod shells, or abraded, unidentifiable shells occur in the gravel fraction.

Metamorphic grains: Elongated, subrounded grains of phyllite and schist (Fig. 6c) showing parallel alignment of mica flakes, have been recognized in a few samples. They never constitute more than 5 per cent of the framework grain population.

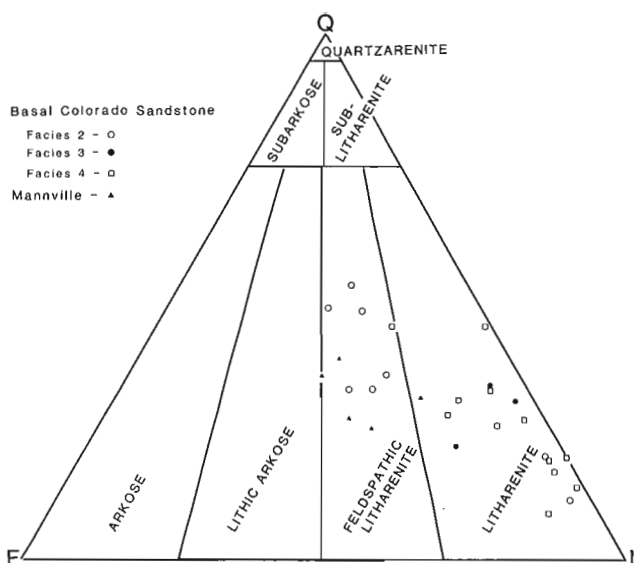


Figure 5. QFL (Quartz-Feldspar-Lithic grain) diagram for 31 modal analyses. Folk's (1974) sandstone classification scheme has been used for division into classes.

Volcanic grains: Rounded grains showing an intergranular texture (Fig. 6d) with feldspar microlites have been identified in several samples. They constitute less than 2 per cent of total grains but become more dominant (5-10%) in the underlying Mannville rocks.

Feldspar: Feldspar content of the samples varies between 6 and 33 per cent (Fig. 5). Microcline and albite are the two most common varieties. The degree of alteration varies from entirely fresh, unaltered grains to completely decomposed grains that leave behind a "ghost" outline in a clay matrix. It is believed that a considerable part of the clay matrix may have been a product of alteration of feldspar grains. Feldspar grains vary in degree of alteration, and the predominance of fresh, unaltered grains of feldspar in the BCS suggests multiple sources.

Glauconite

Glauconite occurs in the BCS in two forms: 1. framework grains of rounded, elliptical pellets (Fig. 6e) with characteristic marginal cracks, or 2. incipient glauconite occurring within the clayey matrix. Glauconite content is maximum (3%) in the graded beds of the storm facies (Facies 4), especially when these beds form the base of the sequence, indicating that during the first onset of transgression, relative sea level rise was rapid, clastic input was cut off, and sedimentation was slow. All these conditions are required for glauconite formation (Odin and Letolle, 1980).

Heavy minerals

Twenty seven samples were subjected to heavy liquid separation. However, because of heavy mineral separation problems, it was decided to record a qualitative or semi-quantitative table of heavy minerals (see Table 2). Heavy minerals are illustrated in Figure 6f.

Table 2. Summary of heavy mineral data and inferred provenances.

Heavy Mineral	Frequency	Provenance
Zircon (euhedral)	common	Acid igneous
Zircon (well rounded)	common	Sedimentary
Tourmaline (subhedral)	common	Acid igneous
Apatite (subhedral)	abundant	Acid igneous, Volcanic (?)
Kyanite (Prismatic, angular)	rare	Metamorphic
Chloritoid (irregular)	common	Metamorphic
Staurolite (irregular, angular)	rare	Metamorphic
Garnet (irregular, angular)	rare	Metamorphic

As is apparent from Table 2, both igneous, metamorphic (deep crustal) and sedimentary (supracrustal) sources are indicated by the heavy mineral suite. The suite is very similar to the one obtained from the underlying Mannville Group (Mellon, 1967; Carrigy, 1963; Carrigy and Mellon, 1964) and its equivalent, the Gates Formation (Leckie, 1986).

Clay matrix

Most sandstones of the BCS unit are clean. A clay matrix occurs only in a few places in the tidal sandy facies (Facies 2) and in the finer grained bioturbated sandstones (Facies 5), and always comprises less than 15 per cent of the total volume of rock. However, the low energy sediments of the underlying Mannville Group contain a high percentage of clay matrix (30-40%).

Some clay matrix is a product of alteration of feldspar grains, and as such is of secondary origin. However, clay of primary origin produced as mud-drapes on ripples and small sand waves during the slackwater period, may be redistributed by burrowers and form an interstitial matrix (Fig. 6g) in a "swirley bedded" or "burrow mottled" sandstone (Facies 5). Both types of clay matrix are mineralogically diverse. They contain kaolinite, illite, and 2:1, interstratified, mixed layer phyllosilicates.

Compaction

In a few samples from Facies 3 sandstones, the quartz and chert grains occur without cement or interstitial clay and instead show sutured grain-to-grain contacts and rare microstylolites (Fig. 6h). A period of compaction, perhaps postdating the siderite cementation phase, has affected this facies and in places reduced its porosity to zero. Some grain-fracturing and deformation of semiplastic grains such as mudclasts has accompanied this phase of compaction.

Cement

The clean, well-sorted, coarse and medium grained sandstones of Facies 2, 3 and 4, with well rounded (granule fraction) and subrounded (sand fraction) grains, have pore-filling cements instead of matrix, and these include quartz, pyrite, siderite, calcite and barite (Fig. 7a-d). Calcite and siderite occur both as pore-filling cement and replacement (Fig. 7a, b, e, f).

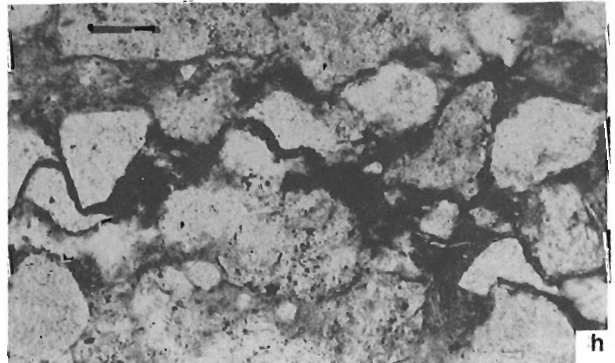
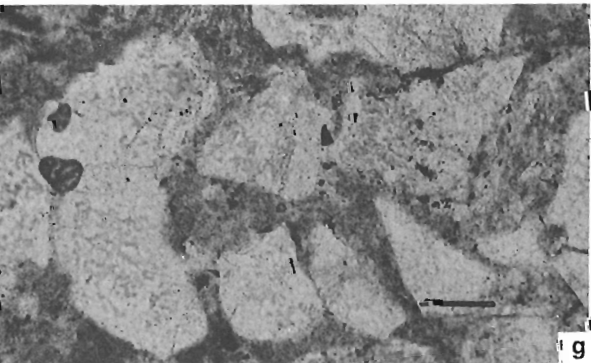
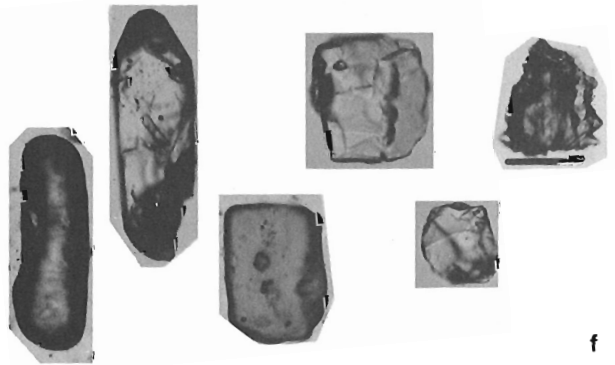
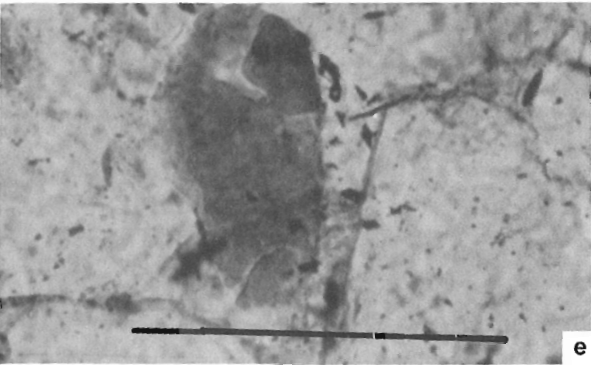
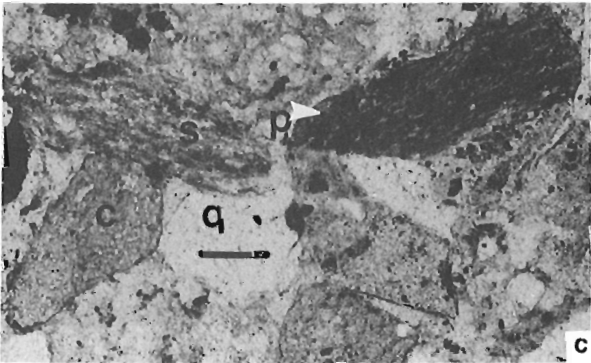
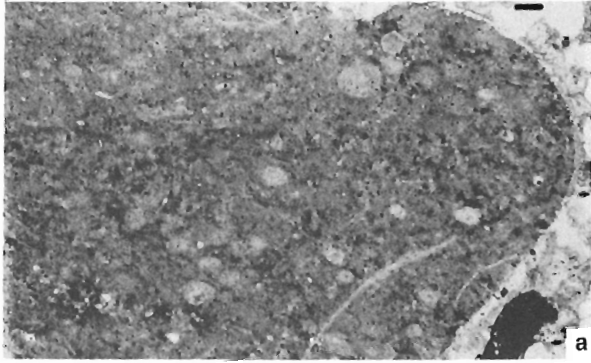


Figure 6. Thin section photomicrographs of the Basal Colorado Sandstone. Bar = 0.1 mm. **a.** Spiculite chert grain. Circular cross-sections of spicules are visible. **b.** Microcrystalline chert grain, nondiagnostic of provenance. **c.** Metamorphic rock fragments: s, schist; p, phyllite; q, quartz; c, chert. **d.** Volcanic rock fragment with microlites of feldspar showing intergranular texture. **e.** Glauconite pellet with marginal cracks. **f.** Heavy minerals, left to right: zircon (well rounded, euhedral), tourmaline, apatite, garnet, staurolite. **g.** Pockets of clay matrix in bioturbated sandstone (Facies 5). **h.** Microstylolite in fine grained sandstone (Facies 5).

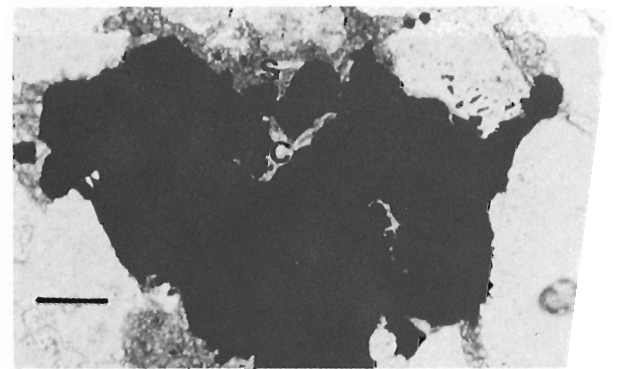
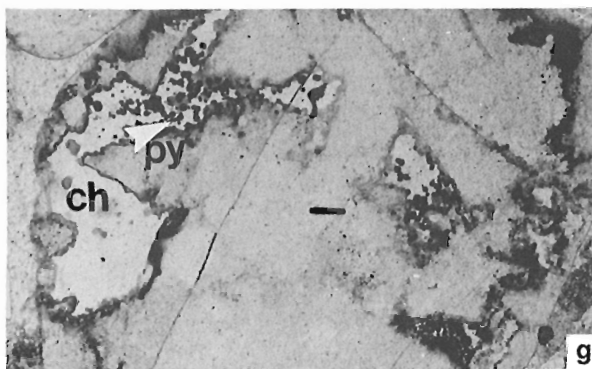
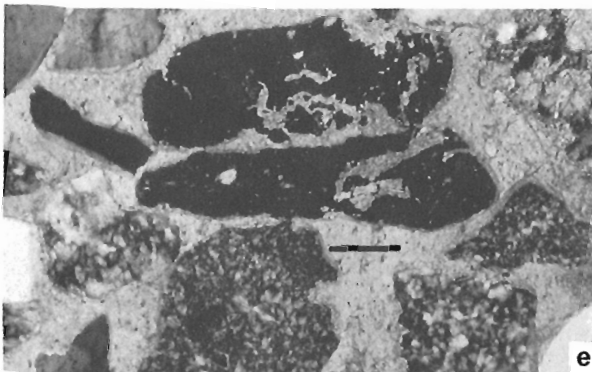
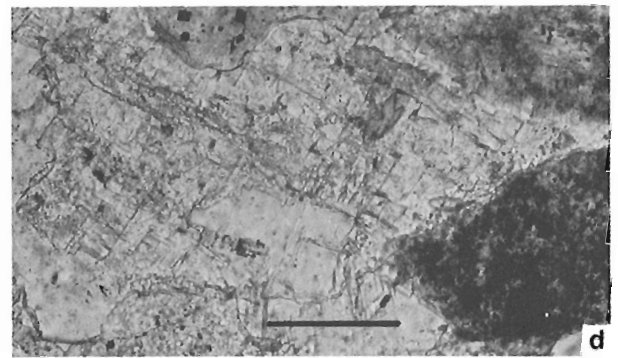
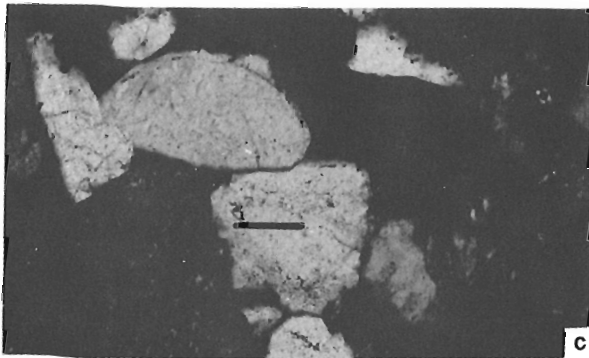
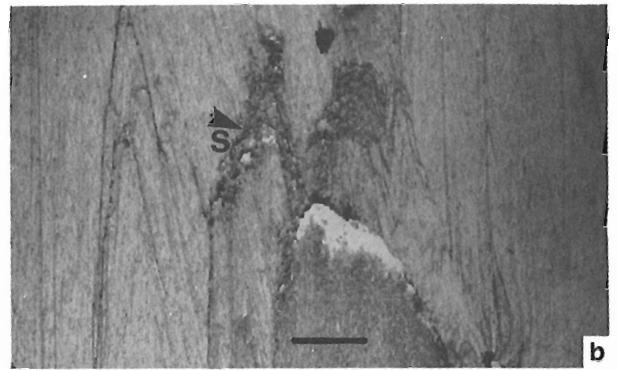
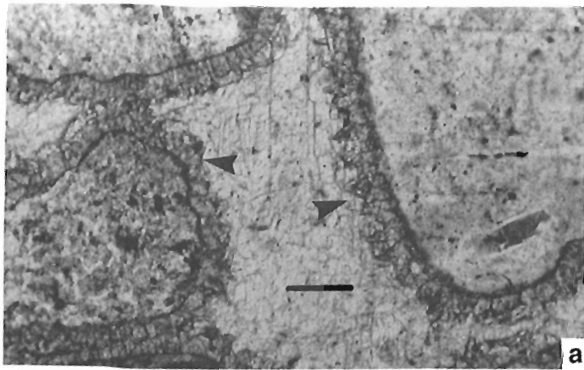


Figure 7. Photomicrographs showing relationships between cements in the Colorado Sandstones. Bar = 0.1 mm. **a.** Clast rim (arrows) of siderite rhombs outlining quartz and chert grains. Poikilotopic calcite fills intergranular pores. **b.** Cone-in-cone structure in calcite. Siderite (s) occupies space between cones. **c.** Quartz overgrowth (arrow) (crossed nicols). **d.** Barite cement with high relief and two right-angled cleavages. **e.** Chert grain being replaced by calcite cement (crossed nicols). **f.** Quartz grain being replaced by siderite. **g.** Chert grain partly dissolved and then replaced by void-filling chalcedony (ch) which in turn, is partly replaced by framboidal pyrite (py). **h.** Pyrite replacing calcite (c) and siderite (s) cements.

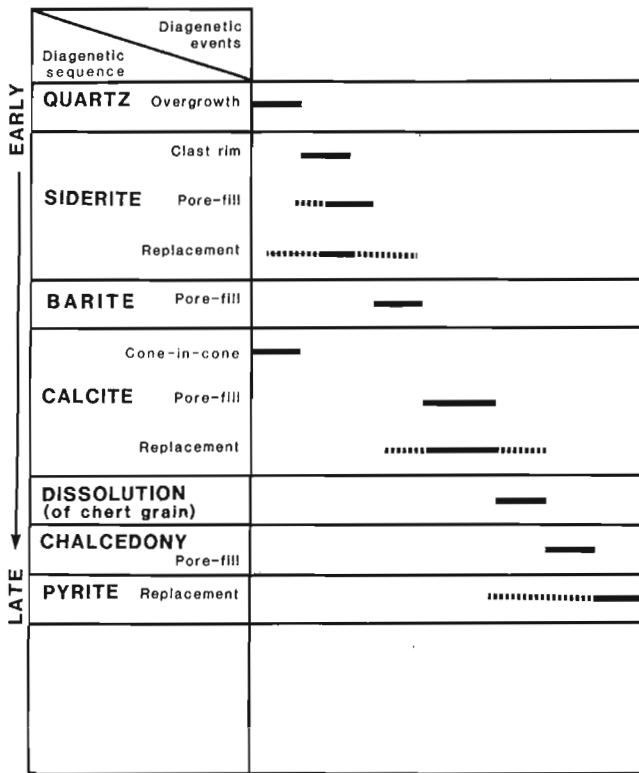


Figure 8. Paragenetic sequence of cements in the Basal Colorado Sandstone.

Quartz: Quartz overgrowths of framework grains (Fig. 7c) are encased in both siderite and calcite cements and are therefore older than both. Volumetrically, quartz cement is not significant in the BCS.

Siderite: Siderite occurs in three main forms: 1. rhombs of siderite lining clasts (Fig. 7a), 2. as anhedral grains filling in pore spaces, and 3. as irregular, patchy grains replacing clay matrix. Examples of pore-filling calcite cement encasing siderite (Fig. 7a) illustrate that the siderite cement formed earlier than the calcite.

Calcite: Poikilotopic calcite cement (Fig. 7a) is ubiquitous in the coarser and cleaner sandstones. It occurs mainly as a pore-filling cement, but there are also examples of replacement of framework grains (Fig. 7e).

An occurrence of cone-in-cone limestone (Fig. 7b) with prismatic calcite crystals occurring in bundles has been found in a 0.2 m thick layer at the top of the BCS unit in the Tidal Can Chief Cessford well (11-18-22-10W4, 2799 ft./1853 m). The fact that siderite rhombs occur between the cones suggests that they formed later.

Pyrite: Framboidal pyrite, disseminated grains and pyritized burrows, shells and mudclasts are the common modes of occurrence of pyrite.

There is some evidence of chert grains dissolving to produce intragranular voids. These voids were later filled by chalcedony, which, in turn, was replaced by framboidal pyrite (Fig. 7g). Calcite and siderite cements are also replaced by pyrite (Fig. 7h). Replacement of clay matrix by pyrite in patches is also common. Pyrite filling large, open pores is not common.

Barite: Barite cement (Fig. 7d) has been found in one sample of Facies 2 sandstone. It occurs as a pore filling, poikilotopic cement enclosing earlier siderite cement and surrounded by later calcite cement. Although barite cement (Carozzi, 1960) commonly replaces calcite cement, the relationship here indicates barite as being a slightly earlier pore-filling cement.

A study of 58 thin sections in which the paragenetic relationships of three cements and the compaction phase have been analysed revealed a paragenetic sequence shown schematically in Figure 8. Of the cements, quartz overgrowth and cone-in-cone calcite seem to have been the first to form, followed by clast-rim siderite, pore-fill siderite, barite, pore-fill calcite, and chalcedony, in that order. Replacement by first siderite, then calcite and finally pyrite followed. Dissolution of chert grains predated precipitation of chalcedony. Cementation seems to be the major porosity reducing process in the Basal Colorado Sandstone; grain welding plays a very minor role.

CONCLUSIONS

The above study shows that the petrography of the BCS is related to its facies. Cement, matrix and diagenetic alterations were also controlled by initial grain size and mineralogy of the grains. More specific conclusions are:

1. Grain size becomes successively finer and better sorted from the storm sand layers (Facies 4), to the tidal gravel waves (Facies 3), to the tidal, small sand wave zone (Facies 2), to the tidal, rippled and bioturbated sand sheet (Facies 5).
2. The sandstones contain considerable amounts of chert grains. The coarser facies (Facies 3 and 4) have a dominance of chert over quartz, and the finer facies (Facies 2 and 5) have a dominance of feldspar.
3. Sponge spiculites constitute a large number of the chert grains. Other chert varieties are microcrystalline quartz (non-diagnostic) and rare, chalcedonic chert (possibly evaporitic).
4. Shale clasts, siderite clasts, volcanic, and metamorphic rock fragments are minor in occurrence.
5. Glauconite is concentrated near the base and the top of the BCS unit, indicating probable hiatuses.
6. Heavy mineral suites indicate igneous (apatite), metamorphic (garnet, kyanite, chloritoid) and multicycle sedimentary (well rounded zircon) source rocks.
7. The paragenetic sequence shows early quartz cement followed successively by cone-in-cone calcite, siderite, barite and poikilotopic calcite. Compaction took place after siderite cementation. Dissolution of chert grains was followed by precipitation of pore-filling chalcedony, which, in turn, was replaced by pyrite.
8. The clay matrix has two distinct origins. Kaolinitic and illitic clay were derived from alteration of feldspar grains, and kaolinite and mixed layer 2:1 clay were deposited as detrital, clay-forming mud drapes over ripples during slack water, and later redistributed by burrowers as matrix within the sand fraction.

REFERENCES

Banerjee, I.

1986: The Basal Colorado Sandstone (Lower Cretaceous) in the Cessford Field, Alberta (tide versus storm origin of a basal transgressive sandstone); 1986 Core Conference; Canadian Society of Petroleum Geologists, p. B-1, B-7.

— Tidal sand sheet origin of the Basal Colorado Sandstone (Albian): A subsurface study in the Cessford Field, Southern Alberta, Canada; Canadian Society of Petroleum Geologists, Bulletin (in press).

Belderson, R.H.

1986: Offshore tidal and non-tidal sand ridges and sheets: differences in morphology and hydrodynamic setting, in Shelf sands and sandstones; Canadian Society of Petroleum Geologists, Memoir 11, p. 293-301.

Carozzi, A.V.

1960: Microscopic sedimentary petrology; New York, John Wiley and Sons, 485 p.

Carrigy, M.A.

1963: Petrology of coarse-grained sands in the lower parts of the McMurray, in The K.A. Clarke Volume, Carrigy, M.A. (ed.); Research Council of Alberta, Information Series, No. 45, p. 43-54.

Carrigy, M.A. and Mellon, G.B.

1964: Authigenic clay mineral cements in Cretaceous and Tertiary sandstones of Alberta; Journal of Sedimentary Petrology, v. 34, no. 3, p. 461-472.

Folk, R.L.

1974: Petrology of Sedimentary Rocks; Hemphill's, Austin, Texas, 170 p.

Leckie, D.

1986: Petrology and tectonic significance of Gates Formation (early Cretaceous) sediments in northeast British Columbia; Canadian Journal of Earth Sciences, v. 23, p. 129-141.

Mellon, G.B.

1967: Stratigraphy and petrology of the Lower Cretaceous Blairmore and Mannville Groups, Alberta foothills and plains; Research Council of Alberta, Bulletin 21, 270 p.

Odin, G.S. and Letolle, R.

1980: Glauconitization and phosphatization environments: a tentative comparison; in Society of Economic Paleontologists and Mineralogists, Special Publication no. 29, p. 227-237.

Rapson, J.E.

1965: Petrography and derivation of Jurassic-Cretaceous Clastic rocks, Southern Rocky Mountains, Canada; American Association of Petroleum Geologists Bulletin, v. 49, p. 1426-1452.

Schultheis, N.H. and Mountjoy, E.,

1978: Cadomin conglomerate of western Alberta — a result of early Cretaceous uplift of the Main Ranges; Bulletin of Canadian Petroleum Geology, v. 26, p. 297-342.

A comparison between the biomarker geochemistry of some samples from the Lower Jurassic Nordegg Member and western Canada Basin oil sands and heavy oils

M.G. Fowler, P.W. Brooks, and R.W. Macqueen
Institute of Sedimentary and Petroleum Geology, Calgary

Fowler, M.G., Brooks, P.W., and Macqueen, R.W., *A comparison between the biomarker geochemistry of some samples from the Lower Jurassic Nordegg Member and western Canada Basin oil sands and heavy oils*; in *Current Research, Part D, Geological Survey of Canada, Paper 89-1D*, p. 19-24, 1989.

Abstract

The distributions of biomarkers observed in extracts from five samples of the Lower Jurassic Nordegg Member of western Alberta are compared to biomarker distributions previously described from Lower Cretaceous heavy oils and oil sand bitumens of the Western Canada Basin. The five Nordegg samples, obtained from two widely separated exploration wells, give biomarker distributions indicating a highly anoxic carbonate depositional environment that allowed extensive reworking of primary organic matter. There are several significant differences between the Nordegg biomarker patterns and those of the heavy oils and oil sand bitumens. These include the ratio of pristane to phytane, the lack of 28,30-bisnorhopanes, the low abundance of diasteranes relative to regular steranes and tricyclic terpanes to 17 α (H)-hopane. If these results are representative of the regional biomarker character of the Nordegg, it is unlikely that the Nordegg was a major contributor to the Western Canada Basin Cretaceous oil sands and heavy oils.

Résumé

Les distributions de marqueurs biologiques observées dans des extraits de cinq échantillons du membre Nordegg du Jurassique inférieur dans l'ouest de l'Alberta sont comparées à des distributions décrites antérieurement de marqueurs biologiques dans des pétroles lourds et des bitumes de sables pétrolifères du Crétacé inférieur provenant du bassin ouest-canadien. Les cinq échantillons du membre Nordegg, prélevés dans deux puits d'exploration très distants, établissent les distributions des marqueurs biologiques, indiquant qu'un environnement fortement anoxique, propice au dépôt de carbonates, a permis un remaniement en profondeur de la matière organique primaire. Il y a plusieurs différences importantes entre ces distributions et celles des pétroles lourds et des bitumes de sable pétrolifère. Ces dernières indiquent le rapport pristane/phytane, l'absence de 28-30-bisnorhopanes, la faible concentration de diastéranes par rapport à celle des stéranes ordinaire, et de terpanes tricycliques par rapport au 17 α (H)-hopane. Si ces résultats sont représentatifs du caractère régional des marqueurs biologiques du membre Nordegg, il est peu probable que ce dernier ait contribué de façon importante à la formation des sables pétrolifères et des pétroles lourds du bassin de l'Ouest canadien pendant le Crétacé.

INTRODUCTION

The identity of the source rocks of the oil sands and heavy oils of the Western Canada Basin remains unknown. One of the most reliable methods of making oil-oil and oil-source rock correlations is by comparing the distributions of certain classes of biomarker compounds. Considerable effort has been expended at the Institute of Sedimentary and Petroleum Geology in examination of the biomarker distributions of heavy oils and oil sand bitumens from the Western Canada Basin (Fowler and Brooks, 1987; Brooks et al., in press, 1988) and biomarker studies are now underway on conventional oils from this basin. There are, however, insufficient data published on the biomarker distributions of the possible source rocks of these nonconventional hydrocarbons to allow oil-source correlations to be made.

Recently, it has been suggested that the Nordegg Member of the Lower Jurassic Fernie Formation was a major source of the hydrocarbons of the Lower Cretaceous oil sands and heavy oils (Creaney and Allan, 1988). A preliminary evaluation of the Nordegg by Stasiuk et al. (1988) indicated that this unit has excellent source potential, showing high TOC values and containing Type I organic matter.

In this brief report, the biomarker distributions of five of the samples examined by Stasiuk et al. (1988) are described and compared to the biomarker distributions observed in Western Canada oil sands and heavy oils by Brooks et al. (in press). The samples originate from two boreholes in western Alberta. The organic matter in the samples from the more northerly borehole (9-26-87-7W6) was found by Stasiuk et al. (1988) to be marginally mature with respect to oil generation, and significantly less mature than the organic matter from a borehole at 2-36-68-4W6, which is within the peak zone of oil generation.

EXPERIMENTAL

The methods of analysis used in this study, namely bitumen extraction and fractionation, gas chromatography and gas chromatography - mass spectrometry, are described in detail in Brooks et al. (in press).

RESULTS AND DISCUSSION

Extraction data are provided in Table 1. The extract and hydrocarbon yields obtained after extraction of the Nordegg samples using azeotropic chloroform-methanol (87:13) show a wide variation in values. Those samples with higher TOC contents tend to show lower values for these parameters. The proportion of saturated hydrocarbons is less than 10 per cent in all of the samples. As expected, because their organic matter is more mature, the samples from borehole 2-36-68-4W6 contain a higher proportion of saturated hydrocarbons than the samples from 9-26-87-7W6.

Representative C_{15+} saturate fraction gas chromatograms of the five Nordegg samples are shown in Figure 1. The chromatograms of samples from one borehole resemble each other, but differ from those from the other borehole.

Table 1. Solvent extract data of Nordegg samples

Well	Depth (m)	TOC %	Ext.		HC ¹ %	R&A ² %	SAT %	AROM %
			Yield (mg/g)	HC ¹ Yield (mg/g)				
9-26-87-7W6	1022	23.62	121.8	43.9	36.0	63.8	3.1	32.9
9-26-87-7W6	1027.5	9.32	229.5	76.1	33.2	64.9	3.7	29.4
9-26-87-7W6	1028.4	22.12	87.3	23.4	26.8	65.8	3.7	23.1
2-36-68-4W6	2056.6	14.37	70.9	30.3	42.7	51.5	9.3	33.4
2-36-68-4W6	2060.3	9.20	138.8	50.9	36.7	57.0	8.7	28.0

¹HY = hydrocarbons: saturates (SAT) and aromatics (AROM)
²R&A = resins and asphaltenes

The gas chromatograms of samples from borehole 9-26-87-7W6 generally show a smooth distribution of n-alkanes, which decrease in abundance with increasing carbon number up to about C_{27} . The sample from a depth of 1022 m shows a slight odd predominance between nC_{15} and nC_{17} (Fig. 1a). There is no evidence of a significant, higher land plant contribution to any of the samples. The abundance of acyclic isoprenoids (as indicated by the pr/nC_{17} ratio; Table 2) and polycyclic alkanes relative to the n-alkanes decreases with depth for the three samples. Such a trend is often attributed to increasing maturity, but this is unlikely in this case because of the narrow depth range of the samples. This trend also correlates with increasing Hydrogen Index values for the organic matter of these samples (Stasiuk et al., 1988), indicating that it could be due to a change in organic matter type; that is, to a more lipid-rich, Type I organic matter. All three samples show low pr/ph values (Table 2) indicating that deposition of the sediments probably occurred under highly anoxic conditions (Didyk et al., 1978).

The two samples from borehole 2-36-68-4W6 show a similar n-alkane distribution to the samples from 9-26-87-7W6 but they are superimposed on a much larger "hump" of unresolved compounds. These samples contain much lower abundances of acyclic isoprenoids and polycyclic alkanes relative to n-alkanes than those from 9-26-87-7W6 (Table 2), probably because of their greater maturity. They also show slightly higher pr/ph values (Table 2) but these are still considerably less than those reported by Brooks et al., (in press) of between 1.1 and 2.0 in Lloydminster heavy oils, where these compounds have not been removed by biodegradation.

Representative m/z 191 and m/z 217 mass fragmentograms are shown in Figures 2 and 3 respectively, and several biomarker parameters are given in Table 2. Hopanes are present in much higher concentrations than steranes in all five of the Nordegg extracts, indicating a major microbial contribution to the organic matter of these sediments (Ourisson et al., 1979).

Maturity dependant parameters such as the ratio of the 20S and 20R $5\alpha(H)$, $14\alpha(H)$, $17\alpha(H)$ steranes or the ratio of the $5\alpha(H)$, $14\beta(H)$, $17\beta(H)$ to the $5\alpha(H)$, $14\alpha(H)$, $17\alpha(H)$ steranes are in agreement with the results of Stasiuk et al. (1988), and indicate that the samples from 2-36-68-4W6 are more mature than those from 9-26-87-7W6.

The principal objective of this report is to compare the biomarker composition of the Nordegg samples to those of the Western Canada Cretaceous oil sands and heavy oils examined by Brooks et al. (in press). In some parameters, such as the relative abundance of $C_{27}:C_{28}:C_{29}$ regular steranes (Table 2), the Nordegg does resemble the Cretaceous samples, there are, however, several significant differences, as follows:

1. In none of the five Nordegg samples were 28, 30 bis-norhopanes detected. These compounds are present in all Lower Cretaceous samples analysed by Brooks et al. (in press).
2. The Nordegg samples contain very low abundances of diasteranes. This is probably a reflection of the low content of acidic clay minerals associated with Nordegg sediments. Acidic clay minerals are known to catalyse

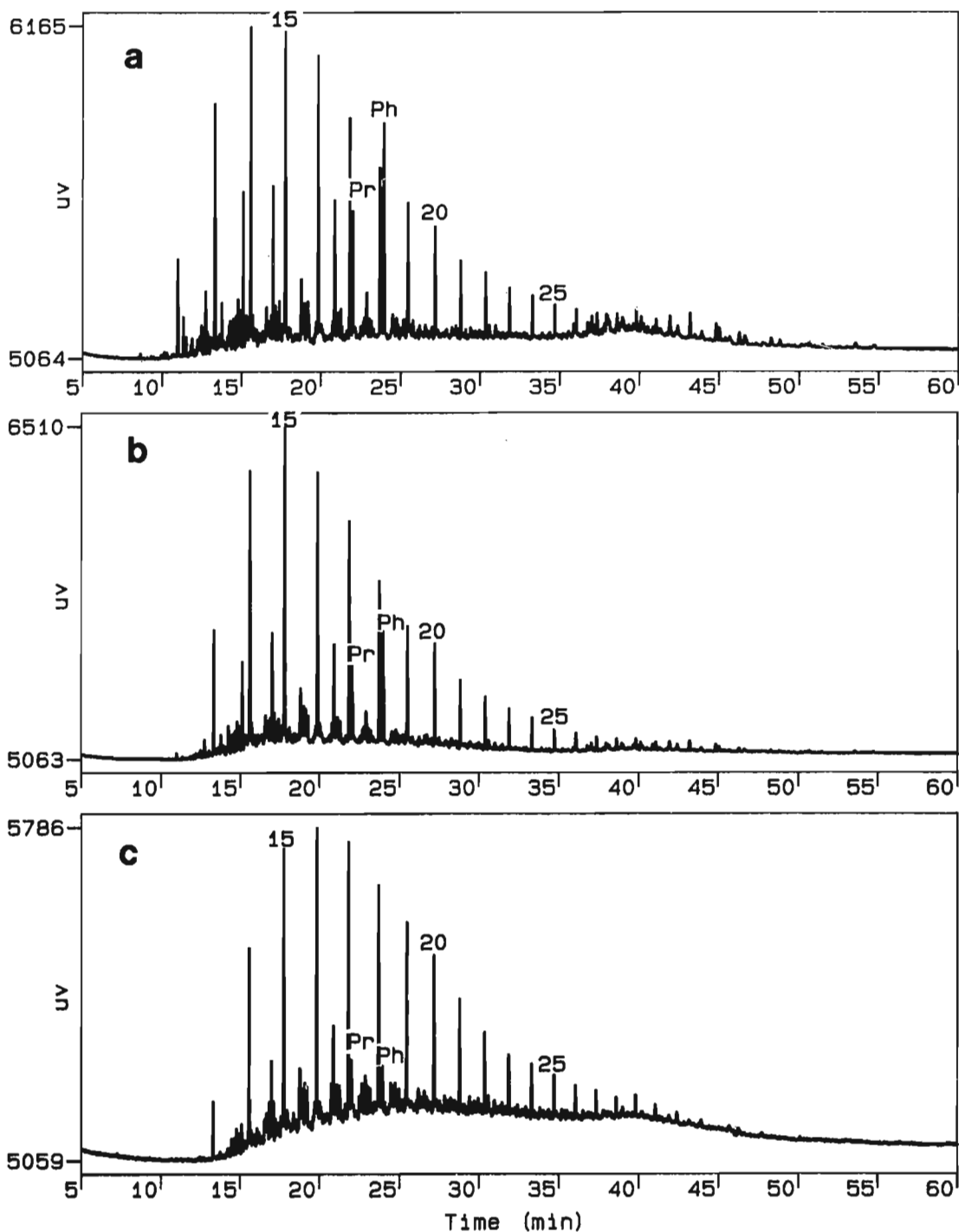


Figure 1. Gas chromatograms of the saturated hydrocarbon fractions of three Nordegg samples; a. 9-26-87-7W6, 1022 m; b. 9-26-87-7W6, 1028.4 m; c. 2-36-68-4W6, 2056.6 m. 15, 20, and 25 are C_{15} , C_{20} and C_{25} n-alkanes; pr is pristane; and ph is phytane.

the rearrangement of steranes to diasteranes. (Sieskind et al., 1979). Diasteranes are present in much higher concentrations in the Cretaceous oil sands and heavy oils, the biomarker distributions of which have not been affected by biodegradation.

3. The ratio of the $18\alpha(\text{H})$ -trisorhopane (Ts) to the $17\alpha(\text{H})$ -trisorhopane (Tm) is believed to be affected by factors similar to those that influence the ratio of diasteranes to regular steranes; that is, lithology and

maturation (Seifert and Moldovan, 1978). The samples from borehole 9-26-87-W6 show very low values for this parameter (Table 2) which, along with the low abundance of diasteranes in these samples, is expected for carbonate samples at this low level of maturity. The Nordegg samples from well 2-36-68-4W6 show much higher Ts/Tm values (Table 2). Since these samples contain no diasteranes, the higher Ts/Tm values are presumably due to their greater maturity compared to

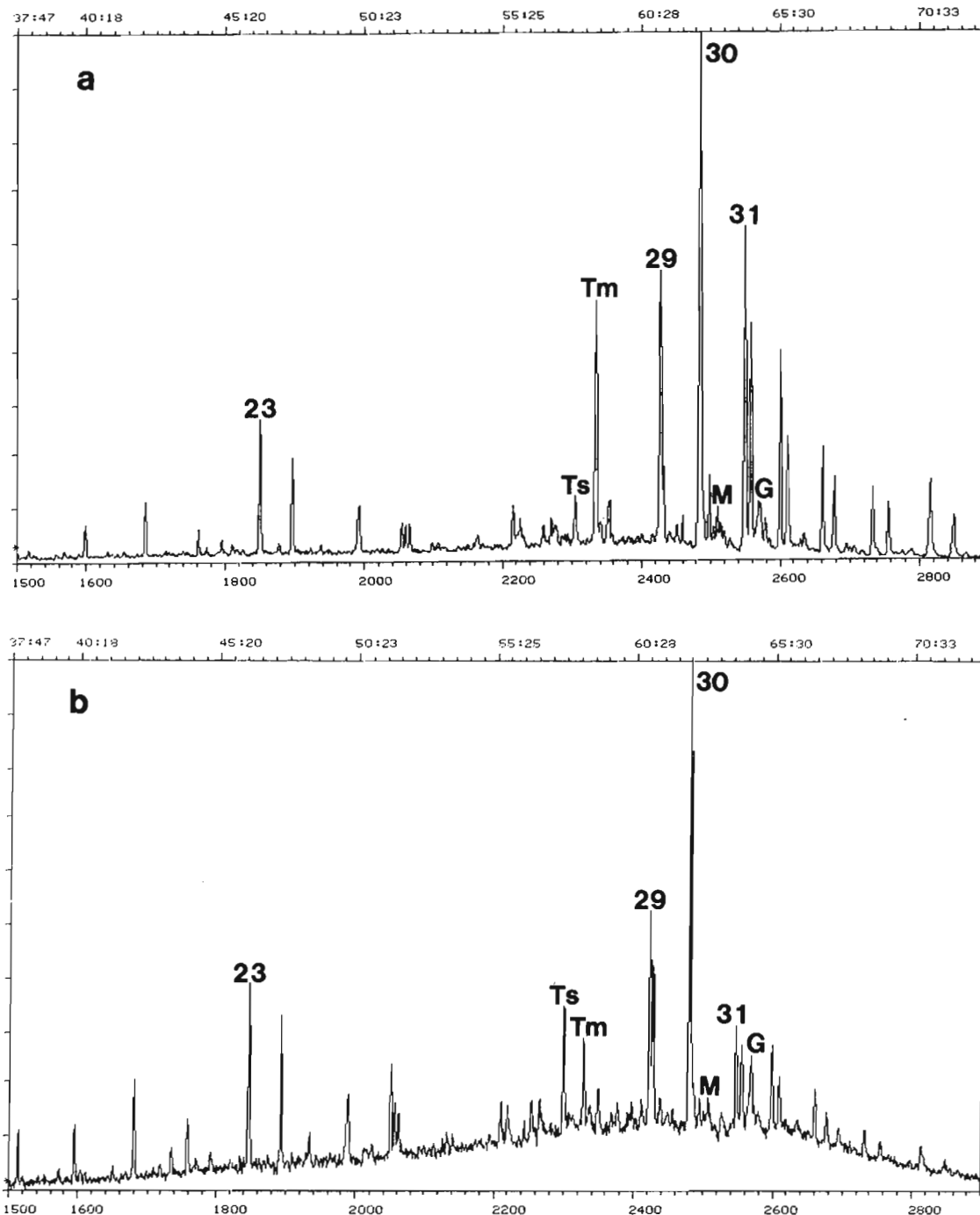


Figure 2. m/z 191 fragmentograms showing the terpene distributions of a. 9-26-87-7W6, 1022 m and b. 2-36-68-4W6, 2060.3 m. 23 is the C_{23} tricyclic terpene; 29-31, the C_{29} - C_{31} $17\alpha(\text{H})$, $21\beta(\text{H})$ - hopanes; Ts is the $18\alpha(\text{H})$ -trisorhopane; Tm is the $17\alpha(\text{H})$ -trisorhopane; M is $17\beta(\text{H})$, $21\alpha(\text{H})$ -hopane; and G is gammacerane.

the samples from 9-26-87-W6, rather than an increase in clay content. The range of Ts/Tm values reported by Brooks et al. (in press) is intermediate between the values for the Nordegg samples in the two boreholes. However, it is possible that Nordegg organic matter, at a level of organic maturation intermediate between the samples examined here, could give Ts/Tm ratios similar to those of the heavy oils and tar sand bitumens.

4. The amount of tricyclic terpanes relative to $17\alpha(\text{H})$ -hopane in the Nordegg samples (see C23/C30 ratio, Table 2) is highest in the more mature samples from borehole 2-36-68-4W6, but even these values (up to 0.48) are lower than those (>0.49) in the Cretaceous heavy oils and tar sand bitumens reported by Brooks et al. (in press).

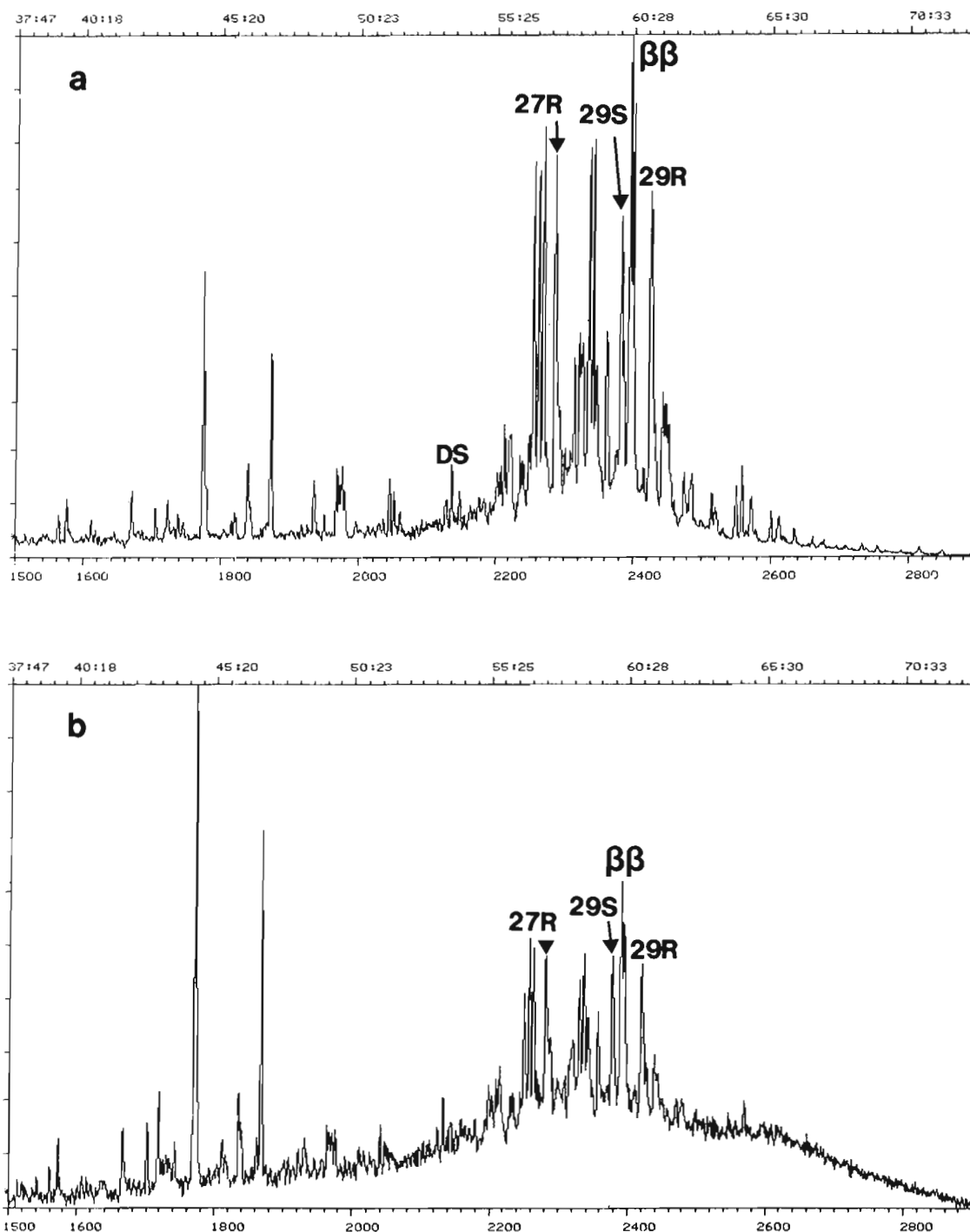


Figure 3. m/z 217 fragmentograms showing the sterane distributions of a. 9-26-87-7W6, 1022 m and b. 2-36-68-4W6, 2060.3m. DS is $13\beta(\text{H})$, $17\alpha(\text{H})20\text{S}$ -diasterane; 27R is $5\alpha(\text{H})$, $14\alpha(\text{H})$, $17\alpha(\text{H})$ 20R - cholestane; 29S is the 24-ethyl - $5\alpha(\text{H})$, $14\alpha(\text{H})$, $17\alpha(\text{H})$ 20S - cholestane; 29R is the 24 - ethyl - $5\alpha(\text{H})$, $14\alpha(\text{H})$, $17\alpha(\text{H})$ 20R - cholestane; and $\beta\beta$ are the 24 - ethyl - $5\alpha(\text{H})$, $14\beta(\text{H})$, $17\beta(\text{H})$ - cholestanes.

Table 2. Biomarker ratios of Nordegg samples

Well	Depth m	pr/nC ₁₇ ¹	pr/ph ²	Steranes						Terpanes			
				C ₂₉ ³	C ₂₉ ⁴	C ₂₉ ⁵	% ⁶	% ⁶	% ⁶	Ts/ Tm ⁷	C ₃₀ ⁸	C ₂₃ / C ₃₀ ⁹	Gm/ C ₃₀ ¹⁰
				α α α S/ α α α R	BB/ α α α R	D/ α α α	α β β	α β β	α β β		α β β α		
9-26-87-7W6	1022	0.73	0.66	0.82	1.40	0.19	32	33	35	0.21	7.65	0.26	0.06
9-26-87-7W6	1027.5	0.50	0.62	0.94	1.23	0.21	32	31	37	0.25	17.1	0.19	0.08
9-26-87-7W6	1028.4	0.39	0.60	0.92	1.41	0.24	34	27	39	0.28	10.3	0.15	0.17
2-36-68-4W6	2056.6	0.18	0.68	1.04	1.41	⁻¹¹	40	24	36	1.33	14.1	0.48	0.13

¹ratio of pristane to n-heptadecane

²ratio of pristane to phytane

³α (H), 14 α (H),, 17 α (H) 20(S)/5 α (H), 14 α (H), 17 α (H), 20(R)-C₂₉ steranes

⁴5 α (H), 14β(H),, 17β(H)/5 α (H), 14 α (H),, 17 α (H) 20(R)-C₂₉ steranes

⁵13β(H), 17 α (H) 20S-diacholestane/5 α (H), 14 α (H), 17 α (H) 20R-cholestane

⁶Normalized proportion of C₂₇:C₂₈:C₂₉ 5 α (H), 14β(H), 17β(H) steranes

⁷18 α (H)-trishnorhopane/17 α (H)- trishnorhopane

⁸17 α (H)-hopane/17β(H) - moretane

⁹C₂₃tricyclic terpene/17 α (H) - hopane

¹⁰Gammacerane/17 α (H) - hopane

¹¹Diasteranes in extremely low abundance

CONCLUSIONS

The distribution of biomarkers in the five Nordegg samples examined indicates that deposition of these sediments occurred in a highly anoxic, marine carbonate environment that allowed extensive microbial reworking of the primary organic matter. This is in agreement with the proposal that the Nordegg was deposited in a zone of oceanic upwelling (Stasiuk et al., 1988).

There are several significant differences between the biomarker distributions of the Nordegg samples and the Cretaceous heavy oil and oil sand bitumens reported by Brooks et al. (in press). These include the ratio of pristane to phytane, and, in the Nordegg samples, the lack of 28,30-bishnorhopanes, the low abundance of diasteranes relative to regular steranes, and tricyclic terpanes to 17 α (H)-hopane. These results indicate that the Nordegg was not a major contributing source, at least in the area where these samples originated, to the heavy oil and oil sand bitumens. However, this study is based only on the study of five samples from two locations and it is possible that the Nordegg may show considerable areal variation in its geochemical characteristics. There is an obvious need for further, more systematic study before the Nordegg can be ruled out as a contributor to the Western Canada oil sands/heavy oils.

ACKNOWLEDGMENTS

We wish to thank S. Achal and M. Northcott for technical assistance.

REFERENCES

- Brooks, P.W., Fowler, M.G., and Macqueen, R.W.
1988: Biomarker geochemistry of Cretaceous oil sands/heavy oils and Paleozoic carbonate trend bitumens, Western Canada Basin; in Preprint Volume IV of the 4th UNITAR/UNDP International Conference on Heavy Crude and Tar Sands, August 7-12, 1988, Edmonton, Alberta, Paper 134, 18 p.
- In press: Biological marker and conventional organic geochemistry of oil sands/heavy oils, Western Canada Basin; Organic Geochemistry.
- Creaney, S. and Allan, J.
1988: Hydrocarbon generation and migration in the Western Canada Sedimentary Basin. Presented at meeting on Classic Petroleum Provinces; Geological Society of London, May 11, 1988.
- Didyk, B.M., Simoneit, B.R.T., Brassell, S.C. and Eglinton, G.
1978: Organic geochemical indicators of paleoenvironmental conditions of sedimentation; Nature, v. 272, p. 216-222.
- Fowler, M.G. and Brooks, P.W.
1987: Organic geochemistry of Western Canada Basin tar sands and heavy oils. 2. Correlation of tar sands using hydrous pyrolysis of asphaltenes; Journal of Energy and Fuels, v. 1. p. 459-467.
- Ourisson, G., Albrecht, P., and Rohmer, M.
1979: Palaeochemistry and biochemistry of a group of natural products: the hopanoids; Pure and Applied Chemistry, v. 51, p. 709-729.
- Seifert, W.K. and Moldovan, J.M.
1978: Applications of steranes, terpanes and monoaromatics to the maturation, migration and source of crude oils; Geochimica et Cosmochimica Acta, v. 42, p. 77-95.
- Sieskind, O., Joly, G., and Albrecht, P.
1979: Simulation of the geochemical transformation of sterols: superacid effect of clay minerals; Geochimica et Cosmochimica Acta, v. 43, p. 1675-1679.
- Stasiuk, L.D., Osadetz, K.G., and Goodarzi, F.
1988: Preliminary source rock evaluation of the Nordegg Member (lower Jurassic), Alberta; in Current Research, Part D, Geological Survey of Canada, Paper 88-1D, p. 51-56.

Regional geology and hydrocarbon occurrences in the Wabamun Group, west-central Alberta

A. Hamid Majid

Institute of Sedimentary and Petroleum Geology, Calgary

Majid, A. H., *Regional geology and hydrocarbon occurrences in the Wabamun Group, west-central Alberta*; in *Current Research, Part D, Geological Survey of Canada, Paper 89-1D*, p. 25-33, 1989.

Abstract

There are two distinct Wabamun play types in the Peace River Arch area. The first, typified by the Normandville and Beaton fields, occurs where a porous limestone of stromatoporoid boundstone and peloidal grainstone facies with primary and secondary porosity serves as the reservoir. Based on examination of cuttings and cores, similar boundstone and grainstone facies are defined in other parts of the Peace River Arch.

The second play type is typified by the Tangent and Eaglesham fields, where dolomite with intercrystalline and fracture porosity serves as the reservoir. Dolomitization occurred as a late-stage burial process and is facies independent; it apparently progressed from the base of the Wabamun upward. Mapping the known major northeastern and northwestern Wabamun fault trends has not served as a predictive tool for dolomitization trends. Several areas are highlighted where thick dolomite occurs.

The preliminary results of this study, which is part of a pilot assessment project on Devonian sour gas currently underway, show a significant potential for oil and gas discoveries in the Wabamun Group.

Résumé

Il y a deux types distincts de zones pétrolifères Wabamun dans la région de l'arche de Peace River. Le premier, caractérisé par les champs de Normandville et de Beaton, se trouve là où un calcaire poreux à faciès de pierre de bornage stromatoporéide et de calcaire à débris jointifs péloïdal avec porosité primaire et secondaire sert de réservoir. Un faciès semblable de pierre de bornage et de calcaire à débris jointifs se retrouve dans d'autres parties de l'arche de Peace River.

Le deuxième type de zone pétrolifère est caractérisé par les champs de Tangent et d'Eaglesham où de la dolomie à porosité intercrystalline et de fracture sert de réservoir. La dolomitisation est le produit d'un enfouissement tardif et est indépendante du faciès; elle semble avoir progressé depuis la base de la zone Wabamun vers le haut. Une fois reportées sur des cartes, les directions principales de la faille de Wabamun vers le nord-est et le nord-ouest n'ont pas permis de prévoir les directions de la dolomitisation. Plusieurs zones sont mises en évidence là où la dolomie est épaisse.

Les résultats préliminaires de l'étude, qui fait partie d'un projet d'évaluation en cours sur les gaz corrosifs du Dévonien, indiquent que le groupe de Wabamun pourrait renfermer d'importantes quantités de pétrole et de gaz.

- | | |
|-----------------|-------------------|
| 1. Tangent | 7. Grande Prairie |
| 2. Normandville | 8. Clair |
| 3. Eaglesham | 9. George |
| 4. Cindy | 10. Oak |
| 5. Peoria | 11. Royce |
| 6. Teepee | 12. Beaton |

Oil ● Gas ☀

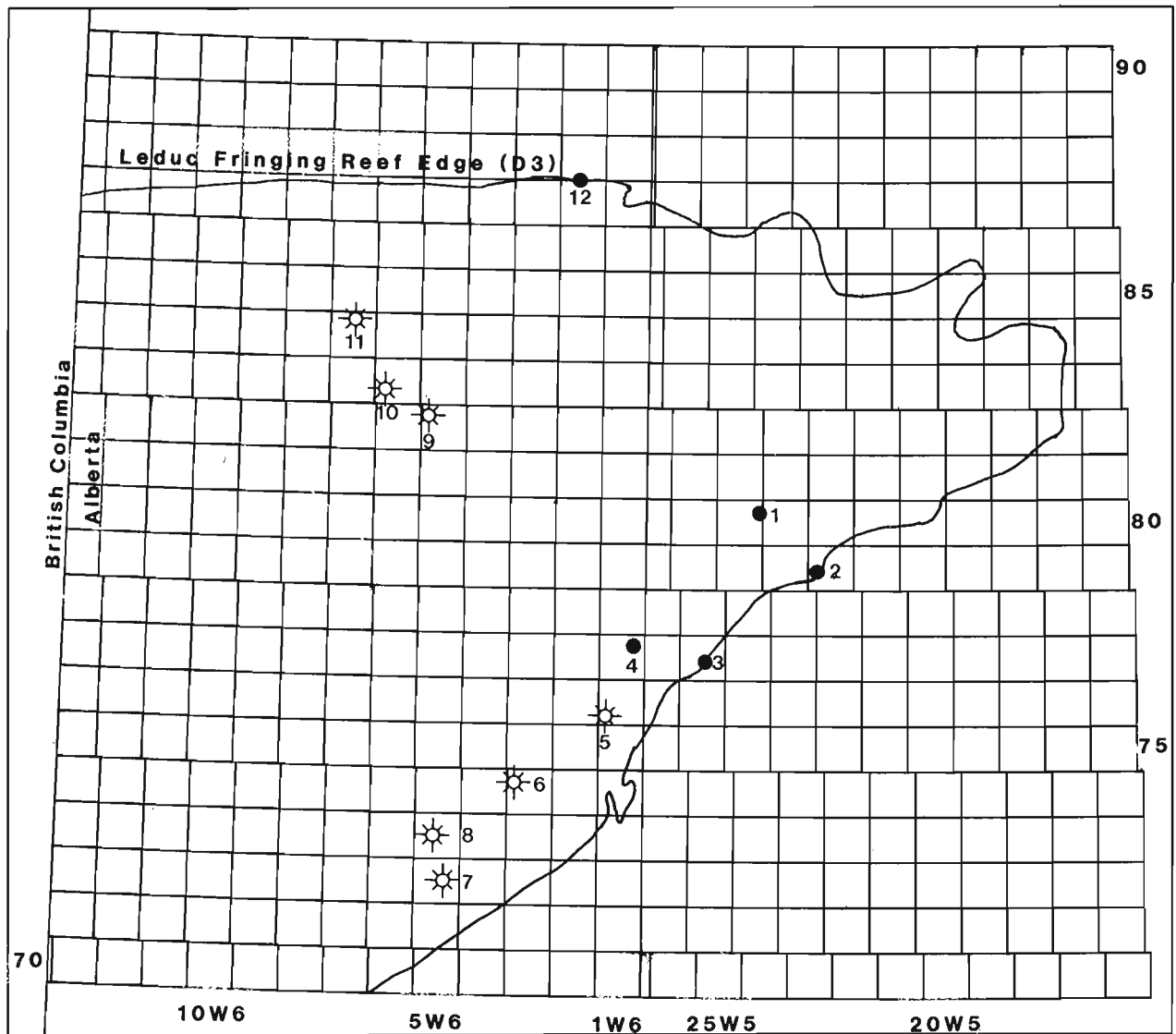
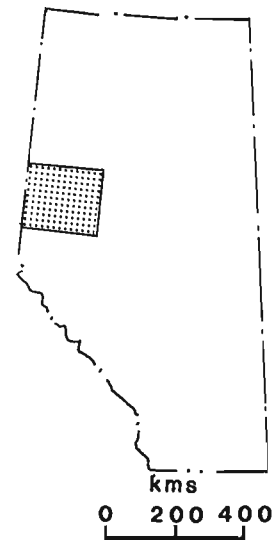


Figure 1. Location map showing the distribution of the established oil and gas fields in the Wabamun Group.

INTRODUCTION

This paper is an initial product of a pilot project currently being conducted by the staff of the Petroleum Resource Appraisal Secretariat at the Institute of Sedimentary and Petroleum Geology on Devonian sour gas resource assessment of the Western Canada Sedimentary Basin. The primary objective of the gas resource analysis is to determine the resource endowment of the region. Resource assessment is not addressed here, because the project is in its preliminary stage. This paper covers the regional subsurface geology and hydrocarbon occurrences in the Wabamun Group in west-central Alberta (Fig. 1).

The project area covers about 46 000 km² and contains twelve hydrocarbon fields in the Wabamun Group reservoir (Fig. 1). These fields are: *oil* — Normandville, Tangent, Eaglesham, Beaton and Cindy; *gas* — Teepee, Royce, Oak, George, Grand Prairie, Clair and Peoria. The reservoirs in these fields are mostly dolomite. However, the Normandville and Beaton production is from limestone of stromatoporoid boundstone and peloidal grainstone facies. Therefore, the primary objective of this paper is to summarize dolomite and limestone distribution and to show to what extent the dolomite distribution is related to the major known fault trends in the area. Other objectives of the paper are to describe the depositional style of the Wabamun Group and its relationship to the known play types, and to identify areas that have some potential for hydrocarbon traps in the Wabamun Group.

STRATIGRAPHY

The age of the Wabamun Group is Famennian (Late Devonian). In the study area, the Wabamun is characterized by a remarkably uniform lithology. It is overlain by dark shales of the Exshaw Formation (Table 1); the boundary between the two formations is marked by a distinctive signature on gamma-ray logs. The contact between the Wabamun Group and the underlying Graminia Formation of the Winterburn Group cannot easily be distinguished on logs. Sample examination is required to select the precise location. The top of the Graminia Formation is placed at the top of a relatively thin unit of quartzose, silty carbonate. The Wabamun Group has been correlated both biostratigraphically and lithologically with the Palliser Formation, which outcrops in the Front Ranges of the Rocky Mountains (Belyea and McLaren, 1956). The Palliser Formation is composed of massive limestones, and was divided by DeWit and McLaren (1950) into a lower Morro Member and an upper Costigan Member. Geldsetzer (1982) subdivided the Palliser Formation into lower and upper units based on the outcrop section in northeast British Columbia.

In the District of Mackenzie and northeastern British Columbia, the Wabamun Group is equivalent to two formations. The lower, known as the Tetcho Formation, is composed of dark grey to dark brown mudstone, locally peloidal and shaly. This unit grades upward into Kotcho Formation, a predominantly dark grey, fissile shale, which locally includes bituminous shale (Belyea, 1962). In southeastern

Table 1. Table of formations (after Podruski, et al., 1987).

EPOCH/AGE		SEQUENCE	NORTHERN ALBERTA	PEACE RIVER	CENTRAL ALBERTA	WILLISTON BASIN
LATE DEVONIAN	FAMENNIAN	PALLISER	KOTCHO	WABAMUN	WABAMUN	BIG VALLEY
			TETCHO		STETTLE	BIG VALLEY
	FRASNIAN	SASK SUBSEO	TROUT RIVER	GRAMINIA SILT	GRAMINIA SILT	TOROUAY
			KAKISKA	NISKU	BLUESHIRE	CROWFOOT
			REDKNIFE		NISKU (unsubdivided)	
			JEAN MARIE		LEDUC	IRETON
FORT SIMPSON	DUVERNAY	DUVERNAY				
MIDDLE DEVONIAN	GIVETIAN	BEAVER HILL SUBSEO	SLAVE POINT	UPPER SLAVE POINT	SWAN HILLS	SOURIS RIVER
			WATERWAYS	WATERWAYS	WATERWAYS	
	EIFELIAN	HUME-DAWSON	FT VERMILION	LOWER SLAVE POINT	SLAVE POINT	FT VERMILION
			WATT MTN	FT VERMILION	WATT MTN	
			BISTCHO	WATT MTN	WATT MTN	First Red Bed
			MUSKEG (Upper Anhydrite)	MUSKEG	MUSKEG/PRAIRIE	PRAIRIE
			Zama	Keg River Sandstone	UPPER WINNIPEGOSIS	UPPER WINNIPEGOSIS
			Lower Anhydrite			
			Black Creek Salt	CHINCHAGA	LOWER WINNIPEGOSIS	LOWER WINNIPEGOSIS
			LOWER KEG RIVER	CHINCHAGA	CONTACT RAPIDS	ASHERN
UPPER CHINCHAGA	CHINCHAGA	COLD LAKE	COLD LAKE			
LOWER CHINCHAGA	ERNESTINA LAKE	ERNESTINA LAKE	ERNESTINA LAKE			
COLD LAKE	BASAL RED BEDS	LOTSBERG	Basal Red Beds			
EARLY DEVONIAN	EMSIAN	DELORME	BASAL RED BEDS	Basal Red Beds		
SIEGENIAN						
GEDINIENIAN						

GSC

Alberta, and particularly in the Stettler area, the Wabamun was divided by Wonfor and Andrichuk (1956) into the Big Valley (fossiliferous limestone with minor interbeds of crystalline dolomite) and Stettler (evaporites with interbeds of very fine grained dolomite) formations. In Saskatchewan, Montana, and Manitoba, the Wabamun Group is correlated with the Three Forks Formation. In the Peace River Arch area of Alberta and British Columbia, the Wabamun Group has been subdivided by Halbertsma and Meijer Drees (1987) into six, mostly shallowing-upward, carbonate sequences based primarily on geophysical logs.

STRUCTURAL SETTING

The Peace River Arch area has been subjected to tectonic activity since post-Cambrian time. The distribution of Granite Wash Formation sediments indicates that crustal uplift forming the Peace River Arch was accompanied by complex block faulting, and was subsequently modified by periods of erosion and rejuvenation of tectonic elements (DeMille, 1958). During Middle and Late Devonian time,

the Peace River Arch slowly subsided, resulting in onlap of Devonian sediments and emplacement of Devonian fringing reefs at favourable locations on the arch. Thick Mississippian and Pennsylvanian(?) sections are preserved in pre-Permian downfaulted blocks that may follow earlier trends (DeMille, 1958).

Rejuvenation of old blocks accompanied by normal faulting initiated the collapse of the Peace River Arch during the late Paleozoic (Lavoie, 1958), and the formation of a depositional trough. Drilling in the Normandville area supports the hypothesis of rejuvenation of old basement fault blocks subsequent to the deposition of the Late Mississippian Upper Debolt Formation (Lavoie, 1958). By the onset of Mississippian time, infilling by late Paleozoic sediments had resulted in a gently rolling topography. Tectonic activity during the Mesozoic was moderate; however, minor reactivations of old faults, probably coincident with the Laramide Orogeny, were sufficient to produce fracturing and warping of overlying sediments (Williams, 1958), as the Peace River Arch again became a positive feature in Late Cretaceous time.

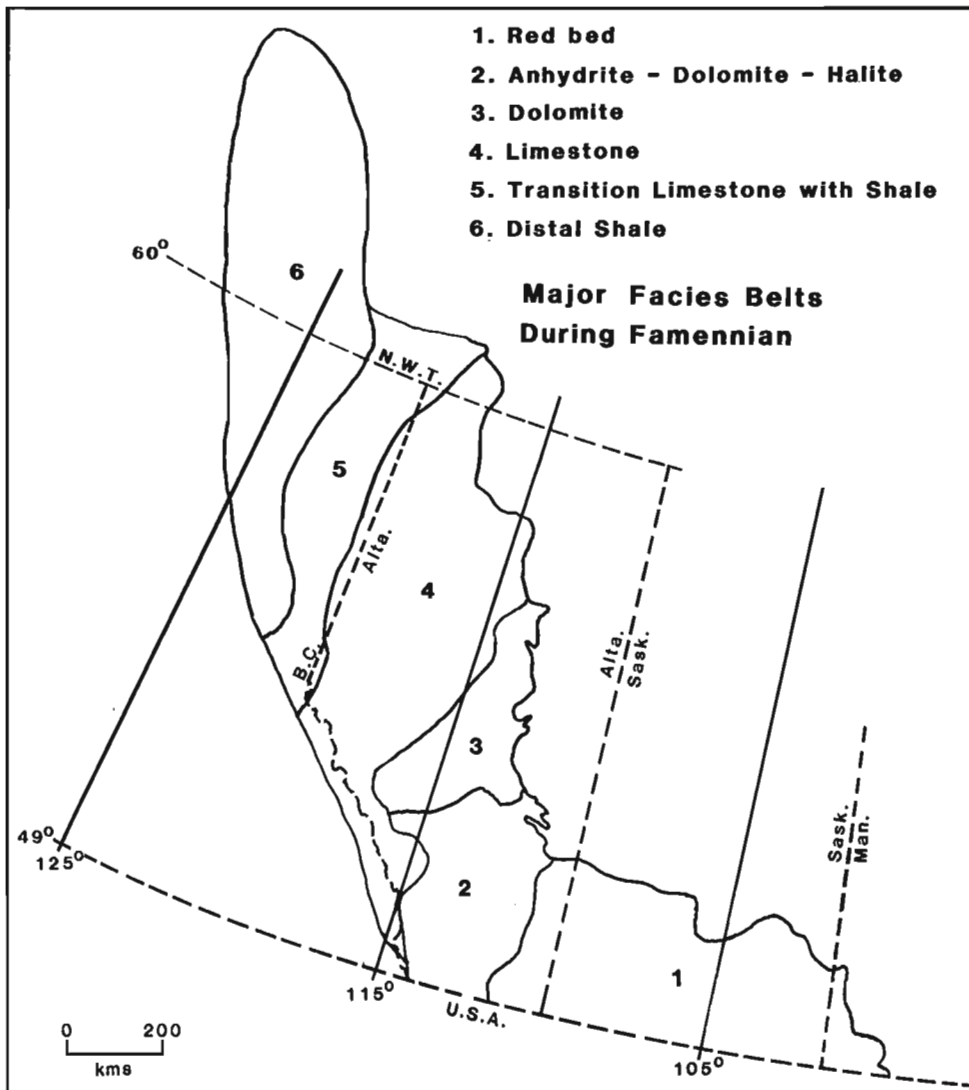


Figure 2. Major facies belts within the Palliser sequence (after Moore, in press).

REGIONAL FACIES CHANGE: DEPOSITIONAL MODEL

The Palliser sequence (Moore, in press) (see Table 1) was deposited at the beginning of the Famennian, which is characterized by a major faunal change. The Famennian was a time of relative quiet in the south (Alberta and Saskatchewan) in spite of the structural activities in the far north (District of Mackenzie) and the influx of the first molasse into the region (Tuttle Formation, Moore, in press). Six depositional facies belts were developed during Famennian time (Moore, in press) (Fig. 2 and Table 1):

1. Red bed facies: Three Forks Group and Lyleton Formation.
2. Mixed clastic - evaporite - carbonate facies: Torquay Formation.
3. Evaporite-carbonate facies: Stettler and Big Valley formations.
4. Carbonate facies: Wabamun and Palliser formations.
5. Carbonate - shale facies: Tetcho and Kotcho formations.
6. Shale facies: Besa River Formation.

The lithological characteristics of the sedimentary rocks and the absence of physical breaks between units (distinct shelf-basin setting) during the Famennian argue for a ramp configuration that extended from Manitoba to the southern part of the District of Mackenzie. The Wabamun Group in the study area is up to 250 m thick and is characterized by a remarkably uniform lithology with high lime mud content, low faunal diversity and a peloidal nature. These characteristics argue for the deposition of the Wabamun Group in an environment of restricted water circulation, resulting in abnormal salinity and depleted nutrients. The modern analog of this Wabamun restricted shelf environment falls between the extremes of the level-bottomed Bahama Bank and compartmentalized Florida Bay environments. It is clear that there is no evidence of large barrier islands or reefal buildups in the study area and its vicinity to act as barriers to water circulation during Famennian time. Therefore, it is postulated that the vast expanses of shallow water would have acted to dampen normal wave or current energy and enhance restriction. The small patch reefs or bioherms in the Normandville area (Nishida et al., 1985) and in the other parts of the study area are local and did not act as barriers. The best depositional model for the Peace River Arch area during the Famennian is the "homoclinal ramp with isolated shallow and downslope buildups" described by Read (1985) (see Fig. 3).

HYDROCARBON PRODUCTION AND DOLOMITIZATION

Hydrocarbons in the Wabamun Group occur in two distinct play types. The first is a porous stromatoporoid boundstone and peloidal grainstone which occurs about 65 to 75 m below the top of the Wabamun. The Normandville and Beaton oil fields are examples of this play type. The porosity of this play is primary intergranular and intragranular

enhanced by leaching and fracturing. The second play type involves dolomite, with intercrystalline and fracture porosity, typified by the Tangent and Eaglesham oil fields. The production in these fields generally is from the top of the Wabamun in either dolomite or dense but fractured limestone assumed to be connected to reservoir dolomite. With the exception of the Normandville and Beaton fields, all the established hydrocarbon fields occur within the dolomitized section. Dolomitization is the most important diagenetic feature controlling the porosity and permeability patterns within the Wabamun Group and thus controlling the exploration concept in the study area.

Several types of dolomite textures and fabrics are recognized from cores and thin sections of cores and cuttings:

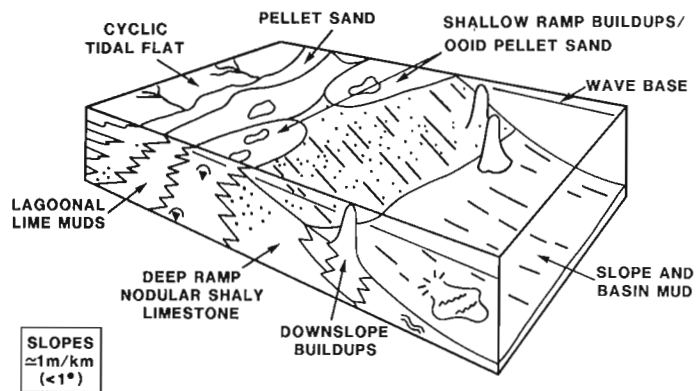
1. Fine grained, matrix-selective dolomite.
2. Coarse grained dolomite localized along stylolites.
3. Medium coarse grained, pore-filling dolomite.
4. Fine to coarse grained dolomite associated with fractures and breccia zones.

The pattern of dolomitization in the Wabamun suggests that the dolomitizing fluid was derived from below and that the dolomitization in the Wabamun is facies independent. The dolomitizing fluid may have been from the underlying Winterburn and Ireton, and perhaps laterally through the Granite Wash Formation. Evidence indicates that most of the dolomitization was of late diagenetic origin. Large dolomite crystals are observed in stylolites and hairline fractures in limestones, indicating a post-compaction stage of growth. In the CDN-SUP Tangent well (9-23-80-24W5) for example, a repetition of the section by reverse faulting in the Wabamun has left dolomite in the footwall and limestone in the hanging wall, suggesting that dolomitization occurred after faulting.

The most intriguing question regarding exploration strategy in the Wabamun play is: what controls the dolomitization? Stoakes (1987) suggested that the dolomitization in the Tangent field was fault-controlled. It is important to know whether this conclusion applies to the other parts of the study area. To shed light on the problem, several computer-generated maps were constructed. These included structural, and first and second order residual maps of the Wabamun and Debolt formations. In addition, a Wabamun lithology map (Fig. 4) has been constructed by utilizing neutron-density porosity logs and Canadian Stratigraphic Services data as well as core and sample descriptions (where the first two sources were not available). By mapping all fault trends using these maps, it was hoped that a dolomitization fairway might be defined, allowing a better understanding of the process of dolomitization as well as providing an exploration prediction tool.

It is clear from the well data that the occurrence of hydrocarbon in the Normandville field is both structurally and stratigraphically controlled; that is, the Normandville fault bisects the field (see also Nishida, 1987). Yet the Wabamun in this field is not dolomitized. It is interesting also to note that the Winterburn Group in the Normandville and Beaton fields is undolomitized.

Figure 3. Depositional model for the Peace River Arch area during Famennian (after Read, 1985).



GSC

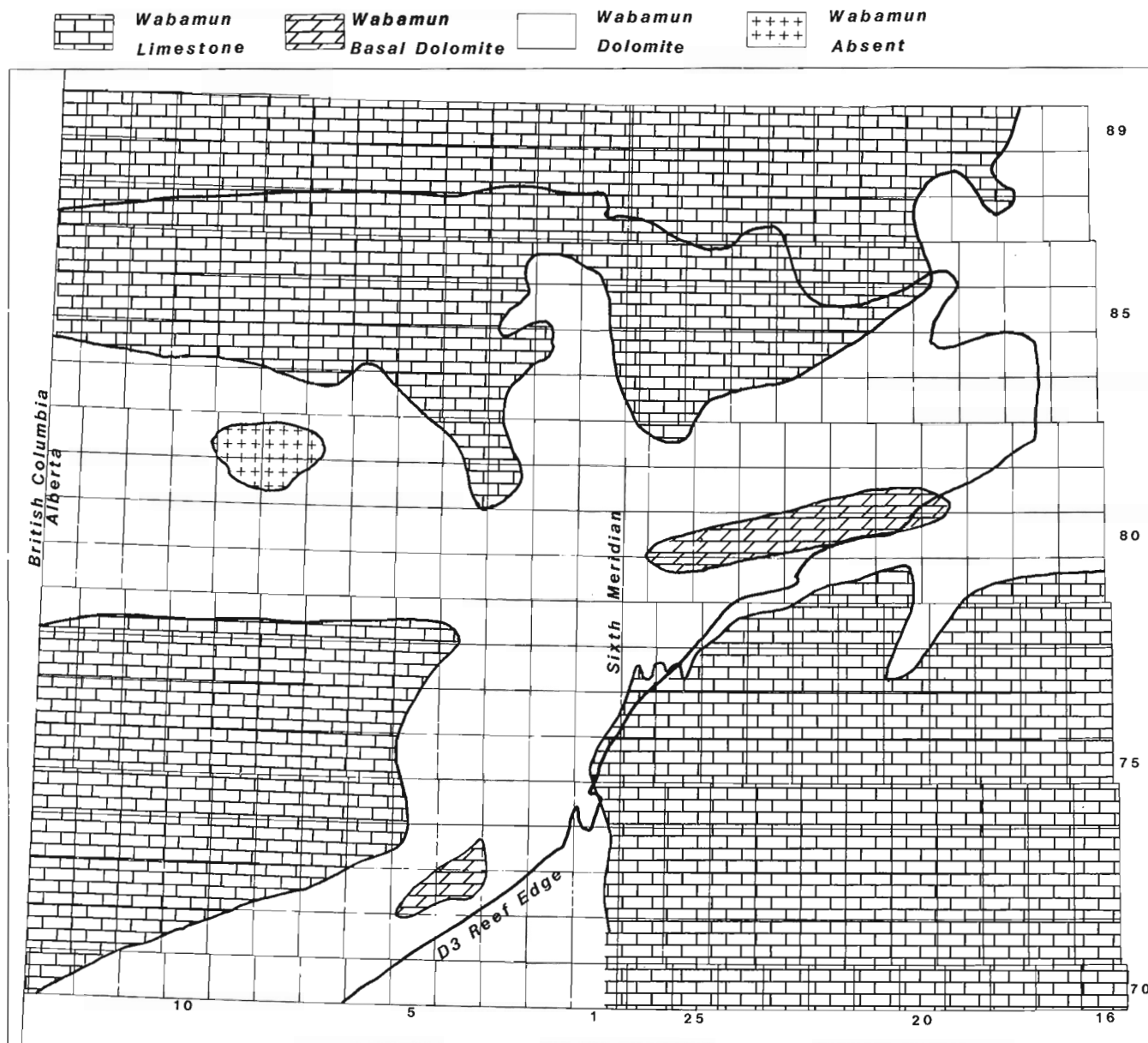


Figure 4. Generalized lithology map of the Wabamun Group.

Structural and residual maps of the Wabamun show that major northeast and northwest striking faults did not serve as mechanisms for dolomite development. Thus, mapping major known faults alone is not a predictive tool for dolomitization. Alternatively, the intersection of major fault trends (Normandville, Dunvegan and Peace River) with minor ones, or intersections of minor faults with the Leduc fringing reef edge may control the development of dolomite and hence the reservoir. The relative significance of open fracture and joint systems in the dolomitization processes should be investigated.

SELECTED OIL AND GAS FIELDS

There are five oil and seven gas fields in the study area (Fig. 1). Of these, three oil and two gas fields are described and some exploration concepts are discussed in the following section.

Normandville oil field

This field produces from the Leduc and Wabamun units. The lithology of the Wabamun in this field is limestone, and the reservoir consists of about 8 to 10 m of stromatoporoid boundstone and peloidal grainstone occurring about 75 m below the top of the Wabamun. The northeast boundary of the field is marked by the Normandville fault, which has a downthrow of as much as 120 m at the top of the Wabamun. A drape of 30 m over the Leduc fringing reef accounts for closure at the Wabamun level. The porosity is generally 6 to 12 per cent, and is of primary type, particularly in the peloidal grainstone, and leached secondary type enhanced by fracture. Pore-filling calcite and/or dolomite account for the reduction of porosity and permeability. The stromatoporoids that make up the patch reef at this field are of primitive *labechia* type (Fig. 5), which survived the Frasnian-Famennian crisis that caused the extinction of the Frasnian and Givetian stromatoporoids (Nishida et al., 1985; Nishida, 1987).

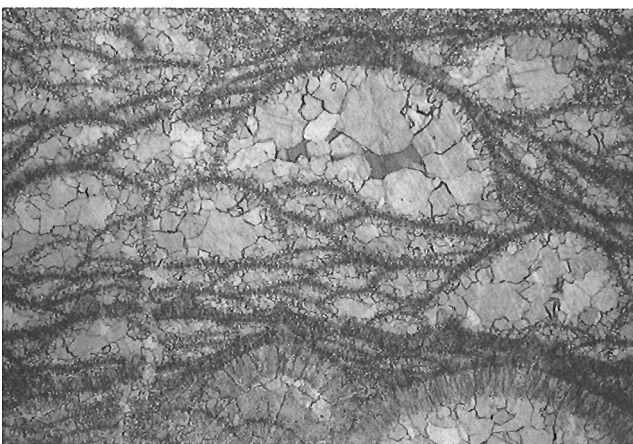


Figure 5. Photomicrograph showing the stromatoporoid (*labechia*) boundstone producing zone at the Normandville field. The width across the photomicrograph is 6 mm.

Because the producing zones in this and the Beaton field are from stromatoporoid boundstone (Fig. 5) and peloidal grainstone (Fig. 6), attempts have been made through examination of cores and cuttings to recognize similar lithologies throughout the study area. Some of the locations where boundstone and grainstone occur are outlined in Figure 8 and should be investigated further for porosity and trap assessment.

Tangent oil field

The best producing well in this field comes from a dolomitized Wabamun reservoir (Fig. 7). The production is from the top of the Wabamun, immediately below the Exshaw, which acts as a seal. The highest oil to water ratios are from wells that are just west of the Normandville fault. Wells in Wabamun limestone are either dry and abandoned or were suspended shortly after completion. However, a few limestone wells produce at low flow rates (6-10 m³/d). Wells drilled in dolomite produce up to 180 m³/d.

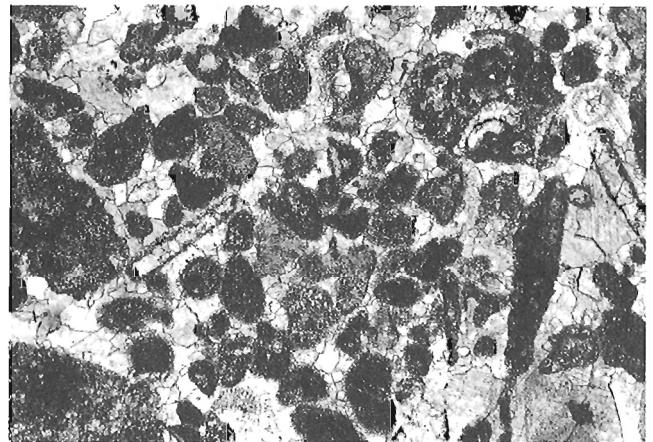


Figure 6. Photomicrograph showing porous peloidal grainstone from Normandville oil field. The width across the photomicrograph is 3 mm.

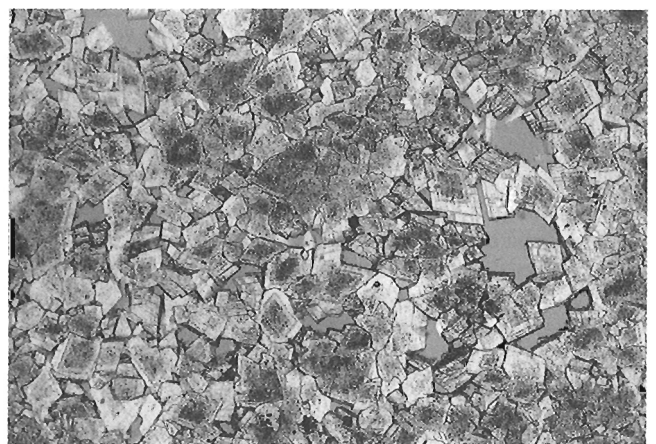


Figure 7. Intercrystalline porosity in the dolomite reservoir of the Tangent oil field. The width across the photomicrograph is 3 mm.

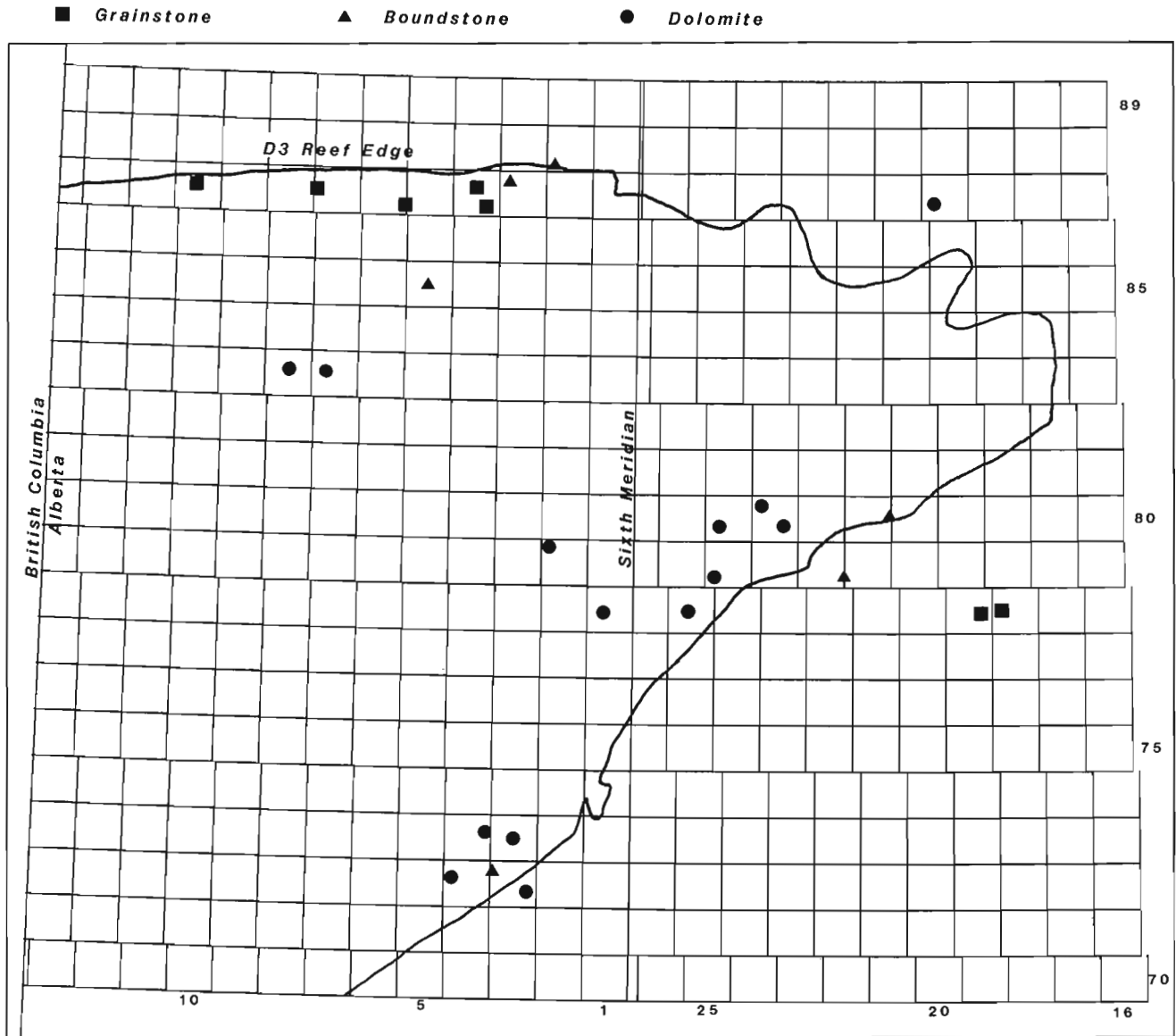


Figure 8. Location of porous grainstone, boundstone and dolomite recognized by lithological descriptions of cuttings and cores.

Dolomitization at Tangent is fault controlled (Stoakes, 1987). The pattern of dolomitization in both the vertical and the lateral dimensions is interesting. Wells only 400 m apart show a change from tight limestone to porous, producing dolomites. The trend of dolomitized wells is in a southwesterly direction away from the Normandville fault. Furthermore, in the case of Wabamun dolomitized wells, the dolomite extends from the top of the Wabamun to the Winterburn, which is also dolomitized. However, many wells in the Tangent vicinity display a dolomitized section at the base of the Wabamun with tight, nonprospective limestone at the top.

Eaglesham oil field

The Wabamun reservoir in this field consists of dolomite exhibiting both fracture and vuggy porosity. In the surrounding dry holes, the Wabamun is limestone. This field

occurs on the Leduc fringing reef edge and within the fairway of basal Wabamun dolomitization. In the Mogul et al. Eaglesham well (5-15-77-25W5), just north of the producing Wabamun wells in this field, an anomalously thick portion of the lower Wabamun is dolomitized. This area, as well as Township 78 Range 25W5, should be considered for further investigation.

Teepee gas field

This field shares some similarities with the Tangent field. It produces from limestone and dolomite units. Dolomite wells occur in close proximity to limestone wells. The gas production in this field comes from a variety of zones throughout the Wabamun, not just from the top of the Wabamun, as is the case in the Tangent. The producing zone in the limestone wells has primary and leached-grain porosity, whereas the dolomite has intercrystalline porosity. Geological controls do not provide evidence of major faulting in the

vicinity of the field and core examination does not show fracture and breccia zones. This may indicate that this dolomitization was not fault-controlled but stratigraphically controlled, with the dolomitizing fluid probably coming from below.

Royce gas field

This field produces from dolomite units that have fracture and intercrystalline porosity. The pattern of dolomitization in this field is spatially related to the zero edge of the Wabamun, where it passes into the Granite Wash Formation. It is postulated that the dolomitizing fluid was expelled during compaction of the Granite Wash sediments along preferred intervals in the Wabamun Group. Cores from this field show extensive fracturing.

CONCLUSIONS AND EXPLORATION IMPLICATIONS

The Wabamun Group over the Peace River Arch area exhibits a uniform, original lithology of muddy, crinoidal sediments with local boundstone-grainstone and dolomite. The lithological characteristics and stratigraphic position of the Wabamun argue for deposition in a restricted shelf environment. Since there is no evidence of a large barrier island or reefal buildups during the Famennian in the Peace River Arch area, it is postulated that the vast expanse of shallow water dampened normal wave or current energy and resulted in restricted flow. The Wabamun Group passes gradually into basinal facies of the Besa River Formation in northeastern British Columbia and District of Mackenzie. The basin represents a homoclinal ramp with isolated shallow ramp and downslope buildups (Read, 1985).

Porosity and permeability are enhanced by dolomitization and fracturing. Dolomitization is the most common reason for hydrocarbon accumulation in all but two established fields in the Wabamun Group. The association of known faults with hydrocarbon accumulation is not always clear-cut, particularly in areas along the major northeastern and northwestern fault trends. It is perhaps the intersection of the major fault trends with the Leduc fringing reef edge and/or with minor fault trends that is the controlling factor for dolomite development.

Based on core, sample, and log examinations, several potential areas are highlighted where stromatoporoid boundstone and peloidal grainstones occur (Fig. 8). In addition, several other areas are highlighted where anomalously thick dolomite sections occur or are expected to be developed (Fig. 8). The author believes that these areas have some merit for further investigation. Inevitably, it will only take one successful well to open up this area to active exploration.

ACKNOWLEDGMENTS

The initial drafts of this manuscript were reviewed by G.R. Davies, J.A. Podruski, N.J. McMillan and P.F. Moore and their comments helped to improve the final text. The writer

thanks the following for stimulating discussions: N.C. Meijer Drees, H.L. Halbertsma, F. Chappell, E.W. Mountjoy, and H.H.J. Geldsetzer. G. Fullmer carried out the compiling of the computer-generated maps and drafted the figures.

REFERENCES

- Belyea, H.R.**
1962: Upper Devonian formations, southern part of Northwest Territories, northeastern British Columbia and northwestern Alberta, Canada; Geological Survey of Canada, Paper 61-69.
- Belyea, H.R. and McLaren, D.J.**
1956: Devonian sediments of Bow Valley and adjacent areas; Alberta Society of Petroleum Geologists; Sixth Annual Field Conference Guidebook, p. 66-91.
- DeMille, G.**
1958: Pre-Mississippian history of the Peace River Arch; Journal of the Alberta Society of Petroleum Geologists, v. 6 p. 61-68.
- DeWitt, R. and McLaren, D.J.**
1950: Devonian sections in the Rocky Mountains between Crowsnest Pass and Jasper, Alberta; Geological Survey of Canada, Paper 50-23.
- Geldsetzer, H.H.J.**
1982: Depositional history of the Devonian succession in the Rocky Mountains southwest of the Peace River Arch; in Current Research, Part C, Geological Survey of Canada, Paper 82-1C, p. 54-64.
- Halbertsma, H.L. and Meijer-Dress, N.C.**
1987: Wabamun limestone sequences in northcentral Alberta; in Devonian lithofacies and reservoir styles in Alberta, F.F. Krause and O.G. Burrowes (eds.); Canadian Society of Petroleum Geologists, 13th Core Conference and Display, p. 21-37.
- Lavoie, D.H.**
1958: The Peace River Arch during Mississippian and Permian-Pennsylvanian time; Journal of the Alberta Society of Petroleum Geologists, v. 6, p. 69-74.
- Moore, P.F.**
— Devonian; in Sedimentary Cover of the North American Craton, D.F. Stott and J.D. Aitken (eds.); Geological Survey of Canada, Geology of Canada, no 6 (also Geological Society of America, The Geology of North America, v. D-1). (in press).
- Nishida, D.K.**
1987: Famennian stromatoporoid patch reef in the Wabamun Group, west-central Alberta, Canada; in Devonian lithofacies and reservoir styles in Alberta, F.F. Krause and D.G. Burrowes (eds.); Canadian Society of Petroleum Geologists, 13th Core Conference and Display, p. 63-72.
- Nishida, D.K., Murray, J.W., and Stearn, C.W.**
1985: Stromatoporoid hydrocarbon traps in Upper Devonian (Famennian) Wabamun Group, north-central Alberta, Canada; American Association of Petroleum Geologists, Bulletin, Convention Issue, v. 69, p. 293.
- Podruski, J.A., Barclay, J.E., Hamblin, A.P., Lee, P.J., Osadetz, K.G., Procter, R.M. and Taylor, G.C.**
1988: Conventional oil resources of western Canada (light and medium); Geological Survey of Canada, Paper 87-26.
- Read, J.F.**
1985: Carbonate platform facies models; American Association of Petroleum Geologists, Bulletin, v. 69, p. 1-21.
- Stoakes, F.A.**
1987: Fault-controlled dolomitization of the Wabamun Group, Tangent field, Peace River Arch Alberta; in Devonian lithofacies and reservoir styles in Alberta, F.F. Krause and O.G. Burrowes (eds.); Canadian Society of Petroleum Geologists, 13th Core Conference and Display, p. 73-85.
- Williams, G.K.**
1958: Influence of the Peace River Arch on Mesozoic strata; Journal of the Alberta Society of Petroleum Geologists, v. 6, p. 74-81.
- Wonfor, J.S. and Andrichuk, J.M.**
1956: The Wabamun Group in the Stettler area, Alberta; Alberta Society of Petroleum Geologists, Journal, v. 4, no. 5, p. 99-111.

Association of enhanced hydrocarbon generation and crustal structure in the Canadian Williston Basin

Kirk G. Osadetz, Lloyd R. Snowdon, and Laverne D. Stasiuk¹
Institute of Sedimentary and Petroleum Geology, Calgary

Osadetz, K.G., Snowdon, L.R., and Stasiuk, L.D., Association of enhanced hydrocarbon generation and crustal structure in the Canadian Williston Basin; in *Current Research, Part D, Geological Survey of Canada, Paper 89-1D*, p. 35-47, 1989.

Abstract

The fundamental control on the hydrocarbon resource potential of pre-Upper Devonian hydrocarbon plays in the Canadian Williston Basin is a long-lived crustal structure, the hinge of which lies along the 103rd meridian of longitude, and the present structural expression of which is the Nesson Anticline. The ancestral structural feature was much larger and broader, and differential subsidence through the early Paleozoic served to either localize or exclude the deposition of potential petroleum source rocks from its hinge. The structure is coincident with a distinctive physical domain in the basement crust that is characterized by electrical conductivity anomalies and elevated heat flows. The elevated heat flows have enhanced the generation of hydrocarbons in strata that were not sufficiently buried to generate hydrocarbons on a regional scale in a normal geothermal environment. For the Upper Ordovician oil-source system, the activity of the arch served to exclude rich source rocks from the locus of elevated thermal maturities. The result is a tremendous potential hydrocarbon resource that is largely immature.

Résumé

L'élément fondamental de contrôle des ressources potentielles en hydrocarbures des zones pétrolières antérieures au Dévonien supérieur dans le bassin canadien de Williston est une structure crustale ancienne dont la charnière repose sur le 103^e méridien et dont l'expression structurale est l'anticlinal de Nesson. Cette structure ancienne était beaucoup plus longue et large, et la subsidence différentielle pendant la Paléozoïque inférieur a permis de localiser ou d'exclure le dépôt de roches mères potentielles provenant de la charnière. La structure coïncide avec un domaine physique distinct dans la croûte du socle, qui est caractérisée par des anomalies de conductivité électrique et des flux thermiques élevés. Ces derniers ont favorisé la production d'hydrocarbures dans des couches qui n'étaient pas assez enfouies pour produire des hydrocarbures à l'échelle régionale dans un environnement géothermique normal. Dans le système des roches mères de l'Ordovicien supérieur, l'activité de l'arche a contribué à exclure des roches mères riches du lieu de maturité thermique élevée. Il en est résulté une énorme quantité de ressources potentielles en hydrocarbures qui sont en grande partie prématurées.

¹ Energy Research Unit and Department of Geology, University of Regina, Regina, Saskatchewan SAS 0A2.

INTRODUCTION

Setting

There is a marked contrast between the habitat of oils in the American and Canadian portions of the Williston Basin. In the Canadian part of the basin, oil is primarily produced from Carboniferous strata, whereas in the American portion of the basin, much of the reserve occurs in older Paleozoic horizons, particularly the Ordovician and Silurian. Brooks et al. (1987) and Williams (1974) determined that these two petroleum provinces were generally characterized by oils of distinctive compositions, as a result of their derivation from differing source rocks. The family of oils occurring primarily in Ordovician reservoirs was originally attributed to potential source rocks in the Winnipeg Formation (Williams, 1974). Thomas (1968) suggested that sources of these oils lay in the microdolomite beds of the Herald Formation. Kendall (1976) and later Kohm and Loudon (1978, 1982) suggested that rich "kukersitic" beds within the Yeoman Formation were the source rocks, exclusively on the basis of organic richness. Recent work (Osadetz et al., work in progress) has determined that suitable source rocks of similar composition occur at several stratigraphic levels within the Winnipeg Formation and the Bighorn Group. In the Canadian part of the basin, the thickest accumulations occur within the upper part of the Yeoman Formation.

Current investigations have attributed a tremendous petroleum potential, in excess of 5 Billion bbls. of oil equivalent, to Ordovician source rocks in the Canadian portion of the Williston Basin. Unfortunately, most of the source is thermally immature and only a small fraction of the total petroleum potential is inferred to have migrated out of these sources, a total of 193,000,000 bbls of oil.

Elevated thermal maturities occur in geographically restricted areas where the source rocks are presently at depths greater than 2950 m. The geographic extent of thermally mature source rocks occurs approximately along the 103rd meridian of longitude within the first three townships north of the international border. This region is coincident with elevated levels of thermal maturity in the Bakken Formation (Price et al., 1984) and Winnipegosis Formation potential source rocks; a region of higher reflectance and coal quality in the Tertiary Ravenscrag Formation (Cameron, in press); present geothermal gradient anomalies in the Paleozoic succession (Majorowicz et al., 1986), and structure in the crust as indicated by the Nesson Anticline (Carlson and Anderson, 1965) and recent magnetotelluric studies (Majorowicz et al., 1988).

This paper describes the importance of elevated crustal heat flows in controlling hydrocarbon generation in the Canadian Williston Basin. An understanding of the controls on hydrocarbon generation provides practical information regarding the controls and risks on exploration plays. In particular, this analysis indicates that prospects in the current Ordovician play, characterized by short migration pathways through the mudstone dominated shelf, should also have demonstrable physical connection to faults and fractures that are the conduit of hot fluids responsible for elevated thermal maturities.

More attractive are combined stratigraphic-structural plays with longer migration pathways and larger drainage areas.

Technique

There are numerous methods by which potential petroleum source rocks can be recognized (Tissot and Welte, 1978, Part V, Chapter 1). Some techniques, petrography for example, are qualitative while other techniques, primarily chemical, are quantitative. The quantitative techniques attempt to determine a relationship between the organic material in the rock and its ability to yield hydrocarbons.

The Rock-Eval anhydrous pyrolysis-organic carbon analysis technique allows the evaluation of shows of oil, oil and gas generation potential, and thermal maturity, and as well provides an indication of the organic matter type in potential petroleum source rocks (Espitalie et al., 1985; Tissot and Welte, 1978, p. 443-447). Rock-Eval analysis results in five parameters: S1, S2, S3, TOC and Tmax. The S1 parameter measures the free or adsorbed hydrocarbons that are volatilized at moderate temperatures (<300°C) during the experiment. The S2 parameter measures the quantity of hydrocarbons and hydrocarbon-like compounds liberated from kerogen in the rock sample during step-wise progressive heating (300-600°C at 25°C/min) after the adsorbed hydrocarbons have been driven off. The S3 parameter measures the organic CO₂ generated from the kerogen. All of these parameters are measured in milligrams of product per gram of rock sample, which is equivalent to kilograms of product per tonne of sample. The Total Organic Carbon (TOC), is measured in weight per cent. Tmax is the temperature corresponding to the maximum rate of hydrocarbon generation, the top of the S2 peak, during the thermal cracking phase of the the experiment.

Source rock potential is defined as being a function of the amount of TOC, as a function of lithology and the S2 parameter value (Table 1). It is common practice to rate carbonate rocks with lower TOC as comparable to clastic rocks with higher TOC, because leaner carbonate rocks give comparable amounts of hydrocarbons in solvent extracts (Tissot and Welte, 1978, p. 430; Gehman, 1962). The results of Rock-Eval experiments have been correlated with other measures of source rock potential (Espitalie et al., 1985; Tissot and Welte, 1978).

Source rock studies in the Canadian portion of Williston Basin identified several intervals with potential (Osadetz and Snowdon, 1986a, 1986b; Osadetz et al., work in progress). However, thin (though important) horizons may be missed either due to too coarse a sampling interval or because they are poorly represented in cuttings collections. Under such circumstances it is necessary to obtain samples from cores to adequately describe these lithologies. Such sampling allows regional variations of source rock richness and maturity to be mapped. While potential source rocks in the Winnipeg Formation are identifiable from well cuttings, the kukersites in the Bighorn Group could only be identified from core samples. Only samples from cores are reported (Table 2).

Table 1. Criteria for Rating Potential Source Rocks

Total Organic Carbon (TOC) value (weight per cent)		
Rating	%TOC in shales	%TOC in carbonates
Poor	0.00-0.50	0.00-0.12
Fair	0.50-1.00	0.12-0.25
Good	1.00-2.00	0.25-0.50
Very good	2.00-4.00	0.50-1.00
Excellent	>4.00	>1.00

S2 value (mg of hydrocarbons/g of rock)	
Rating	S2 value
Poor	Less than 2.00
Fair	2.00-5.00
Good	Greater than 5.00

Source rocks may be further characterized by both chemical and petrographic techniques. Petrographic source rock characterization is essential to an understanding of the biological composition and environment of deposition of the source rock. Solvent extractions from sources provide compositional information that can be compared to the composition of oils. Hydrocarbons extracted from source rocks have compositions that are controlled by the biochemistry of contributing organisms, the depositional environment, diagenetic reactions accompanying the polymerization of the kerogen, and the source rock thermal maturity (Brooks et al., 1987).

Stratigraphic setting

The Winnipeg Formation (Fig. 1) is a thin, dominantly clastic, largely marine formation of Middle Ordovician age (Lefever et al., 1987; Anderson, 1982; Paterson, 1971; Vigrass, 1971; Fuller, 1961; Carlson, 1958). It is up to 135 m thick and progressively onlaps Precambrian basement and Upper Cambrian to Lower Ordovician Deadwood Formation from the east and south. It is bounded on the west by an onlap limit and on the north and east by erosional edges of pre-Middle Devonian and Recent age, respectively. Throughout North Dakota, where the Winnipeg has group status, it is characterized by a lithological succession of: the sandstone dominated Black Island Formation, a medial shale (the Icebox Formation), and an upper carbonate unit (the Roughlock Formation) (Lefever et al., 1987; Carlson, 1960, 1958). In southeastern Saskatchewan and southern Manitoba, the Winnipeg Formation is composed of a lower, sandstone dominated Black Island Member and an overlying, shale dominated Icebox Member (Paterson, 1971; Vigrass, 1971). Along its western and northern margins, the complete succession is sandstone dominated.

The Bighorn Group, a succession of Upper Ordovician to lowermost Silurian limestone, dolostone and evaporite, is approximately 230 m thick in southeastern Saskatchewan and conformably overlies the Winnipeg Formation. It consists of four, lithologically distinctive formations (Fig 1). The lowest formation, Yeoman, is predominantly burrow-mottled or plane laminated lime- and dolomudstone and wackestone (Kendall, 1976). Lesser amounts of other lithologies are also present, particularly, thin beds and laminae of kukersite, a finely laminated bituminous lime mudstone that is locally called kerogenite (Kendall, 1976; Kohm and Loudon, 1978, 1982). The overlying Herald Formation comprises three formal members: Lake Alma, Coronach and Redvers; they are composed predominantly of dolostones and evaporites, and are distinguishable by anhydritic beds at the tops of the lower two members (Kendall, 1976). The Stony Mountain Formation is divisible into a lower bioclastic limestone, the Harthaven Member, a medial, argillaceous, bioclastic floatstone and mudstone of limestone and dolostone, the Gunn Member, and the upper, Gunton Member, composed of dolostones and commonly capped by a laminated dolomudstone and anhydrite. The overlying Stonewall Formation, comprising dolostone and lesser evaporites, straddles the Ordovician-Silurian boundary.

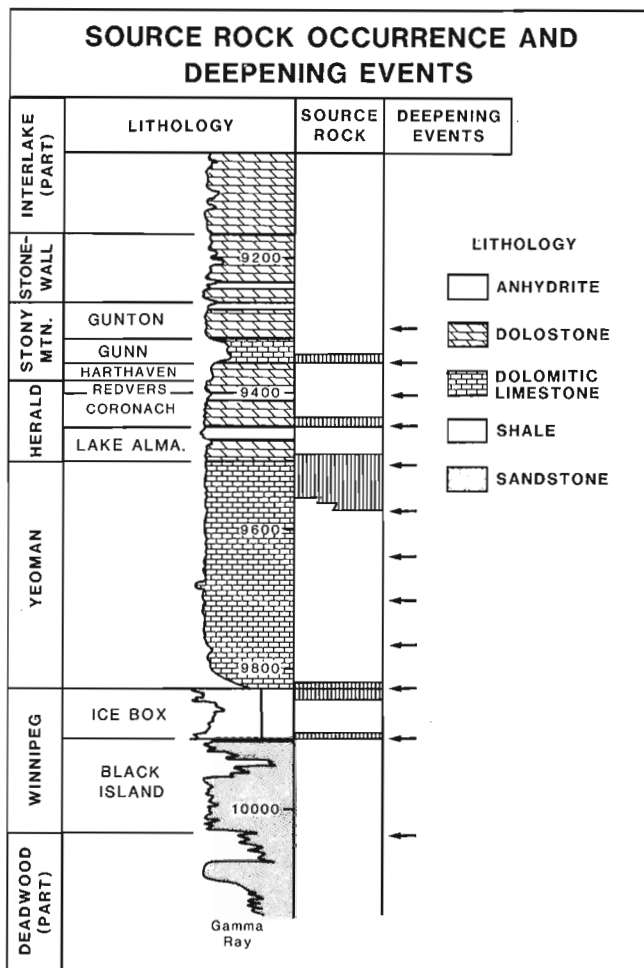


Figure 1. Lithological succession of Ordovician rocks in Canadian Williston Basin indicating the stratigraphic position of potential source rock intervals identified in this study.

Table 2. Results of Rock-Eval experiments for potential Ordovician source rocks

<u>Yeoman Formation</u>								
Location	Depth (M)	Tmax (°C)	S1 (mg/g)	S2 (mg/g)	S3 (mg/g)	TOC (%)	HI	OI
08-16-002-14W2	3053	453	0.15	4.92	0.30	0.84	585	35
03-20-002-16W2	3076	456	0.44	121.60	0.64	13.95	871	4
03-20-002-16W2	3071	455	0.28	72.42	0.61	8.54	848	7
06-13-002-19W2	3021	455	0.96	57.92	0.40	6.83	848	5
06-13-002-19W2	3020	455	0.92	88.67	0.76	10.55	840	7
07-23-003-17W2	2990	455	1.05	106.23	0.40	14.21	747	2
07-23-003-17W2	2992	455	1.83	103.90	0.47	12.79	812	3
07-23-003-17W2	2990	456	1.57	128.26	2.56	15.64	820	16
03-26-004-20W2	2830	453	0.68	90.99	0.49	9.91	918	4
06-11-004-21W2	2830	451	0.56	61.44	0.48	6.61	929	7
06-11-004-21W2	2829	449	0.70	18.03	0.39	2.04	883	19
08-02-006-16W2	2696	450	0.60	86.38	0.53	9.16	943	5
08-02-006-16W2	2689	449	0.88	27.52	0.40	3.16	870	12
08-02-006-16W2	2686	454	0.16	18.63	0.32	2.24	831	14
12-13-007-19W2	2993	442	0.62	5.58	0.58	1.89	295	30
16-20-008-10W2	2445	453	2.37	147.98	0.59	16.69	886	3
16-20-008-10W2	2446	451	1.12	113.73	0.52	12.94	878	4
16-20-008-10W2	2446	453	1.07	146.03	2.53	15.28	955	16
16-20-008-10W2	2446	455	3.21	158.69	3.37	17.07	929	19
16-20-008-10W2	2455	450	0.36	5.46	0.40	1.04	525	38
16-20-008-10W2	2447	449	0.35	5.09	0.43	0.82	620	52
06-32-008-16W2	2459	453	3.70	202.70	1.23	22.29	909	5
06-32-008-16W2	2466	453	0.22	4.22	0.34	0.55	767	61
03-14-008-20W2	2577	446	2.72	116.03	0.14	12.12	957	1
03-14-008-20W2	2577	447	2.30	93.60	1.20	10.09	927	11
03-14-008-20W2	2576	446	0.85	52.00	1.10	6.33	821	17
03-14-008-20W2	2598	441	0.05	1.15	0.05	0.29	396	17
06-05-008-22W2	2532	450	0.20	14.81	0.40	1.72	861	23
14-11-014-16W2	2136	449	0.87	33.33	0.63	3.82	872	16
14-11-014-16W2	2126	440	0.60	6.92	0.57	1.58	437	36
02-04-022-15W2	1733	448	3.42	203.98	1.07	22.05	925	4
02-04-022-15W2	1732	452	3.48	339.10	3.03	34.94	970	8
02-04-022-15W2	1732	450	2.86	291.05	2.91	30.47	955	9
02-04-022-15W2	1732	452	3.38	268.25	3.38	28.49	941	11
02-04-022-15W2	1733	451	2.13	243.10	3.10	23.98	1013	12
01-25-023-16W2	1599	448	1.03	113.01	0.83	12.21	925	6
01-25-023-16W2	1603	447	0.52	57.09	0.64	6.52	875	9
04-10-033-01W3	1466	427	0.44	57.91	4.27	7.90	733	54
03-14-008-20W2	2576	432	0.93	47.68	0.83	5.33	894	15
11-27-001-17W2	3066	452	2.19	2.60	0.48	1.06	245	45
11-14-002-09W2	2980	458	0.51	0.79	0.47	0.43	183	109
12-13-002-19W2	3016	441	1.49	0.80	0.61	0.48	166	127
<u>Winnipeg Formation, Icebox Member</u>								
Location	Depth (M)	Tmax (°C)	S1 (mg/g)	S2 (mg/g)	S3 (mg/g)	TOC (%)	HI	OI
01-04-020-32W1	1391	435	1.08	96.19	1.76	10.41	924	16
01-04-020-32W1	1375	442	0.00	4.28	0.15	0.53	807	28
05-15-010-02W2	2286	439	0.29	6.39	0.15	1.25	511	12
05-15-010-02W2	2285	438	0.24	2.10	0.08	0.57	368	14
05-15-010-02W2	2282	440	0.17	4.72	0.33	1.07	441	30
05-15-010-02W2	2282	438	0.33	4.91	1.16	1.03	476	112
05-15-010-02W2	2282	435	0.10	4.79	0.35	1.02	469	34
05-15-010-02W2	2285	431	0.00	1.15	0.35	0.27	425	129
03-14-008-20W2	2595	446	0.04	1.59	0.04	0.38	418	10
03-14-008-20W2	2593	445	0.04	1.01	0.19	0.21	480	90

Table 2 (cont.)

<u>Stoney Mountain Formation, Gunn Member</u>								
Location	Depth (M)	Tmax (°C)	S1 (mg/g)	S2 (mg/g)	S3 (mg/g)	TOC (%)	HI	OI
02-11-010-09W2	2273	447	1.65	177.60	0.95	22.20	800	4
<u>Herald Formation, Redvers Unit</u>								
Location	Depth (M)	Tmax (°C)	S1 (mg/g)	S2 (mg/g)	S3 (mg/g)	TOC (mg/g)	HI (%)	OI
02-08-003-14W2	2930	449	0.11	5.62	0.38	0.76	739	50
02-11-010-09W2	2286	425	0.19	0.59	0.94	0.63	93	149
<u>Herald Formation, Coronach Member</u>								
Location	Depth (M)	Tmax (°C)	S1 (mg/g)	S2 (mg/g)	S3 (mg/g)	TOC (%)	HI	OI
13-23-001-17W2	3044	443	1.06	2.97	0.05	0.68	436	7
<u>Yeoman Formation</u>								
Location	Depth (M)	Tmax (°C)	S1 (mg/g)	S2 (mg/g)	S3 (mg/g)	TOC (%)	HI	OI
03-08-001-11W2	3193	458	0.80	8.52	0.40	4.06	209	9
03-08-001-11W2	3186	459	0.61	1.30	0.42	0.99	131	42
10-25-001-15W2	3142	458	0.50	93.33	0.75	13.01	717	5
10-25-001-15W2	3144	455	0.85	30.62	0.54	5.28	579	10
10-25-001-15W2	3142	456	0.93	27.54	2.91	4.63	594	62
10-25-001-15W2	3115	449	0.19	3.22	0.51	0.75	429	68
10-25-001-15W2	3143	443	2.83	2.28	0.59	0.79	288	74
01-14-001-17W2	3109	448	0.50	62.91	0.60	7.78	808	7
01-14-001-17W2	3094	449	0.19	11.07	0.63	1.59	696	39
01-14-001-17W2	3107	447	0.64	14.07	1.14	2.86	491	39
07-23-001-17W2	3074	456	0.11	10.93	0.27	1.64	666	16
13-23-001-17W2	3076	452	0.64	134.25	0.29	15.54	863	1
13-23-001-17W2	3076	458	0.56	171.61	0.64	19.87	863	3
13-23-001-17W2	3082	457	2.78	210.35	0.87	26.35	798	3
13-23-001-17W2	3074	455	0.07	8.80	0.59	1.62	543	36
13-23-001-17W2	3062	441	0.40	3.75	0.50	0.79	474	63
13-23-001-17W2	3068	449	1.78	2.17	0.50	0.71	305	70
11-27-001-17W2	3072	454	0.92	12.74	0.52	2.41	528	21
16-36-001-18W2	3062	451	4.37	158.39	0.85	19.12	828	4
16-36-001-18W2	3072	452	2.80	19.50	0.39	3.10	629	12
16-36-001-18W2	3052	443	0.64	3.25	1.57	1.10	295	142
15-09-002-14W2	3069	448	1.29	26.76	1.04	4.57	585	22
15-09-002-14W2	3065	448	1.84	26.56	1.74	5.33	498	32
15-09-002-14W2	3070	446	2.72	4.89	1.41	1.63	300	86
08-16-002-14W2	3052	456	0.93	33.63	0.36	4.97	676	7

LITHOLOGY AND OCCURRENCE OF POTENTIAL SOURCE ROCKS

Potential petroleum source rocks occur within a restricted number of lithologies and stratigraphic positions in the Winnipeg Formation and Bighorn Group in southeastern Saskatchewan. In the Winnipeg Formation (Table 2) black, fissile shales and rusty black, lithic greywacke (rock fragments consisting of limonitic oolites), occur as laminae, beds or partings in predominantly green shales. They commonly contain sparse disarticulated and broken fragments of arthropods and inarticulate brachiopods. The green shales and silty shales that are common in the Winnipeg Formation have no petroleum potential. A prominent shale marker in the upper portion of the Black Island Member (Paterson, 1971, p. 12) was not sampled for this study.

Potential source rocks are restricted to the Icebox Member, commonly lying at or near the contact of two sequences defined by Vigrass (1971) (Fig. 1). Only a small number of cores have been analyzed, and the areal distribution of potential petroleum source rocks has not been mapped. However, some zones can be correlated between wells tens of kilometres apart, and the general potential of intervals corresponds well with the facies distribution outlined by Vigrass (1971). Source rock intervals are inferred to persist through the facies in which they occur.

The thickest potential source rock interval occurs in 4.4 m of black, fissile shale, and oolitic, lithic greywacke at the top of the Winnipeg Formation in the Whitebear Crown well (5-15-10-2W2). In this well, beds occur in the upper offshore mudstone facies belt of Vigrass (1971). The Flint Cutarm well (1-4-20-32W1) lies in the transitional facies belt where it overlies the basin margin sand facies. In this well, potential petroleum source rocks occur both near the top of the Icebox Member, as thin laminae and partings in beds of green shale, and near the base of the Member in a fissile, brown shale that is interbedded with a few thin beds of bioturbated sandstone. The lower interval overlies a sandstone near the top of the lower basin margin sandstone facies succession. Samples of core from the Pangman well (3-14-8-20W2) and cuttings from the nearby Parry No. 1 well (16-8-9-21W2) reveal a persistent, lean, potential petroleum source rock interval near the contact with the Black Island Member in the upper part of the formation. Better potential sources are recognized at the top of the Icebox Member in cuttings from the Parry well.

In general, potential source rocks appear to occur either near the top or the base of the Icebox Member. The lower horizon is richer and more persistent. It coincides with the base of the upper transgressive sequence defined by Vigrass (1971), particularly in the offshore mudstone facies belt.

Within the Bighorn Group, potential petroleum source rocks occur in the Yeoman, Herald, and Stoney Mountain formations (Table 2). In the Yeoman Formation, source rocks occur as thin laminae; laminae and thin beds of laminated, pale yellowish brown, bituminous lime mudstone with a resinous lustre (kukersite or kerogenite); as thin laminae interbedded with beds of kukersitic crinoidal floatstones, that are commonly dark brown to earthy black in

colour; and as laminae in thin beds of bioturbated lime mudstone. Kukersite beds have distinct contacts with burrow-mottled or thinly laminated lime- and dolomudstones and wackestones. Kukersites commonly overlie and infill submarine hardgrounds and are often gradational upward into lime mudstones. Contacts of thin laminae are commonly distinct and are sometimes stylolitized. Variations in thickness of kukersites represent variations in accumulation and not diagenetic condensation as suggested by Kendall (1976).

In several instances, burrows extend from the overlying burrow-mottled carbonates into the kukersites. The extent of bioturbation grades from nonexistent to complete, consisting predominantly of *Thalassinoides*-like Type II burrows as described by Derby and Kilpatrick (1985). Reworking by burrowing completely degrades the source rock potential of kukersites.

Kukersites occur at several levels in the Yeoman Formation, either within the upper 15 or 20 m of the formation, or near the base of the formation. They are up to 0.5 m thick, although commonly they occur as four to six very thin beds and laminae, less than one centimetre thick, of plane, thinly laminated kukersite and carbonate. Individual beds can be correlated between wells, and in some cases, log "picks" at similar stratigraphic position are associated with kukersites.

Kukersite beds in the upper portion of the formation occur in restricted areas. The vast majority of potential source rocks are from wells located in the first 23 townships between ranges 9 and 21 west of the second meridian. This region is overlain by a section of the Lake Alma Member, which is more than 15 m thick. Other regions where the Lake Alma Member is as thick occur east of 103° west longitude. In these regions, the Yeoman Formation is not well represented in cores and its source rock potential cannot be assessed. If thickening of the Lake Alma Member in these eastern areas indicates depressions on the shelf, the kukersites will probably lie lower in the Yeoman Formation than those toward the west; the uppermost cycle of the formation is characterized in the east by restricted shelf deposits in this area (Kendall, 1976). Kukersites occurring near the base of the formation, like the sample from the Imperial Pangman well (3-14-8-20W2), appear to underlie the main area of source rock development recognized in the upper part of the formation.

Potential petroleum source rocks occur in all three members of the Herald Formation. Within the Lake Alma Member they have been identified from core descriptions, and occur as thin laminae in thin beds of bioclastic wackestone and bioturbated mudstone. They occur in the same area as potential sources in the upper Yeoman Formation. Together they comprise two cycles, one in the upper Yeoman Formation and the other in the Lake Alma Member. One potential source rock has been analyzed from the Coronach Member (12-23-001-17W2) (Table 2). Its significance cannot be assessed. Potential source rocks also occur in the Redvers Unit (Table 2). These sources are recognizable in the same areas as the upper Yeoman-Lake Alma source rocks (e.g., 02-08-003-14W2) and but are absent away from that area (e.g., 02-11-010-09W2). Source rocks are concentrated

near the base of this unit; however, their lateral extent cannot be determined with the available results. An indication of petroleum source rock potential in the argillaceous, bioclastic wackestones of the Gunn Member of the Stoney Mountain Formation suggests the presence of thin, yet rich sources of unknown distribution and thickness (02-11-010-09W2).

SOURCE ROCK POTENTIAL AND PETROGRAPHY

Winnipeg Formation

Potential petroleum source rocks from the Winnipeg Formation have a variable petroleum potential (Table 2). Concentrations of up to 10.41% TOC occur, although the average abundance is only 1.67%. Pyrolysis S2 yields of up to 96.19 kg/tonne characterize the sample having the richest TOC abundance. The average S2 yield of 10 samples is only 12.71 kg/tonne, whereas an average yield of only 3.44 kg/tonne characterizes the sample set if the richest sample is not considered. There is a strong linear correlation between TOC and total petroleum potential (S1+S2), such that $S1 + S2 = -3.10 + 9.59(\text{TOC})$. The average total petroleum potential of these sources is 12.92 kg/tonne. This represents an aggregate average that may not be characteristic of specific facies. The marked difference of the petroleum potential of the sample from the basal part of the Icebox Member in the upper offshore mudstone facies belt is probably indicative of improved source rock potential associated with this depositional environment. Samples from the transitional facies belt settings, although numerically the largest portion of this sample set, may not be characteristic of Winnipeg lithologies with the greatest potential.

Petrography indicates that organic material in Winnipeg Formation sources is an alginite associated with acritarchs and chitinozoa. The alginite is composed of agglomerations

of cup-like structures of the alga *Gloeocapsomorpha prisca* Zalesky 1917 (Plate 1). Source rocks also contain fragments of brachiopods and arthropods and limonitic oolites. The contributing organic material is entirely marine, not unexpected from rocks of this age. Hydrogen Indices (S2/TOC) range from 368 to 924, characteristic of both Type II and Type I organic material. The presence of *G. prisca* in samples with Type II Hydrogen Index values suggests a variation in Hydrogen Index results, either from varying degrees of mixing of alginitic, Type I organic material with marine, Type II organic material contributed by other organisms, or by variable amounts of diagenetic degradation.

Big Horn Group

Potential petroleum source rocks occur exclusively in kukersites in the Yeoman Formation (Table 2). Kukersite beds contain up to 34.9% TOC with an average of 8.44% TOC from 66 samples. Pyrolysis yields up to 339 kg of hydrocarbons/tonne of rock (S2 peak). An average yield is 71.67 kg/tonne. There is a strong linear correlation between TOC abundance and total petroleum potential (S1+S2), such that $(S1+S2) = -7.50 + 9.52(\text{TOC})$. The mean total hydrocarbon potential is 72.85 kg/tonne. Cores suggest that at least 23 cm of source rock underlies the source rock sub-basin.

Samples from kukersites and argillaceous carbonates from the Herald and Stoney Mountain formations are commonly lean, less than 1.05% TOC (Table 2). One sample from the Gunn Member, of the Stoney Mountain Formation, contained 22.2% TOC and exhibited an S2 yield of 177.6 kg of hydrocarbons/tonne. A sample of the kukersite bed in the Lake Alma Member of the Bead Lake well (6-8-4-21W2) pictured by Kendall (1976, Plate XXIIIB) could not be found at the core repository, but this bed has an appearance similar to the rich sources in the Yeoman Formation.

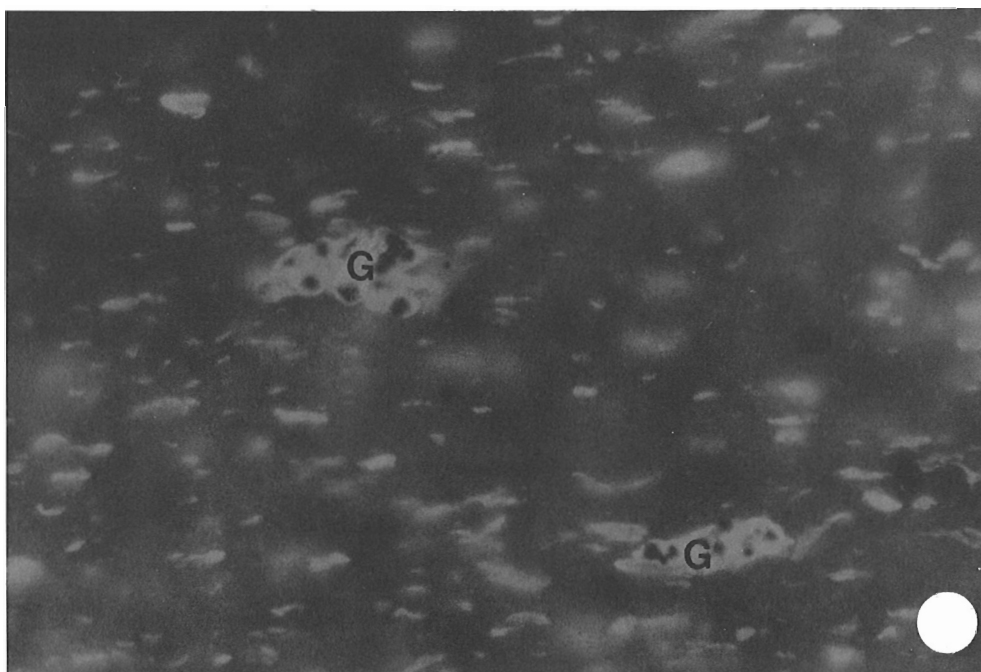


Plate 1. Incident ultraviolet light photomicrograph of Ordovician Winnipeg Formation (Icebox Member) consisting of *Gloeocapsomorpha*-type alginite (G). The alginite bodies are generally disseminated, display agglomerations of cup-like structures and can be associated with acritarchs and chitinozoan remains (5-15-10-2W2; 2281.94 m).

Hydrogen indices of Yeoman and Stoney Mountain rich sources are all very high, commonly greater than 800 for thermally immature samples. Oxygen indices are generally very low, commonly below 20. Petrographic examination indicates that the kukersites are made up of an alginite composed exclusively of *Gloeocapsomorpha prisca* (Plate 2). These rocks are Type I marine source rocks containing algal material similar to that found in the underlying Winnipeg Formation sources.

THERMAL MATURITY

Winnipeg Formation

Maturation indicators suggest that all the samples from the Winnipeg shales are immature, although the reliability of standard indices of thermal maturity is uncertain (see below). Production indices are low, (<10 per cent) and Tmax values do not appear to vary with depth (Table 2). Due to the component of Type I organic material it is unlikely that these parameters (Tmax, Production Index) can be used successfully to identify the onset of hydrocarbon generation. Only the Pangman well (3-14-8-20W2) lies near the region of thermally mature Bighorn Group source rocks. A sample from the Yeoman Formation in the Pangman well is immature (Table 2), and similarly, a lack of maturity is inferred for the Winnipeg Formation. Because of the similarity of source material it is expected that Winnipeg Formation potential sources that underlie mature Big Horn Group source rocks will also be mature.

Big Horn Group

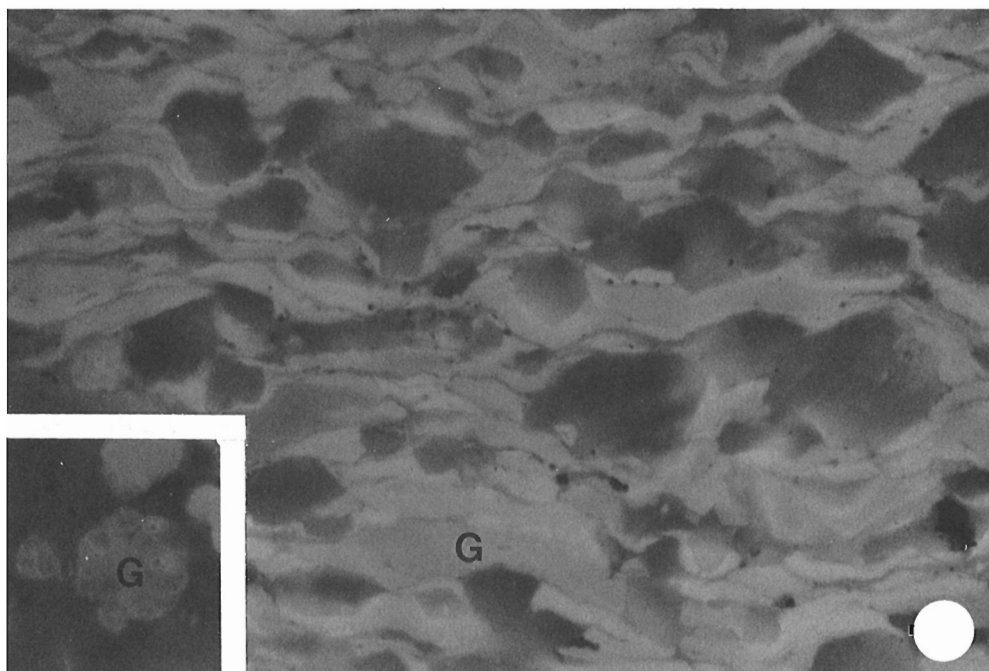
Unlike other organic matter types, the thermal maturity of Type I source rocks in the Big Horn Group is not reflected by the maximum temperature of the S2 peak (Tmax) during the cracking phase of the Rock-Eval experiment (Table 2).

Production Index, $S1/(S1+S2)$, commonly equals 0.10 with the onset of thermal maturity in other source rock types (Tissot and Welte, 1978; p. 453-455). Thermal maturity is positively correlated with Transformation Ratio, $(HI_0-HI)/HI_0$, (where HI_0 is the initial Hydrogen Index of thermally immature source rock, and HI is the Hydrogen Index of the sample, $S2/TOC$). Although Transformation Ratio behaves predictably for kukersitic sources, its correlation with Production Index is poor. Coherent behaviour of the Transformation Ratio with depth and the strong linear relationship between petroleum potential ($S1+S2$) and Total Organic Carbon can be employed to identify the onset of hydrocarbon generation and migration.

If the Hydrogen Index values of thermally immature samples are plotted as a function of depth, the result should be linear (Fig. 2). Samples that have generated hydrocarbons will have depleted S2 values and those that have expelled hydrocarbons will exhibit lower total petroleum potential ($S1+S2$) than the S2 value of immature samples of similar composition. If the total petroleum potential is normalized with respect to TOC abundance, the resulting ratio is a pseudo-hydrogen index, the residual petroleum potential (RPP). This ratio can be plotted against depth to identify hydrocarbon expulsion by comparison to the trend of thermally immature samples (Fig. 2). For Type I source rocks, Hydrogen Index values greater than 765 (Transformation Ratio = 10%) are immature to marginally mature (Espitalie et al., 1985).

If the RPP of Yeoman Formation kukersites is plotted against present depth, a strong linear relationship characterizes samples that are immature (Fig. 2). Below 2950 m present depth, the RPP exhibits a wide range of values, from thermally immature (zero Transformation Ratio) to thermally mature (Transformation Ratio = 80%). This indicates the occurrence of the oil window below 2950 m present depth in geographically restricted areas. The oil

Plate 2. Incident ultraviolet light photomicrograph of Ordovician Red River Formation (Yeoman Member) rich in *Gloeocapsomorpha*-type alginite (G) in an orientation perpendicular to bedding. Insert in lower left corner is a section parallel to bedding, displaying agglomeration of cup-like structures, typical of colonial algae (G) (6-32-18-16W2; 2458.82 m).



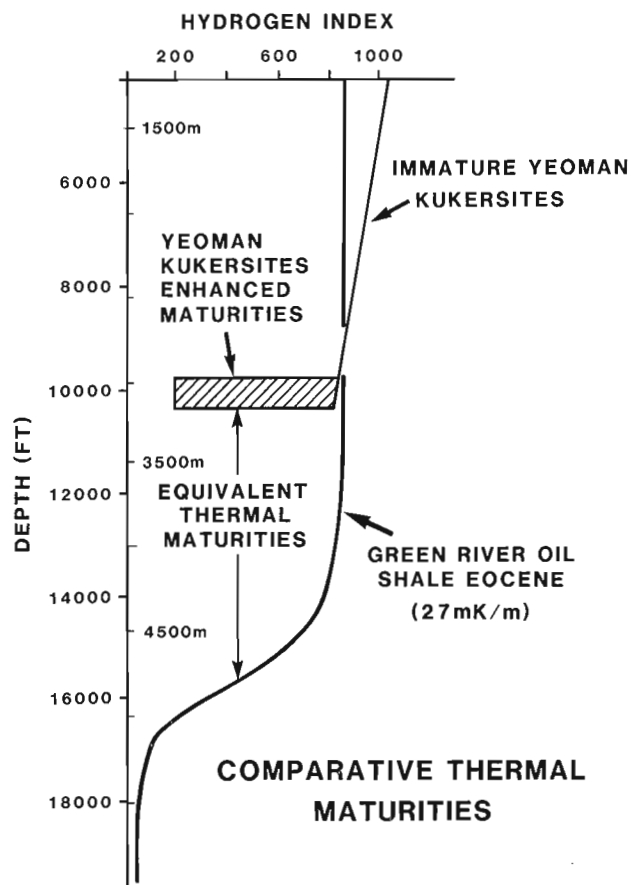


Figure 2. Variation of Hydrogen Index (S₂/TOC) with depth for Ordovician kukersite compared to Green River Oil Shale Type I source rock.

window for the Green River Formation (another Type I source rock) occurs at approximately 4200 m (Fig. 2), nearly 50 per cent deeper than that observed for the Yeoman samples. Coalification gradients in the Green River Formation suggest that geothermal gradients were approximately 27 mK/m during its maturation (cf. Middleton, 1982). Thermally mature Ordovician kukersites require geothermal gradients commonly in excess of 35 mK/m and as high as 42 mK/m to attain observed levels of Transformation Ratio, if the kinetics are the same.

Other techniques such as solvent extract yield are also used to characterize the thermal maturity of source rocks and to identify the onset of hydrocarbon generation. However, solvent extracts from the Yeoman and Winnipeg formations do not behave in the expected manner. This is attributable to the peculiar chemistry of the precursor organisms. Stains are generally restricted to depths in excess of 2800 m (Tables 4, 5), supporting the 2950 m oil window depth inferred from Rock-Eval data (Fig. 2). Percentages of hydrocarbons in solvent extracts from unstained source rocks (Table 3) and their lack of variation with depth cannot be interpreted using standard indications of thermal maturity (40-60 % hydrocarbons in total extract). In fact, samples with the largest Transformation and RRP ratios (10-25-01-15W2; 3141.8 m) have substantially lower

extractable hydrocarbons than immature samples (02-04-22-15W2; 1732 m). Even stains commonly have an unexpectedly low proportion of hydrocarbons in their solvent extracts (Table 4). The restriction of stains to depths greater than 2800 m and the inference, from pyrolysis data, that the top of the oil window lies at approximately 2950 m provide a more reliable indication of hydrocarbon generation than solvent extract data alone.

Association of crustal structure and elevated thermal maturity

Elevated thermal maturity of Ordovician petroleum source rocks in southeastern Saskatchewan is observed to be controlled by present burial depth and geographic location. Stratigraphic reconstruction indicates that no more than approximately 300 m of erosion has occurred in the region of thermally mature source rock since Eocene time. Samples of kukersitic source rock lying at depths below the inferred top of the oil window (2950 m) and in western geographic locations (eg., 6-13-2-19W2, Table 2) have high RPP's and are inferred to be thermally immature. These observations indicate that burial depth alone was neither sufficient to generate oil on a regional scale nor the sole control on the thermal maturity of these source rocks.

The highest levels of thermal maturity and hydrocarbon expulsion, as determined from the RPP, are exhibited by samples at present depths below 2950 m and lying closer to the 103rd meridian of longitude (eg., 3-8-1-11W2, Table 2). Using the RPP, the geographic extent of the oil window can be outlined to lie between Ranges 9 and 18 west of the second meridian. Yet samples in Ranges 16, 17 and 18 west of the second meridian exhibit a considerable range of RPP values in a single well. This pattern indicates that the intensity of hydrocarbon generation increases toward the 103rd meridian of longitude. Unfortunately, the kukersitic sources are a facies of the Big Horn Group, the initial distribution of which was controlled by a persistent, paleogeographic element, the axis of which lay at approximately Range 16 west of the second meridian (104°W), and extended no farther east than Range 9 west of the second meridian. This prevents accurate assessment of the regional pattern of thermal maturity beyond the depositional limit of the source rocks. To assess the control of crustal structure on thermal maturity requires the consideration of additional factors.

The Nesson Anticline is a geological structure on the bedrock surface of the outcropping Montana and Fort Union groups. Its hinge is located approximately along the 103rd meridian of longitude extending from near the centre of the Williston Basin to approximately the Canadian border. There is considerable evidence of differential subsidence of the present structure and its environs throughout the Phanerozoic (Lefever et al., 1987). In the Canadian portion of the basin, there is clear evidence that a much larger crustal structure, ancestral to the current anticline, exerted a control on the depositional environments of several units throughout the Phanerozoic. Significant activity of the ancestral structure is recorded by its differential subsidence history during the Upper Ordovician. During the Upper

Ordovician, the arch was a positive feature identifiable by a reorientation of facies boundaries in the upper Yeoman and lower Herald formations along a north-south axis (Kendall, 1976). The hinge of the arch was the site of a mud dominated shelf that served as the major control on the eastern margin of the starved source rock subbasin in the Late Ordovician epeiric sea (Osadetz et al., work in progress). This pattern of subsidence and inferred control on source rock accumulation on the western flank of the structure affected the hydrocarbon potential of these Ordovician source rocks.

The axis of the ancestral Nesson structure is also the site of elevated crustal heat flows. The thermal history of this structure is not yet completely known but several facts are

certain. Elevated geothermal gradients occurred in association with this structure at the time of maximum burial depth (Early Eocene) as indicated by the RPP values in Ordovician sources and elevated coal reflectances in Tertiary strata (Cameron, in press). Currently, the same region is characterized by elevated geothermal gradients in Paleozoic rocks (Majorowicz et al., 1986). Present gradients are comparable to those inferred from the Transformation Ratio of Ordovician sources and attributed to late Mesozoic and Paleogene times. New data from Middle Devonian source rocks corroborates these observations and shall be reported in a later publication. The hinge of the structure is coincident with elevated Tmax values for Type II Bakken source rocks in the American portion of the Basin as mapped by Price et al. (1984). Majorowicz et al. (1988) have recently commented

Table 3. Solvent extracts from potential Ordovician source rocks

<u>Yeoman Formation</u>					
Location	Depth (M)	Total yield	%Hydrocarbons (%) (mg/gTOC)	TOC	TransformationRatio (%)
02-04-22-15W2	1732.1	17.78	44.74	22.05	1.9
16-20-08-10W2	2445.6	46.00	53.30	16.69	0
16-20-08-10W2	2446.5	12.82	53.19	12.94	0
06-32-08-16W2	2453.7	29.53	58.78	16.27	0
07-23-03-17W2	2990.0	30.70	40.90	14.21	4.1
13-27-01-17W2	3076.2	10.63	46.25	17.71	0
03-20-02-16W2	3076.5	8.64	26.29	13.95	0
13-27-01-17W2	3082.0	23.99	49.40	26.35	5.9
10-25-01-15W2	3141.8	106.61	38.96	13.01	11.1
<u>Winnipeg Formation, Icebox Member</u>					
Location	Depth (M)	Total yield	%Hydrocarbons (mg/gTOC)	TOC (%)	
01-04-20-32W1	1375.0	35.80	32.94	0.53	
01-04-20-32W1	1391.1	10.98	26.56	10.41	
05-15-10-02W2	2281.7	23.33	45.45	1.03	
05-15-10-02W2	2282.7	22.73	26.39	1.07	
05-15-10-02W2	2285.7	23.80	30.69	1.25	

Table 4. Solvent extraction of oil stains in Bighorn Group

Location	Depth (M)	Total yield	%Hydrocarbons (mg/gTOC)	TOC (%)
06-28-03-12W2	2876.0	1474.67	54.29	1.44
07-23-03-17W2	2989.7	1027.95	45.75	5.09
08-16-02-14W2	3037.6	1733.02	80.83	1.53
11-27-01-17W2	3071.0	1495.73	57.55	1.17

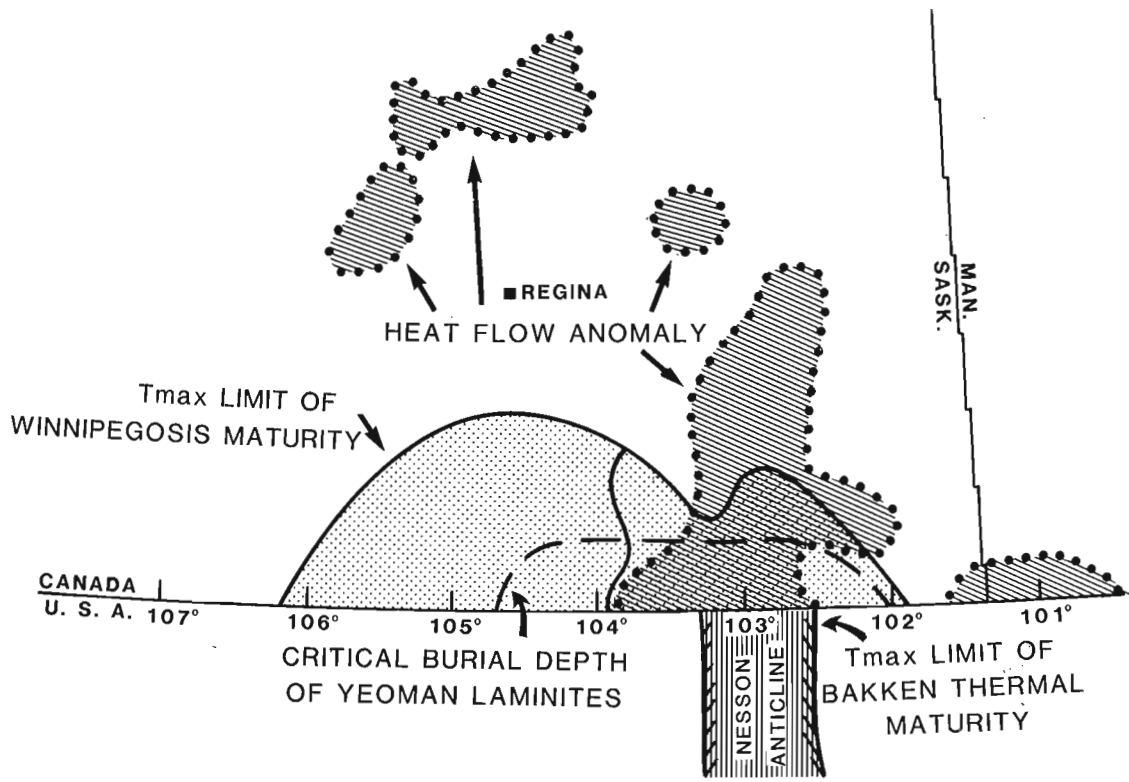


Figure 3. Indications of enhanced thermal maturity associated with the Nesson Anticline at the 103rd meridian of longitude.

Table 5. Results of Rock-Eval experiments on oil stains in Ordovician rocks

Location	Depth (M)	<u>Bighorn Group</u>						
		Tmax (°C)	S1 (mg/g)	S2 (mg/g)	S3 (mg/g)	TOC (%)	HI	OI
07-23-001-17W2	3063	433	4.12	1.26	0.48	0.84	150	57
07-23-001-17W2	3075	448	1.74	2.93	0.47	0.73	401	64
11-27-001-17W2	3071	444	5.61	3.99	0.51	1.17	341	43
11-27-001-17W2	3059	436	2.61	0.75	0.51	0.38	197	134
08-16-002-14W2	3038	429	13.45	1.50	0.41	1.53	98	26
08-16-002-14W2	3035	452	7.55	3.46	0.53	1.85	187	28
08-16-002-14W2	3036	455	2.78	2.70	0.36	1.28	210	28
08-16-002-14W2	3035	447	7.18	2.39	0.83	1.94	123	42
08-16-002-14W2	3049	439	3.72	2.88	0.56	1.06	271	52
08-16-002-14W2	3054	441	2.67	1.78	0.99	0.76	234	130
12-13-002-19W2	3018	455	0.12	8.80	0.36	1.42	619	25
06-28-003-12W2	2876	434	7.52	4.16	0.68	1.44	288	47
02-08-003-14W2	2931	401	4.76	0.88	0.40	0.56	157	71
04-22-003-15W2	2937	443	3.82	1.37	0.88	0.75	182	117
07-23-003-17W2	2988	447	13.43	9.09	1.71	3.21	283	53
07-23-003-17W2	2989	443	2.37	1.66	0.43	0.69	240	62
07-23-003-17W2	2990	445	20.00	18.58	4.48	5.09	365	88
11-02-003-21W2	2864	443	1.56	0.93	0.46	0.35	265	131
06-11-004-21W2	2818	443	0.64	0.88	0.40	0.36	244	111
08-02-006-16W2	2678	442	2.09	1.53	0.52	0.48	318	108
16-20-008-10W2	2444	439	1.76	2.12	0.60	0.54	392	111

on the coincidence of a number of these features and their association with a revised position of the North American Central Plains Conductivity Anomaly as deduced from recent magnetotelluric soundings.

The spatial coincidence or association of these geological and physical domains indicates that the ancestral structure of the Nesson Anticline was a crustal structure that exerted a fundamental control on the depositional history of source rock facies and their subsequent thermal maturation. Upper Ordovician source rocks accumulated on the western flank of this feature during a period when it acted as a positive tectonic element. Subsequent burial has been demonstrated to be insufficient to mature Ordovician source rocks regionally.

This region has been the locus of high heat flows and elevated thermal maturities. The Ordovician oil-source system in Canada suffers from the fact that the ancestral Nesson structure was a positive tectonic element at the time that potential source rocks accumulated on its western flank. This effectively removed most Ordovician sources in Canada from the region of enhanced thermal maturity and lowered the extent of hydrocarbon generation in Ordovician source rocks. Organic matter type probably enhanced this discrepancy, as Type I source rocks have significantly higher thresholds of hydrocarbon generation than to Type II source rocks (cf. Espitalie et al., 1985).

CONCLUSIONS

The Nesson Anticline is the present expression of a long-lived crustal structure, the hinge of which lies along the 103rd meridian of longitude. The much broader ancestral feature has affected the hydrocarbon potential of the basin. Its differential subsidence history with respect to its environs has led to the exclusion, as in the Upper Ordovician, of rich potential source rocks along its hinge line. This differentially subsiding crustal structure coincides with the North American Central Plains Conductivity Anomaly and is the locus of elevated geothermal gradients (Majorowicz et al., 1988). The pattern of thermal maturity and rate of hydrocarbon generation in Upper Ordovician kukersitic source rocks indicates geothermal gradients as high as approximately 40°C/km on the western flank of the structure through at least late Mesozoic and Paleogene time. These gradients are comparable to those currently observed by Majorowicz et al. (1986) in Paleozoic rocks. These elevated geothermal gradients controlled the generation of hydrocarbons in a region that was insufficiently buried for the generation of hydrocarbons to have occurred.

This structural feature is the fundamental control on the hydrocarbon resource potential of Ordovician plays for hydrocarbon in the Canadian Williston Basin. Its effect on the Upper Ordovician oil source system has been to exclude very rich source rocks from the region of elevated thermal maturities. The result is a low efficiency of oil generation, only about 193,000,000 bbls, from a source rock interval with a potential in excess of 5 billion bbls of oil equivalent. This play has not been extensively exploited in spite of favourable estimates of its resource potential.

REFERENCES

- Anderson, T.C.**
1982: Exploration history and hydrocarbon potential of the Ordovician Winnipeg Formation in the southern Williston Basin; in Fourth International Williston Basin Symposium Proceedings, J.E. Christopher and J. Kaldi (eds.), Saskatchewan Geological Society, Special Publication No. 6, p. 19-25.
- Brooks, P.W., Snowdon, L.R., and Osadetz, K.G.**
1987: Families of oils in southeastern Saskatchewan; in Proceedings of the Fifth International Williston Basin Symposium, C.G. Carlson and J.E. Christopher (eds.), Bismarck, North Dakota, June 15-17, 1987, Saskatchewan Geological Society, Special Publication No. 9, p. 253-264.
- Cameron, A.R.**
—: Regional patterns of reflectance distribution in lignites of the Ravenscrag Formation, Saskatchewan, Canada; *Journal of Coal Geology* (in press).
- Carlson, C.G.**
1958: The stratigraphy of the Deadwood-Winnipeg interval in North Dakota and northwestern South Dakota; Proceedings of the Second International Williston Basin Symposium, Regina, April 23-25, 1958, Saskatchewan Geological Society and North Dakota Geological Society, p. 20-26.
1960: Stratigraphy of the Winnipeg and Deadwood formations in North Dakota; North Dakota Geological Survey, Bulletin 35, 149 p.
- Carlson, C.G., and Anderson, S.B.**
1965: Sedimentary and tectonic history of North Dakota part of Williston Basin; American Association of Petroleum Geologists, Bulletin, v. 49, p. 1-15.
- Derby, J.R. and Kilpatrick, J.T.**
1985: Ordovician Red River Dolomite Reservoirs, Killdeer Field, North Dakota; in Carbonate Petroleum Reservoirs, P.O. Roehl and P.W. Choquette (eds.), Springer-Verlag, p. 61-69.
- Espitalie, J., Deroo, G. and Marquis, F.**
1985: Rock Eval Pyrolysis and Its Applications: Preprint; Institut Français du Pétrole, Géologie No. 27299, 72 p. English translation of, La pyrolyse Rock-Eval et ses applications, Première, Deuxième et Troisième Parties, in *Revue de l'Institut Français du Pétrole*, v. 40, p. 563-579, 755-784; v. 41, p. 73-89.
- Fuller, J.G.C.M.**
1961: Ordovician and contiguous formations in North Dakota, United States; American Association of Petroleum Geologists, Bulletin, v. 45, p. 1334-1363.
- Gehman, H.M. Jr.**
1962: Organic matter in limestones; *Geochimica et Cosmochimica Acta*, v. 26, p. 885-897.
- Kendall, A.C.**
1976: The Ordovician carbonate succession (Bighorn Group) of southeastern Saskatchewan; Saskatchewan Department of Mineral Resources, Report 180, 185 p.
- Kohm, J.A. and Loudon, R.O.**
1978: Ordovician Red River of eastern Montana and western North Dakota: relationships between lithofacies and production; in 1978 Williston Basin Symposium — the Economic Geology of the Williston Basin, Proceedings of the Montana Geological Society 24th Annual Conference, Billings Montana, p. 99-117.
1982: Ordovician Red River of eastern Montana and western North Dakota: relationships between lithofacies and production; in Fourth International Williston Basin Symposium Proceedings, J.E. Christopher and J. Kaldi (eds.), Saskatchewan Geological Society, Special Publication No. 6, p. 27-28.
- Lefever, J.A., Lefever, R.D., and Anderson, S.B.**
1987: Structural evolution of the central and southern portions of the Nesson Anticline, North Dakota; in Proceedings of the Fifth International Williston Basin Symposium, C.G. Carlson and J.E. Christopher (eds.), Bismarck, North Dakota, June 15-17, 1987, Saskatchewan Geological Society, Special Publication No. 9, p. 147-156.
- Lefever, R.D., Thompson, S.C., and Anderson, D.B.**
1987: Earliest Paleozoic history of the Williston Basin in North Dakota; in Proceedings of the Fifth International Williston Basin Symposium, C.G. Carlson and J.E. Christopher (eds.), Bismarck, North Dakota, June 15-17, 1987, Saskatchewan Geological Society, Special Publication No. 9, p. 22-36.

- Majorowicz, J.A., Jones, F.W., and Jessop, A.**
1986: Geothermics of the Williston Basin in Canada in relation to hydrodynamics and hydrocarbon occurrences; *Geophysics*, v. 51, p. 767-779.
- Majorowicz, J.A., Jones, F.W., and Osadetz, K.G.**
1988: Heat flow environment of the electrical conductivity anomalies in the Williston Basin, and occurrence of hydrocarbons; *Canadian Bulletin of Petroleum Geology*, v. 36, no. 1, p. 86-90.
- Middleton, M.F.**
1982: Tectonic history from vitrinite reflectance; *Geophysical Journal of the Royal Astronomical Society*, v. 68, p. 121-132.
- Osadetz, K.G. and Snowdon, L.R.**
1986a: Petroleum source rock reconnaissance of southern Saskatchewan; in *Current Research, Part A*, Geological Survey of Canada, Paper 86-1A, p. 609-617.
1986b: Speculation on the petroleum source rock potential of portions of the Lodgepole Formation (Mississippian) of southern Saskatchewan; in *Current Research, Part B*, Geological Survey of Canada, Paper 86-1B, p. 647-651.
- Paterson, D.F.**
1971: The Winnipeg Formation (Ordovician) of Saskatchewan; Saskatchewan Department of Mineral Resources, Report 140, 57 p.
- Price, L.C., Ging, T., Daws, T., Love, A., Pawlewicz, M., and Anders, D.**
1984: Organic metamorphism in the Mississippian-Devonian Bakken shale, North Dakota portion of the Williston Basin; in *Hydrocarbon source rocks of the Greater Rocky Mountain region*, J. Woodward, F.F. Meissner and J.L. Clayton (eds.); Rocky Mountain Association of Geologists, Denver, p. 83-134.
- Thomas, G.E.**
1968: Notes on textural and reservoir variations of Ordovician microdolomites, Lake Alma-Beaubier producing area, southern Saskatchewan; Saskatchewan Department of Mineral Resources and Saskatchewan Geological Society, Core Seminar on Pre-Mississippian rocks of Saskatchewan, October 3-4, 1968, Regina.
- Tissot, B.P. and Welte, D.H.**
1978: *Petroleum Formation and Occurrence: A New Approach to Oil and Gas Exploration*; Springer-Verlag, 538 p.
- Vigrass, L.W.**
1971: Depositional framework of the Winnipeg Formation, Manitoba and eastern Saskatchewan; Geological Association of Canada, Special Paper No. 9, p. 225-234.
- Williams, J.A.**
1974: Characterization of oil types in Williston Basin; *American Association of Petroleum Geologists, Bulletin*, v. 58, p. 1243-1252.

Modelling of stress refraction in sediments around the Peace River Arch, western Canada

J.S. Bell and P.F. Lloyd¹
Institute of Sedimentary and Petroleum Geology, Calgary

Bell, J.S. and Lloyd, P.F., Modelling of stress refraction in sediments around the Peace River Arch, western Canada; in Current Research, Part D, Geological Survey of Canada, Paper 89-1D, p. 49-54, 1989.

Abstract

Breakout orientations measured in many wells in northern Alberta and British Columbia show that the principal horizontal stresses are deflected over the Peace River Arch. Instead of the regional NE-SW azimuth for S_{Hmax} , the larger horizontal principal stress is directed NNE-SSW.

Two-dimensional finite element modelling of this stress refraction within the sediments overlying the Peace River Arch shows that the cause could be lateral variations in the elastic properties of the rocks.

Résumé

Dans un grand nombre de puits du nord de l'Alberta et de la Colombie-Britannique, des mesures des directions des éclats de roche indiquent que les contraintes principales horizontales sont déviées au-dessus de l'arche de Peace River. Contrairement à S_{Hmax} dont la direction régionale est NE-SW, la contrainte principale horizontale, qui est plus importante, a une direction NNE-SSW.

La modélisation bidimensionnelle par éléments finis de cette réfraction des contraintes dans les sédiments recouvrant l'Arche de Peace River indique que la cause pourrait être des variations latérales des propriétés élastiques des roches.

¹ Norcen Energy Resources Ltd., 715 - 5th Avenue S.W., Calgary, Alberta T2P 2X7.

INTRODUCTION

Shortly after breakouts began to be widely used for mapping horizontal principal stress orientations in western Canada (Gough and Bell, 1981) it became apparent that the larger horizontal principal stress was oriented approximately northeast-southwest in most parts of the Western Canadian Basin except over the Peace River Arch. Fordjor et al. (1983) noted that, between 55° and 57°N, in northwest Alberta and northeast British Columbia, the breakout azimuths show a significant anticlockwise rotation relative to those to the south and north. From this they inferred that stress trajectories were rotated in the region, as illustrated subsequently by Bell and Babcock (1986). Fordjor et al. (op. cit.) suggested that, since the area in which this stress axis rotation was observed coincided approximately with the subcropping Peace River Arch, this basement feature was responsible (Fig. 1, 2).

In this note, we offer an explanation for the bending of horizontal principal stress axes, and illustrate it by means of two-dimensional finite element modelling.

PEACE RIVER ARCH

The Peace River Arch has a history of protracted, intermittent uplift and erosion. It appears to have been an emergent feature during Ordovician and Silurian time and underwent erosion in Early Devonian time (Porter et al., 1982). Middle and Late Devonian sediments rimmed and overlapped what was then a northeasterly extending peninsula but, in Carboniferous and Permian time, the Peace River Arch subsided to become the locus of sedimentation in the region (McCrossan and Glaister, 1964). Burial by Mesozoic and Tertiary sediments and subsequent Tertiary erosion (Porter et al., 1982) has left the Peace River Arch as a high-standing, Precambrian-cored, peninsula-like uplift, which locally elevates the southwest-dipping basement surface that floors the Western Canadian Basin (Fig. 1). In many papers,

the Peace River Arch is illustrated by outlining the depositional edge of the upper Slave Point Formation (for example, Podruski et al., 1988), but here we define the arch structurally and outline the area over which the basement surface is elevated above the regional homocline (Fig. 2).

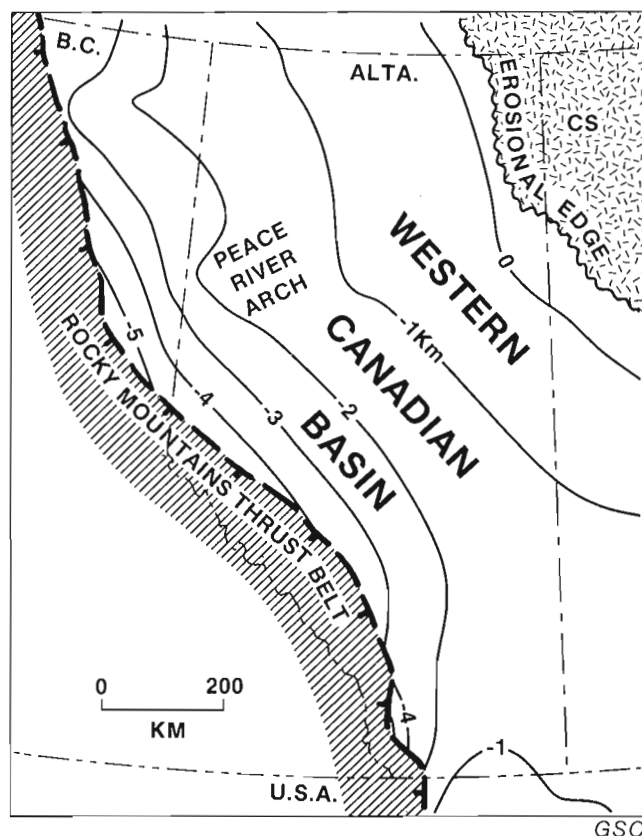
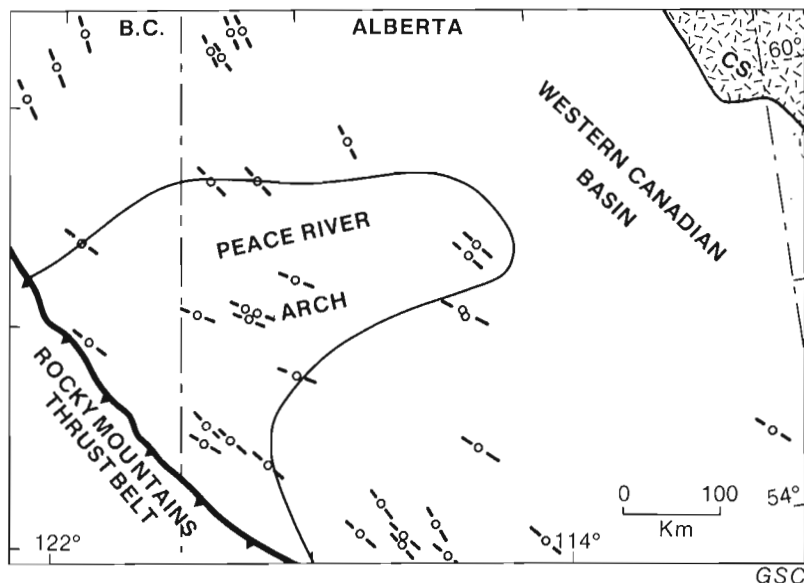


Figure 1. Basement structure of the Western Canadian Basin contoured in kilometres below sea level. Note the elevated Peace River Arch area. CS, Canadian Shield.

Figure 2. Mean breakout azimuths for 35 wells on and around the Peace River Arch. Small circles indicate well locations; bars denote mean azimuths of borehole breakouts. CS, Canadian Shield.



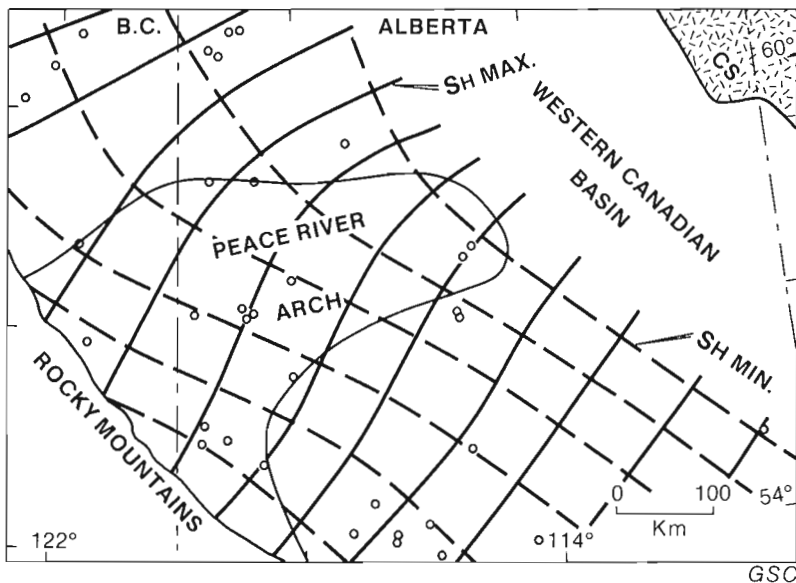


Figure 3. Stress trajectory map of the Peace River Arch area. Solid lines show the directions of the larger horizontal principal stress, S_{Hmax} . Dashed lines denote the corresponding directions of the smaller horizontal principal stress, S_{Hmin} . Small circles indicate well locations. CS, Canadian Shield.

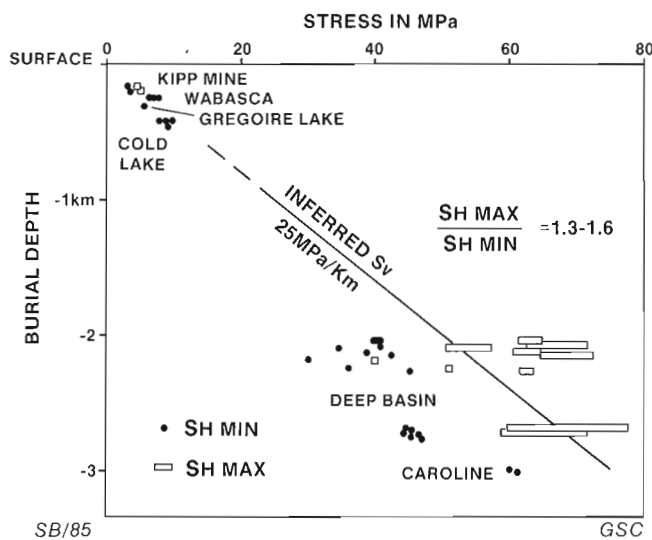
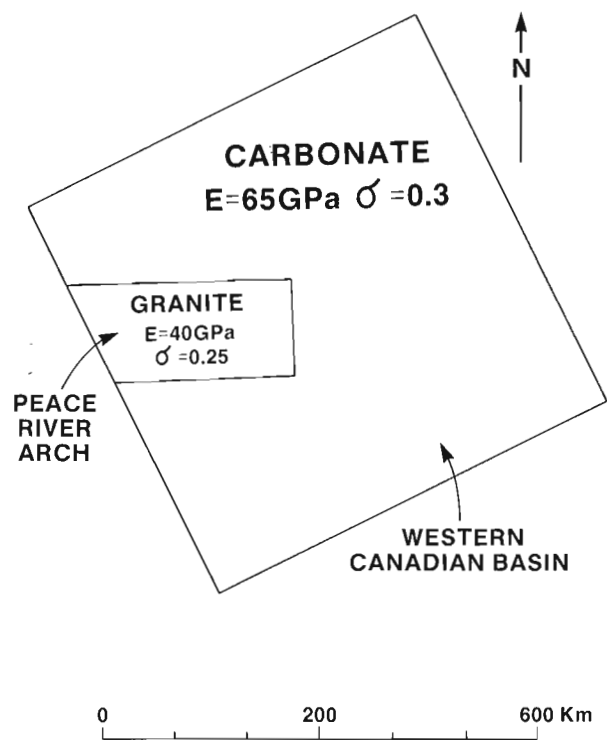


Figure 4. Stress magnitude data from the Western Canadian Basin. Note that the S_{Hmax} values are calculated, not measured, in the Deep Basin of Alberta.

In-situ stress orientations and magnitudes around the Peace River Arch

Horizontal principal stress trajectories in the Western Canadian Basin have been mapped from borehole breakouts by Bell and Babcock (1986), and their mean breakout azimuths for 35 wells over and around the Peace River Arch are illustrated in Figure 2. All breakouts in these wells occur in the Paleozoic and Mesozoic sequences overlying the Precambrian crystalline basement, and were measured at burial depths ranging from 112.5 to 3990.8 m. As yet, the breakout orientations have not been analysed stratigraphically to determine whether there are significant changes related to rock units or structural position, so only the mean breakout azimuths for each well are considered here. Statistically, most of them fall into single populations with small standard deviations (Fordjor et al., 1983; Bell and Babcock, 1986).



ELASTIC CONSTANTS used in model

GSC

Figure 5. Two-dimensional plate model of the Western Canadian Basin and Peace River Arch with a carbonate/granite contrast. E, Young's Modulus in gigapascals; σ , Poisson's ratio.

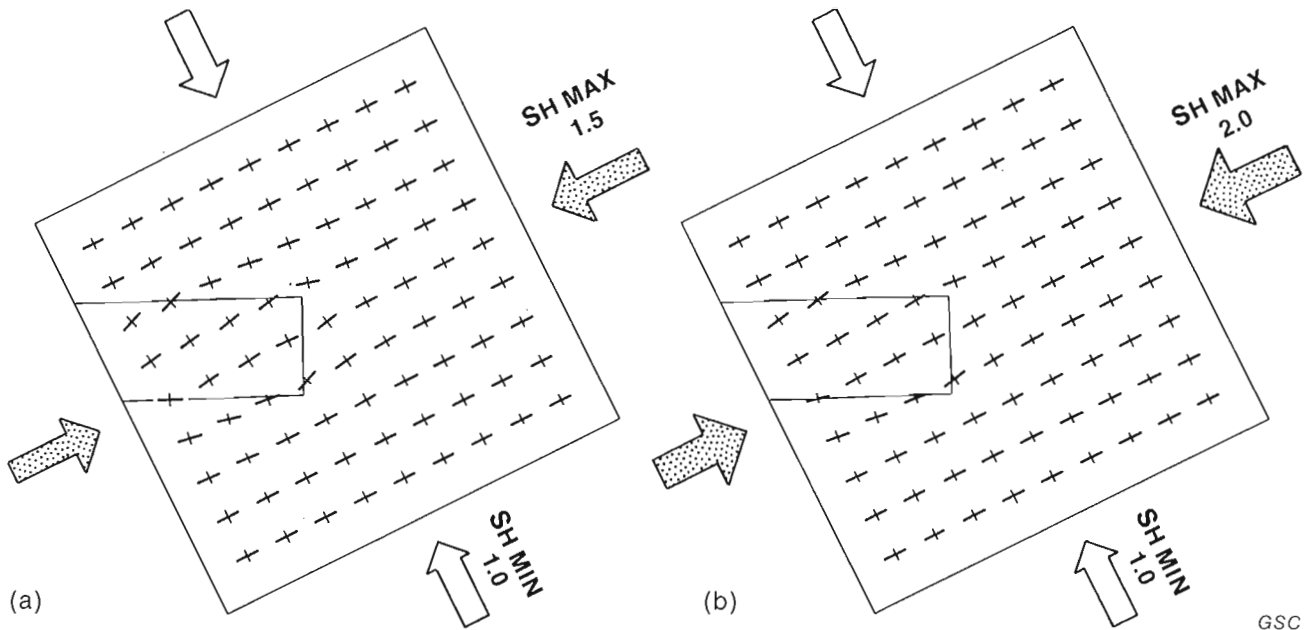


Figure 6. (a) Stress trajectories projected across Peace River Arch model with S_{Hmax} 50% larger than S_{Hmin} . (b) Stress trajectories projected across Peace River Arch model with S_{Hmax} twice as large as S_{Hmin} .

GSC

Following Bell and Gough (1979), the mean breakout axis is equated with the smaller horizontal stress, S_{Hmin} , and the larger horizontal principal stress, S_{Hmax} , is projected perpendicular to the mean breakout axis at the well location. In this way, the stress trajectory map (Fig. 3) was constructed. It portrays the interpreted compressive stress trajectories that are acting within the sedimentary section above and around the Peace River Arch, and refers largely to rocks buried between depths of 1000 and 2500 m.

Unfortunately, there is little information on stress magnitudes in the area. Kry and Gronseth (1982) used microfracturing techniques to measure S_{Hmin} between depths of 2073 and 2765 m in two wells in the Deep Basin immediately to the south of the Peace River Arch. They calculated the larger horizontal principal stress from the relationship: $H_{max} = 3H_{min} - P_r - P_o$, where P_r is the fracture opening pressure and P_o the pore pressure in the rock (Bredehoeft et al., 1976). The vertical principal stress was equated to an overburden load that increased at 25 megapascals per kilometre (Fig. 4). The measured and estimated values for the two horizontal principal stresses gave Kry and Gronseth (op. cit.) an $S_{Hmax}:S_{Hmin}$ ratio ranging from 1.3:1 to 1.6:1 and averaging 1.5:1. It is the ratio between the principal horizontal stresses, rather than their absolute values, that determines how stress trajectories are refracted by lateral contrasts in the properties of compressed materials.

Modelling

In order to test the hypothesis that the refraction of stress trajectories observed in the Peace River Arch area is caused by contrast in elastic properties between the basement and sediments, we considered an elastic plate with a built-in contrast in elastic properties. For simplicity, we have modelled

a plate composed of carbonates surrounding an angled, rectangular block of granite (Fig. 5) and assigned values of E (Young's Modulus) and σ (Poisson's Ratio) based on average measured values for rock samples (Clark, 1966). This represents a simplified simulation of a plate that lies largely within Paleozoic rocks and cuts the Precambrian core of the Peace River Arch. The plate represents a thin horizontal slice and allows the problem to be treated in two dimensions, which simplifies the stress analysis. A plane stress condition is assumed because the active tectonic stresses are horizontal, approximately in the plane of the model. The stress-strain relationship is assumed to be linear and the simplified elasticity equations are solved using the finite element method. In simulation A (Fig. 6a), boundary stresses are applied uniformly to the edges of the plate in the ratio of 1.5:1. This induces stresses of the same magnitude and direction within the plate away from the granite region (Fig. 5) corresponding to the regional stress field, but within and around the granite region the directions are significantly different. There is clearly a qualitative similarity between the model stress trajectories and the observed configuration. In both there is an outward bending of the maximum stress around the Peace River Arch and an inward bending of the minimum stress to the east of the Arch. The model stress directions within the granite region cannot be compared directly with the observed directions because no stress directions were measured in basement.

The above model uses a stress ratio that we believe is close to that acting today. In a subsequent simulation (Fig. 6b) we applied stresses to the edge of the plate in a ratio of 2:1, higher than observed. The resulting stress trajectories show much less refraction around the granite body, demonstrating that the smaller the ratio of horizontal principal stresses, the greater may be their deflection across areas with lateral variations in the elastic properties of the stressed rocks.

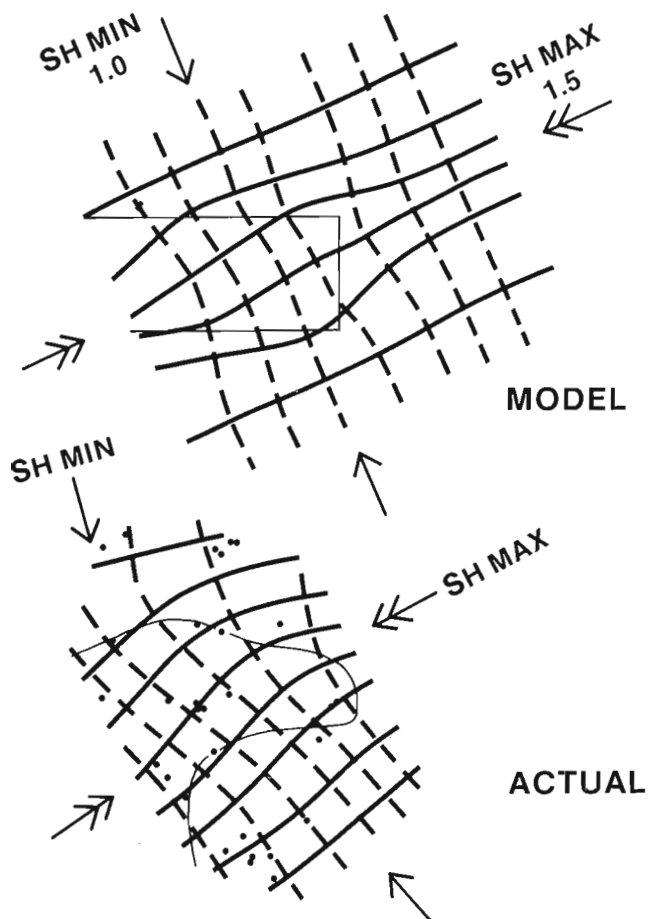


Figure 7. Comparison between modelled and actual horizontal principal stress trajectories across the Peace River Arch.

A comparison between the modelled stress trajectories when the $S_{Hmax}:S_{Hmin}$ ratio is 1.5:1 and the interpreted orientations is shown in Figure 7. There is sufficient similarity to support the hypothesis that contrasts in the elastic properties of rocks around the Peace River High are the cause of the observed deflection of stress trajectories.

IMPLICATIONS

The results reported above are very clearly tentative first steps in modelling stress trajectories in the Western Canadian Basin. The technique has been used to elucidate fault and fracture geometry in deformed zones (e.g. Hafner, 1951; Odé, 1957) but, until the recognition of breakouts as stress orientation indicators (Bell and Gough, 1979), there has not been enough information to delineate regional compressional axes, recognise anomalous areas, or map stress orientations in sufficient detail to encourage controlled modelling.

In the case of the Peace River Arch, further development of this model will need to include a three-dimensional analysis. The three-dimensional model would have similar horizontal dimensions to the two-dimensional model, and the vertical dimension would correspond to the thickness of the elastic lithosphere that is able to transmit elastic stresses.

The basement surface would be approximated by the triangular sides of tetrahedral finite elements, based on depth to basement maps. Stresses would be applied to the sides of the block as in the two-dimensional model. Individual wells could be located in the model and predicted breakout azimuths along the lengths of these wells could be derived. This would allow a more complete comparison between the model and the actual stresses. It would also indicate whether vertical changes in stress directions over basement highs should be expected. More refined estimates of the elastic properties of the sedimentary section and basement should also be made from well logs and seismic studies. Obviously, a greater density of horizontal stress orientation measurements is also desirable.

Clearly, models of this complexity have potential economic applications. Since hydraulic fractures form normal to the direction of the least principal stress (Hubbert and Willis, 1957), a three-dimensional model of stress trajectories in rocks overlying a basement high would be an invaluable tool for engineers planning to stimulate reservoirs by controlled induced fractures. This study also warns that one should be careful about extrapolating expected hydraulic fracture orientation directions across basement highs since, over them, in-situ stress directions may not conform to regional trends, and fractures may occur in unexpected directions. Moreover, the same phenomenon may also occur around other structures that exhibit lateral changes in elastic properties, such as faults, domes, or intrusions. Our results may also be relevant to the interpretation of petrofabric analyses in terms of paleostress directions. If lateral changes in rock type give rise to changes in elastic properties, the local petrofabric may not indicate the true direction of regional stresses active at the time the rock was deformed.

What is more alarming to consider is that, if principal stress magnitude contrasts were low, a rather negligible lateral variation in elastic response might produce a significant orientation change in compressional features such as fold axes. Paleostress deflection around boudins is well recognized, but other, larger-scale, "salients" are not usually attributed to elasticity contrasts.

ACKNOWLEDGMENTS

The authors are most grateful to A.M. Jessop and D.N. Skibo for reviewing the manuscript and suggesting improvements, to Claudia Thompson for typing the text and to G.M. Grant for drafting the figures.

REFERENCES

- Bell, J.S. and Gough, D.I.
1979: Northeast-southwest compressive stress in Alberta: evidence from oil wells; *Earth and Planetary Science Letters*, v. 45, p. 475-482.
- Bell, J.S. and Babcock, E.A.
1986: The stress regime of the Western Canadian Basin and implications for hydrocarbon production; *Bulletin of Canadian Petroleum Geology*, v. 34, p. 364-378.
- Bredehoeft, J.D., Wolff, R.G., Keys, W.S., and Shuter, E.
1976: Hydraulic fracturing to determine the regional in-situ stress field, Piceance Basin, Colorado; *Geological Society of America, Bulletin*, v. 87, p. 250-258.

- Clark, S.P., Jr.**
1966: Handbook of Physical Constants; Geological Society of America, Memoir 97, 587 p.
- Fordjor, C.K., Bell, J.S., and Gough, D.I.**
1983: Breakouts in Alberta and stress in the North American plate; Canadian Journal of Earth Sciences, v. 20, p. 1445-1455.
- Gough, D.I. and Bell, J.S.**
1981: Stress orientations from oil well fractures in Alberta and Texas; Canadian Journal of Earth Sciences, v. 18, p. 638-645.
- Hafner, W.**
1951: Stress distributions and faulting; Geological Society of America, Bulletin, v. 62, p. 373-398.
- Hubbert, M.K. and Willis, D.G.**
1957: Mechanics of hydraulic fracturing; AIME Petroleum Transactions, v. 210, p. 153-166.
- Kry, P.R. and Gronseth, J.M.**
1982: In situ stresses and hydraulic fracturing in the Deep Basin; 33rd Annual Technical Meeting of the Petroleum Society of the Canadian Institute of Mining and Metallurgy, Paper 82-33-21, Calgary, Canada, June 6-9, 1982.
- McCrossan, R.G. and Glaister, R.P. (editors)**
1964: Geological history of Western Canada; Alberta Society of Petroleum Geologists, 232 p.
- Odé, H.**
1957: Mechanical analysis of the dike pattern of the Spanish Peaks area, Colorado; Geological Society of America, Bulletin, v. 68, p. 567-578.
- Podruski, J.A., Barclay, J.E., Hamblin, A.P., Lee, P.J., Osadetz, K.G., Procter, R.M., Taylor, G.C., Conn, R.F., and Christie, J.A.**
1988: Conventional oil resources of Western Canada (light and medium); Geological Survey of Canada, Paper 87-26, 149 p.
- Porter, J.W., Price, R.A., and McCrossan, R.G.**
1982: The Western Canadian Sedimentary Basin; in The Evolution of Sedimentary Basins, P.E.Kent, M.H.P. Bott, D.P. MacKenzie and C.A. Williams (eds.); Royal Society, London, 338 p.

Geology of the northern Solitude Range, Western Rocky Mountains, British Columbia

L.P. Gal¹, E.D. Ghent¹, and P.S. Simony¹

Gal, L.P., Ghent, E.D., and Simony, P.S., *Geology of the northern Solitude Range, Western Rocky Mountains, British Columbia*; in *Current Research, Part D, Geological Survey of Canada, Paper 89-1D*, p. 55-60, 1989.

Abstract

The Porcupine Creek Anticlinorium (PCA) is the dominant structural feature of the northern Solitude Range. Cambrian Gog Group strata unconformably overlie the middle Miette Group in broad, upright folds in the core of the PCA. Cambrian Chancellor Group strata on the western flank of the PCA form overturned folds and have been affected by two phases of deformation, in contrast to the older rocks exposed in the core of the PCA. A décollement at the base of the Chancellor Group is inferred to have been active early in the development of the anticlinorium. Metamorphic grade increases east to west from chlorite-chloritoid zone to kyanite zone. Microtextural observations suggest that the peak of metamorphism occurred during late deformation to post latest deformation (defined by a crenulation cleavage).

Résumé

L'anticlinorium de Porcupine Creek (APC) est l'élément structural dominant dans le nord des monts Solitude. Les couches du groupe cambrien de Gog recouvrent de façon discordante le groupe intermédiaire de Miette en formant de larges plis droits au centre de l'APC. Les couches du groupe cambrien de Chancellor sur le flanc ouest de l'APC font partie de plis renversés et ont subi deux phases de déformation, contrairement aux roches plus anciennes qui sont exposées au centre de l'APC. Un décollement à la base du groupe de Chancellor aurait été actif au début de la formation de l'anticlinorium. Le degré de métamorphisme augmente d'est en ouest depuis une zone de chlorite-chloritoïde jusqu'à une zone kyanite. Des observations sur la microstructure indiquent que le métamorphisme a été le plus intense vers la fin de la période de déformation et après la dernière (tel qu'indiqué par le clivage le long des microplis).

¹ Department of Geology and Geophysics, University of Calgary, Calgary, Alberta T2N 1N4.

INTRODUCTION

During the field seasons of 1987 and 1988, the Porcupine Creek Anticlinorium (PCA) was mapped at 1:20 000 scale in the northern Solitude Range of the Western Rocky Mountains (Figs. 1, 3). This area lies within the northwest part of the Rogers Pass map area, (82 N/W 1/2), mapped by Wheeler (1963). Laboratory work included petrographic examination of thin sections, and electron microprobe and X-ray diffraction analysis of samples.

REGIONAL GEOLOGY

The western Rocky Mountains are composed of Upper Proterozoic and lower Paleozoic miogeoclinal metasediments. These are separated from the more highly metamorphosed and deformed rocks of the Selkirk Mountains by the Rocky Mountain Trench (RMT) (Simony et al., 1980). The Purcell Thrust follows the trace of the RMT, and truncates the western flank of the PCA (Price and Mountjoy, 1980). It is offset by the west-side down Chancellor normal fault (Meilliez, 1972; Ferri, 1984).

The PCA, a gently southeast plunging fold complex, imparts a southeast trending structural grain to the area. Foliations and axial planes of minor folds fan across the anticlinorium, dipping northeast on the west flank of the structure, and southwest on the east flank. In the Solitude Range, the PCA is outlined by the competent Gog Group, and is box-like in profile (Meilliez, 1972).

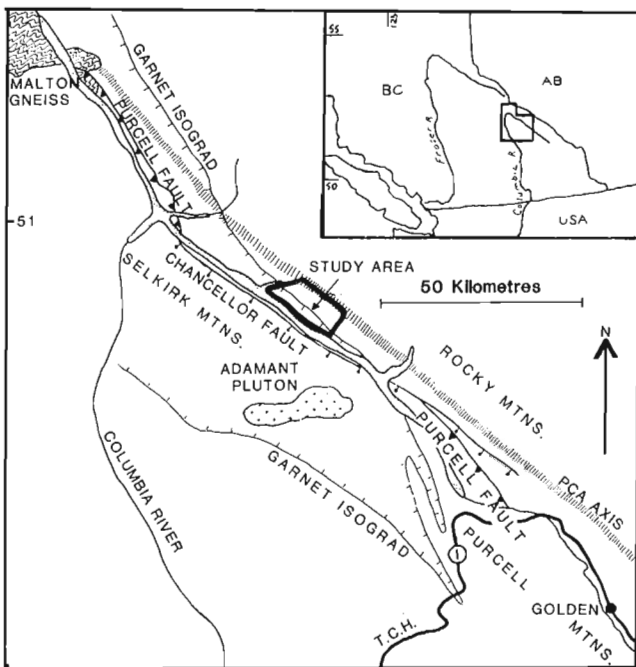


Figure 1. Geological map of the western Rocky Mountains, British Columbia, and location of the northern Solitude Range.

STRATIGRAPHY

The stratigraphic sequence extends from the Proterozoic (Windermere) Miette Group to the Middle Cambrian Chancellor Group (Fig. 2). The oldest Miette strata, exposed in cirques south of Sophist Mountain, comprise at least 400 m of monotonous, coarse quartz and quartzo-feldspathic pebble and granule conglomerates ("grits") with thin siltstone interbeds. Above these grits are approximately 300 m of grey-green and brownish slates. Lensoidal grit beds up to 30 m thick occur in the slate unit near the Gog contact. In the Sullivan River valley, no slate unit is present, and fine granule conglomerates lie directly beneath the Gog Group. Comparison with the Miette Group of the Jasper area (Mountjoy, 1962; McDonough and Simony, 1984) suggests that the contact is a major unconformity. The thick grit unit probably belongs to the middle Miette Group, hence some 2000 m of upper Miette Group slate, siltstone and carbonate are missing. Locally, the unconformity truncates grit beds.

The three formations of the Gog Group (Mountjoy, 1962) have been recognized in the Solitude Range. The lowermost McNaughton Formation is 300 m thick and consists predominantly of quartzite. It is characterized by a 90

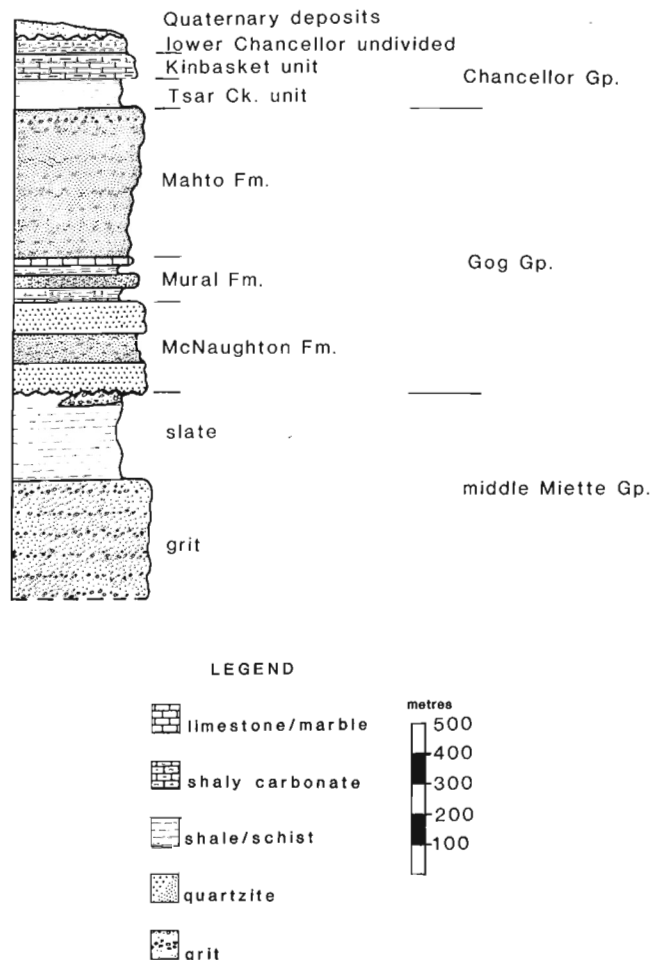


Figure 2. Generalized stratigraphic section, northern Solitude Range.

m thick basal unit of white quartzite. Overlying the McNaughton is the recessive Mural Formation, comprising 150 m of slate, carbonate and minor quartzite. It is capped by 15 m thick *Archeocyathid*-bearing limestone. The topmost Mahto Formation consists of approximately 550 m of interbedded slate and quartzite, with minor carbonate near the top. The westernmost Mahto Formation is more pelitic than in exposures in the core of the PCA. The upper 50 m contains metre-thick grit units and interbedded quartzite and pelite. Consequently, the Mural Formation and overlying Mahto Formation of the western Rockies closely resemble the Donald Formation of the northern Purcell Mountains (Wheeler, 1963) and we propose that they are correlative and continuous.

The Gog Group is overlain by the lower Chancellor Group, informally divided into the Tsar Creek and the Kinbasket units by Fyles (1960). The Tsar Creek unit is a dark grey pelite with thin carbonate laminae. It grades upward into the Kinbasket unit, a blue-grey, laminated, micritic limestone. Overlying the limestone are tan weathering calcareous slates and platy limestones assigned to the undivided lower Chancellor Group. Stratigraphic thicknesses are difficult to estimate due to extreme deformation, but are about 100 m for the Tsar Creek and 150 m or more for the Kinbasket unit (Meilliez, 1972).

Alkalic dykes (syenites and monzo-syenites) intrude the Kinbasket unit northwest of Caribou Creek. A small plug of syenite and nepheline syenite intruding the Mahto and Mural formations was exposed south of the mouth of the Sullivan River prior to flooding of Kinbasket Lake. These bodies display a foliation that is parallel to the cleavage in the limestone and pelites, and have been recrystallized. They may be related to the Late Devonian Ice River intrusions (Currie, 1975).

Bedding-parallel amphibolite layers, locally garnet-bearing, occur in western exposures of the Mahto Formation. These range from a few centimetres to 2 m in thickness.

STRUCTURE

Both the western flank and the central core of the PCA are exposed in the study area (Fig. 3). The core of the anticlinorium is composed of a pair of large, upright, cylindrical anticlines with an intervening syncline. Fold plunges are at low angles, both to the northwest and southeast. Late, steep faults, with throws of several hundred metres, cut the limbs of these folds (Fig. 4). These faults likely permitted the continued rise of the anticlinorium after ductile deformation had ceased.

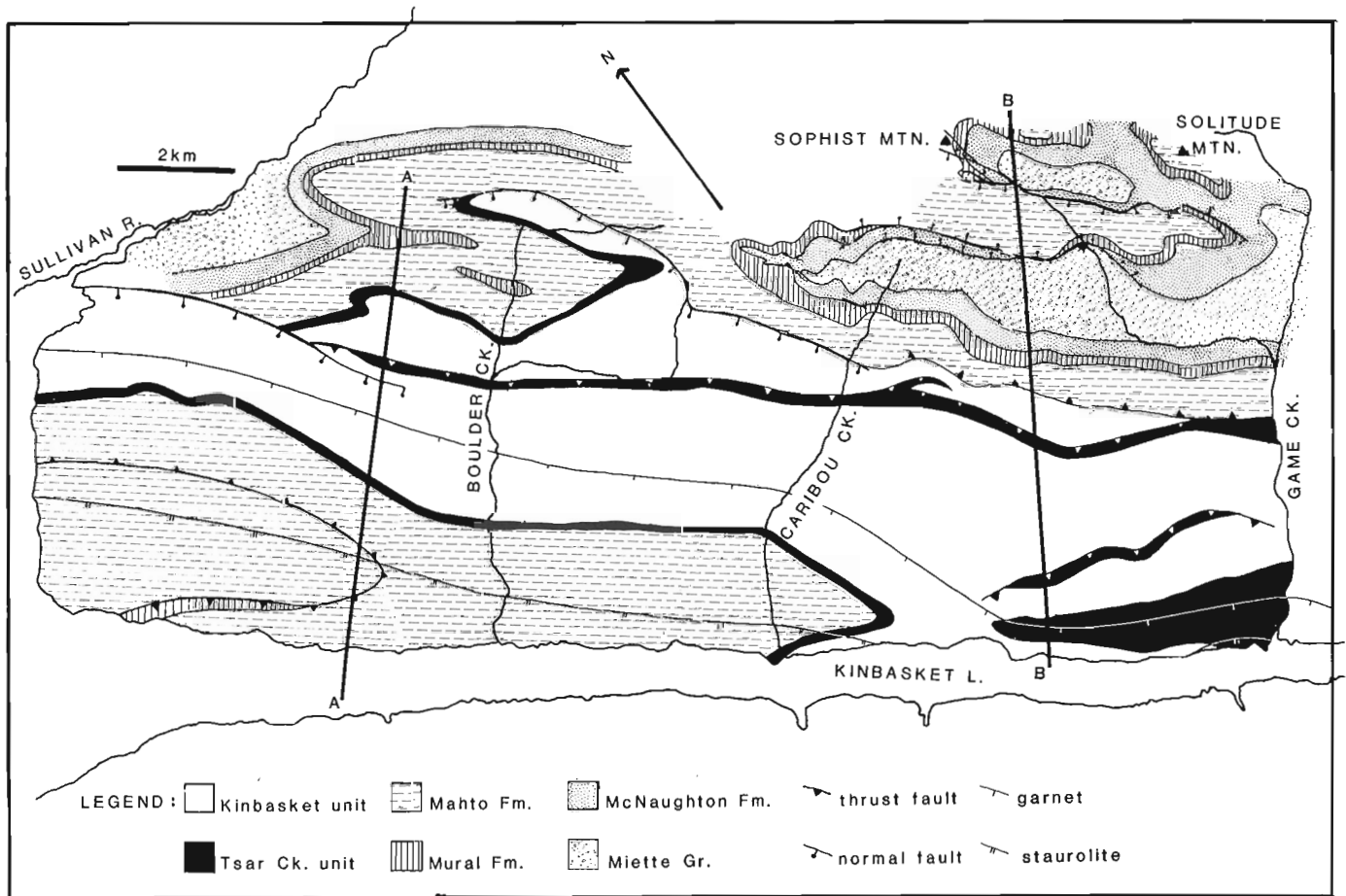


Figure 3. Geological map of the northern Solitude Range. The kyanite isograd and fold axial traces are omitted for clarity.

A single axial planar cleavage is present in all the divisions of the Gog and Miette groups in the core of the PCA. The Mural Formation also shows only one cleavage, but had a more ductile response to deformation than the adjacent quartzites. Locally, the Mural strata are sheared and strongly folded, and the formation apparently acted as a layer of high ductility between the competent McNaughton and Mahto formations (Meilliez, 1972).

The Chancellor Group is exposed on the western flank of the anticlinorium. Evidence of two phases of deformation is apparent in the Chancellor strata, and in Mahto strata in a northeast overturned anticline on the distal, southwest flank of the PCA. The early foliation or cleavage (S_1) in these rocks is parallel to bedding. S_1 cleavage is folded both on a mesoscopic and a microscopic scale, and a spaced crenulation cleavage (S_2) is developed. S_2 is axial planar to minor folds. The two cleavages are associated with two styles of mesoscopic folding observed in the Tsar Creek and Kinbasket units. The F_1 folds are isoclinal, exhibiting stretched limbs and thickened hinges. These are locally

refolded by more open, chevron or angular F_2 folds. Boudins formed in competent beds and amphibolites during the first phase of deformation were folded by F_2 folds.

Generally, the Chancellor and Gog groups display different degrees and styles of deformation. This is in part due to the relative competencies of the rock types involved; however, the presence of refolded folds and two cleavage fabrics in the Chancellor Group indicate that this package underwent an earlier phase of deformation, when, it is inferred, a décollement was activated near the base of the Tsar Creek unit (Ferri, 1984). Thus the S_2 cleavage in the Chancellor Group and western exposures of the Mahto Formation may correlate temporally with the single cleavage in the PCA core (Fig. 6).

In the slopes immediately east of Kinbasket Lake, a northeast-overturned anticline (Fyles, 1960; Wheeler, 1963) exposes Mahto Formation from Cariboo Creek northward across the Sullivan River (Fig. 3). Grit-bearing upper Mahto beds occur immediately adjacent to the overlying Tsar Creek pelites, and are repeated in the core of the

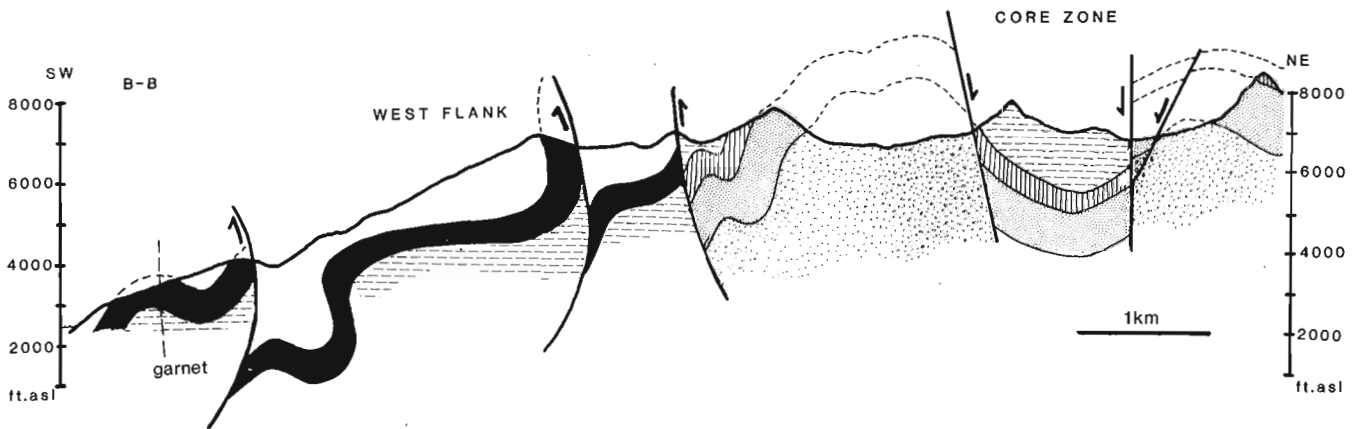


Figure 4. Schematic cross-section B-B (section line indicated on Figure 3). Stratigraphic patterns correspond to legend on Figure 3.

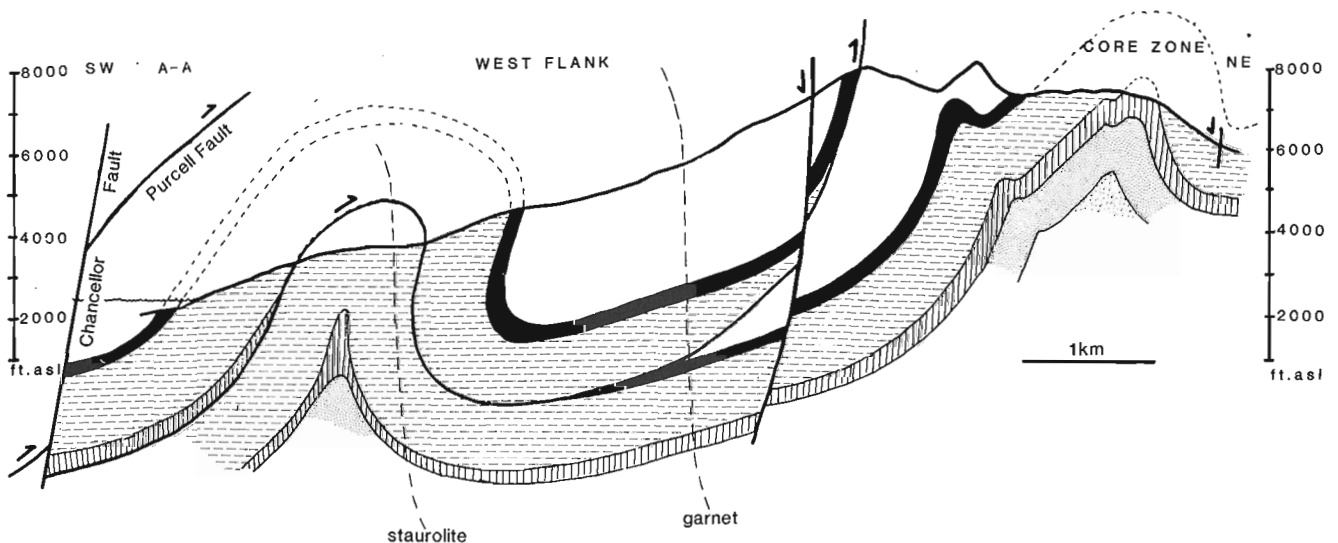


Figure 5. Schematic cross-section A-A (section line indicated on Figure 3). Stratigraphic patterns correspond to legend on Figure 3.

fold. A pure marble, corresponding to the upper Mural Formation, was mapped by one of us (P.S.S.) prior to the 1973 flooding of Kinbasket Lake. This Mural marble structurally overlies upper Mahto Formation grit, pelite and quartzite. These relationships, in conjunction with the excessive thickness of Mahto Formation exposed in the core of the anticline, indicate that the Mahto Formation is duplicated by a thrust fault that is now folded (Fig. 5). The fault must underlie the syncline to the east, cored by Kinbasket limestone, and pass upward and eastward into the décollement at the base of the Tsar Creek unit. The overlap of Mahto on Mahto suggests a minimum dip slip of some 4 km.

METAMORPHISM

The metamorphic grade increases from east to west in the study area, toward a metamorphic high in the Selkirk Mountains west of the RMT. The facies series is Barrovian, increasing from lower greenschist to lower amphibolite

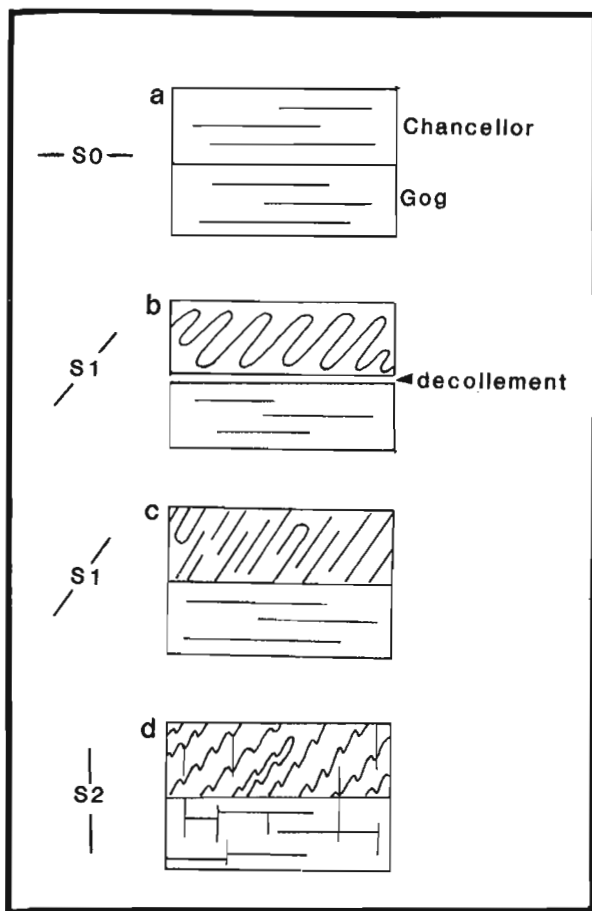


Figure 6. Schematic representation of the time relationship between structural fabrics of the Gog (and Miette) groups in the core of the PCA and Chancellor Group strata on the west flank. **a.** S_0 is original bedding prior to deformation; **b.** initiation of early, tight folding and foliation in Chancellor Group strata above a décollement; **c.** bedding is sheared parallel to foliation (S_0 parallel S_1); and **d.** initiation of S_2 crenulation cleavage in Chancellor Group strata, and cleavage in Gog Group rocks. Refolding of early layer-parallel folds in the Chancellor Group is illustrated.

Table 1. Mineral assemblages of pelites and calcipelites from metamorphic zones of increasing grade

Zone	Assemblage (+ Qtz + Ms + accessories)
Chl-Cld	1. Chl + Py 2. Chl + Cld +/- Czo
Grt	3. Chl + Cal + Bt + Ep 4. Chl + Cld + Czo + Grt + Pl 5. Cal + Czo + Bt + Pl + Grt + Ts 6. Bt + Grt + Pl
St	7. Pl + Grt + St +/- Chl, Cal, Ep 8. Bt + Grt + St +/- Pl
Ky	9. Grt + Ky +/- Pl, Bt 10. Grt + Bt + St + Ky + Pl
accessories	Dol, Ep, Gr, Ilm, Py, Rt, Tur, Zr

Mineral abbreviations (after Kretz, 1983)			
Bt	Biotite	Ky	Kyanite
Cal	Calcite	Ms	Muscovite
Chl	Chlorite	Pl	Plagioclase
Cld	Chloritoid	Py	Pyrite
Czo	Clinozoisite	Rt	Rutile
Dol	Dolomite	St	Staurolite
Ep	Epidote	Tur	Tourmaline
Gr	Graphite	Ts	Tschermakite
Grt	Garnet	Zr	Zircon
Ilm	Ilmenite		

facies, in which kyanite is the stable aluminosilicate. Typical pelitic assemblages from different zones are presented in Table 1. The first occurrences of garnet, staurolite and kyanite were mapped (Fig. 3). The isograds cut across lithological units, trend slightly obliquely to structural trends, and are apparently unfolded. They must postdate the early folded thrust that they overprint. The isograds are quite closely spaced, and their map pattern suggests that the isogradic surfaces dip steeply northeast.

Chloritoid is common in the low-grade slates, particularly in the Miette and Chancellor Group pelites. The chloritoid-forming reaction is enigmatic. X-ray diffraction analyses indicate that pyrophyllite and/or kaolinite, which might be expected to form chloritoid (Hoschek, 1969), are very rare or absent in the lowest grade slates. The preservation of chloritoid in garnet cores, while staurolite is present in the matrix, suggests that chloritoid was consumed in the production of staurolite, although direct replacement was not observed.

The first appearance of biotite is spotty, and could not be continuously mapped. Bulk composition probably restricted crystallization of biotite. It is uncommon in the aluminous Tsar Creek unit and does not coexist with chloritoid.

Near the garnet isograd, highly aluminous amphiboles occur in the Tsar Creek calc-schists. These ferrotschermakites (Leake, 1978) are rare in pelites and are probably due to the high Al and Ca content of the Tsar Creek unit (cf. Thompson and LeClair, 1987). The amphiboles are found in assemblages containing so many phases that equilibrium amongst them is doubtful.

In the staurolite zone, rutile pseudomorphs replace ilmenite as the dominant oxide, suggesting that ilmenite reacted with Al-Si phases to produce staurolite + rutile (see also Craw, 1978). Garnet zoning profiles from staurolite-bearing pelites support this interpretation, as they show a distinct drop in the almandine component toward their rims. Kyanite occurs more commonly in quartz veins and pegmatitic pods within schists than in the matrix.

Garnet-biotite (Ferry and Spear, 1976) and calcite-ferrous dolomite thermometry (Anovitz and Essene, 1987) were used to explore for any temperature gradient preserved by assemblages throughout the area. Chloritoid-chlorite zone temperatures (from calcite-dolomite) range from 400 to 480°C, whereas garnet and staurolite zone temperatures (from garnet-biotite) range from 480 to 540°C. Stable existence of staurolite in the kyanite zone suggests that temperatures did not exceed 600°C (Carmichael, 1978, and written comm.). Chlorite-chloritoid grade aluminous pelites of the Chancellor Group some 12 km southeast of the Solitude Range were studied by Ghent et al. (in press). They estimated equilibration temperatures of 345°C, which can be considered a minimum for the lower grade rocks of the Solitude Range.

Pressures were estimated from plagioclase — Al₂SiO₅ — garnet equilibria (Ghent, 1976; Ghent et al., 1979), giving a spread from 450 to 900 MPa. Garnet-plagioclase-muscovite-biotite equilibria (Ghent and Stout, 1981) yielded results in a somewhat narrower range: 450 to 750 MPa. The wide ranges are probably due to inhomogeneities in feldspar compositions on the microscopic intergrain and intragrain scale, perhaps due to peristerite exsolutions. Craw (1978) estimated pressures of 500 MPa in the Park Ranges about 45 km to the northwest.

Throughout the study area, metamorphic crystallization seems to have been initiated before, and to have outlasted the latest deformation (i.e., crenulation foliation). In low grade slates, porphyroblasts have grown after the last deformation; in the highest grade schists, only staurolite, kyanite and garnet rims have porphyroblast-matrix microfabrics that indicate syn- and post-tectonic growth. The peak conditions were syn- and post-D₂, as is evident from kyanite blades that overprint S₂ schistosity but are locally kinked by it. Evidently, the conduction of heat through the area proceeded more slowly than the D₂ deformation associated with the PCA development.

Movement on the décollement at the base of the Chancellor Group, the folded thrust, and other F₁ deformation structures, predated the peak metamorphism. Folding associated with the PCA (e.g., broad folds in the core) was well underway during the peak of metamorphism, although the overturning of folds on the western flank may have occurred later. Steep faults in the core of the PCA, and the Purcell and Chancellor faults, are postmetamorphic structures.

ACKNOWLEDGMENTS

A. Silas and C. Velu provided assistance in the field. Fieldwork was supported by EMR contract 69-4981 to Simony,

and laboratory work by NSERC grant A-4379 to Ghent. M. McMechan and T. Gordon reviewed the manuscript. S. Digel reviewed earlier drafts.

REFERENCES

- Anovitz, L.M. and Essene, E.J.**
1987: Phase equilibria in the system CaCO₃-MgCO₃-FeCO₃; *Journal of Petrology*, v. 28, p. 389-411.
- Carmichael, D.M.**
1978: Metamorphic bathozones and bathograds: a measure of the depth of post-metamorphic uplift and erosion on the regional scale; *American Journal of Science*, v. 278, p. 769-797.
- Craw, D.**
1978: Metamorphism, structure and stratigraphy in the southern Park Ranges (Western Rocky Mountains), British Columbia; unpublished M.Sc. thesis, University of Calgary, 140 p.
- Currie, K.L.**
1975: The geology and petrology of the Ice River Alkaline Complex, British Columbia; *Geological Survey of Canada, Bulletin 245*.
- Ferri, F.**
1984: Structure of the Blackwater Range, British Columbia; unpublished M.Sc. thesis, University of Calgary, 143 p.
- Fyles, J.T.**
1960: Geological reconnaissance of the Columbia River between Bluewater Creek and Mica Creek, British Columbia; British Columbia Minister of Mines, Annual Report, 1959, p. 90-105.
- Ghent, E.D.**
1976: Plagioclase-garnet-Al₂SiO₅-quartz: a potential geobarometer; *American Mineralogist*, v. 61, p. 710-714.
- Ghent, E.D., Robbins, D.B., and Stout, M.Z.**
1979: Geothermometry and geobarometry of metamorphosed calciliculates and pelites, Mica Creek, British Columbia; *American Mineralogist*, v. 64, p. 874-895.
- Ghent, E.D. and Stout, M.Z.**
1981: Geobarometry and geothermometry of plagioclase-biotite-garnet-muscovite assemblages; *Contributions to Mineralogy and Petrology*, v. 76, p. 92-97.
- Ghent, E.D., Stout, M.Z., and Ferri, F.**
in Chloritoid-paragonite-pyrophyllite and stilpnomelane bearing rocks near Blackwater Mountain, Western Rocky Mountains, British Columbia.
- Hoschek, G.**
1969: The stability of staurolite and chloritoid and their significance in metamorphism of pelitic rocks; *Contributions to Mineralogy and Petrology*, v. 22, p. 208-232.
- Kretz, R.**
1983: Symbols for rock-forming minerals; *American Mineralogist*, v. 68, p. 277-279.
- Leake, B.E.**
1978: Nomenclature of amphiboles; *Canadian Mineralogist*, v. 16, p. 501-520.
- Meilliez, F.**
1972: Structure of the southern Solitude Range, British Columbia; unpublished M.Sc. thesis, University of Calgary, 112 p.
- Mountjoy, E.W.**
1962: Mount Robson (southeast) map-area; Rocky Mountains of Alberta and British Columbia; *Geological Survey of Canada, Paper 61-31*.
- Price, R.A. and Mountjoy, E.W.**
1970: Geological structure of the Canadian Rocky Mountains between Bow and Athabasca Rivers — a progress report; *Geological Association of Canada, Special Paper 6*, p. 7-26.
- Simony, P.S., Ghent, E.D., Craw, D., Mitchell, W., and Robbins, D.B.**
1980: Structural and metamorphic evolution of the northeast flank of the Shuswap Complex, southern Canoe River area, British Columbia; *Geological Society of America, Memoir 153*, p. 445-461.
- Thompson, P.H. and Leclair, A.D.**
1987: Chloritoid-hornblende assemblages in quartz-muscovite pelitic rocks of the Central Metasedimentary Belt, Grenville Province, Canada; *Journal of Metamorphic Geology*, v. 5, p. 415-436.
- Wheeler, J.O.**
1963: Rogers Pass map-area, British Columbia and Alberta (82 N W 1/2); *Geological Survey of Canada, Paper 62-32*.

**A preliminary report on stratigraphy and sedimentology of
the lower and middle Chancellor Formation
(Middle to Upper Cambrian) in the zone of facies transition,
Rocky Mountain Main Ranges, southeastern British Columbia**

W.D. Stewart¹

Institute of Sedimentary and Petroleum Geology, Calgary

Stewart, W.D., A preliminary report on stratigraphy and sedimentology of the lower and middle Chancellor Formation (Middle to Upper Cambrian) in the zone of facies transition, Rocky Mountain Main Ranges, southeastern British Columbia; in Current Research, Part D, Geological Survey of Canada, Paper 89-1D, p. 61-68, 1989.

Abstract

The Middle to Upper Cambrian Chancellor Formation is the basinal equivalent of eight carbonate and clastic formations that accumulated on a broad platform to the east. On the basis of detailed stratigraphic and sedimentological studies, the sequence is divisible into at least seven major stratigraphic units in and near the zone of facies transition. All of these units are composed largely of fine grained, hemipelagic sedimentary rocks, and contain a variety of sedimentological features typical of deep-water carbonate slopes. These include peri-platform talus blocks, intraformational truncation surfaces, slide masses, submarine channels, debris flows, and graded calcarenites. Spectacular examples of these features occur in the basinal equivalents of the Eldon and Pika formations, which display large-scale slide surfaces truncating up to 150 m of platform margin and slope strata, channels up to 23 m deep, and megaconglomerates containing platform-derived blocks of Epiphyton boundstone ranging up to a few tens of metres across.

Résumé

La formation de Chancellor du Cambrien moyen à supérieur est l'équivalent bassinale de huit formations de carbonates et de roches clastiques qui se sont accumulées sur une grande plate-forme à l'est. Selon des études stratigraphiques et sédimentologiques détaillées, la série est divisible en au moins sept grandes unités à l'intérieur et à proximité de la zone de transition du faciès. Toutes ces unités sont en grande partie composées de roches sédimentaires hémipélagiques à grain fin et contiennent une variété de caractères sédimentologiques propres aux talus de carbonates des eaux profondes: bloc de talus de bordure de plate-forme, surfaces d'intra-formation tronquées, masses de déjection, chenaux sous-marins, coulées de débris et calcarénites classées. On trouve des exemples frappants dans les équivalents bassinaux des formations d'Eldon et de Pika qui comportent des surfaces de glissement très grandes qui tronquent jusqu'à 150 m de large de plate-forme, ainsi que des mégaconglomérats contenant des blocs de pierre de bornage Epiphyton provenant de la plate-forme et atteignant des dizaines de mètres de largeur.

¹ Department of Geology, University of Ottawa, and Ottawa-Carleton Geoscience Centre, Ottawa, Ontario, K1N 6N5

INTRODUCTION

The Middle to Upper Cambrian Chancellor Formation, in southeastern British Columbia, has long been recognized as the basal equivalent of eight, well documented, carbonate and clastic formations that were deposited on a broad, stable platform to the east. However, the stratigraphy and sedimentology of the formation have been little documented due to structural complexity, poor biostratigraphic control, and incomplete exposure of the platform-to-basin transition at most stratigraphic levels. As a result, four key aspects of Chancellor sedimentation remain to be clarified:

1. The paleogeographical context of the "Chancellor basin".
2. The stratigraphy and correlation of the Chancellor divisions recognized during regional mapping.
3. The sedimentology of the sequence.
4. The style of facies transition between the various Chancellor divisions and equivalent rocks on the platform.

This report summarizes the results of the 1987 and 1988 field seasons, during which the stratigraphy and sedimentology of the lower and middle Chancellor Formation were investigated in the zone of facies transition. Most of the study was concentrated in a core area immediately west of the continental divide in Yoho and Kootenay National parks (Fig. 1). This area coincides with the central complex belt of thrust faults and tight folds described by Cook (1975) along the boundary between the eastern and western Main Ranges of the southern Rocky Mountains. Reconnaissance work was also carried out as far northwest as Mt. Laussedat, and as far southeast as Mount Assiniboine Provincial Park and Tangle Peak (Fig. 1).

To date, 28 stratigraphic sections have been measured, comprising about 9 km of Chancellor and equivalent strata. About 250 rock specimens have been collected for petrographic study. These include a large number of allochthonous, platform-derived blocks, essential for reconstructing the composition of the now largely destroyed platform margin. A modest number of trilobites have also been collected, chiefly from the lower Chancellor. Attempts to recover acritarchs from selected samples proved unsuccessful due to the incipient metamorphism experienced by these rocks.

PREVIOUS WORK

The Chancellor Formation was initially named by Allan (1911, 1914) for a predominantly slate sequence exposed near Chancellor Peak, 19 km south of Field, British Columbia (Fig. 1). No measured type section was ever formally designated. Allan also assigned a limestone sequence exposed on nearby Mt. Dennis and Mt. Burgess to the Chancellor, which he considered to be of Late Cambrian age. In a later geological synthesis, however, North and Henderson (1954) recognized that the Chancellor was, in fact, the lateral equivalent of both Middle and Upper Cambrian strata to the east.

Cook (1970, 1975) established for the first time a basic three-fold, gross subdivision in the Chancellor for regional mapping purposes. He further subdivided the middle and upper Chancellor into two and three units, respectively. Cook's basic correlation of these units with the eastern platform sequence has been followed in Figure 2.¹

The essential structural elements of the study area have been summarized by Balkwill (1972) and Cook (1975). They are also illustrated on maps and cross-sections by Price and Mountjoy (1972), Cook (1975), Price et al. (1978a, 1978b, 1979), Leech (1979), and Balkwill et al. (1980).

With certain important exceptions, only scattered stratigraphic information was available from the Chancellor Formation prior to this study. Incomplete measured sections from various parts of the formation have been described by Deiss (1940), Rasetti (1951) and Aitken (in press). Of particular importance is McIlreath's (1977) detailed stratigraphic and sedimentological analysis of the basal equivalents of the Cathedral, Stephen and adjoining formations. These basal units form part of the lower Chancellor, as defined in this report.

REGIONAL PALEOGEOGRAPHICAL SETTING

Middle and Upper Cambrian sedimentation took place on a low-latitude, regionally east-west oriented, passive margin flanking the North American craton (Aitken, in press). In the region of the study area, sediments were deposited in three major environments (Aitken, 1966, 1978): 1. a shallow to moderately deep inshore basin, where sediments accumulated in distinct, but temporally shifting inner detrital and middle carbonate facies belts; 2. a peritidal shoal complex (outer margin of the middle carbonate belt), usually confined to a narrow zone a few tens of kilometres wide and apparently localized by a persistent, paleotopographic feature named the Kicking Horse Rim by Aitken (1971); and 3. an open basin, where Chancellor sediments were deposited in relatively deep water (outer detrital facies belt)².

The platform succession is characterized by large-scale sedimentary cycles (Grand Cycles of Aitken 1966, 1978), which are inferred to be the product of major, cyclical shifts in the boundary between the inner detrital and middle carbonate belts. Since the fine grained, deep-water carbonate sediments in the Chancellor would have been derived almost exclusively from the platform, these fundamental changes in the character of platform sedimentation should have had a profound influence on sedimentation in the basin.

¹ An alternate correlation proposed by McIlreath (1977) equated the lower middle Chancellor with the Field Member of the Eldon Formation. New lithostratigraphic and fossil evidence from this study, however, tends to support Cook's (1975) correlation.

² The configuration and tectonic setting of this basin remain controversial, and will not be discussed further in this report.

AGE		FOSSIL ZONES	WESTERN LITHOFACIES (COOK, 1975; AITKEN, IN PRESS; THIS REPORT)	EASTERN LITHOFACIES (AITKEN AND GREGGS, 1967; McLREATH, 1977; AITKEN, IN PRESS)			
UPPER CAMBRIAN	DRESBACHIAN	ELVINIA	OTTERTAIL FM.	LYELL FM.			
		DUNDERBERGIA					
		APHELASPIS					
		CREPICEPHALUS					
MIDDLE CAMBRIAN	CEDARIA	CEDARIA	UPPER CHANCELLOR	UPPER	UPPER	SULLIVAN FM.	
			MIDDLE	MIDDLE			
			LOWER	LOWER			
		MIDDLE CHANCELLOR	OKE UNIT	UNDIVIDED ELDON - PIKA - ARCTOMYS - WATERFOWL RIM CARBONATES	WATERFOWL FM.		
			DUCHESNAY UNIT		ARCTOMYS FM.		
		PARK UNIT	VERMILION SUB-UNIT		PIKA FM.		
			?		ELDON FM.		
			TOKUMM SUB-UNIT		FIELD MBR.		
		LOWER CHANCELLOR	BASINAL STEPHEN EQUIVALENT		WAPTA MBR.	WAPUTIK MBR.	STEPHEN FM.
			AMISKWI MBR.		NARAO MBR.		
			BASINAL CATHEDRAL EQUIVALENT (TAKAKKAW TONGUE)		CATHEDRAL FM.		
			NAISET FM.		MOUNT WHYTE FM.		
LOWER CAMBRIAN	BONNIA - OLENELLUS	GOG GROUP					
	NEVADELLA	GOG GROUP					
	FALLOTASPIS	GOG GROUP					

Figure 1. Locations of measured sections and geographic features in the study area.

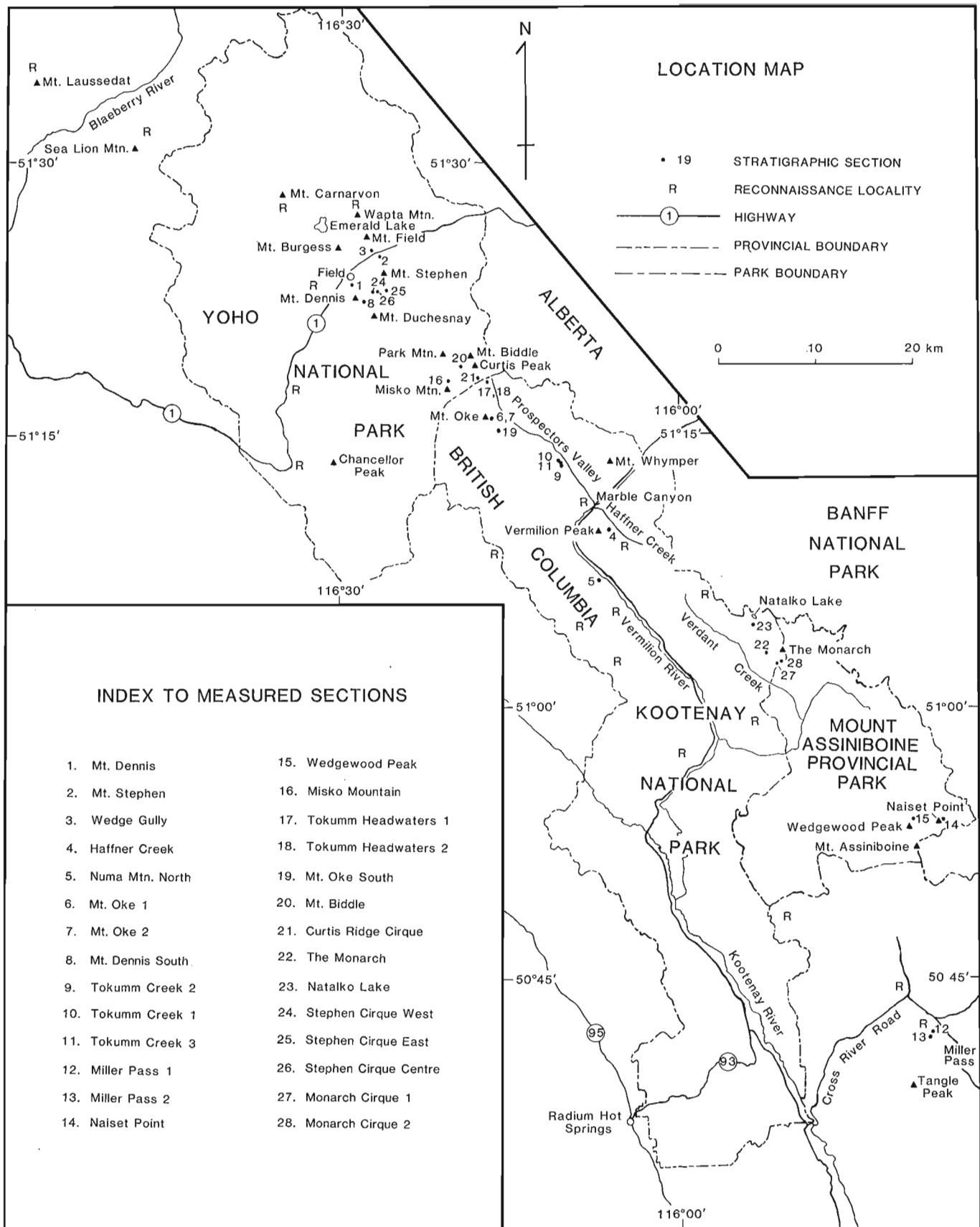


Figure 2. Correlation chart for stratigraphic units in the Chancellor (western lithofacies) and equivalent platform rocks (eastern lithofacies).

STRATIGRAPHIC NOMENCLATURE

The stratigraphy of the Chancellor is now well enough established in the study area to elevate its status to that of a group, composed of at least seven formations. Until this is formalized in print, however, informal nomenclature will be used for new stratigraphic units introduced below.

The lower Chancellor comprises four units in the zone of facies transition, listed as follows in ascending stratigraphic order (Fig. 2): 1. the basinal equivalent of the Mount Whyte Formation, named the Naiset Formation by Deiss (1940); 2. the basinal equivalent of the Cathedral Formation, named the Takakkaw Tongue by Aitken (in press)¹; 3. the basinal equivalent of the Stephen Formation, recently subdivided by Aitken (in press) into the Amiskwi and Wapta members²; and 4. the basinal equivalent of the undivided Eldon and Pika formations, informally referred to here as the Park unit³. The Park unit is further divisible into a lower Tokumm sub-unit, and an upper Vermilion sub-unit.

The overlying middle Chancellor is informally divided into the Duchesnay and Oke units⁴. These correspond, respectively, to the lower middle Chancellor and upper middle Chancellor subdivisions recognized by Cook (1975).

SUMMARY OF STRATIGRAPHIC AND SEDIMENTOLOGICAL OBSERVATIONS

Lower Chancellor

Naiset Formation

The Naiset Formation was named by Deiss (1940) from a type section at Naiset Point in Mount Assiniboine Provincial Park. The type section was remeasured as part of this study, together with six other sections at Naiset Point, Wedgewood Peak, The Monarch, Natacko Lake, Mt. Stephen and Mt. Field (Sections 2, 3, 14, 15, 22, 23, and 27; Fig. 1)⁵.

The thickness of the Naiset varies from 0 to more than 200 m, with values increasing basinward from the Kicking Horse Rim. The type section is about 150 m thick. All trilobites recovered from the formation during this and earlier studies have been referred to the *Plagiura* - '*Poliella*' Zone, indicating that the Naiset is correlative with the Mount Whyte Formation on the platform (Fig. 2).

The Naiset Formation unconformably overlies the Gog Group in all but one area, and is conformably and gradationally succeeded by the Cathedral Formation or its basinal equivalent, depending on locality. The exception is at The Monarch (Section 28, Fig. 1), where the Naiset conformably overlies and passes abruptly eastward into platform carbonate rocks assigned for mapping purposes to the Cathedral Formation. Where not destructively dolomitized,

this sequence is in a reef-flat facies strongly resembling that described by McIlreath (1977) immediately east of the Cathedral Escarpment on Mt. Stephen. In turn, the platform carbonates rest with angular unconformity on the Gog Group along the crest of the Kicking Horse Rim.

The dominant rock types in the Naiset Formation are monotonous, massive terrigenous mudstone and laminated shale. Laminated, crosslaminated or burrowed siltstone and fine grained sandstone are interlaminated at some horizons. Planar parted to ribbon limestone occurs at the base of the formation at The Monarch and Natacko Lake⁶. At both localities, it is separated from the main mudstone sequence by an interval containing huge peri-platform talus blocks and a series of debris flows (the latter containing megaclasts up to 12 by 13 m in size). Elsewhere in the formation, slide units characterized by syndimentary overfolds and homogenized beds are fairly common, as are smaller scale intraformational truncation surfaces.

The stratigraphic and sedimentological relationships observed at The Monarch suggest a striking parallel with the Cathedral Escarpment at Field. At The Monarch, an abrupt facies change is apparent, with a carbonate sequence in reef-flat facies on one side, and deep-water sediments containing huge blocks of peri-platform talus on the other. Hence, the platform margin was probably characterized at least locally by an escarpment during early Naiset time. This may have been a short-lived feature, however, in view of the absence of coarse, platform-derived material in the upper Naiset and overlying basinal Cathedral equivalent.

Basinal equivalent of Cathedral Formation

The basinal equivalent of the Cathedral Formation was thoroughly documented in the Field area by McIlreath (1977). Aitken (in press) later named this unit the Takakkaw Tongue, as it demonstrably thins westward into the basin. The only other locality where equivalent basinal rocks have been found in the study area is at The Monarch (Sections 22 and 27; Fig. 1).

At Section 22, the thickness of the basinal Cathedral (243 m) is almost identical to that at the type section designated by Aitken (in press) on Mount Stephen. However, there is insufficient lateral exposure to determine whether the sequence at The Monarch also thins basinward. No new fossils were collected, but the basinal Cathedral is known to range from the *Plagiura* - '*Poliella*' Zone to a point within the *Glossopleura* Zone on Mt. Stephen (Fritz, 1971; Fig. 2). The unit is succeeded conformably by argillaceous strata of the basinal Stephen equivalent.

At The Monarch, the basinal Cathedral is dominantly composed of monotonous, planar parted to ribbon limestone and its dolomitized equivalent. Internally deformed slide units occur at some levels, and intraformational truncation surfaces are very abundant in parts of the sequence. The unit is capped by a clast-supported debris flow containing both

¹ Previously the "thin Cathedral" of Fritz (1971) and McIlreath (1977).

² Previously the "thick Stephen" of Fritz (1971) and McIlreath (1977).

³ Named after Park Mountain (Fig. 1), one of the localities where this stratigraphic unit is exposed.

⁴ Names after Mt. Duchesnay and Mt. Oke (Fig. 1)

⁵ Sections 2, 3, 14 and 15 follow the same, or nearly the same, line of measurement as earlier sections measured by J.D. Aitken (Aitken, in press).

⁶ Planar parted limestones are predominantly thin bedded limestone sequences in which the beds are separated by relatively planar layers of dolomite, argillaceous dolomite, or shale up to 1 cm thick. In ribbon limestones, the intervening layers are more than 1 cm thick. Both facies are of relatively deep-water origin.

slope-derived lime mudstone and platform-derived grainstone clasts. Aside from this single occurrence, however, the abundant debris flows and peri-platform talus blocks seen in the Takakkaw Tongue at Field are conspicuously absent.

Basinal Equivalent of Stephen Formation

The basinal equivalent of the Stephen Formation was studied in detail on Mt. Stephen and Mt. Field by McIlreath (1977). Similar rocks occur at The Monarch, where only the lower 96 m of the sequence are exposed (Section 22, Fig. 1). By comparison, complete sections of the basinal Stephen equivalent near Field are about 275 m thick. In that area, the unit ranges from the upper *Glossopleura* Zone to the lower *Bathyriscus* - *Elrathina* Zone (Fritz, 1971; Fig. 2).

At The Monarch, the basinal Stephen is composed dominantly of laminated shale and massive, terrigenous mudstone. The argillaceous rocks commonly contain thin, spaced interbeds, lenticular interbeds and nodules of limestone. Many of these are structureless, but some are graded or laminated grainstone layers and starved ripple horizons. Thicker, intraclast grainstone beds occur in the lower part of the unit. The top of the exposure is dominated by a series of clast-supported debris flow units up to 3 m thick. These contain slope- and platform-derived clasts up to 0.7 by 2.8 m in size, set in a dolomitic argillite matrix.

Park Unit (Basinal equivalent of Eldon and Pika)

The Park unit incorporates the basinal equivalents of the Eldon and Pika formations. The unit is extensively exposed along Haffner Creek (Section 4), along the southwest wall of Prospectors Valley (Sections 9, 10, 11, 17 and 18), at Mount Biddle (Sections 20 and 21), on the northeast face of Park Mountain, and along the ridge connecting Mt. Stephen and Mt. Dennis (Sections 24, 25 and 26). The Park unit is conformably overlain by argillaceous rocks of the lower middle Chancellor (Duchesnay unit).

Along the full length of Prospectors Valley, the Park unit overlies clearly recognizable platform Cathedral, Stephen and lower Eldon strata. The lower Eldon consists of planar parted to ribbon limestone (the basal "black limestone band" widely recognized in the eastern Main Ranges), which is capped by a thin sequence of massive, burrow mottled limestone. Thicknesses of the recognizable Eldon sequence range from about 100 m to about 245 m, depending on locality.

The platformal, lower Eldon limestones are succeeded vertically by the Tokumm sub-unit, which consists of up to 180 m of dominantly planar parted to ribbon limestone and minor shale. Slide units, intraformational truncation surfaces, occasional thin debris flows, and rare peri-platform talus blocks of *Epiphyton* boundstone occur in the sequence. Agnostid trilobites from the middle and upper parts of the Tokumm sub-unit have been referred to the *Ptychagnostis gibbus* subzone of the *Bathyriscus* - *Elrathina* Zone (W.H. Fritz, unpublished report, 1987)¹.

The Tokumm sub-unit is in turn overlain by up to 250 m of mixed argillaceous and carbonate strata, the Vermilion sub-unit. The sequence is composed largely of intercalated shale and ribbon limestone. Internally deformed slide units of all scales are common, and the sequence is punctuated throughout by relatively thin (less than 2-3 m) debris flow units. In Section 11, large-scale channels with up to 23 m of intraclast - ooid grainstone fill are incised into the underlying shales. Even more impressive, however, are thick megaconglomerate units in the upper part of the sequence. These contain blocks of *Epiphyton* boundstone ranging up to a few tens of metres across, surrounded by a matrix of argillaceous dolomite and poorly sorted, slope- and platform-derived clasts. The megaconglomerates are inferred to be the deposits of major debris flows generated by platform margin collapse.

Collectively, the debris flows, channels, slide masses, and occasional peri-platform talus blocks in the Vermilion sub-unit all appear, from a distance, as a series of "grey bodies" encased in brown weathering, dolomitic shale and argillaceous limestone. The sub-unit thus forms a distinctive marker that can be traced through much of the study area.

The Eldon-Pika platform margin was probably characterized by a low-angle, carbonate ramp. Exceptional exposures along the Stephen - Dennis ridgeline and at two other localities indicate that this feature was subject to large-scale, periodic failure.

In the eastern part of the Stephen Cirque (Section 25), horizontally bedded dolomites of the upper Eldon Formation (above the Field Member) are truncated by a large-scale slide surface, which is overlain by a thick sequence of deep-water argillites and ribbon carbonates assigned to the Vermilion sub-unit. The surface cuts at least 0.5 km eastward into the platform sequence, and a minimum of 150 m of platform strata are missing. A comparable feature is also present at the same stratigraphic level in the headwaters of Verdant Creek. A third slide surface, in a slightly more basinward position, truncates about 100 m of lower Eldon equivalent strata near Mt. Biddle (Section 20). The existence of these large-scale slide scars provides a plausible explanation for the origin of megaconglomerates and other coarse, platform-derived debris in the basinal sequence.

Middle Chancellor

Duchesnay unit

Strata belonging to the lower middle Chancellor have been informally assigned to the Duchesnay unit (Fig. 2). Complete and relatively undeformed sections of this unit are present on Mt. Dennis (Sections 1 and 8, Fig. 1). Elsewhere in the study area, the Duchesnay unit is invariably strongly deformed or poorly exposed. Partial sections have, however, been measured at Haffner Creek, Mt. Oke, Numa Mountain and Miller Pass (Sections 4, 19, 5 and 13). The sequence is about 400 m thick at Mount Dennis, and is conformably and gradationally overlain by the Oke unit (upper middle Chancellor).

¹ It is noteworthy that fauna belonging to the same subzone are also characteristic of the Field Member of the Eldon Formation (W.H. Fritz, personal communication).

No fossils were found in the core part of the study area, aside from unidentifiable agnostid trilobites at Misko Pass. At the extreme southeastern end of the study area near Miller Pass, however, a large number of trilobites referable to the *Bolaspidella* Zone were recovered from beds tentatively assigned to the basal part of the Duchesnay unit. A trilobite from the same zone was also recovered from talus in the Numa Mountain section, but its source could not be identified. At present, the unit is tentatively correlated with the Arctomys Formation on the platform (Fig. 2).

The Duchesnay unit is lithologically heterogeneous. The sequence is dominantly composed of argillaceous rocks with frequent intercalations of ribbon to planar parted limestone generally measuring less than 3-4 m in thickness. Lenses and thin interbeds of ooid- intraclast grainstone and packstone occur sporadically in the limestones. Thin, clast- and matrix-supported limestone conglomerates (debris flow units), containing predominantly slope-derived clasts, are particularly abundant in the lower half of the unit.

Oke unit

The upper Middle Chancellor, informally named the Oke unit in this report, is well exposed from Mount Dennis southeastward to Prospectors Valley. Elsewhere, the unit tends to be strongly deformed. Complete sections have been measured at Mt. Oke and Misko Mountain (Sections 7 and 16, together with a supplementary section at locality 19), and an incomplete section has been measured on the south side of Mt. Dennis (Section 8). The unit is approximately 400 m thick.

No fossils were recovered from the Oke unit, despite extensive searches. A single collection from the upper part of the sequence at Natural Bridge (near Emerald Lake) has been assigned to the upper *Bolaspidella* Zone (W.H. Fritz in Cook, 1975). The unit is tentatively correlated with the Waterfowl Formation on the platform (Fig. 2).

The Oke unit is composed largely of ribbon limestones containing a significant component of carbonate sand. Interbedded lithologies include slate, argillaceous nodular limestone, laminated and crosslaminated dolomite, and a variety of calcarenites. The ribbon limestones contain a wealth of sedimentary structures not seen in similar rocks elsewhere in the Chancellor. Graded beds, laminated and ripple crosslaminated units, and starved ripple horizons are all very common. Limestone conglomerate (debris flow) units are rare, and where found contain exclusively slope-derived, argillaceous limestone clasts set in an argillaceous or dolomitic matrix. Synsedimentary deformation features are also relatively uncommon, and peri-platform talus blocks are absent. The character of this sequence is compatible with a lime sand, shoal-dominated, carbonate ramp model for the Waterfowl margin.

FURTHER WORK

A short field season is planned in 1989 to investigate remaining problems in Chancellor stratigraphy and sedimentology. Additional exposures of the platform-to-basin transition at the Eldon-Pika level will be examined

immediately northeast of Mt. Duchesnay and in the headwaters of Verdant Creek. New sections of the Park unit will also be measured at Park Mountain and in the headwaters of Haffner Creek. Details of the facies transition at the level of the Arctomys and Waterfowl formations have so far been elusive, and will be further investigated north of Field.

ACKNOWLEDGMENTS

This project forms part of a Ph.D. study at the University of Ottawa. The field component of the study is being funded by the Institute of Sedimentary and Petroleum Geology, Calgary, as an activity under Project No. 213-7298. The writer is indebted to Environment Canada (Parks) and the Ministry of Parks of the Province of British Columbia for permission to conduct fieldwork in Yoho National Park, Kootenay National Park, and Mount Assiniboine Provincial Park. J.D. Aitken and D.G. Cook (ISPG, Calgary) and B.R. Rust (University of Ottawa) have provided valuable guidance throughout. All trilobites collected during this study have been identified by W.H. Fritz (GSC Ottawa).

REFERENCES

- Aitken, J.D.
1966: Middle Cambrian to Middle Ordovician cyclic sedimentation, southern Rocky Mountains of Alberta; *Bulletin of Canadian Petroleum Geology*, v. 14, p. 405-441.
1971: Control of lower Paleozoic sedimentary facies by the Kicking Horse Rim, southern Rocky Mountains, Canada; *Bulletin of Canadian Petroleum Geology*, v. 19, p. 557-569.
1978: Revised models for depositional Grand Cycles, Cambrian of the southern Rocky Mountains, Canada; *Bulletin of Canadian Petroleum Geology*, v. 26, p. 515-542.
1981: Cambrian stratigraphy and depositional fabrics, southern Canadian Rocky Mountains, Alberta and British Columbia; in *The Cambrian System in the southern Canadian Rocky Mountains, Alberta and British Columbia*, M.E. Taylor (ed.); *Second International Symposium on the Cambrian System, Guidebook for Field Trip 2*, p. 1-27.
—: Middle Cambrian stratigraphy of the southern Rocky Mountains, Canada; *Geological Survey of Canada, Bulletin* (in press).
- Aitken, J.D. and Greggs, R.G.
1967: Upper Cambrian formations, southern Rocky Mountains of Alberta, an interim report; *Geological Survey of Canada, Paper* 66-49.
- Allan, J.A.
1911: *Geology of the Ice River District, British Columbia*; *Geological Survey of Canada, Summary Report* 1910, p. 135-144.
1914: *Geology of the Field map area, British Columbia and Alberta*; *Geological Survey of Canada, Memoir* 55.
- Balkwill, H.R.
1972: *Structural geology, lower Kicking Horse River region, Rocky Mountains, British Columbia*; *Bulletin of Canadian Petroleum Geology*, v. 20, p. 608-633.
- Balkwill, H.R., Price, R.A., Cook, D.G., and Mountjoy, E.W.
1980: *Geology of Golden (east half), British Columbia*; *Geological Survey of Canada, Map* 1496A (1:50 000).
- Cook, D.G.
1970: A Cambrian facies change and its influence on structure, Mount Stephen - Mount Dennis area, Alberta - British Columbia; *Geological Association of Canada, Special Paper* No. 6, p. 27-39.
1975: *Structural style influenced by lithofacies, Rocky Mountain Main Ranges, Alberta - British Columbia*; *Geological Survey of Canada, Bulletin* 233.
- Deiss, C.
1940: Lower and Middle Cambrian stratigraphy of southeastern British Columbia; *Geological Society of America, Bulletin*, v. 51, p. 731-794.

Fritz, W.H.

1971: Geological setting of the Burgess Shale; Proceedings of the North American Paleontological Convention, Part 1, p. 155-1170.

Leech, E.B.

1979: Kananaskis Lakes (west sheet); Geological Survey of Canada, Open File Map 634 (1:126 720).

McIlreath, I.H.

1977: Stratigraphic and sedimentary relationships at the western edge of the Middle Cambrian carbonate facies belt, Field, British Columbia; unpublished Ph.D. thesis, University of Calgary, Calgary, Alberta, 259 p.

North, F.K. and Henderson, G.G.L.

1954: Summary of the geology of the southern Rocky Mountains of Canada; Alberta Society of Petroleum Geologists, Guidebook, Fourth Annual Field Conference, p. 15-81.

Price, R.A., Balkwill, H.R., and Mountjoy, E.W.

1979: Geology of McMurdo (east half), British Columbia; Geological Survey of Canada, Map 1501A (1:50 000).

Price, R.A., Cook, D.G., Aitken, J.D., and Mountjoy, E.W.

1980: Geology of Lake Louise (west half), Alberta; Geological Survey of Canada, Map 1483A (1:50 000).

Price, R.A. and Mountjoy, E.W.

1972: Geology of Banff (west half), Alberta; Geological Survey of Canada, Map 1483A (1:50 000).

Price, R.A., Mountjoy, E.W., and Cook, D.G.

1978a: Geology of Mount Goodsir (west half), British Columbia; Geological Survey of Canada, Map 1477A (1:50 000).

1978b: Geology of Mount Goodsir (east half), British Columbia; Geological Survey of Canada, Map 1476A (1:50 000).

Rasetti, F.

1951: Middle Cambrian stratigraphy and faunas of the Canadian Rocky Mountains; Smithsonian Miscellaneous Collections, v. 116, no. 5.

Measurement frequency requirements for permafrost ground temperature monitoring: analysis of Norman Wells pipeline data, Northwest Territories and Alberta

Margaret M. Burgess and Daniel W. Riseborough¹
Terrain Sciences Division

Burgess, M.M. and Riseborough, D.W., Measurement frequency requirements for permafrost ground temperature monitoring: analysis of Norman Wells pipeline data, Northwest Territories and Alberta; in Current Research, Part D, Geological Survey of Canada, Paper 89-1D, p. 69-75, 1989.

Abstract

Monthly ground temperature observations are a major component of the permafrost and terrain monitoring program along the Norman Wells pipeline. The reliability of low frequency manual field measurements in characterizing the annual ground thermal regime was examined using high frequency ground temperature data from depths of 1 to 5 m, recorded by a data logger at one of the monitoring sites from October 1985 to October 1987. Low frequency data sets were extracted from the logger data, and temperature and running mean annual temperature curves were generated using cubic spline interpolation. Comparison of created curves with measured high frequency data curves revealed that timing of measurements as well as frequency are critical for characterizing the annual wave and obtaining reliable mean annual temperature. Important measurement times are periods of rapid change in the summer months, and the onset of the "zero-curtain". The current monthly field program provides reliable temperature estimates at depths from 1 m and below; if necessary, a reduction to a 6 week measurement interval would be acceptable.

Résumé

Les observations mensuelles de la température du sol constituent un élément important du programme de surveillance du pergélisol et du terrain le long du pipeline de Norman Wells. La fiabilité des mesures basse fréquence prises manuellement sur le terrain pour caractériser le régime thermique annuel du sol a été examiné à l'aide de données haute fréquence de la température du sol à des profondeurs de 1 à 5 m, relevées par un enregistreur de données à l'un des emplacements de surveillance d'octobre 1985 à octobre 1987. Des ensembles de données basse fréquence ont été extraits des données de l'enregistreur, et des courbes de température et des courbes des moyennes mobiles de température annuelle ont été établies par interpolation à l'aide d'une spline cubique. La comparaison entre ces courbes et les courbes des mesures haute fréquence a révélé que la répartition dans le temps et la fréquence des mesures sont des facteurs critiques pour caractériser l'onde annuelle et obtenir une température annuelle moyenne fiable. Dans la répartition des mesures dans le temps, il est important de tenir compte des périodes de changement rapide en été et de la "période zéro". Le programme actuel de mesures mensuelles sur le terrain produit des estimations de la température qui sont fiables à des profondeurs de 1 m et plus; au besoin, il serait acceptable de réduire l'intervalle de mesure à 6 semaines.

¹ Department of Geography, Carleton University, Ottawa, Ontario K1S 5B6

INTRODUCTION

The Geological Survey of Canada (GSC) cooperates with the Department of Indian and Northern Affairs (INAC) in a multidisciplinary Permafrost and Terrain Research and Monitoring Program along the 869 km long Norman Wells, N.W.T. to Zama, Alberta buried oil pipeline. A major component of this program involves monitoring the ground thermal regime at 13 instrumented sites established along the pipeline route. Ground temperature data are gathered during monthly field observation and data collection trips, undertaken since pipeline operation began in April 1985. The temperature data are collected to characterize both the annual temperature wave and trends in mean annual temperature in order to assess changes to the thermal conditions of the discontinuous permafrost terrain caused by pipeline related activity and natural phenomena.

This report presents the results of an analysis undertaken in 1988 to examine the feasibility of reducing the frequency of field temperature measurements while continuing to characterize adequately the ground thermal regime. The analysis uses high frequency (3 readings/day) ground temperature data at depths of 1 to 5 m, recorded by a data logger installed at one of the monitoring sites, to evaluate the reliability of low frequency measurements (monthly or less frequent).

The results of this study have served as a useful guide to the future planning of the thermal aspects of the field monitoring program and should be of interest to those designing shallow geothermal and geotechnical monitoring programs focusing on the zone of seasonal and annual ground temperature fluctuations.

BACKGROUND

The Norman Wells pipeline is the first completely buried oil pipeline constructed within the discontinuous permafrost zone of northwestern Canada. The 324 mm diameter, uninsulated pipeline is buried at an average depth of 1 m. Oil is chilled to near 0°C before delivery to Interprovincial Pipe Line (NW) Ltd. in Norman Wells and thereafter undergoes no further refrigeration along the 869 km to Zama, northern Alberta. These design features were adopted in order to minimize ground thermal disturbance and to assure pipeline integrity under possible conditions of thaw settlement or frost heave, since much of the terrain along the pipeline route consists of thaw sensitive or frost susceptible soils (Kay et al., 1983; Nixon et al., 1984).

Monitoring the ground thermal regime forms part of a larger multidisciplinary Permafrost and Terrain Research and Monitoring Program established by INAC in 1983 following the signing of an Environmental Agreement with the pipeline operator, Interprovincial Pipe Line (NW) Ltd. (IPL). The monitoring program provides Canadians with an important opportunity to assess the impacts on the northern physical environment of the construction and operation of this first small diameter "ambient" temperature pipeline in permafrost terrain.

In order to observe and quantify the effects on permafrost and terrain, 13 INAC/GSC instrumented sites were

established along the pipeline route (Fig. 1) at locations representing the major soil types and ground thermal conditions encountered throughout the discontinuous permafrost zone. Thermal instrumentation at these sites is designed to monitor changes in the ground temperature regime, both on and off the right-of-way, as well as changes in the pipe temperature regime.

The monitoring program relies on measurements and observations obtained during helicopter-supported field visits, since a permanent haul road was not required for pipeline construction and operation. A schedule of monthly field trips was instituted in order to quantify the seasonal ground temperature cycle, as well as document surface and vegetation change both at the monitoring sites and along the right-of-way in general. Field trips are generally undertaken by members of the monitoring program throughout the summer months and by INAC district staff during the winter. Selected sites, where regular access throughout the winter months was not initially scheduled or where a more detailed temperature record was of interest, have also been equipped with automatic data acquisition systems (Sea-Data Model 1250).

In fiscal year 1988/1989, a less frequent manual thermal data measurement program at all sites was considered in order to perhaps reduce helicopter logistic costs. To examine the feasibility and quantify the reliability of a reduced ground thermal measurement program, an analysis using the time series collected with one of the data loggers was therefore undertaken. The analysis involved an examination of errors in measured temperatures as well as in calculated mean annual temperatures, for various sampling frequencies and selected measurement depths.

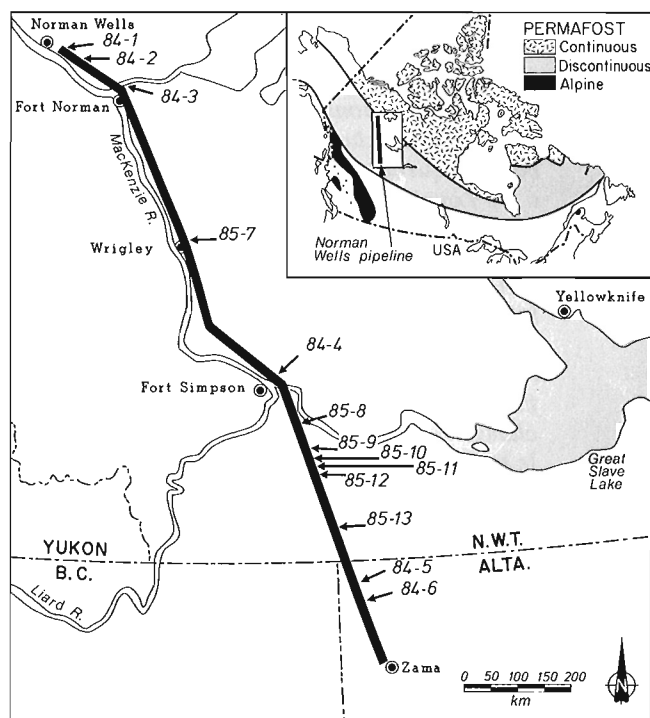


Figure 1. Location of Norman Wells pipeline permafrost and terrain research and monitoring sites.

GROUND TEMPERATURE MEASUREMENT PROGRAM

Temperature instrumentation

At the INAC/GSC monitoring sites, ground temperature cables have been installed in boreholes ranging from 5 to 20 m in depth and located both on and off the pipeline right-of-way. Several monitoring sites have more than one instrumented transect, or thermal fence, for a total of 23 thermal fences. The ground temperature cables are positioned to examine both the short and long term effects of right-of-way clearance, pipeline trenching and operation, and changes resulting from natural phenomena. The cables generally contain 10-11 temperature sensors, either at 50 cm spacing in the shorter cables or 1 to 3 m spacing in the longer cables. Details on the instrumentation and listings of data are published annually as GSC Open Files (e.g. Burgess 1987).

The temperature sensors are thermistors (semiconductor devices in which electrical resistance varies inversely as a function of temperature); the main type of sensors used is the YSI44033, although YSI44032 sensors are installed at two locations. All cables connected to Sea-Data loggers are made with YSI44033 sensors. The sensors are calibrated to an absolute accuracy of $\pm 0.1^\circ\text{C}$. The resolution of the manual measurement system (digital multimeter) and of the Sea-Data loggers is of the order of 0.01° to 0.02°C . The 64 channel data Sea-Data Model 1250 automatic data acquisition systems were set to collect data every 8 hours and twenty minutes. The loggers require servicing twice a year, in late spring and early fall, for data retrieval (data storage is on cassette tape) and battery replacement. To date six loggers have been installed; four in 1985 and two in 1987.

Analytical procedures

The data acquired manually during the approximately monthly field trips constitute an irregularly spaced time series, occasionally with gaps of 1-2 months. The ground temperature envelope, the minimum and maximum ground temperatures during a year, and the yearly active layer depth are generally determined directly from the data set for each cable. In addition, since the seasonal temperature fluctuations may mask a general long term trend, mean annual and running mean annual temperatures are also calculated for each sensor. The mean annual temperature is of particular importance, since any change upward indicates the potential vulnerability of permafrost sites to future thaw.

In order to calculate mean annual values, an interpolation program is first used to generate regularly and more closely spaced temperatures from the approximately monthly measurements. Interpolation can be defined as mathematical curve fitting in order to obtain estimates between measured values. Although the ground thermal regime is fundamentally harmonic and Fourier series expansion is often a preferable interpolation technique for ground temperature data, particularly where gaps of several months may exist in the record (Burgess, 1983), a cubic spline interpolation routine was selected for the analysis of the Norman Wells data.

The spline interpolation method was chosen for several reasons. The Fourier technique necessitates data manipulations to ensure the first and last observations are separated by a period of time equal to the fundamental period, or some whole multiple thereof; such manipulations are not necessary with the spline interpolation. Furthermore, when the data analysis first began the length of the data record at many monitoring sites was not long enough for the Fourier

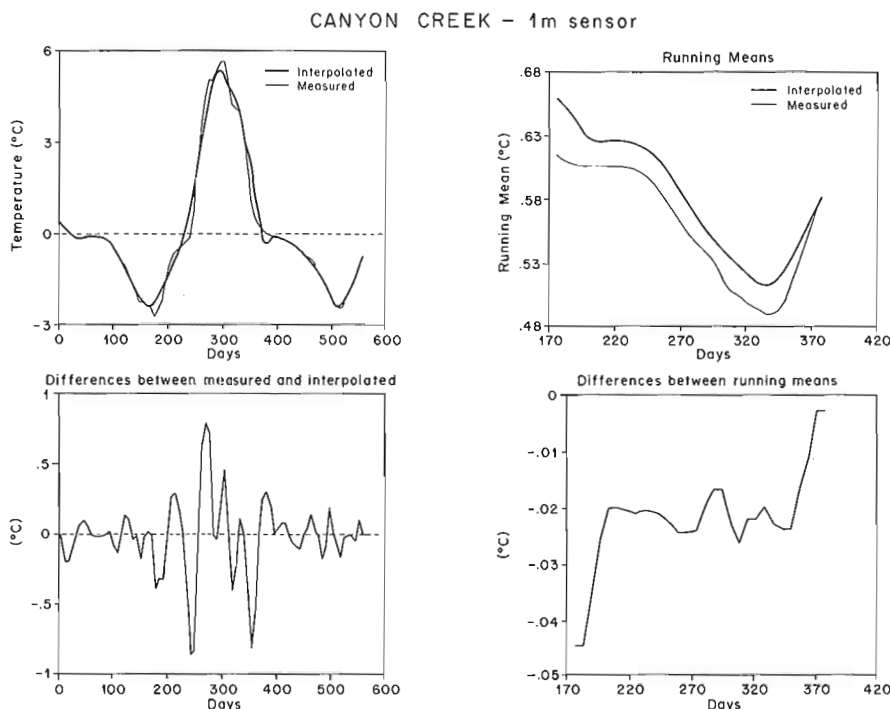


Figure 2. Canyon Creek 1 m sensor: Comparison of measured and interpolated temperature curves based on a 4 week measurement interval (simulation of the current field measurement program).

CANYON CREEK - 2.5m sensor

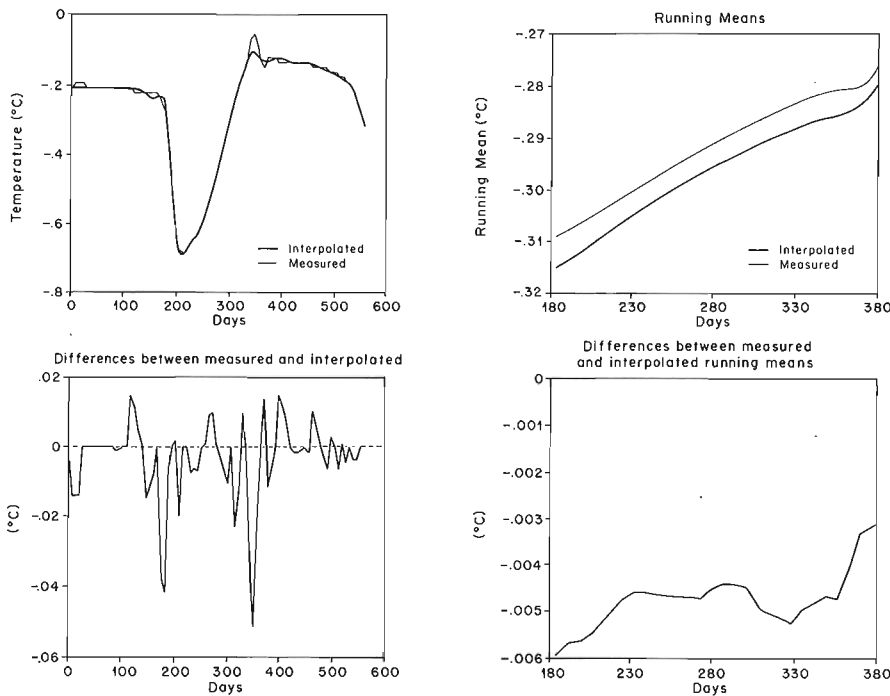


Figure 3. Canyon Creek 2.5 m sensor: Comparison of measured temperature curves and estimated curves based on a 4 week measurement interval (simulation of the current field measurement program).

technique to be applicable. Finally, there was a general absence of large data gaps in the Norman Wells data.

Cubic spline interpolation uses the measured values to generate third degree polynomial equations ("cubic" polynomial curves) which pass through the data points in succession. The polynomials are "splined" (i.e., they form a smooth curve) at each data point by ensuring the first and second derivatives (i.e., the slope and rate of change of slope) of the curves are matched. Interpolations for particular dates are obtained using the equations generated.

For the Norman Wells monitoring sites weekly temperature estimates are generated from the approximately monthly measurements. Mean annual temperatures are then calculated from these weekly estimates (average of 52 weekly values), and running mean annuals calculated in steps of 1 week. This procedure and calculations on the monthly data sets collected to October 1987 are presented by Riseborough et al. (1988). Preliminary results have also been discussed by Burgess (1988) and Burgess and Harry (1988).

MEASUREMENT FREQUENCY EVALUATION

Data logger time series

The Sea-Data logger temperature data from cable T1 at monitoring site 84-2A Canyon Creek was selected for most of the data frequency evaluation exercise. An uninterrupted two year data record, from October 1985 to October 1987, was unique to this site and allowed an examination of the reliability of running means. The site is located about 20 km south of Norman Wells; the T1 cable is 5 m deep and positioned on the right-of-way 2 m from the pipeline. The site is underlain by permafrost to depths of 25 m; a thin (5 m) and coarse till with low ice content overlies fractured shale.

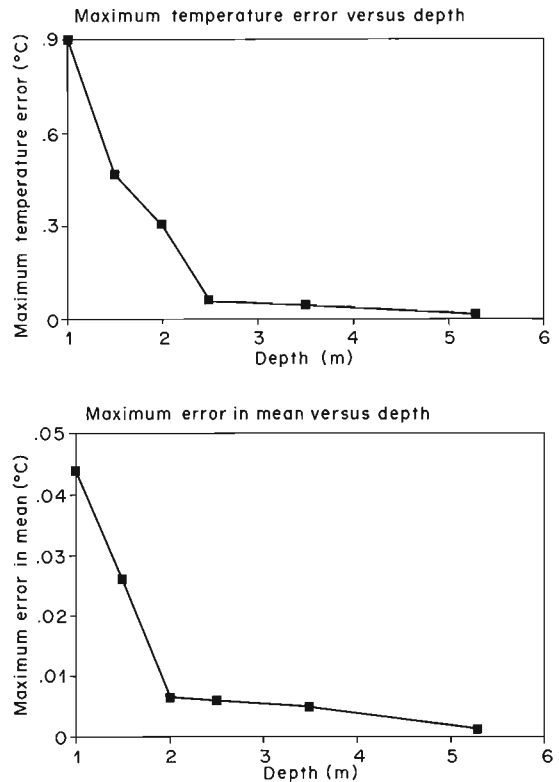


Figure 4. Maximum temperature error and maximum error in running mean annual temperature as a function of depth, 4 week measurement interval.

The pipe lies within a portion of the right-of-way that had been previously cleared in the 1960s for the proposed Canadian National Telecommunications alignment. The T1 cable is also located in this previously cleared portion.

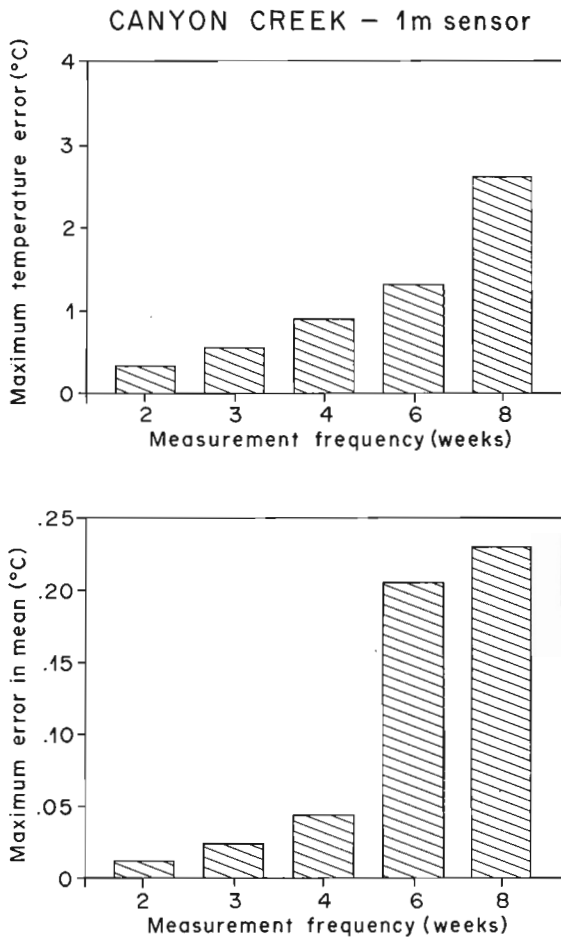


Figure 5. Maximum temperature error and maximum error in running mean annual temperature as a function of measurement frequency, sensor at 1 m depth.

CANYON CREEK - 1m sensor
Measurement Frequency Analysis

42 day Measurement interval

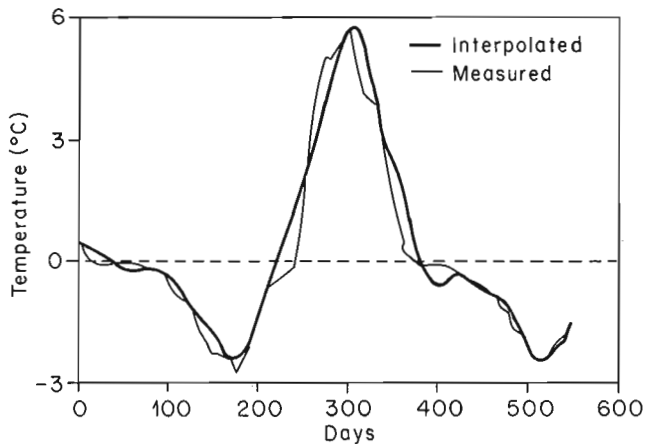


Figure 6. Comparison of measured temperature curves and estimated temperature curves for a 6 week measurement intervals, 1 m sensor.

Methodology

The 2A-T1 data logger set was used to create data files of the type obtained with the manual temperature recording, by extracting data points at various intervals.

To simulate the current manual measurement program for example, temperature data were extracted from the logger data sets at four week intervals. These "created" data files were given to the cubic spline interpolation program, which supplied temperature estimates at one week intervals, as well as running mean annual temperatures based on these estimates. The estimates thus generated were compared to the weekly measured temperature curves, while the running means calculated from the interpolated temperatures were compared to the running mean curve calculated from the measured data logger temperatures.

The interpolated temperature and running mean curves were deemed "reliable" to the extent that they reproduced the actual, that is, measured curves. The error analysis involved the determination of the absolute value of the largest error obtained (measured minus estimated) and in that sense may be viewed as worst case. Sensors at depths ranging from 1 to 5.3 m were examined.

RESULTS

Current measurement program

Several general observations can be made based on the comparison of measured and interpolated temperature curves. Results from the 1 m and 2.5 m sensor are shown in Figures 2 and 3. The largest temperature errors are for periods of rapid change, generally in the summer. The maximum error in the estimated temperatures is of the order of 10 % of the annual temperature range for depths of 1 m or more. For sensors located within the active layer (the layer above the permafrost that undergoes an annual freeze/thaw cycle), interpolation does not properly account for transitions through the zero curtain in the fall (the persistence of zero temperature, 0oC, for a considerable period of time during the freezing and thawing process due to latent heat effects).

The estimated running mean curves closely follow the true running mean curves; the errors are principally in the absolute value of the mean. The maximum error in the running mean usually occurs at the beginning or end of the data set, where the interpolation is constrained on one side only.

Figure 4 summarizes the maximum error in temperature and the maximum error in the running mean as a function of depth. For both parameters, the error decreases rapidly with depth. The interpolation error falls within the limits of uncertainty in the measurement by 2.5 m depth coincidentally the first measurement depth at which the ground is perennially frozen. The error in the means is less than the uncertainty in the measurement for all depths examined.

Alternate measurement frequencies

For this analysis the reliability of data in the near surface is the principal concern in order 1) to examine thermal

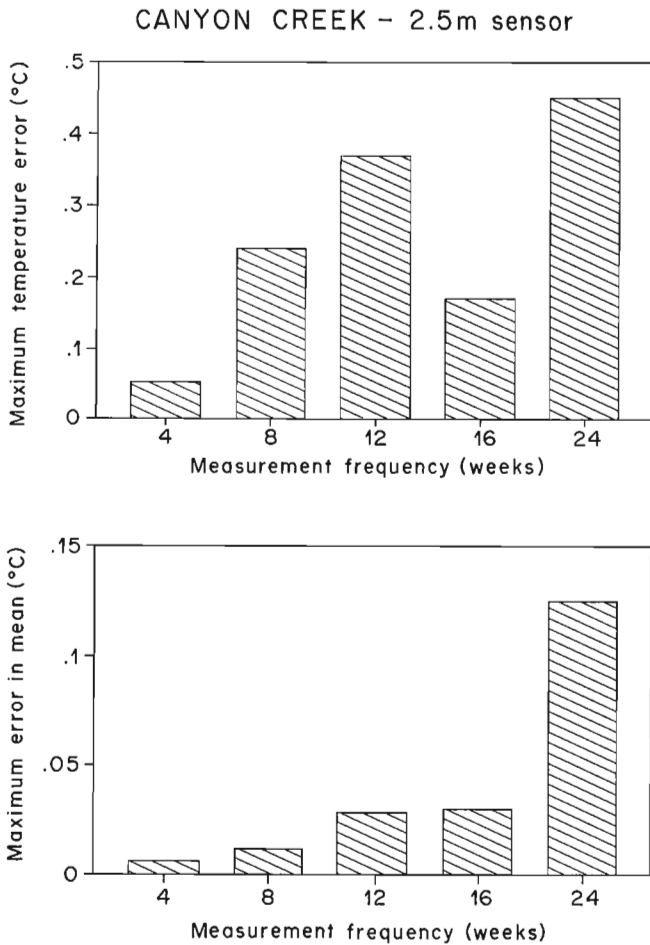


Figure 7. Maximum temperature error and maximum error in running mean annual temperature as a function of measurement frequency, 2.5 m sensor.

changes which have not yet propagated to great depth, such as those resulting from clearing, construction, shallow pipe burial and operation and 2) to monitor adequately seasonal changes in the active layer and thaw depths.

Alternative measurement frequencies were investigated using the Canyon Creek data for three depths (1, 2.5, and 5.3 m). Frequencies of from 2 to 8 weeks were examined for the 1 m sensor, and 4 to 24 weeks were examined for the other depths. Data were extracted from the 84-2A-T1 logger data set for the desired interval and the interpolated curve generated. Again estimated and measured temperature and mean curves were compared.

The resulting errors for the 1 m sensor are summarized in Figure 5. The temperature error increases steadily over the measurement interval from 2 to 6 weeks, with a jump at 8 weeks. The estimated and measured curves for the 6 week interval are shown in Figure 6. For the running means the error jumps between the 4th and 6th weeks with the 6 week interval error being only twice the uncertainty in the temperature measurement (Figure 5).

The resulting errors for the 2.5 m and 5.3 m sensors are shown in Figure 7 and 8.

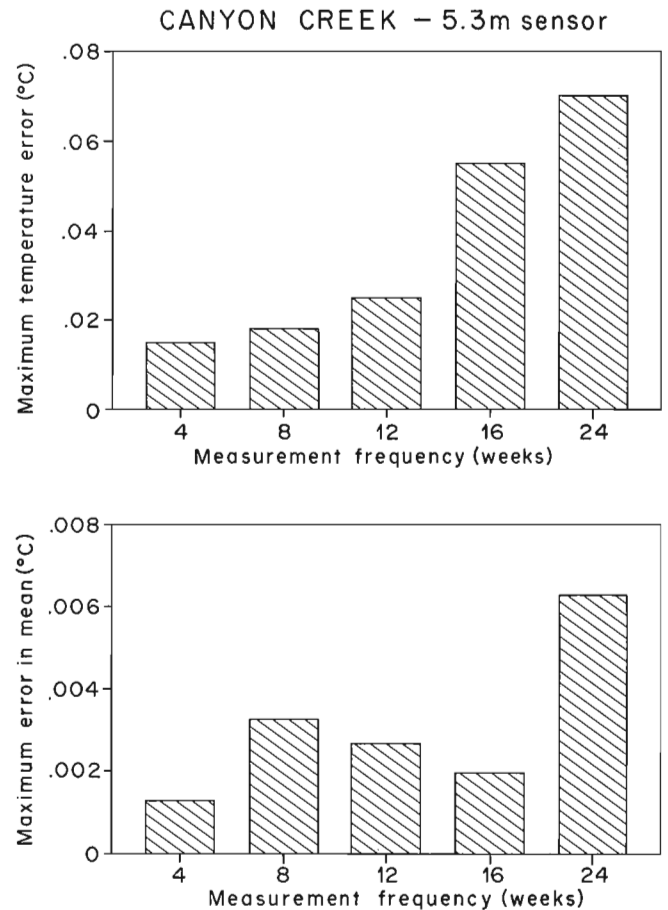


Figure 8. Maximum temperature error and maximum error in running mean annual temperature as a function of measurement frequency, 5.3 m sensor.

Variable frequency

The seasonal pattern of error in the temperature estimates (being greatest in the summer) suggests the possibility of varying the measurement interval over the year. A period of 6 weeks in the winter and either 3 weeks in the summer (for the same number of trips/year as the current total of 12) or 4 weeks in the summer (for 10 trips/year) results in a more even distribution of temperature errors throughout the year. A 3 or 4 week interval over the summer is also desirable from the point of view of visual observations and evaluation along the right-of-way of drainage and erosion, water crossings, slope conditions, and general terrain performance. A reduced interval over the winter would also limit the number of trips during the time of year when operating conditions are at their coldest and daylight is short.

CONCLUSIONS AND RECOMMENDATIONS

1. "Monthly" measurements are adequate for monitoring the long term temperature trend at depths from 1 m and below.
2. A critical time for measurements appears to be the time of freezeback. Although the temperature estimate error may

not be the maximum, the greatest error in the mean annual estimate appears to occur when the onset of freezeback is missed. The largest error in temperature occurs during periods of rapid change, generally in the summer.

3. As a first level of reduction in the thermal measurement program, a combined measurement interval of every 4 weeks in the summer and every 6 weeks in the winter months (from freezeback until the snow cover has gone) would be recommended. This would reduce the total number of field trips to 10 each year.

4. A reduction in field trips to a 6 week measurement interval throughout the year (for a total of 8 trips per year) would still provide reliable estimates of the temperature wave at depths from 1 m and below. A further reduction to an 8 week interval would not be recommended for temperature measurements in the near surface, since the maximum temperature error for the 1 m sensor doubled from 6 to 8 weeks.

5. These conclusions are based on the analysis of data from one site whose specific characteristics, that is, soil temperatures and thermal properties, are not representative of conditions at all monitoring sites. The application of the results to the whole monitoring program, however, is not unreasonable given that the amplitude of the 1 m annual wave at Canyon Creek 84-2A-T1 is equal to or greater than that observed at most of the other permafrost sites.

6. A useful extension of the analysis would be to examine sites with different terrain conditions (such as higher ice contents, warmer/and or colder soil temperatures, unfrozen soil). Such a study may allow an understanding of the relationships between depth of measurement, frequency of measurement and the ground thermal regime in dimensionless terms.

ACKNOWLEDGMENTS

We particularly thank Vic Allen, Permafrost Research Section, for the Sea-Data logger installation and maintenance, and the development of the software for data retrieval, translation, and conversion of data files for this analysis on IBM compatible microcomputer.

The Permafrost and Terrain Research and Monitoring Program is coordinated by Kaye MacInnes, Indian and Northern Affairs, Yellowknife. Many other individuals within INAC, EMR, IPL, Agriculture Canada, and National Research Council Canada also provide support and cooperation. The thermal monitoring has been primarily funded by INAC's Northern Affairs Program, with contributions from the Northern Oil and Gas Action Program (NOGAP). Additional funding and other assistance has also been provided by IPL and by the former Earth Physics Branch of the Energy Mines and Resources, Geological Survey of Canada, and the Federal Panel on Energy Research and Development.

REFERENCES

Burgess, M.M.

1983: Analysis of the ground thermal regime at Norman Wells and Fort Good Hope: 1971-1974; unpublished Masters thesis, Carleton University, Ottawa, Ontario, 153 p.

1987: Norman Wells pipeline monitoring sites ground temperature data file: 1986; Geological Survey of Canada, Open File 1621, 24 p. + appendices. 1988: Permafrost and terrain preliminary monitoring results, Norman Wells pipeline, Canada; in Proceedings of the Fifth International Conference on Permafrost, Trondheim, Norway, August 1988, p. 916-921.

Burgess, M.M and Harry, D.G.

1988: Norman Wells pipeline permafrost and terrain monitoring: Geothermal and geomorphic observations; in Preprint Volume, 41st Canadian Geotechnical Conference, Kitchener, Ontario, October 1988, p.354-363.

Kay, A.E., Allison, A.M., Botha, W.J., and Scott, W.J.

1983: Continuous geophysical investigation for mapping permafrost distribution, Mackenzie Valley, N.W.T., Canada; in Proceedings of the Fourth International Conference on Permafrost, Fairbanks, Alaska, 1983, National Academy of Sciences, p. 578-583.

Nixon, J.F., Stuchly, J., and Pick, A.R.

1984: Design of Norman Wells pipeline for frost heave and thaw settlement; in Proceedings, Third International Symposium on Off-shore Mechanics and Arctic Engineering (American Society for Mechanical Engineers), New Orleans, February 1984, Paper No. 83-OMA-303.

Riseborough, D.W., Patterson, D.E., and Smith, M.W.

1988: Computer analysis of Norman Wells pipeline thermal data; Geological Survey of Canada, Open File 1898, 120 p.

Late Quaternary marine record of the Cape Parry — Clinton Point region, District of Mackenzie, N.W.T.

Daniel E. Kerr¹
Terrain Sciences Division

Kerr, D.E., *Late Quaternary marine record of the Cape Parry — Clinton Point region, District of Mackenzie, N.W.T.*; in *Current Research, Part D, Geological Survey of Canada, Paper 89-1D*, p. 77-83, 1989.

Abstract

A preliminary investigation of stratigraphic sections and raised marine geomorphic features in the Cape Parry — Clinton Point area, north-central District of Mackenzie has made it possible to reconstruct late glacial and postglacial marine environments of deposition. In the early stages of deglaciation, recessional moraines, deltas, and outwash fans were formed on Parry Peninsula as a result of the receding Amundsen Gulf lobe. Ice marginal lakes with deltas also developed, impounded between this lobe and the more elevated terrain of the Melville Hills. Further retreat of the ice mass led to the marine incursion from the west during which the sea penetrated along the southern margin of the Amundsen Gulf lobe and inundated the coastal lowlands, beginning with Cape Parry, through to Paulatuk and eventually reaching Clinton Point. Marine deltas mark the limit of submergence in these areas, although some are related to successively lower sea levels. Marine limit varies from approximately 46 m a.s.l. near Clinton Point to 6 m a.s.l. near Cape Parry to the northwest. This decreasing trend in elevation is the result of differential isostatic uplift which can be traced further east along the mainland coast.

Résumé

Un examen préliminaire de coupes stratigraphiques et de caractéristiques géomorphologiques marines soulevées dans la région du cap Parry et de la pointe Clinton dans le centre-nord du district de Mackenzie a permis de reconstituer des environnements sédimentaires marins du glaciaire récent et du postglaciaire. Pendant les premières étapes de la déglaciation, des moraines de retrait, des deltas et des cônes de déjection fluvio-glaciaires se sont formés dans la péninsule Parry à cause du retrait du lobe du golfe d'Amundsen. Des lacs marginaux glaciaires avec deltas se sont aussi formés, emprisonnés entre ce lobe et les collines Melville. En se retirant davantage, la masse de glace a permis l'incursion de la mer par l'ouest, ses eaux pénétrant le long de la marge méridionale du lobe du golfe d'Amundsen et inondant les basses-terres côtières, à commencer par le cap Parry, Paulatuk et finalement jusqu'à la pointe Clinton. Les deltas marins marquent la limite de subsidence dans ces régions, même si certains sont associés à des niveaux de la mer successivement plus bas. La limite marine varie d'environ 46 m au-dessus du niveau de la mer près de la pointe Clinton à 6 m près du cap Parry au nord-ouest. Cette tendance à la baisse de l'altitude tient à un soulèvement isostatique différentiel qui peut être retracé plus loin à l'est le long du littoral continental.

¹ Department of Geology, University of Alberta, Edmonton, Alberta T6G 2E3

INTRODUCTION

The Cape Parry — Clinton Point study area (Fig. 1) comprises Parry Peninsula, Darnley Bay, and the coastal lowlands north of the Melville Hills. This region was investigated during the summer of 1988 in order to record the marine stratigraphy and the major raised marine geomorphic features. Twenty stratigraphic sections were measured, of which seven are summarized in Table 1. These sections represent sedimentary sequences of glaciomarine and marine deposits associated with the retreat of the last ice sheet from this area. A series of perched deltas records the approximate limit of marine submergence as well as successively lower sea levels.

As few geologists have previously worked in this region, our knowledge of the marine history is rather limited. O'Neill (1924) made several general observations regarding Pleistocene deposits along the arctic coast. Mackay (1952, 1958) mapped major glacial landforms, such as end moraines, eskers, and glacial lineations, and discussed the glacial history of the region. Klassen (1971) did preliminary surficial geology mapping in the study area. More recent

work was carried out by J-S. Vincent in 1985 who first recognized evidence for marine submergence south of Darnley Bay and who provided age estimates for deglaciation. Immediately to the east of the study area, St-Onge and McMartin (1987) mapped the surficial deposits on the basis of morphosedimentary zones, and Kerr (1987) provided an account of the marine stratigraphic sequences.

STRATIGRAPHIC RECORD OF THE MARINE SUBMERGENCE

Section 114, situated in north-central Parry Peninsula (Fig. 1) at an elevation of 5 m a.s.l. (top of section), consists of stratified sand and silt, capped by active eolian cliff-top dunes (Table 1). These laminated to bedded, fine grained sediments (Fig. 2) have both sharp and gradational upper and lower boundaries, and are fossiliferous in the lower half of the section. The foraminifera *Elphidium clavatum* and *Pseudopolymorphina novangliae*, as well as the marine ostracode *Cytheropteron montrosiense*, are in an excellent state of preservation and show no sign of abrasion due to transport; many ostracodes were found as paired valves.

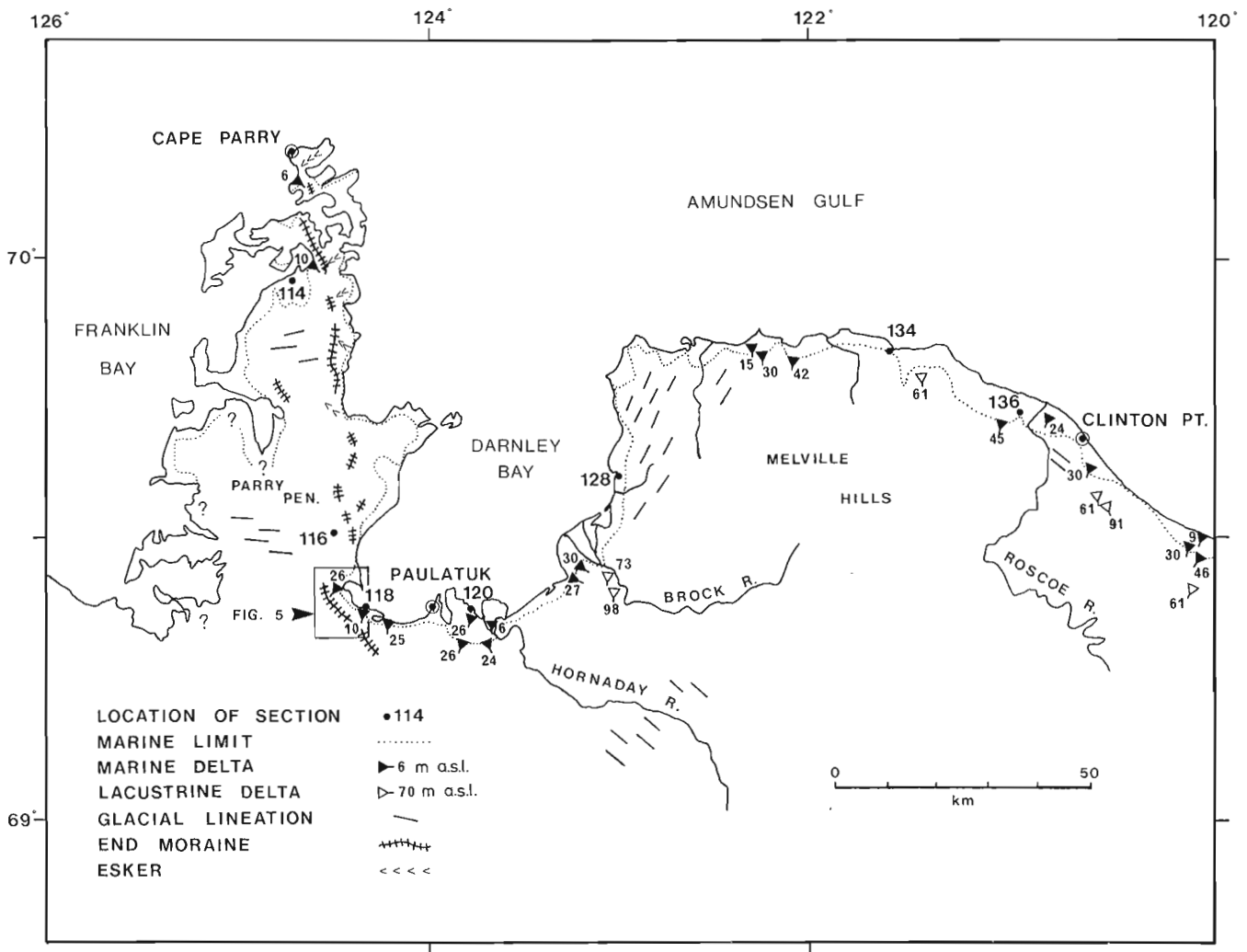


Figure 1. Location map of the Cape Parry — Clinton Point region, showing areas submerged by the postglacial sea and related geomorphic features.

Table 1. Stratigraphy of the Cape Parry — Clinton Point region

Thickness	Material	Thickness	Material
A. Stratigraphy of section 114 on Parry Peninsula, 5 m a.s.l.		D. Stratigraphy of section 120 east of Paulatuk, 26 m a.s.l.	
0.5 m	Eolian sand, fine grained, light brown, finely laminated	2.5 m	Interbedded, medium to coarse grained, light grey sand and laminated fine, grey sand with coal fragments and rare twigs
1.0 m	Sand, fine grained, light brown, massive to poorly laminated	1.5 m	Massive to poorly laminated, medium grained grey sand
1.5 m	Sand, fine grained, grey-brown, thinly bedded, fossiliferous	1.8 m	Laminated, medium grained sand, forming cross-stratification dipping 20° towards 065°
2.0 m	Thinly bedded fine sand and silt, grey brown, interbedded with silty clay horizons, fossiliferous	2.2 m	Thinly bedded to laminated, medium grained, dark grey sand, with thin horizons of coal fragments
B. Stratigraphy of section 116 on Parry Peninsula, 30.5 m a.s.l.		7.0 m	Fine sand and silt, grey-brown, planar laminations and ripple-drift crosslaminations, paleocurrents towards 045°-060°
0.2 m	Sandy peat	1.75 m	Interbedded, brown, medium grained sand and dark silty clay
0.75 m	Cryoturbated fine sand and silt, light grey, sporadic occurrence of rounded gravel and cobble clasts, contorted organic pods	3.0 m	Fine sand and silt strata interbedded with silt beds
0.6 m	Fine sand and silt, light grey, thinly bedded, containing silty clay lenses	1.5 m	Massive silt and clay with stringers of medium grained sand
3.0 m	Sand, medium to fine grained, grey, finely laminated	4.0 m	Thinly bedded to laminated fine sand, silty sand and silt layers interbedded with horizons of coal fragments
3.0 m	Coarse sand, dark grey, with minor gravel, thin horizons of coal fragments; planar crossbedded strata dipping 20°-30° towards 030°-350°	E. Stratigraphy of section 128 on east side of Darnley Bay, 6.5 m a.s.l.	
1.0 m	Medium grained grey sand, with thin horizons of coal fragments; planar crossbedded strata, dipping 10° towards 345°	1.3 m	Fine sand, silt, and clay, massive, fossiliferous
1.5 m	Massive coarse sand, dark grey, containing small coal lenses	1.2 m	Silt and clay, massive to poorly stratified, with fossiliferous horizon
2.0 m	Medium grained grey sand, massive to poorly laminated, interbedded with a coarse sand horizon with abundant coal fragments	0.2 m	Medium to fine grained sand, silt, and clay with rare small cobbles, massive
C. Stratigraphy of section 118 west of Paulatuk, 10 m a.s.l.		2.8 m	Unstratified diamicton, sand-silt matrix, numerous gravel to cobble clasts, angular to rounded
0.4 m	Poorly stratified sandy gravel with small cobbles, cryoturbated	1.0 m	Covered
1.0 m	Medium to coarse sandy gravel, grey brown, unstratified to thinly bedded, with lenses of pebbles and cobbles	F. Stratigraphy of section 134 north of Melville Hills, 16.5 m a.s.l.	
6.0 m	Fine grained grey sand, beds alternating with fine sandy silt, forming crossbedded strata dipping 30° towards 335°; rare gravel clasts in lower section and discontinuous layers of coal fragments throughout	3.0 m	Interstratified medium to fine grained sand, silt, and clay, laminated to thinly bedded, fossiliferous near top
2.5 m	Interbedded, dark brown silty clay and medium grained, brown sand beds with thin horizons of coal fragments	1.5 m	Unstratified diamicton, sand-silt matrix angular to rounded gravel and cobble clasts
		3.0 m	Bedrock
		G. Stratigraphy of section 136 near Roscoe River, 24 m a.s.l.	
		3.5 m	Interbedded medium to fine grained sand and coarse sandy gravel strata, planar laminated to thinly bedded, fossiliferous in lower half
		4.5 m	Fine grained sand and silt, massive to poorly stratified, fossiliferous
		4.0 m	Interstratified sandy silt and silty clay, laminated to thinly bedded
		6.0 m	Silt and clay, dark grey, massive

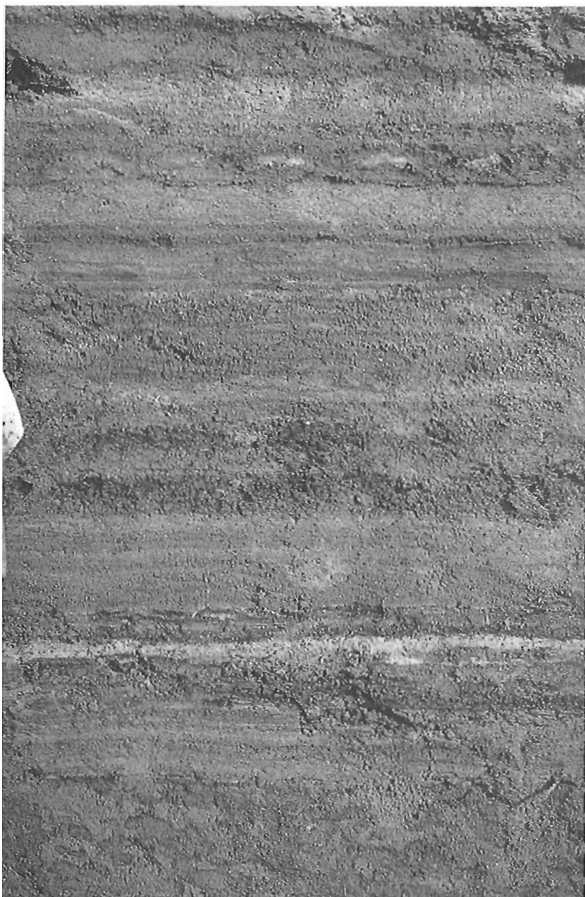


Figure 2. Shallow water marine laminated and thinly bedded sand and silt from section 114.

Section 116, located in south-central Parry Peninsula at 30 m a.s.l. (Fig. 1), is composed of a series of interstratified planar and crossbedded sands (Table 1) which contain high proportions of coal fragments derived from the local bedrock. Paleocurrent directions of crossbedded strata suggest a flow towards the northeast to northwest. This site is on the edge of a large, discontinuous, ice marginal outwash complex which covers large areas of the peninsula. There is, however, no direct evidence linking this site to a marine environment, so it is not yet known whether it was or was not built in contact with the sea.

Section 118, west of Paulatuk (Fig. 1), is at 10 m a.s.l. and represents a coarsening upward sequence (Table 1) in which fossiliferous, bottomset, stratified silty clay grades vertically into crossbedded foreset sand, overlain by topset gravel with cobbles (Fig. 3). The marine fossils *Elphidium orbiculare* and *Cytheropteron montrosiense* are well preserved and show no evidence of being reworked. Paleocurrent directions indicate a flow towards the northwest. Coal fragments are relatively abundant in the crossbedded unit.

A more complex sedimentary sequence is found in section 120, east of Paulatuk at the mouth of the Hornaday River (Fig. 1), at an elevation of 26 m a.s.l. Here, as in section 118, a coarsening upward trend occurs (Table 1). Stratified sand, silt, and clay grade up into crosslaminated



Figure 3. Marine deltaic sequence of section 118 where foreset crossbedded sands are overlain by topset gravel with cobbles.



Figure 4. Massive diamicton unit of section 128, overlain by poorly stratified silty clay.

sand with paleocurrents towards the northeast, overlain by planar and crossbedded sand with a similar flow direction. Rare twigs are found in the uppermost sandy unit, as are coal fragments which also occur throughout the section. This site may also be part of an ice marginal outwash system built in contact with the sea, as it forms a mound rising above the surrounding lowlands.

Section 128 on the east side of Darnley Bay (Fig. 1) at 6.5 m a.s.l. is the most westerly occurrence of a fine grained matrix-supported diamicton which can be seen in sections along the coastline north of the Melville Hills and which continues farther east along the mainland coast (Kerr, 1987). The stony massive diamicton (Table 1) is overlain by a sandy silty clay unit which contains in situ shells of *Hiatella arctica*, the foraminifera *Elphidium orbiculare*, *E. bartletti*, and *Pseudopolymorphina novangliae*, as well as the ostracode *Cytheropteron montrosiense*. A comparable stratigraphic sequence occurs in section 134 (Table 1), located north of the Melville Hills, at 16.5 m a.s.l. (Fig. 1). The unstratified diamicton is underlain by bedrock and overlain by interlaminated sand, silt, and clay (Fig. 4). Near the surface, these sediments yielded fossils of *Hiatella arctica* and *Elphidium bartletti*.

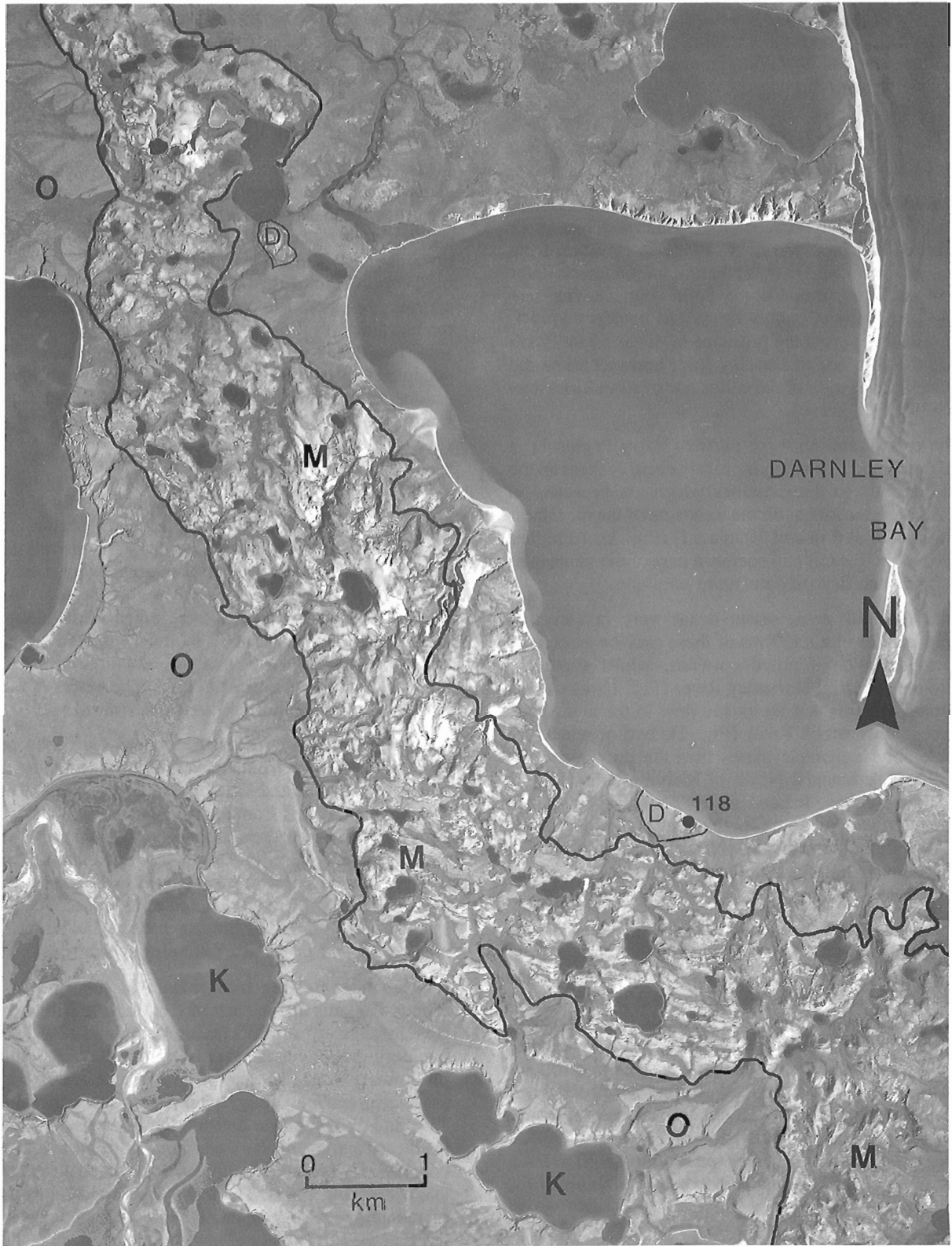


Figure 5. Air photograph of the area 15 km west of Paulatuk (Fig. 1). To the west and south of the end moraine complex (M), extensive outwash plains (O) are pitted with kettle lakes (K). Deltas (D) and section 118 occur northeast of the moraine. NAPL A18922-37

A coarsening upward trend occurs in section 136 near Roscoe River (Fig. 1, Table 1). Basal silty clay grades vertically into stratified sand and silt which in turn grades into sand and gravel. Fossils of *Hiatella arctica* and *Portlandia arctica* were recovered from these units.

GEOMORPHIC FEATURES OF THE MARINE EPISODE

The coastline of the Cape Parry — Clinton Point region is dotted with a series of perched marine deltas and, to a lesser extent, raised beaches. The deltas range in elevation from 6 m a.s.l. south of Cape Parry to 98 m a.s.l. on Brock River and 91 m a.s.l.¹ south of Clinton Point (Fig. 1). They are generally composed of pebbly sands and bouldery gravel. O'Neill (1924) reported the presence of deltas 15 to 25 km inland on the east side of Darnley Bay; however, time did not permit investigation of the deltas nor of strandlines during the 1988 field season.

In the central and northern parts of Parry Peninsula, a series of north-south trending moraines occur; eskers on the east side lead up to the moraines which are breached in places. At these locations, on the west side of the moraines, two deltas occur at 6 m and 10 m a.s.l. (Fig. 1). At higher elevations in the central and southern part of the peninsula, fans and outwash deposits are more common.

In the Paulatuk area, seven deltas vary in elevation between 6 and 26 m a.s.l. Two of these may be associated with local deposits of pitted outwash, whilst some are related to the ancestral Hornaday River (Fig. 1), as well as other fluvial systems that no longer flow in the area. Four deltas occur near Brock River (Fig. 1), two of which are at considerably higher elevations than the previously discussed deltaic sediments. North of Melville Hills (Fig. 1) the remaining deltas, located up to 25 km apart, range from 9 to 91 m a.s.l. Some of those at higher elevations (61-91 m) were built in contact with the ice, exhibiting such features as kettle lakes and collapse structure, and lateral gradations into kames.

As noted earlier, raised beaches may be found within the study area, although they are not as common or as spectacular as in other coastal regions of the arctic islands or the mainland. O'Neill (1924) recorded beach deposits south of Paulatuk at 21 m a.s.l. and up to 30 m a.s.l. farther west. Few beaches occur on Parry Peninsula, but they become increasingly evident, albeit discontinuous, as one follows the coastline to the east from Paulatuk and the Brock River delta to Clinton Point. Although none were observed above 30 m a.s.l., well developed flights of beaches of limited extent may rise from present-day sea level to 15-20 m a.s.l. in many small coastal embayments north of Melville Hills.

DISCUSSION

During the last glacier advance, ice flow occurred around the higher land of the Melville Hills as indicated by the local pattern of glacial lineations (Mackay, 1958). This resulted

in the Amundsen Gulf lobe flowing towards the west and southwest, and a second lobe south of the Melville Hills advancing towards the northwest. According to Dyke and Prest (1987), the area was ice covered from at least 18 000 to 13 000 BP, and was ice free by 12 000 BP. The Early and Late Wisconsinan limits of glaciation are thought to lie 50 km west of Parry Peninsula.

During deglaciation, the north-south trending recessional moraines on Parry Peninsula were formed (Fig. 1); they record the successive frontal positions of the Amundsen Gulf lobe (O'Neill, 1924; Mackay, 1958) as it receded towards the east. Fans and outwash plains were deposited on the west side of the moraines by glacial streams whose courses are marked in places by eskers on the east side of the moraines (Fig. 5). In the northern part of Parry Peninsula, two deltas were constructed into the sea which then occupied the isostatically depressed coastal regions. The sediments in section 114 were deposited at this time in a shallow, quiet water environment.

Proglacial lakes also developed during the early stages of deglaciation in the coastal zone as a result of meltwater accumulating between the more elevated terrain of the Melville Hills and the lobe of ice occupying Amundsen Gulf which blocked drainage to the sea. Northward flowing streams built deltas into these lakes which were successively lowered or drained as the ice front retreated (Mackay, 1958). Six lacustrine deltas were noted in the study area: two along Brock River at 73 m and 98 m a.s.l., one north of the Melville Hills at 61 m a.s.l., and three east of Clinton Point at 61 m, 61 m and 91 m a.s.l. The extent of these ice marginal lakes has not yet been determined.

Further shrinking of the Amundsen Gulf lobe resulted in marine incursion from the west along its southern margin between Paulatuk and Clinton Point; the limit of marine submergence varies from approximately 46 m a.s.l. east of Clinton Point and decreases to the west, attaining 6 m a.s.l. near Cape Parry (Fig. 1). Debris flows originating from this melting ice margin, which terminated in the sea at this time, are responsible for the diamicton units of sections 128 and 134. The fine grained sediments that overlie the diamictons were deposited in the sea following ice retreat.

Meltwater flowing from masses of stagnant ice inland around Paulatuk and in parts of the Melville Hills is responsible for outwash deposits (sections 116 and 120) and raised bouldery gravel deltas east of Darnley Bay. Based on this preliminary work, the elevation of these features and the associated marine stratigraphic record (sections 114, 118, 134, and 136) indicate that marine limit rises towards the southeast margin of the study area, a trend that continues considerably farther east along the mainland coast (St-Onge and McMartin, 1987). The few deltas found below the limit of submergence suggest that the bulk of sedimentation took place in the early stages of the transgression, so that considerably less sediment was supplied by a smaller number of rivers during the marine regression. The deltaic sequence of section 118 is an example of such deltas built in the latter stages of regression. The coarsening upward trend observed in section 136 is also characteristic of this typical offlap sequence.

¹ Elevation measured by helicopter altimeter, probable accuracy ± 6 m (Stan A. Smith, Associated Helicopters, personal communication, 1988).

Few radiocarbon dates are available in the study area. In the Paulatuk region, peat overlying deltaic sediments was collected by J-S. Vincent and D.A. St-Onge from 2 m a.s.l. and yielded an age of 5100 ± 100 BP (GSC-4410), whereas wood and peat collected by D.A. St-Onge from a sandy channel deposit at 2-3 m a.s.l. gave an age of 9600 ± 100 BP (GSC-4480). The oldest date, $11\,280 \pm 100$ (TO-217), was derived from shells collected by J-S. Vincent at 6 m a.s.l. between Hornaday and Brock rivers, east of Paulatuk. Thus sea level was between 25 and 6 m a.s.l. about 11 300 years ago and had regressed to below 2-3 m by 9600 BP in the Paulatuk area. However, it is possible to define further the sea level history of this area, as wood collected by J-S. Vincent (9400 ± 120 BP, GSC-4143) at 1 m a.s.l. indicates that sea level could not have been much higher than 1 m a.s.l. 9400 years ago. Vincent (1983), working on Banks Island to the north of the study area, concluded that based on marine shells, the postglacial sea was at approximately 21 m a.s.l. by about $11\,200 \pm 100$ BP (GSC-2545; Lowdon and Blake, 1980). This appears to be compatible with the data presently available from the Paulatuk area, although additional ^{14}C dating will further help elucidate the temporal framework of the marine record.

ACKNOWLEDGMENTS

This study is part of a continuing PhD research project investigating the stratigraphic nature of glaciomarine and marine sediments along the mainland coast of the Northwest Territories. Field work was made possible with the logistical and financial support of Indian and Northern Affairs Canada (in particular W.A. Padgham, Geology Division), and Geological Survey of Canada (in particular, D.A. St-Onge). Thanks are also extended to G. Hobson, P. Lapointe, and F. Hunt, Polar Continental Shelf Project, without whose assistance this project could not have been

undertaken. All unpublished radiocarbon dates presented in this report were supplied by J-S. Vincent, who in addition, also provided much appreciated constructive comments which improved an earlier version of this report. I would also like to thank the station supervisors of BAR-4, PIN Main, and PIN-1 DEW line sites for their cooperation.

REFERENCES

- Dyke, A. and Prest, V.**
1987: Paleogeography of northern North America 18 000 — 5 000 years ago; Geological Survey of Canada, Map 1703A.
- Kerr, D.E.**
1987: Preliminary interpretation of the stratigraphy of the marine offlap sequence in the Clifton Point area, District of Mackenzie; in Current Research, Part A, Geological Survey of Canada, Paper 87-1A, p. 153-157.
- Klassen, R.W.**
1971: Surficial geology, Franklin Bay, Brock River, District of Mackenzie; Geological Survey of Canada, Open File 48.
- Lowdon, J.A. and Blake, W., Jr.**
1980: Geological Survey of Canada radiocarbon date list XX; Geological Survey of Canada, Paper 80-7.
- Mackay, J.R.**
1952: Physiography of the Darnley Bay area, N.W.T., The Canadian Geographer, no. 2.
1958: The Anderson River map-area, N.W.T.; Geographical Branch, Memoir 5, Department of Mines and Technical Surveys.
- O'Neill, J.**
1924: The geology of the Arctic Coast of Canada, West of the Kent Peninsula; Report of the Canadian Arctic Expedition 1913-18, v. XI, Geology and Geography, Part A; King's Printer, Ottawa.
- St-Onge, D.A. and McMartin, I.**
1987: Morphosedimentary zones in the Bluenose Lake region, District of Mackenzie; in Current Research, Part A, Geological Survey of Canada, Paper 87-1A, p. 89-100.
- Vincent, J-S.**
1983: La géologie du Quaternaire et la géomorphologie de l'île de Banks, arctique canadien; Commission géologique du Canada, Mémoire 405.

Frost heave of subaqueous lake-bottom sediments, Mackenzie Delta, Northwest Territories

C.R. Burn¹

Burn, C.R., *Frost heave of subaqueous lake-bottom sediments, Mackenzie Delta, Northwest Territories; in Current Research, Part D, Geological Survey of Canada, Paper 89-1D, p. 85-93, 1989.*

Abstract

During winter 1987-88 the frost heave regime of lake-bottom sediments was studied at four sites near Inuvik, Northwest Territories. Frost heave was measured with telescoping tubes and magnets; by precise levelling; and by determining the excess water content of core samples obtained during drilling. The lake-bottom thermal regime was monitored with thermistor cables. Maximum of the lake ice thickness in March, including icing and intrusive ice at the bottom of the ice cover, was almost 90 cm. The maximum measured frost penetration into lake sediments was 130 cm. Lake-bottom heave of up to 20 cm was measured over the winter at the sites; ice segregation accounted for approximately 15 cm of the total displacement. Segregated ice lenses 0.5 to 2 cm thick were commonly observed in the core samples. Intrusive ice masses were also recovered. Water migration induced by freezing led to desiccation of some sediments.

Résumé

Au cours de l'hiver 1987-1988, le régime de soulèvement par le gel des sédiments lacustres a été étudié à quatre emplacements près d'Inuvik dans les Territoires du Nord-Ouest. Le soulèvement par le gel a été mesuré au moyen de tubes télescopiques et d'aimants; par nivellement précis; et par évaluation de l'eau en excès dans des échantillons de carottes prélevées en cours de forage. Le régime thermique du fond lacustre a été surveillé à l'aide de câbles à thermistors. L'épaisseur maximale de la glace lacustre, était de 90 cm en mars. La pénétration maximale du givre dans les sédiments lacustres, telle que mesurée, était de 130 cm; la ségrégation de la glace représentait environ 15 cm du déplacement total. Plusieurs lentilles de glace de ségrégation de 0,5 à 2 cm d'épaisseur ont été observées dans les échantillons. Des masses de glace intrusive ont aussi été récupérées. La migration d'eau due au gel a asséché certains sédiments.

¹ Department of Geography, University of British Columbia, Vancouver, British Columbia V6T 1W5

INTRODUCTION

During winter, after water has frozen to the bottom of shallow arctic lakes, the frost line may penetrate underlying sediments. Mackay (1967) and Shilts and Dean (1975) have suggested that sub-ice frost action may be responsible for patterned ground on the bottoms of some lakes in the districts of Mackenzie and Keewatin. Patterned ground at the bottom of other lakes may have formed subaerially and then been submerged (Dionne, 1974; Walters, 1983).

Mackay (1967, p. 39-43) demonstrated that considerable frost heave may occur on exposed surfaces of drained lakes and that some frost action may take place beneath an ice cover. Saturated, fine grained, lake-bottom sediments, in which the temperature gradient may be gentle, should provide an environment conducive to ice segregation and frost heave. While the development of polygonal ground in such environments may be restricted to areas underlain by permafrost, other features, for example, frost-heaved boulders and mud boils, may result from seasonal frost penetration alone (Shilts and Dean, 1975, p. 652).

In a similar fashion, seasonal frost may penetrate nearshore marine sediments where sea ice freezes to the seafloor. At sites of active coastal erosion, an active layer, frozen for some of the winter and thawed in summer, may form between submerged permafrost and the seafloor (e.g. Mackay, 1972, 1986; Grigorjev, 1987). Processes associated with permafrost may continue to occur in this environment; for example, Washburn (1979, p. 125) noted frost cracks beneath sea ice which had been frozen to the bottom. This suggests that some submerged ice wedges in the nearshore zone may be active (cf. Mackay, 1986, Fig. 87.11).

Frost heave in the nearshore active layer may be important for coastal engineering, particularly regarding the design of pipelines bringing oil or gas ashore. Although frost heave may be reduced in a saline environment (Chamberlain, 1983), the waters of the Beaufort Sea in the outer Mackenzie Delta are diluted with fresh water. Results presented by Burn (1987) indicate that considerable ice masses may develop seasonally in the seafloor sediments of this region.

Field studies were conducted in winter 1987-88 in order to examine the frost-heave regime of subaqueous sediments in the Mackenzie Delta, near Inuvik. The results of the study are presented here.

SITE CONDITIONS

Two lakes were selected for study, both of which drain into Mackenzie River (Fig. 1); two monitoring sites were installed in each lake. Lake 1 is 7 km southwest of Inuvik, close to "NRC Lake"; Lake 2 is 16 km northwest of Inuvik, downstream along East Channel (Fig. 2). In mid-September, a small boat can enter each lake without difficulty, but after freeze-up, as the Mackenzie stage falls, water drains from the lakes into the channels. Collapsed surface ice indicated that lake level fell by more than 70 cm at Lake 1 between the beginning of freezing and 21 November 1987. Both lakes are surrounded by permafrost, as are most lakes in the Mackenzie Delta (Mackay, 1963).

The lake-bottom sediments are mostly silt. Mean particle-size distributions of 8 samples collected at 50 cm intervals to a depth of 2 m below lake bottom from two boreholes at each lake are: 1 % sand, 82 % silt, 17 % clay (Lake 1); and 0 % sand, 75 % silt, 25 % clay (Lake 2). The difference between the lakes may be due, in part, to distal fining of delta sediments. The sediments have liquid and plastic limits of approximately 30 % and 27 %, respectively, and are classified ML under the Unified Soil Classification. The gravimetric water contents of grab samples collected with an auger at 50 cm intervals to 2 m depth during equipment installation ranged from 32 % to 62 %.

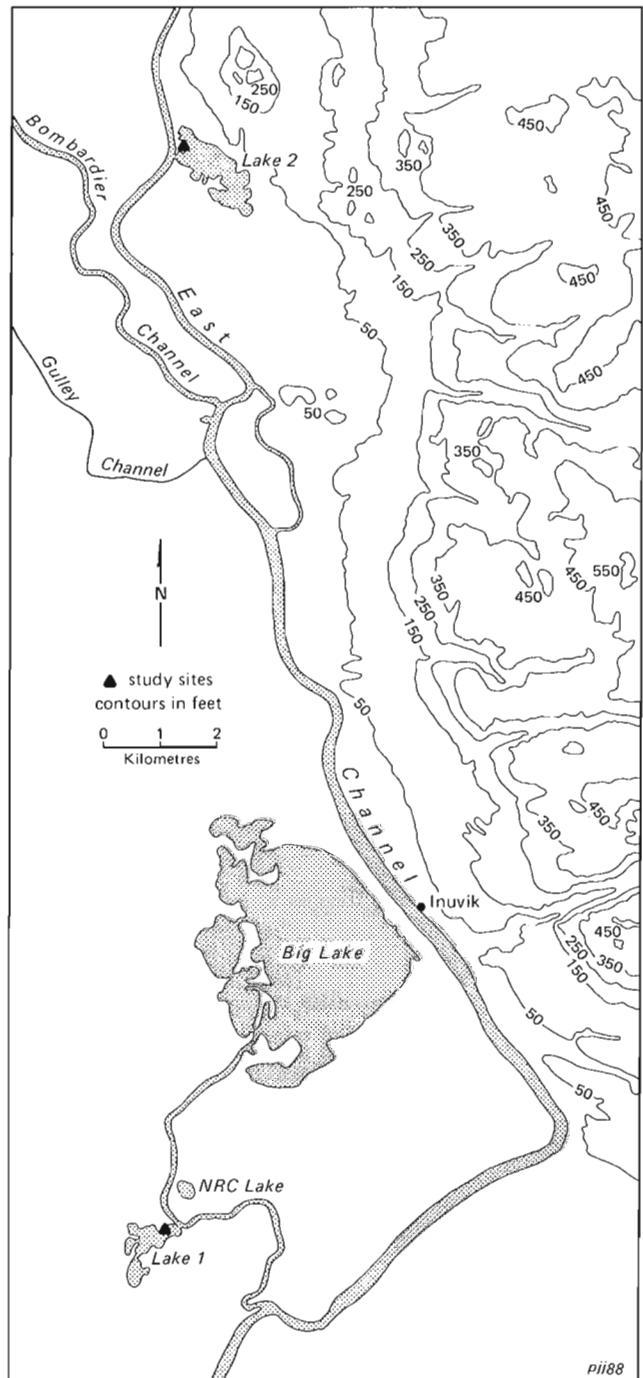


Figure 1. Location of study sites, Mackenzie Delta, Northwest Territories.

By late March 1988, ice thickness at Lakes 1 and 2 had reached 65 cm and 89 cm. Icing (overflow) accounted for some of the ice. The icing may have occurred as a result of continuing recharge of the lakes from a subpermafrost aquifer, or by drainage through the active layer during a comparatively mild early winter. Mean monthly temperatures for the winter and normals for the same period are presented in Table 1. On 28 March, the 0°C isotherm reached a maximum measured depth beneath the ice-sediment interface of 96 cm (Lake 1) and 128 cm (Lake 2).

FIELD TECHNIQUES

The lake-bottom thermal regime and associated frost heave were monitored with equipment installed in late November 1987 (Fig. 3). Sediment temperatures were determined with thermistors spaced at 25 cm intervals from the sediment surface downward for 175 cm. Before installation, the thermistors were calibrated in an ice bath and could be read in the vicinity of 0°C to ± 0.03°C.

Sediment heave was measured with telescoping heave tubes and ring magnets (Mackay et al., 1979; Mackay and Leslie, 1987). One-inch diameter holes were augered into unfrozen lake sediments to a depth of 150 cm, and the equipment was pushed in farther to provide measurements of soil heave in the upper 2 m of sediment. Relative displacement of the heave tubes was measured with calipers to ±0.1 mm. The magnets were located in the soil column with a resolution of ±0.5 mm by a reed switch lowered down an access tube passing through the magnets.

Table 1. Mean monthly temperatures (°C) at Inuvik Airport, September 1987 — March 1988

Observed	4.7	-3.2	-21.7	-21.4	-26.6	-25.0	-19.7
Normal	3.1	-8.1	-20.7	-27.2	-29.6	-28.9	-25.0
Source: Environment Canada (1982).							



Figure 2. Lake 2 on 16 March 1988. Site 2 is in the foreground; the cutline leads to the permafrost benchmark. The west bank of East Channel can be seen behind the snowmobile.

Two benchmarks, for use during levelling surveys, were installed in September 1987 near each lake, one in permafrost and the other on the lake shore between the first and the study sites. The benchmarks comprised 0.5 inch steel rods, 3.5 m long, covered in the active layer and near-surface permafrost by a 2 m-long sleeves of close-fitting, greased aluminum tubing. Collars on the rods protruded into permafrost. It was assumed that the benchmarks in permafrost heaved little; in any event, levelling of the lake surface with respect to the benchmarks provided a *minimum* estimate of total heave after the water column had frozen to the lake-bottom. Over the winter the lake shore benchmarks heaved 3.1 cm and 0.1 cm with respect to the benchmarks in permafrost at Lakes 1 and 2, respectively.

Lake ice elevation was levelled at points marked by dowels along transects lakeward from the shore. Tin cans, 3 cm high and frozen to the lake surface, were used as level markers to provide a stable reference position at each site. Some of the cans were flooded in December/January and could not be located subsequently.

Heave and sediment temperature measurements were made during visits to the sites in late January and March 1988. During the March visits, cores of frozen lake-bottom sediment, 5 cm in diameter, were collected to examine ice lens stratigraphy and to note the depth of frost penetration along the survey transects. The core obtained was brought to the laboratory and thawed in 5.5 cm acrylic tubes in order to determine the excess water content of the frozen zone (Fig. 4). The excess water was then poured off, and the remaining soil dried to determine both volumetric and gravimetric water contents.

RESULTS

Two sites were instrumented in each lake during the November field visit. The thicknesses of frozen materials at the sites in November and during March are summarized in Table 2. Bottom sediments froze at all sites except site 2, Lake 2, where lake ice was still afloat in March.



Figure 3. Site 1, Lake 1 on 16 March 1988. From left to right: heave tubes; thermistor cable; magnet access tube; snowstake.

Lake ice thickness

Lake ice thickness in the Mackenzie Delta near Inuvik is rarely more than 1 m (Mackay, 1963, p. 76). The ice thicknesses determined by drilling at each lake in November and March are indicated by Table 2; ice thickness increased over the winter at both sites. In Lake 1, the final ice thickness of 62 cm comprised approximately 8 cm of icing, 28 cm of ice present in November, and $(25 \times 1.09 =) 27$ cm of ice formed from the November water column. (Icing thickness was measured on a snowstake installed in November which was subsequently partially flooded). At Lake 2, ice thickness on 20 March was 89 cm, overlying 6 cm of water. On 23 November there was only 30 cm of ice and 15 cm of water at this site, which accounts for the underlying water and 40 cm of the March ice. Part of the residual 49 cm is the 17 cm of icing measured at the site. The outstanding 49 cm may be due to groundwater discharge into the lake over the winter.

While Lake 1 is located several kilometres from the edge of the Mackenzie Delta, Lake 2 is part of a system of lakes bounded to the east by the escarpment of the Caribou Hills (Fig. 1). Groundwater may be expected to flow from the hills toward the lake system and to recharge the basin. Lake ice rupture and overflow of discoloured water at "Red" Lake, near Reindeer Station, 30 km north of Lake 2, is attributed to discharge of groundwater through or below permafrost in the Cretaceous shales of the Caribou Hills (J.R. Mackay, personal communication, 1988). If discharge

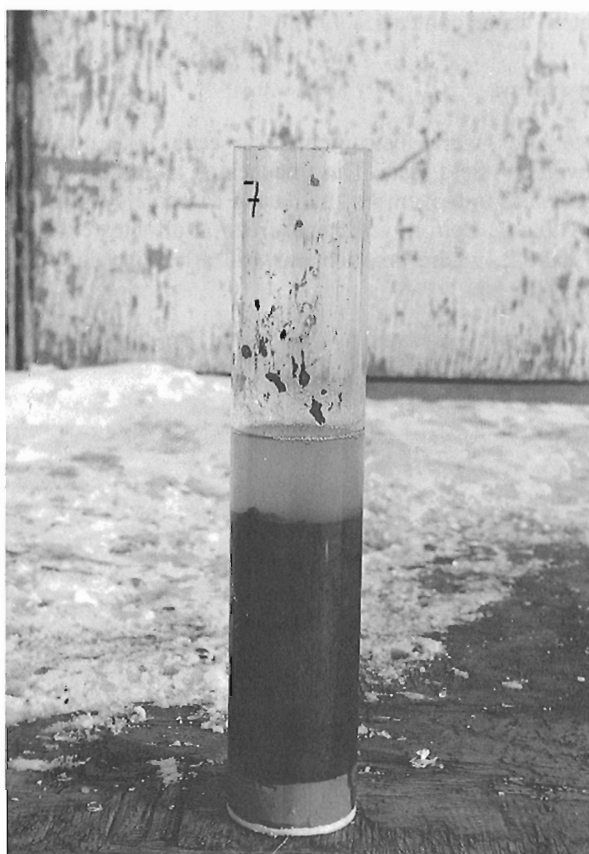


Figure 4. Core sample in acrylic tube after thawing, 20 March 1988.

from Lake 2 into East Channel ceases or is restricted in winter, continuing intrapermafrost or subpermafrost groundwater discharge into the lake system will lead to elevated water pressures beneath the ice cover and uplift of the ice. The distance between the ice surface and lake bottom will increase, and an icing may form if the ice cover ruptures. The rate of groundwater discharge may decline over the winter: active layer discharge directly into the lake, or via streams, will cease; and aquifer recharge in permafrost regions is lowest during this season, resulting in reduced flow of deeper groundwater (Williams, 1970).

Levelling of the ice surface at Lake 2, site 2, indicated an increase in elevation of 48 cm with respect to the permafrost benchmark between 24 November and 16 March (Fig. 5), in agreement with the 49 cm increase of ice thickness described above. Therefore, approximately 45 cm of water (49 cm ice) was added to the lake over the period 23 November to 20 March. This is equivalent to a mean groundwater discharge rate of 4 mm/day (4.4×10^{-6} cm/s) over the period. Levelling of the ice surface on 23 January indicated an increase in elevation of 38 cm over the previous two months. Applying similar reasoning, the discharge rate in December and January can be estimated at 5.7 mm/day (6.6×10^{-6} cm/s), and in February and March at 1.9 mm/day (2.2×10^{-6} cm/s).

The 45 cm of added water comprises 17 cm of icing and 32 cm added to the ice cover below the lake surface. The ground ice equivalent of the lower ice is intrusive ice, formed where water is injected under pressure into a freezing soil or rock. In the present case, the elevated water pressure raised the lake ice; with intrusive ground ice, the elevated pore water pressure raises an overlying layer of frozen soil (e.g., Pollard and French, 1984). On 19 March, when lake ice was drilled at Lake 2, site 2, water rose up the hole to the lake surface, implying an hydraulic head of 89 cm at the base of the ice.

Table 2. Thickness of ice and frozen sediment (cm), Lakes 1 and 2, winter 1987-88

	Lake 1		Lake 2	
	Site 1	Site 2	Site 1	Site 2
Snowdepth	5	8	11	9
Lake ice	25	28	30	30
Water	0	25	0	15
Icy sediment	6	0	10	0
Depth to 0°C*	20	0	35	0
Date of survey	19 November 1987		23 November 1987	
Snowdepth	38	38	43	27
Lake ice	24	62	31	89
Water	0	0	0	5
Icy sediment	78	12	93	0
Depth to 0°C*	92	81	124	0
Date of survey	19 March 1988		20 March 1988	

*Depth of 0°C isotherm below lake bottom.

Lake-bottom thermal regime

Lake-bottom temperature profiles for the period 23 November 1987 to 28 March 1988 are presented in Figure 6. The depth of "ice-bonded" sediment and the extent of visible ice in drill core recovered from each site are also indicated. In this case, "ice-bonded" refers to sediment containing ice that could not be broken by hand. The unfrozen water content of sediment containing ice, but not ice-bonded, was often high enough to provide noticeable plasticity in the recovered core.

The association of sediment temperatures, ice appearance, and plasticity indicates that at the time of drilling, soil ice nucleation temperature was approximately -0.25°C , and that a significant quantity of unfrozen water was present at temperatures as low as -1°C . The implication is of a frozen fringe up to 25 cm thick, corresponding to a temperature difference of 0.75°C (cf. Miller, 1978).

Lake-bottom temperature gradients in the talik were of the order of $1.5^{\circ}\text{C}/\text{m}$ throughout the winter, but somewhat greater above the frost line; in March approximately

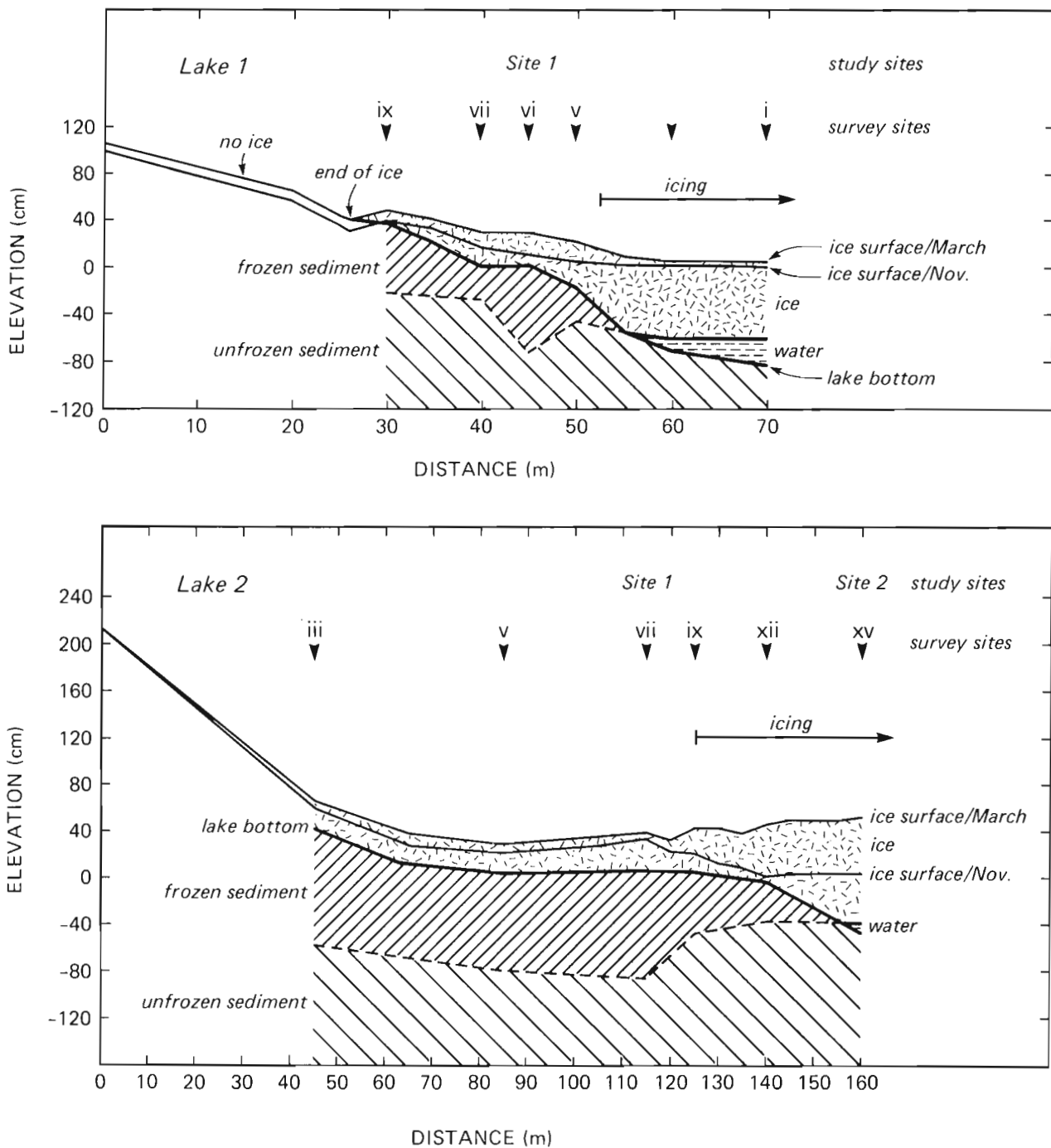


Figure 5. Drilling transects at Lakes 1 and 2, March 1988, with elevation of the lake surface in November 1987.

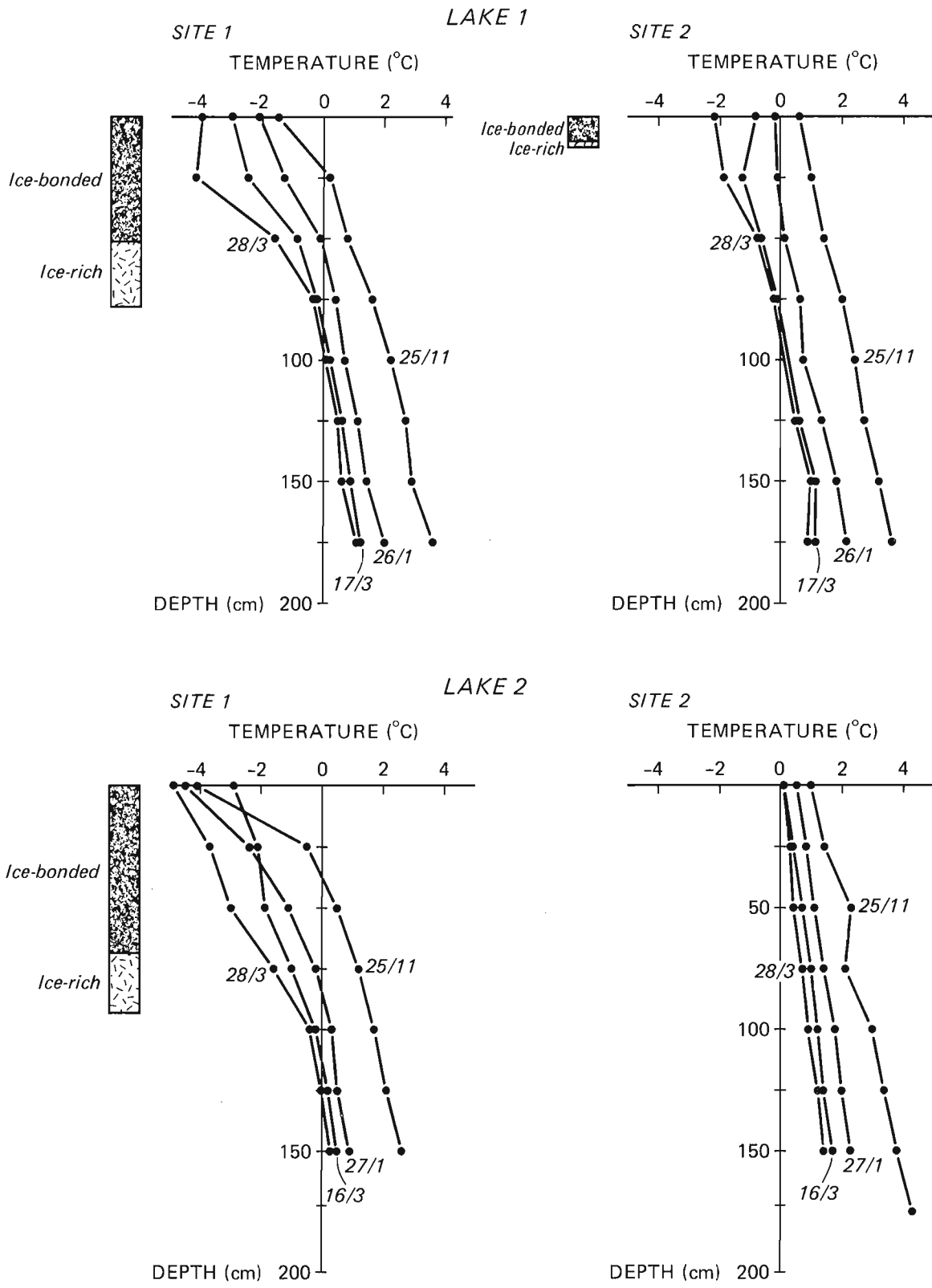


Figure 6. Temperature profiles in lake-bottom sediment, Mackenzie Delta study sites, winter 1987-88, with aspects of drill logs from 19 March 1988.

-4°C/m at Lake 1, and -2°C/m at Lake 2. Where ice was present in the soil, these temperature gradients imply pore pressure gradients of approximately 2.4×10^3 kPa/m and 4.8×10^3 kPa/m, respectively (Edlefsen and Anderson, 1943).

Frost heave

The total heave of lake-bottom sediments at the study sites during the period 22 November to 17 March, determined by heave tubes, magnets, and level survey, is presented in Table 3. Site 2, Lake 2 is excluded from this table because the water column did not freeze through. Table 3 shows agreement between the three techniques, except in the case of heave tubes at Lake 1 after January. Some variation between techniques is also to be expected for the period from November to January, especially with the magnets, to allow for settlement following installation. The most consistent observations were obtained at Lake 2, site 1, where the range between measurement techniques was less than 1 cm. The greatest heave was measured at Lake 1, site 1, where the lake bottom was displaced upward by approximately 20 cm.

The heave recorded in Table 3 includes both soil displacement as a result of the expansion of interstitial water on freezing and segregational heave due to the growth of ice lenses in freezing sediment (Miller, 1978; Smith, 1985). Estimates of segregational heave, determined from the water released by core samples on thawing, are presented in Table 4. These drilling results imply that approximately 15 cm of the observed displacement at Lake 1, site 1 was due to segregational heave. At the other two sites, segregational heave was much less. At Lake 1, site 2 the drill hole was located lakeward of the site, and the frozen sediments were probably undersampled.

Table 3. Total lake-bottom heave (cm), 22 November 1987 to 17 March 1988, Mackenzie Delta sites

Instrument	Heave tubes	Magnets	Level	Mean
November-January				
Lake 1, Site 1	10.05	11.9	10.7	10.8
Lake 1, Site 2	0.0	[1.6]	0.0	0.0
Lake 2, Site 1	6.56	6.7	7.4	6.9
January-March				
Lake 1, Site 1	[2.64]	9.2	9.2	9.2
Lake 1, Site 2	[8.82]	14.0	14.4	14.2
Lake 2, Site 1	2.21	2.4	2.4	2.3
November-March				
Lake 1, Site 1	[12.69]	21.1	19.9	20.5
Lake 1, Site 2	[8.82]	15.6	14.4	15.0
Lake 2, Site 1	9.27	9.1	9.8	9.4
Notes: Observations at Lake 1 on 22 November, 23 January, 17 March Observations at Lake 2 on 24 November, 24 January, 16 March Data in parentheses omitted from calculation of the mean.				

Only minimum estimates of segregational heave can be derived from the excess water contents of drill samples. "Excess water" is determined from the water that may be poured off the sample while the sediment remains saturated. Therefore, the estimate does not include any segregational heave that may have been effected by moisture redistribution within the sample intervals.

Drill records

Summaries of the drill logs obtained at Lakes 1 and 2 are presented in Figure 5. The vertical scale in Figure 5 is referenced to an arbitrary zero, chosen as the lowest elevation of the lake surface during the November survey. The diagrams indicate that frost penetration into bottom sediments was approximately even beneath parts of the lake not covered by icing. The lateral extent of freezing in the sediment body at Lake 1 was primarily controlled by the bottom topography, since the increase in surface elevation between November and March was minimal. The increase in ice thickness during the winter at Lake 2 indicates the influence of water intrusion on the horizontal limit of frost penetration.

The moisture contents of drill core samples are presented in Table 5. At both lakes, samples recovered from the uppermost sediments were ice rich, and contained a significant quantity of excess ice. Horizontal ice lenses 0.5 to 1.5 cm thick were observed in the core. The ice-bonded sediments below this ice-rich horizon were saturated and contained ice lenses 0.5 mm to 2 mm thick. At most drill sites in Lake 1, and some in Lake 2, the samples from this interval did not release excess water upon thawing. Therefore, the ice lenses resulted from local moisture redistribution.

At all sites in Lake 1, the sediments below the ice-rich layer remained saturated. However in Lake 2, at sites over 60 m from the limit of bottom-fast lake ice (survey sites iii and v), sediments more than 60 cm below lake bottom were desiccated in mid-March (Table 5). Moisture supplied from the desiccated zone was drawn to the advancing frost front and contributed to ice lensing in the upper layers. The moisture was not replaced, since horizontal hydraulic gradients in the lake sediment would be considerably less than the vertical pore pressure gradients due to freezing calculated above.

In both lakes at sites within 20 m of the bottom-fast ice (sites ii, iv, 1, 2, Lake 1; site xii, Lake 2), the lowermost 30 cm of core samples containing ice lenses held these lenses

Table 4. Sediment soil displacement and excess ice content of drill core, Mackenzie Delta sites, winter 1987-88.

	Total Heave (cm)	Excess ice (cm)
Lake 1, Site 1	20.5	15.9
Lake 1, Site 2	15.0	4.3
Lake 2, Site 1	9.4	3.8
Note: Excess ice determined from excess water content of drill core samples x1.09.		

Table 5. Water content of drill core samples from survey sites, Lakes 1 and 2, March 1988 (cf. Fig. 5)

Depth (cm)	Excess Water (cm)	Gravimetric %	Volumetric %
Lake 1			
Site ix			
0-15	4.2	102	71
15-32	3.0	62	57
32-46	1.0	43	49
46-61	0.0	49	55
Site vii			
0-13	5.3	101	72
13-28	0.0	44	48
Site vi (Site 1)			
0-13	4.9	87	65
13-28	4.1	64	58
28-52	4.7	87	69
52-77	0.0	43	52
(Site 2)			
0-12	3.9	107	74
12-20	0.0	43	47
Site v			
0-18	6.8	105	72
18-29	3.0	108	74
Lake 2			
Site iii			
0-16	3.2	73	66
16-35	1.5	60	60
35-62	0.0	36	50
62-89	0.0	34	46
89-108	0.0	25	33
Site v			
0-15	2.6	78	67
15-34	1.1	55	58
34-59	0.0	40	52
59-83	0.0	17	22
Site vii (Site 1)			
0-16	3.5	52	52
16-42	0.0	50	55
42-69	0.0	35	42
69-93	0.0	35	40
Lake 2			
Site ix			
0-15	4.8	90	70
15-40	3.5	70	65
40-46	0.4	56	60
52-62	0.0	33	—
Site xii			
0-13	6.2	225	89
13-27	14.0	—	100
27-34	2.3	125	75

in a matrix of soft sediment. Where small sand inclusions were contained in these samples, the inclusions were ice-bonded. The ice lenses in these intervals were up to 1 cm thick.

The ice-bonded sand inclusions imply that sediment temperatures were below 0°C. If the ice lenses were growing by segregation, then, according to the Rigid Ice model (O'Neill and Miller, 1985), the sediments above the large lenses would be thoroughly ice-bonded. At some sites, the sediments below the ice lenses were also plastic, but not saturated. Pore water pressures in these sediments were not above zero gauge pressure at the time of drilling.

At survey site xii, Lake 2 (Fig. 5), an ice lens 14 cm thick was observed, 13 cm below lake bottom. The lens comprised vertical columnar crystals, 1 cm in diameter, with elongated bubbles up to 1 cm long. The lens was devoid of mineral inclusions. Ice-bonded sediments, 7 cm thick, lay below the ice lens. When these were penetrated, water rose to within 8 cm of the surface of the lake ice.

The hydrostatic head in the lake-sediment water and the form of the ice lens suggest that it was intrusive ice, formed from water injected toward the freezing front. The large, continuous columnar crystals imply that the ice formed from bulk water ("pool" ice; Mackay, 1988), rather than by segregation; the analogy between intrusive ground ice and intrusive lake ice has been made above. The site concerned was close to the limit of bottom-fast ice (Fig. 5), and 20 m from site 2, where 32 cm of injected lake ice formed. A continuum between the injected lake and ground ice is implied.

Inspection of Table 5 and Figure 5 indicates that, in general, the excess water (ice) content of frozen lake-bottom sediments increases with distance from the lake shore. Close to shore, most of the excess water is probably drawn into the upper sediments during freezing and contributes to the development of segregated ice lenses. The unfrozen sediments are not replenished from the lake, which is some distance away. Farther from shore, close to the limit of bottom-fast ice, significant quantities of injected ice may be found. An elevated pressure may be generated in the lake water body by recharge beneath an enclosing ice cover and lead to pore water pressures in adjacent sediments sufficient to raise the overlying ice and frozen soil. The ice pressures associated with the injection ice are considerably lower than those required for the formation of segregated ice lenses.

CONCLUSION

The thermal regime, frost heave, and ground ice content of sediments in two lakes near Inuvik, Northwest Territories were examined during winter 1987-88. Segregational frost heave of up to 15 cm was documented at one site. Increases in lake ice thickness and the nature of the ground ice at some sites suggested that considerable quantities of ice may be formed in the lake sediments from water injected toward the frost front, rather than by segregation.

ACKNOWLEDGMENTS

The fieldwork was supported by the Geological Survey of Canada, Imperial Oil Limited and the Inuvik Scientific Research Laboratory. Support at the University of British Columbia was provided by the Killam Committee.

J.R. Mackay, S.R. Dallimore, J.A.M. Hunter, and J.D. Ostrick have given valuable advice and discussion throughout the project. D.A. Sherstone, S.C. Bigras, and M.E. Ferguson made helpful suggestions and provided logistical support during site selection in June 1987. Comments on the manuscript by D.G. Harry and J.A. Heginbottom are appreciated. The figures were drawn by P.J. Jance.

REFERENCES

- Burn, C.R.**
1987: Frost heave tests; in Geotechnical investigations off northern Richards Island, N.W.T., P.J. Kurfurst (ed.); Geological Survey of Canada, Open File 1707, p. 31-37.
- Chamberlain, E.J.**
1983: Frost heave of saline soils; Proceedings, Fourth International Conference on Permafrost, Volume 1; National Academy of Sciences, Washington, D.C. p. 121-126.
- Dionne, J.-C.**
1974: Cryosols avec tirage sur rivage et fond de lacs, Québec central subarctique; *Revue de Géographie de Montréal*, vol. 28, no 4, p. 31-298.
- Edlefsen, N.E. and Anderson, A.B.C.**
1943: Thermodynamics of soil moisture; *Hilgardia*, v. 15, no. 2, p. 31-298.
- Environment Canada**
1982: Canadian Climate Normals, 1951-1980, Temperature and Precipitation — The North, Y.T. and N.W.T.; Atmospheric Environment Service, Ottawa, Ontario, 55 p.
- Grigorjev, N.F.**
1987: Permafrost in the coastal zone of northern Yamal District; Permafrost Research Institute, Yakutsk, 112 p. (in Russian).
- Mackay, J.R.**
1963: The Mackenzie Delta area, N.W.T.; Geographical Branch, Memoir 8, Department of Mines and Technical Surveys, Ottawa, 202 p.
1967: Underwater patterned ground in artificially drained lakes, Garry Island, N.W.T.; *Geographical Bulletin*, v. 9, no. 1, p. 33-43.
1972: Offshore permafrost and ground ice, southern Beaufort Sea, Canada; *Canadian Journal of Earth Sciences*, v. 9, no. 11, p. 1550-1561.
1986: Fifty years (1935-1985) of coastal retreat west of Tuktoyaktuk, District of Mackenzie; in *Current Research, Part A, Geological Survey of Canada, Paper 86-1A*, p. 727-735.
1988: Catastrophic lake drainage, Tuktoyaktuk Peninsula area, District of Mackenzie; in *Current Research, Part D, Geological Survey of Canada, Paper 88-1D*, p. 83-90.
- Mackay, J.R. and Leslie, R.V.**
1987: A simple probe for the measurement of frost heave within frozen ground in a permafrost environment; in *Current Research, Part A, Geological Survey of Canada, Paper 87-1A*, p. 37-41.
- Mackay, J.R., Ostrick, J., Lewis, C.P., and Mackay, D.K.**
1979: Frost heave at ground temperatures below 0°C, Inuvik, Northwest Territories; in *Current Research, Part A, Geological Survey of Canada, Paper 79-1A*, p. 403-406.
- Miller, R.D.**
1978: Frost heaving in non-colloidal soils; Proceedings, Third International Conference on Permafrost, v. 1, National Research Council of Canada, Publication 16529, p. 708-713.
- O'Neill, K. and Miller, R.D.**
1985: Exploration of a rigid ice model of frost heave; *Water Resources Research*, v. 21, no. 3, p. 281-296.
- Pollard, W.H. and French, H.M.**
1984: The groundwater hydraulics of seasonal frost mounds, North Fork Pass, Yukon Territory; *Canadian Journal of Earth Sciences*, v. 21, no. 10, p. 1073-1084.
- Shilts, W.W. and Dean, W.E.**
1975: Permafrost features under arctic lakes, District of Keewatin, Northwest Territories; *Canadian Journal of Earth Sciences*, v. 12, no. 4, p. 649-662.
- Smith, M.W.**
1985: Observations of soil freezing and frost heaving at Inuvik, Northwest Territories, Canada; *Canadian Journal of Earth Sciences*, v. 22, no. 3, p. 283-290.
- Walters, J.C.**
1983: Sorted patterned ground in ponds and lakes of the High Valley/Tangle Lakes region, central Alaska; Proceedings, Fourth International Conference on Permafrost, v. 1; National Academy of Sciences, Washington, D.C., p. 1350-1355.
- Washburn, A.L.**
1979: *Geocryology*; Edward Arnold, London, 406 p.
- Williams, J.R.**
1970: Groundwater in permafrost regions of Alaska; United States Geological Survey, Professional Paper 696, 83 p.

Rock blisters and other frost-heaved landforms in the Bernard Harbour area, District of Mackenzie, N.W.T.

Denis A. St-Onge, Isabelle McMartin,¹ and Ron Avery²
Terrain Sciences Division

St-Onge, D.A., McMartin, I., and Avery, R., Rock blisters and other frost-heaved landforms in the Bernard Harbour area, District of Mackenzie, N.W.T.; in Current Research, Part D, Geological Survey of Canada, Paper 89-1D, p. 95-99, 1989.

Abstract

In the Bernard Harbour area, District of Mackenzie flat surfaces of exposed bedrock display abundant evidence of frost heaving. On dolomite, the most common bedrock type, frost heaving has produced "rock blisters", 1 to 3 m high and 2 to 5 m in diameter, which resemble miniature pingos. Related forms in shaly sandstone are 2 to 3 m deep trenches in regular grid pattern, with individual cells 50 to 120 m wide. Lichen cover and degree of weathering suggest that all frost-heaved features date from the early postglacial when permafrost was being established following ice retreat.

Résumé

Dans la région de Bernard Harbour, district de Mackenzie, des surfaces planes d'affleurements rocheux présentent de nombreux signes de soulèvement par le gel. Sur la dolomie, le principal type de roche en place, le soulèvement par le gel a produit des « pustules rocheuses » de 1 à 3 m de haut et de 2 à 5 m de diamètre qui ressemblent à des pingos miniatures. Associées, des tranchées de 2 à 3 m de profondeur forment dans le grès schisteux un réseau régulier de mailles de 50 à 120 m de côté. La couche de lichen et le degré d'alteration indiquent que tous les éléments soulevés par le gel datent du début du post-glaciaire lorsque le pergélisol s'est formé après le retrait des glaces.

¹ Département des Sciences de la Terre, Université du Québec à Montréal, Montréal, Québec H3C 3J7

² Department of Geology, Queen's University, Kingston, Ontario K7L 3N6

INTRODUCTION

The Bernard Harbour area, District of Mackenzie, as defined in this report, is the peninsula bounded by Coronation Gulf to the east, by Cape Kendall to the south, by longitude 116°x to the west, and by Dolphin and Union Strait to the north (Fig. 1). The area is underlain by flat-lying, lower Paleozoic dolomite and minor sandstones and shales (Fraser et al., 1960). Extensively drumlinized drift, sandy gravel outwash, and glaciomarine sand, silt, and clay discontinuously cover bedrock, revealing extensive outcrop exposures both along valley walls and as large platforms or benches. Dolomite beds, varying in thickness from 5 to 50 cm, are cut by fractures which delineate angular blocks with sides ranging in length from 10 centimeters to 1 m or more. Where recently exposed, the bedrock surface is smoothly grooved and striated, but where it has been exposed for long periods, striations and other flow indicators have been removed, and in many places the surface has been differentially dissolved into a lapiés. The surfaces of these platforms are commonly modified by the presence of mounds and small rounded hills which result from the updoming of the beds of dolomite. These forms are discussed in detail in this report.

NATURE AND SIZE OF MOUNDS

Although rock blisters display great variations in detail, they have the following characteristics in common:

- (1) They occur on presently well drained surfaces of dolomite benches (Fig. 2).
- (2) They are 1 to 3 m high and 3 to 5 m in diameter (Fig. 3).
- (3) A small crater is commonly present at the top with the collapsed blocks occupying the base of the depression (Fig. 3,4).
- (4) Mounds less than 1 m high do not display a collapsed centre.
- (5) They are composed of imbricated angular blocks of dolomite beds which retain the glacially smoothed or the lapiés surface characteristic of the bench surface (Fig. 3).
- (6) The thickness of the tilted blocks, which may comprise several beds, is between 80 to 100 cm (Fig. 4).
- (7) At present there is no ice in the core of the mounds.

The general appearance is that of a jigsaw puzzle pushed up from underneath; when the upward pressure was removed the jagged angularity of the blocks prevented their falling back to their original position.

Similar features to the rock blisters discussed here have been reported from numerous parts of Arctic Canada: the east coast of Hudson Bay (Dionne, 1981), northern Quebec (Payette, 1978), eastern District of Mackenzie (DiLabio, 1978), Baker Lake area, District of Keewatin (Dyke, 1984). In all cases, domed structures occur in jointed or sheeted rock and in discharge areas where water moved in joints and bedding planes.

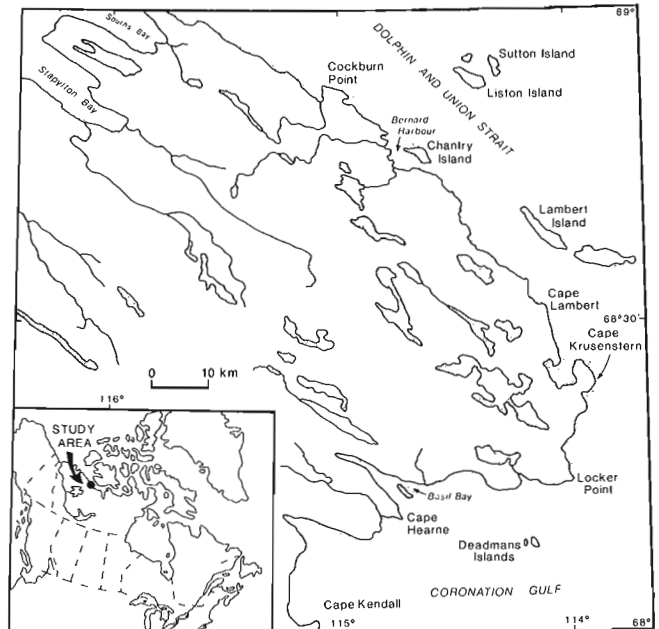


Figure 1. Location map of the Bernard Harbour area, District of Mackenzie.

DISCUSSION

There is no doubt that the rock blisters result from the uplifting of blocks which were part of a glacially smoothed surface of horizontally bedded dolomite. The shape and size of the blocks are closely related to two dominant subvertical sets of fractures trending 340° and 260°, but these fractures are not the controlling factor because the mounds, in many places, are absent from surfaces that are intensely dissected by these near perpendicular dominant sets of fractures.

The Bernard Harbour area, with a mean annual air temperature of 12.5°C, lies well within the continuous permafrost zone (French, 1976). Several excavations in glacial drift and in coarse raised marine beach sediments indicate that the active layer was up to 1.5 m thick in July 1988 and was probably thicker in bedrock (Dyke, 1984). Thus, the condition certainly exists for the formation of pingos and other frost heave features.

Rock pingos have been reported previously from this general area. Craig (1960) showed several on his map and described one as follows: "The pingo near the Harding River at latitude 68°x28' is found in a swampy area beside a small lake. It is seventy feet high and two hundred feet in diameter. The outer surface is dolomite of Lower Paleozoic age In the crater, about ten feet of the rock has been exposed."

A similar but smaller pingo to the one observed by Craig is located in the study area (Fig. 5). It is in part composed of broken slabs of bedrock and occurs in a swampy area; it is between 5 and 6 m high and approximately 20 m in diameter. It was photographed from a low-flying aircraft but was not studied on the ground. Obviously this pingo and the

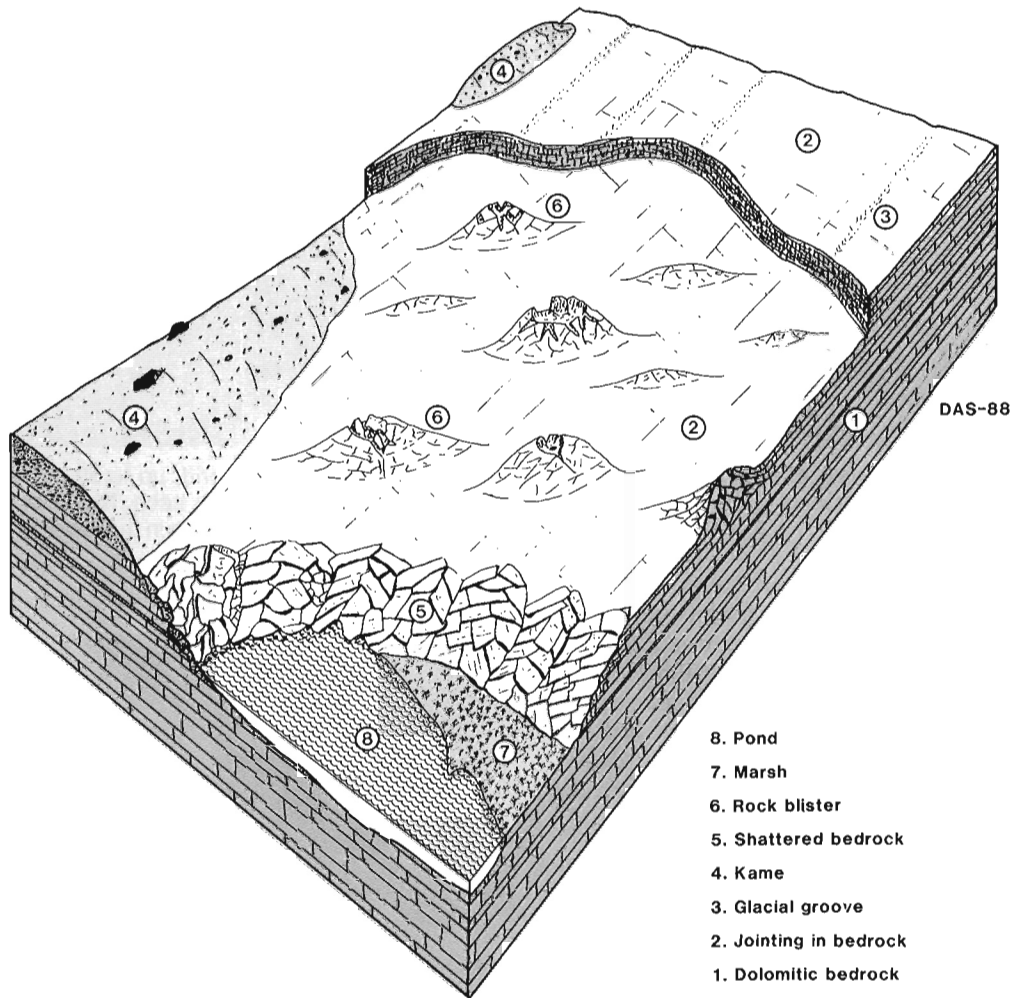


Figure 2. Block diagram showing typical location where rock blisters of various sizes occur.



Figure 3. Group of rock blisters in similar condition to those illustrated in Figure 2. Note the generally even size, dominantly rectangular shape of the blocks, and open central crater. The glacially smoothed surface is clearly visible both on the undisturbed bench surface and on the uplifted blocks. 204662-F.



Figure 4. Detail of the uplifted beds, rectangular blocks, and collapsed centre of a rock blister. Shovel handle is 50 cm long. 204662-B



Figure 5. Pingo in marshy area at 68x37'N, 115x50'W. The debris is predominantly blocks of dolomite. 204662

larger one reported by Craig are ice-cored since they show no evidence of major collapse. The rock blisters in the Bernard Harbour area, however, have no ice core and, furthermore, lichen cover and weathering on block faces clearly indicate that no disturbance has taken place for a long period of time. In his excellent study of frost heaving of bedrock in permafrost regions, Dyke (1984) described "dome-shaped rock heave features" which, although in quartzite, appear identical to the rock blisters discussed here.

Dyke proposed that features formed by the expulsion of excess water pressures in the saturated active layer reach an equilibrium height and show little further movement. Domes are similar to the closed-system type of pingo. Watersaturated fractured dolomite and a progressing freezing plane result in heaving forces from high pore water pressures. In the dolomites of the Bernard Harbour area the near vertical fracture sets and the subhorizontal bedding acted as the controlling discontinuities that favoured the development of ice-cored domes.

Doming of bedrock layers usually produces a dilation and when the ice lens melts, partial collapse or total disruption occurs depending on the relative thicknesses of the ice body and the rock layer. Dyke was successful in predicting the maximum size of dome-type features in central District of Keewatin from relationships between the total dilation and the height of the dome. In the Bernard Harbour area, rock blisters have collapsed and maximum size can only be estimated — approximately 5 m in diameter by 3 m in height. The dilation for that diameter and height was so large that the ice core was exposed, leading to eventual melting and collapse during the annual thaw of the active layer. Once the miniature pingo had collapsed into a mound of blocks, conditions no longer existed for the formation of the high pore water pressures that would allow the process to start again.

AGE OF ROCK BLISTERS

Rock blisters are composed of angular weathered blocks. Given that the only reasonable explanation for their formation is the growth of ice in a confined space and since no ice is present today, when were conditions most favourable for their formation?



Figure 6. Rectangular grid, up to 50 by 120 m, delimited by uptilted shaly sandstone beds. Note trenches extending across raised marine beaches in the lower right of the photograph. 204662-A



Figure 7. Uptilted beds of shaly sandstone forming margins of 50 m rectangles. 204662-D

Because the mounds occur on bedrock surfaces that have been smoothed by glacier ice or by meltwater abrasion, they postdate the last glaciation. No permafrost existed under the surface which was uncovered as the glacier retreated (Washburn, 1979, p. 61). The growth of permafrost would have started soon after the area became ice-free or when the sea retreated from the coastal regions. The melting of snow supplied all the water required to saturate the bedrock surface which had become intensely fractured as a result of decompression by ice removal.

Permafrost established to a depth of a few metres provided the impermeable lower barrier required to generate high pressures in the active layer during the annual freeze-back. The updoming of the rock blisters, resulting from the enormous pressures generated by ice growth in the saturated active layer, shattered the bedrock surface. The uplifted and tilted blocks did not fall back into place but came to rest as an open work fabric which precluded any further development of rock-breaking pressures in the active layer. Each rock blister thus acted as a pressure release valve for the immediate area surrounding it.

Rock blisters represent a particular response to high pressure generated during the annual freeze-back of the active layer of newly established permafrost in this area underlain by beds of dolomite. Similar conditions in other lithological units produced different results. In shaly sandstone in the Locker Point area (Fig. 1) frost heaving has produced rectangular grids up to 50 by 120 m (Fig. 6), bounded by 2 to 3 m deep trenches (Fig. 7) as a result of the uplifting and tilting of beds on either side of presumed vertical fractures.

SUMMARY AND CONCLUSIONS

In the Bernard Harbour area the establishment of permafrost following the last ice retreat created favourable conditions for the generation of pressures sufficiently high in the active layer to induce frost heaving in the jointed, horizontally bedded competent bedrock. The dolomite surface is pock-marked with blisters of uplifted and tilted blocks which resemble miniature relict pingos, commonly with a central crater-like depression. Once uplifted by growth of ground ice in the pressure-confined zone of the active layer, the angular blocks form an open-work system which acts as a pressure release vent. All rock blisters studied on the ground are old, as indicated by the presence of lichens and by weathering surfaces. Thus, it is assumed that most of these forms date from the early Holocene. Present conditions, as evidenced by large rock pingos, are certainly favourable to the growth and preservation of ground ice. Once rock blisters are formed, however, they "open up" the active layer making it impossible for freeze-up to generate the high pressures required to uplift and tilt bedrock blocks. In less competent bedrock, such as shaly sandstone, different forms were generated, but the age and conditions of formation appear to be the same.

ACKNOWLEDGMENTS

We are grateful to the following persons for assistance in the field and for enthusiastic logistical support: M. Potschin and D. Kerr who found time to look at periglacial landforms between drumlins; Peter Newman, the pilot, and Miles Nelson, the engineer, who not only ensured that the helicopter took us where we wanted to go but, more importantly, brought us back to camp at the end of the day; they greatly contributed to the quality of life in camp by constructing a hot water system for the refurbished shower; Rod Stone, the quietly competent radio expediter in Yellowknife went out of his way to provide all the help and assistance to his "farthest away" field crew.

This report benefited from critical review by R.N.W. DiLabio.

REFERENCES

- Craig, B.G.**
1960: Surficial geology of north-central District of Mackenzie, Northwest Territories; Geological Survey of Canada, Paper 60-18, 8 p. and Map 24-1960.
- DiLabio, R.N.W.**
1978: Occurrences of disrupted bedrock on the Goulburn Group, eastern District of Mackenzie; in Current Research, Part A, Geological Survey of Canada, Paper 78-1A, p. 499-500.
- Dionne, J.-C.**
1981: Formes d'éjection périglaciaire dans le Bouclier laurentidien, Québec; *Revue de Géomorphologie dynamique*, vol. 30, p. 113-124.
- Dyke, L.D.**
1984: Frost heaving of bedrock in permafrost regions; *Bulletin of the Association of Engineering Geologists*, v. 21, no. 4, p. 389-405.
- Fraser, J.A., Craig, B.G., Davison, W.L., Fulton, R.J., Heywood, W.W., and Irvine, T.N.**
1960: Geology, north-central District of Mackenzie, Northwest Territories; Geological Survey of Canada, Map 18-1960.
- French, H.M.**
1976: *The Periglacial Environment*; Longman Inc., New York, 309 p.
- Payette, S.**
1978: Les buttes rocheuses d'origine périglaciaire au Nouveau-Québec; *Géographie physique et Quaternaire*, vol. 32, p. 369-374.
- Washburn, A.L.**
1979: *Geocryology, A Survey of Periglacial Processes and Environments*; Edward Arnold (Publishers) Ltd., London, 406 p.

High terrace sediments, probably of Neogene age, west-central Ellesmere Island, Northwest Territories

John G. Fyles
Terrain Sciences Division

Fyles, J. G., *High terrace sediments, probably of Neogene age, west-central Ellesmere Island, Northwest Territories*; in *Current Research, Part D, Geological Survey of Canada, Paper 89-1D*, p. 101-104, 1989.

Abstract

Unconsolidated sands and gravels, containing wood, peat, and other organic remains, are widely distributed on west-central Ellesmere Island beneath high terraces. These high terrace sediments are inferred to represent boreal forest to forest tundra conditions. Preliminary plant macrofossil investigations by J. V. Matthews, Jr. have revealed floral similarities to both the Kap København Formation (late Pliocene) of north Greenland, and the Beaufort Formation on Meighen and Prince Patrick islands (late Miocene).

Résumé

Des sables et graviers non consolidés, contenant du bois, de la tourbe et d'autres restes organiques, sont très répandus dans la partie ouest-centrale de l'île d'Ellesmere, au-dessous de terrasses élevées. Ces sédiments de terrasses élevées se seraient accumulés dans un écosystème de forêt boréale ou de toundra arbustive. Des études préliminaires de macrofossiles végétaux, faites par M. J. V. Matthews, fils, ont révélé l'existence de similarités entre la flore de la formation de Kap København (Pliocène supérieur) du nord du Groenland et celle de la formation de Beaufort dans les îles Meighen et Prince Patrick (Miocène supérieur).

INTRODUCTION

Unconsolidated deposits beneath high terraces on west-central Ellesmere Island were reported by Fyles (1962) to include sandy and gravelly strata containing wood, buried soils, and peat. Wood gnawed by beavers was found in a few places (Harrington, 1978, p. 48). It was suggested that these deposits may be stratigraphically equivalent to the Beaufort Formation of the western Arctic Islands (Craig and Fyles, 1965; Prest, 1970, p. 698-699). Field investigations in 1988 have confirmed the widespread occurrence of the organic materials, apparently in a single stratigraphic unit, and have provided a suite of samples for paleontological study.

NATURE AND OCCURRENCE

The high terrace sediments consist of horizontally stratified unconsolidated fluvial gravel, sand, and silty sand lying beneath near horizontal (gently sloping) gravelly to bouldery surfaces. These sediments rest on low relief ancient valley floors eroded into or bevelled across soft bedrock, commonly of the Eureka Sound Group. The distribution of these benches and associated deposits is delineated on a series of surficial materials maps for west-central Ellesmere Island (Hodgson and Edlund, 1978; Hodgson, 1979). On Fosheim Peninsula (Fig. 1), remnants of an extensive high plain slope gently westward from the foot of the Sawtooth Range at elevation 350 m to the vicinity of the head of Slidre Fiord at elevation 260 m. South of Canon Fiord, high terraces and associated deposits form concordant ancient valley floors 400 to 600 m above sea level, which in part cap the south wall of the fiord itself. The inner valley of Canon Fiord and the valleys occupied by modern rivers entering the fiord from the south are deeply entrenched below the high terrace surface. An extensive network of high terraces and associated plains occurs at 350 to 450 m elevation in the vicinity of Strathcona Fiord and Bay Fiord. Southeastward from the head of Strathcona Fiord they increase progressively in elevation to about 600 m close to the western margin of the ice cap and merge with a broad plain, surmounted by mountain ranges and bedrock hills, which extends southward beyond the head of Vendom Fiord. This "Braskerud's Plain" and associated "driftwood" were discovered in 1899 by members of the Norwegian Arctic Expedition (Sverdrup, 1904, p. 177).

The high terraces are veneered by gravel and diamicton containing cobbles and large blocks or boulders. This surface layer, typically 2 to 3 m thick, apparently has resulted from a succession of sedimentary and erosional processes on the terrace surfaces, but it commonly contains clasts which, because of their striated surface and/or large size, are considered to be glacially transported. In contrast, evidence of glaciation has not been found in the finer sediments beneath or on the buried bedrock surface.

The high terrace sediments, beneath the surface veneer of coarse gravel and diamicton, consist mainly of sand, pebble to cobble gravel, silty sand, and minor silt. Muddy or clayey material is a minor constituent. The strata are horizontal and include thinly laminated, ripple bedded, and cross-stratified layers; however, large-scale cross-stratification is rare.

The most common evidence of plant material in the high terrace sediments is the occurrence of pieces of unaltered wood lying near the base of the stony talus slopes along eroded margins of the high terraces. The few good exposures reveal the local presence of layers of woody and mossy detritus, earthy and highly organic soils containing wood and cones, silt beds containing fine organic material and tiny molluscan shells, and peat of various kinds. The wood ranges from waterworn fragments to logs more than 20 cm in diameter and to small whole trees with strongly tapered trunks characteristic of a treeline environment. All the plant materials are unmineralized and unaltered.

The high terrace sediments differ from place to place in thickness, character of sediment, internal stratigraphic sequence, and enclosed organic materials. As yet, however, it is not known whether the sediments can be divided into sub-units that are traceable from place to place.

EXAMPLES FROM THE HEAD OF STRATHCONA FIORD

The sediments beneath Braskerud Plain (Fig. 2) contain peat beds and detrital plant mats that are yielding a varied and well preserved record of the organisms that lived during accumulation of the high terrace sediments. The following description applies to the best known locality on the upper part of the south wall of Strathcona Fiord immediately south of the head of the fiord (Fig. 1, 3, 4). Here 20 to 60 m of unconsolidated materials forms the top of the valley wall and lies unconformably on the Eureka Sound Group. The low relief upland surface consists of diamicton and is strewn with angular granitoid blocks, some of which exceed 2 m in maximum dimension.

At "A" in Figure 3, where the upland is 420 m above sea level, the diamicton is underlain (in sequence) by the following horizontal strata: 6 m of round-cobble gravel; 3 m

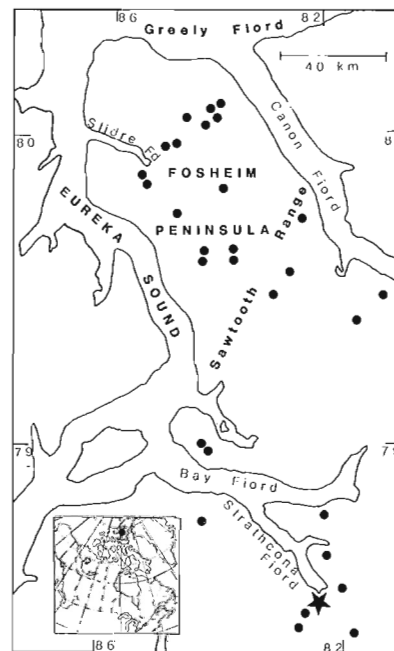


Figure 1. Known occurrences of wood, peat, and other organic remains in high terrace sediments on west-central Ellesmere Island. The star locates "A" and "B" shown in Figure 3.

of pebble gravel; 11 m of crossbedded sand containing pebble lenses, fine coal placers, and isolated fragments of unaltered wood to 8 cm in diameter; and 32 m of thinly bedded fine sand and silty sand, including dark organic silt beds and mats of fine woody plant detritus and moss. Discontinuous pebble and cobble gravel separates the lowest sand from the underlying shale of the Eureka Sound Group.

Approximately 1 km to the west along the top of the south wall of Strathcona Fiord, at "B" in Figure 3, the top of the face is about 30 m lower than at "A" and the following section was recorded (in 1961) beneath the surface layer of bouldery material: 12 m of loose (slumped) pebble gravel; 3 m of fine sand and silt containing pods of peat to 0.4 m thick and wood to 3 cm in diameter; 3 m of sand and pebbly sand; and 2 m of peat containing much wood. A covered interval of about 10 m separates this peat from the highest (shale) outcrop of the Eureka Sound Group. Although the peat beds and other sediments at "B" are at about the same elevation as the detrital organic layers near the base of the high terrace sediments at "A", the intervening face is covered by slumped material and their relative stratigraphic position is not known.



Figure 2. Braskerud Plain, southeast of Strathcona Fiord.

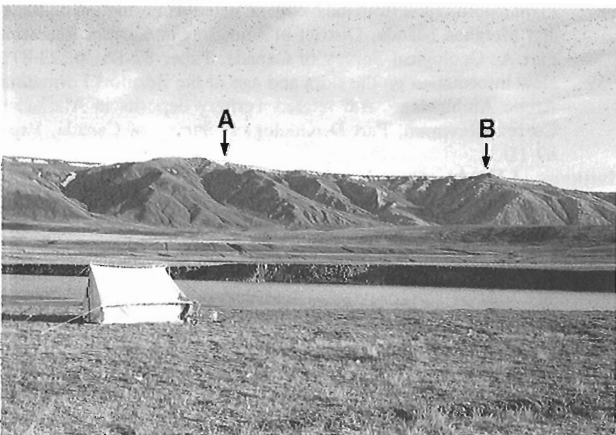


Figure 3. South wall of Strathcona Fiord at the head of the fiord. The upland surface is approximately 350 to 400 m above sea level. High terrace sediments 30-50 m thick occur at the top of the face beneath a bouldery veneer. "A" and "B" mark the top of stratigraphic sections described in the text (cf. Fig. 4).

The 2 m thick peat bed at "B" forms a prominent outcrop (Fig. 5) and has been selected for detailed study. It is referred to below as the "beaver peat". This peat includes felted layers made up entirely of mosses or mosses mixed with vegetative fragments of other aquatic plants. The peat also includes earthy layers consisting of degraded and comminuted organic materials. Pebbles and coarse sand are scattered throughout. Wood commonly lies parallel to the horizontal bedding planes and is mostly less than 10 cm in diameter: trunks appear to represent trees less than 3 m tall, although larger logs (diameter 25 cm) occur on the slumped face. Some pieces of wood have been chewed by beaver, and bones, possibly of beaver, were found at mid-level in the peat bed. Some wood is charred. Larch cones are common and several pieces of wood have been identified as larch (R.J. Mott, unpublished GSC Palynological Report 68-3). Seeds, needles, woody "galls", parts of beetles, and small pelecypod shells are visible on the outcrop surface. The bones collected from this site are being studied by C.R. Harington of the National Museum of Canada, mosses are being identified by L. Ovenden, and palynological analysis is planned.

PRELIMINARY PLANT MACROFOSSIL INFORMATION

Preliminary reports on plant macrofossils from site "B", Figure 3 (J.V. Matthews, Jr., unpublished GSC Plant Macrofossil Reports 88-24 and 88-24a) include 18 taxa from two samples of the beaver peat (FG-88-8a, 8b). These beaver peat samples "display the range of plants that would be expected around a small pond in the subarctic region" and confirm that larch was the dominant tree near this site. The assemblage of plant taxa identified from the beaver peat has similarities to that reported from the Kap København Formation of north Greenland (Funder et al., 1985), and on this

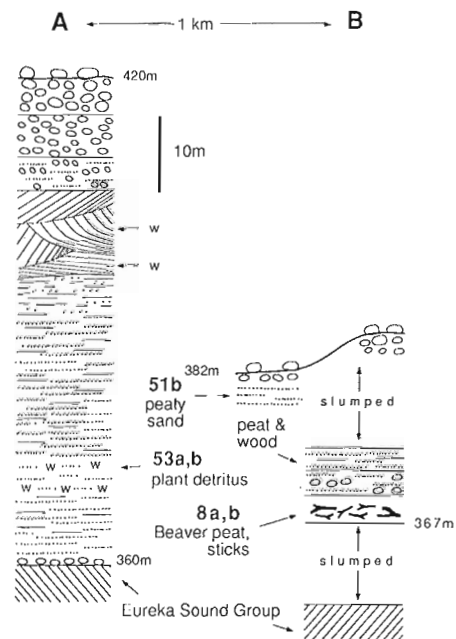


Figure 4. Sections at "A" and "B" (Fig. 3) south of the head of Strathcona Fiord.

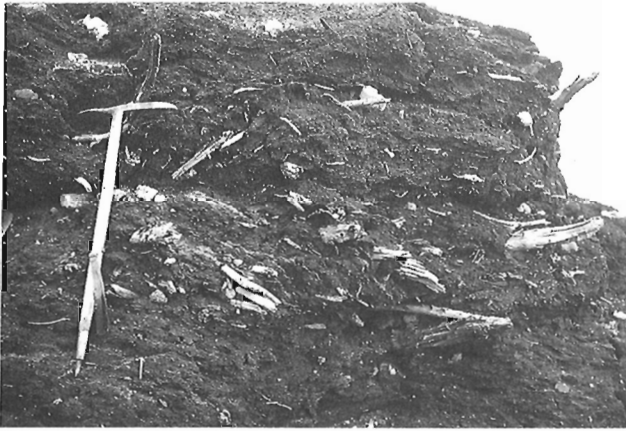


Figure 5. Outcrop of 2 m thick beaver peat bed at "B" (Fig. 3). The pick is 80 cm in length.

basis alone the enclosing strata could be late Pliocene. A single sample (F6-88-51b) from earthy peat 15 m above the beaver peat (at "B", Fig. 3) has yielded, in addition *Pinus*, *Picea* and *Thuja*. *Picea* and *Thuja* are reported at Kap København but *Pinus* is not, and its presence at this locality may indicate somewhat greater age.

Additional evidence of greater antiquity has been provided by plant macrofossils contained in two samples of plant detritus from the other section south of the head of Strathcona Fiord ("A", Fig. 3), approximately 1 km east of the beaver peat locality. These samples (FG-88-53a and FG-88-53b) of plant detritus from thin-bedded silty sands about 10 m above the base of the high terrace sediments were subject to the same preliminary scrutiny as the samples from the beaver peat locality. Although most of the plant macrofossils found in samples 53a and 53b are the same as those from the beaver peat locality (J.V. Matthews, Jr., unpublished GSC Plant Macrofossil Report 88-25), they include *Pinus* and three other taxa (*Comptonia*, "Paliurus type", and *Decodon*) which are not recorded from Kap København. Fossils of *Pinus* and *Comptonia* have been seen in the Beaufort Formation of Meighen Island, whereas seeds of the "Paliurus type" and *Decodon* occur in the Beaufort Formation of Prince Patrick Island and Banks Island but have yet to be recorded on Meighen Island (Matthews, 1987; Matthews et al., in press). Thus, in keeping with latest information on the age of the Beaufort Formation on Meighen Island (Matthews, 1989), these samples (53a, 53b) may suggest late Miocene rather than Pliocene age. Moreover, despite the preliminary nature of the plant macrofossil data cited above, they provide an early warning of significant floral (and age) differences among deposits presently assigned to the high terrace sediments.

SUMMARY

The high terrace sediments represent a stage in the evolution of the landscape of Ellesmere Island involving fluvial planation and boreal forest to forest-tundra conditions prior to formation of fiord valleys and valleys occupied by present rivers. Clear evidence of glaciation contemporaneous with or preceding deposition of these sediments has not been

found. Initial results of plant macrofossil study of peat and plant detritus from high terrace sediments at the head of Strathcona Fiord reveal floral similarities to the Kap København Formation of north Greenland (late Pliocene) in some samples and to the Beaufort Formation on Meighen Island and Prince Patrick Island (late Miocene?) in other, nearby samples.

The name Beaufort Formation has recently been assigned to a sandstone and conglomerate unit on Ellesmere Island, at the head of Makinson Inlet about 100 km southeast of Strathcona Fiord (Riediger et al., 1984). The sediments comprising this occurrence of the Beaufort Formation are somewhat lithified, are tilted with minor folds, and contain fossils indicative of Early Miocene age: thus they are distinct and different from the high terrace sediments discussed here.

I do not intend to apply the name Beaufort Formation to the high terrace sediments on Ellesmere Island, but rather, a locally named lithostratigraphic unit needs to be established to comprise or include these sediments.

REFERENCES

- Craig, B.G. and Fyles, J.G.
1965: Quaternary of Arctic Canada; in Anthropogen Period in Arctic and Subarctic; Transactions of Scientific Research Institute of the Geology of the Arctic, State Geological Committee, U.S.S.R., Moscow, v. 143, p. 5-33.
- Funder, S., Bennike, O., and Feyling-Hanssen, R.W.
1985: Forested arctic: evidence from North Greenland; *Geology*, v. 13, p. 542-546.
- Fyles, J.G.
1962: Surficial geology, Axel Heiberg-Ellesmere Islands, 1961; in Jenness, S.E., Field Work, 1961; Geological Survey of Canada, Information Circular no. 5, p. 4-6.
- Harington, C.R.
1978: Quaternary vertebrate fauna of Canada and Alaska and their suggested chronological sequence; *Syllogeus*, no. 15, 105 p.
- Hodgson, D.A.
1979: Surficial materials, south-central Ellesmere Island, N.W.T.; Geological Survey of Canada, Open File 653.
- Hodgson, D.A. and Edlund, S.A.
1978: Surficial materials and biophysical regions, eastern Queen Elizabeth Islands: Part II; Geological Survey of Canada, Open File 501.
- Matthews, J.V., Jr.
1987: Plant macrofossils from the Neogene Beaufort Formation on Banks and Meighen islands, District of Franklin; in Current Research, Part A, Geological Survey of Canada, Paper 87-1A, p. 73-87.
1989: New information on the flora and age of the Beaufort Formation, Arctic Archipelago, and related Tertiary deposits in Alaska; in Current Research, Part D, Geological Survey of Canada, Paper 89-1D.
- Matthews, J.V., Jr., Ovenden, L., and Fyles, J.G.
—: New data on the late Tertiary Beaufort Formation: Plant and insect fossils from Prince Patrick Island, N.W.T.; *Syllogeus* (in press).
- Prest, V.K.
1970: Quaternary geology of Canada; in Geology and Economic Minerals of Canada; Geological Survey of Canada, Economic Geology Report No. 1.
- Riediger, C.L., Bustin, R.M., and Rouse, G.E.
1984: New evidence for a chronology of the Eurekan Orogeny from south-central Ellesmere Island; *Canadian Journal of Earth Sciences*, v. 21, p. 1286-1295.
- Sverdrup, O.
1904: *New Land*; Longmans, Green and Co., London.

New information on the flora and age of the Beaufort Formation, Arctic Archipelago, and related Tertiary deposits in Alaska

John V. Matthews, Jr.
Terrain Sciences Division

Matthews, J.V., Jr., *New information on the flora and age of the Beaufort Formation, Arctic Archipelago, and related Tertiary deposits in Alaska; in Current Research, Part D, Geological Survey of Canada, Paper 89-1D, p. 105-111, 1989.*

Abstract

*Samples collected in 1988 from the Worth Point Formation at Worth Point, Banks Island lack taxa found at the Late Pliocene Kap København locality in northern Greenland. Consequently, the Worth Point Fm. probably postdates the Kap København Formation. A recent Sr-isotope date on shells of *Arctica* from Meighen Island supports other data that show the Beaufort Formation there is Late Miocene to Early Pliocene — at least 3 million years older than Kap København. Another Sr-isotope date also indicates that the Nuwork Member (Alaska), sometimes correlated with the Beaufort Formation on Meighen Island, is Late Oligocene in age. Newly discovered fossil plants from Duck Hawk Bluffs exposures of the Beaufort Formation support the contention that its flora is of late Early to early Middle Miocene age (Seldovian), perhaps even older. Recent work at Duck Hawk Bluffs also shows that it does not contain two Beaufort units of distinctly different age.*

Résumé

*Des échantillons prélevés en 1988 dans la formation de Worth Point située à la pointe Worth dans l'île de Banks, ne contiennent pas les taxons rencontrés dans le Pliocène supérieur du nord du Groenland, à Kap København. On en déduit que la formation de Worth Point est probablement ultérieure à la formation de Kap København. Une datation récente par les isotopes du Sr, faite sur des coquilles d'*Arctica* recueillies dans l'île de Meighen, confirme d'autres données indiquant que, dans cette région, la formation de Beaufort date du Miocène supérieur au pliocène inférieur, c'est-à-dire plus ancienne d'au moins 3 millions d'années que celle de Kap København. Une autre datation par les isotopes du Sr montre aussi que le membre de Nuwok (en Alaska), qui parfois est corrélé avec la formation de Beaufort dans l'île de Meighen, date de l'Oligocène supérieur. Des fossiles végétaux nouvellement découverts dans des affleurements de la formation de Beaufort aux falaises de Duck Hawk, permettent aussi d'affirmer que cette flore se situe entre la fin du Miocène inférieur et le début du Miocène moyen (Seldovien), ou qu'elle est peut-être même plus ancienne. Des recherches récentes effectuées aux falaises de Duck Hawk montrent aussi que la formation ne contient pas deux unités de Beaufort d'âges nettement différents.*

INTRODUCTION

In 1987 the participants at a Denver Colorado workshop on Neogene environments around the Arctic Basin (Brigham-Grette, 1988) identified several questions requiring study if we are to gain a better understanding of the late Tertiary environmental history of the region. Fuller knowledge of that time period is important because the last time that climate was as warm as is predicted for the next century (Dickinson and Cicerone, 1986) was during the late Tertiary. The Beaufort Formation and related deposits, such as those of the Worth Point Formation and Kap København Formation, provide the best available window on late Tertiary environments of the Arctic.

During the summer of 1988 the author and colleagues J.-S. Vincent, L. Ovenden, J. G. Fyles, and R. Barendregt worked on exposures of the Beaufort Formation at Duck Hawk Bluffs on southern Banks Island and the Worth Point Formation at the type locality near Duck Hawk Bluffs (Fig. 1). Although the samples collected are still being analyzed, the fossils already at hand provide new information on the flora of the Beaufort Formation and its age. Especially significant for correlation are recent strontium isotope dates on marine shells from the Beaufort Formation on Meighen Island, Northwest Territories and the Nuwok Member (Sagavanirtoq Fm.) at Carter Creek, northern Alaska.

Worth Point Formation, southern Banks Island

The Worth Point Fm. at Worth Point (Fig. 1) consists of the fill of a small valley incised into the Beaufort Fm. Kuc (1974) was the first to study plant macrofossils from the Worth Point Fm. at Worth Point. Like the author and his colleagues, he noted the remarkable preservation of some of the fossils, e.g., alder and *Ledum* shrubs still possessing

a few intact leaves and even flowers! One of the objectives of the 1988 work was to collect samples that would enlarge the fossil flora documented by Kuc and possibly yield fossils of insects. We also sought to clarify the stratigraphy of the site (Fyles and Vincent), collect samples for paleomagnetic analysis (Barendregt) and to acquire a complete series of pollen samples (Ovenden).

Kuc showed that Worth Point sediments were deposited at a time when the site lay just inside a larch-dominated tree-line and that climate cooled enough during deposition to render the site treeless by the time the valley had filled. Like Kuc, we observed that the size of tree fossils decreased toward the top of the sequence. At least one of the uppermost peats contains fossils of the obligate tundra beetle *Carabus truncaticollis* Eschz. (Lindroth, 1961). Sections of trees from all levels were collected in the hope that it might be possible to construct a detailed tree ring record of climate change during deposition of the Worth Point valley fill sequence.

Till of the Banks Glaciation, the oldest and most extensive glaciation of Banks Island (Vincent, 1983), caps the exposure at Worth Point. According to paleomagnetic data the till is older than 730 ka (Vincent et al., 1984), but if the Banks Glaciation corresponds with the first major glacial event in the Northern Hemisphere (Ruddiman and Raymo, 1988; Shackleton et al., 1988), it may be as old as 2.5 Ma (J.-S. Vincent, personal communication, 1987). This means the Worth Point Fm. is early Quaternary, possibly even Late Pliocene in age.

Funder et al. (1985) suggested that the Worth Point Fm. may be approximately the same age as the Kap København deposits on northern Greenland (Fig. 1). Kap København organic beds were deposited at a treeline site approximately 2 million years ago (Funder et al., 1985). The Kap København macrofloral assemblage also includes fossils of two

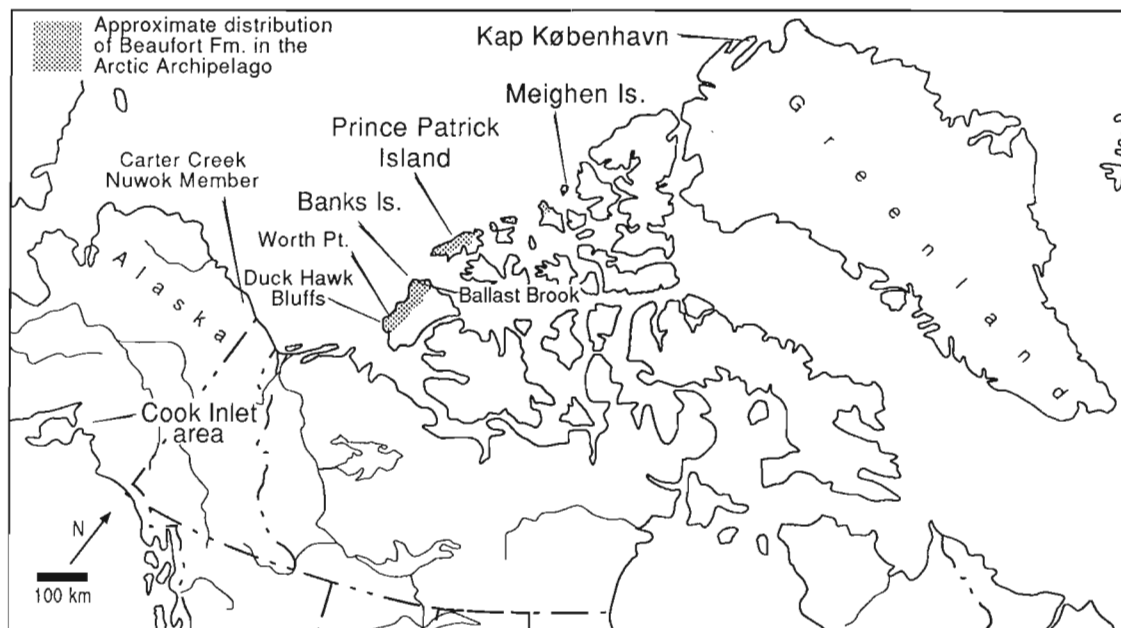


Figure 1. Map showing location of sites mentioned in the text.

extinct plants: one apparently closely related to the fossil species *Myrica eogale* Nikitin and the other, *Aracites Johnstrupii*, presumed to be a member of the arum family (Funder et al., 1988; Bennike and Böcher, in press). The distinctive seeds of *Aracites* also occur in Beaufort Fm. deposits on Banks Island, Prince Patrick Island, and Meighen Island (listed as *Aracispermum* sp. in Matthews, 1987) as well as at a number of late Tertiary sites on the mainland (J.V. Matthews, Jr., unpublished data). Recently they were discovered in pre-Quaternary organic deposits from the Strathcona Fiord region on Ellesmere Island (Fyles, 1989 and J. V. Matthews, unpublished Geological Survey of Canada Macrofossil Reports 88-24 and 88-25). *Aracites* is also recorded in early Pleistocene interglacial deposits in Finland (Aalto and Hirvas, 1987) and Labrador (Klassen et al., 1988).

Aracites seeds are buoyant and indurate. When present in sediments they usually occur in the fraction of the sample which floats on water during processing. Several of the "water float" fractions of Worth Point samples collected in 1988 have been examined, and even though they contain an abundance of remarkably well preserved seeds, *Aracites* has not yet been detected. Only the best preserved seeds of *Myrica* can be reliably referred to either *M. gale* or *M. eogale*. Fossils of the *M. eogale* type do occur in Beaufort deposits, but as yet no *Myrica* fossils of any type have been found in Worth Point sediments.

The treeline flora from Kap København includes trees such as *Taxus* (yew) and *Thuja occidentalis* (eastern white cedar) (Funder et al., 1985; Bennike and Böcher, in press). Although the latter is present in the Beaufort Fm., neither fossils of it nor of *Taxus* have been seen in Worth Point sediments. Thus, even though both Worth Point and Kap København represent similar vegetation, the floristic

similarities expected if both are approximately the same age have not yet emerged. They may be of significantly different age, and if so, Worth Point, with the more depauperate and "modern" flora, is probably the younger of the two, for example, early Quaternary rather than Late Pliocene.

DUCK HAWK BLUFFS, SOUTHERN BANKS ISLAND

One of the best single exposures of the late Tertiary Beaufort Fm. in the entire Arctic is at Duck Hawk Bluffs (DHB) on southern Banks Island (Fig. 1). The site also contains sediments thought to represent the Worth Point Fm. and a complex Quaternary sequence (Vincent et al., 1983; Vincent, 1983; Matthews et al., 1986). The Beaufort sediments at DHB have yielded important plant fossils (Hills et al., 1974; Matthews et al., 1986; Matthews, 1987). Table 1 lists the taxa identified as of October 1988.

Matthews et al. (1986) cited plant macrofossil evidence in concluding that what had previously been considered part of the Worth Point Fm. at section G (Fig. 2) was more likely part of the Beaufort Fm. (Tb₂ in Fig. 2). These deposits occur at only one section and are mostly silt rather than the sand and gravel typical of the Beaufort Fm. at the other DHB sections. Matthews et al. (1986) also noted differences in the Beaufort macrofloras at section G and proposed the two part designation, Tb₂ and Tb₁. Tb₂ was thought to represent an "upper", younger Beaufort unit than Tb₁. Samples from unit Tb₂ collected in 1988 negate this conclusion because they contain many of the same plant fossils seen in the lower part of the section (Table 1). Thus Tb₂ and Tb₁

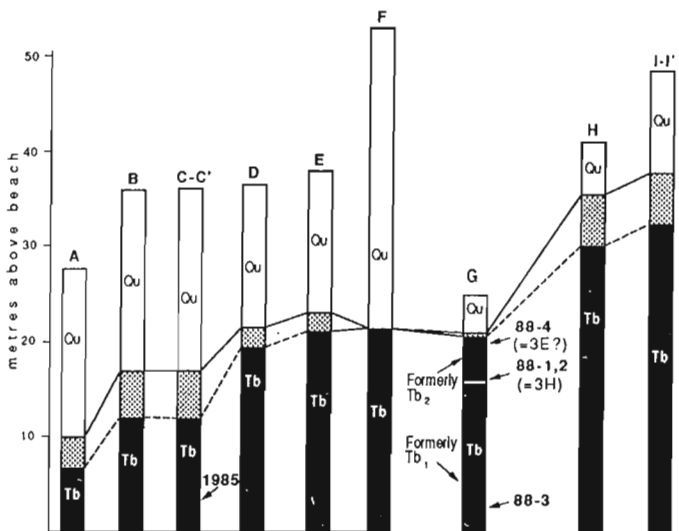


Figure 2. Diagrammatic stratigraphy of Duck Hawk Bluffs, modified from Figure 2B of Matthews et al. (1986). Quaternary deposits (Qu) are not differentiated. Deposits assigned to the Worth Point Fm. — stippled; Beaufort Fm. (Tb) — black. Section G is the one studied in 1988 and the one previously divided into two units Tb₁ and Tb₂ on the basis of supposed differences in the plant macrofossil assemblages.

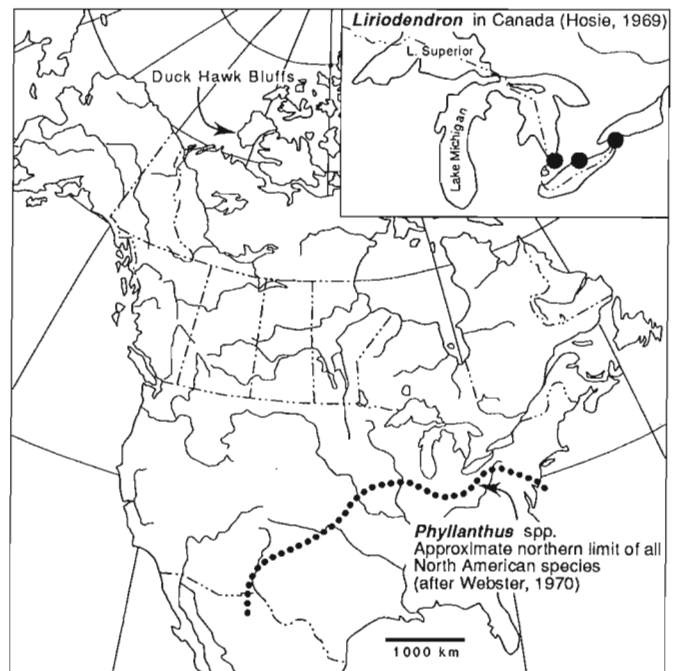


Figure 3. Present distribution of *Liriodendron* and *Phyllanthus*, two of the genera represented by newly discovered fossils from the Beaufort Fm. at Duck Hawk Bluffs.

of Matthews et al., 1986 represent at most only different facies of the Beaufort Fm. at DHB and are not of greatly different age.

The work carried out in 1988 has resulted in the addition of several new plant taxa to the Beaufort Fm. flora at DHB (Table 1). One unexpected find was seeds of *Liriodendron*, the genus now represented by the tulip tree *Liriodendron tulipifera* L.) of the southeastern United States and southernmost Canada. Tulip trees barely reach southern Canada (Fig. 3). Fossils of *Liriodendron* are found in Siberian and east European Miocene floras (Friis, 1985; Lancucka-Srodoniowa, 1966), but this is the first record of *Liriodendron* in Neogene deposits of Arctic North America. The DHB flora is now known to include other plants, for example, *Actinidia* and *Phyllanthus*, which have not been found in any other Beaufort assemblage. The latter, discovered in 1988 samples, is a genus that presently includes approximately 750 species, most of which grow in the Old World tropics (Webster, 1967). Only 8 native species occur in North America (Webster, 1970) and none of them grow in Canada (Fig. 3). Like *Liriodendron*, *Phyllanthus* has been recorded in Neogene assemblages from Europe and Asia (Dorofeev, 1963; Lancucka-Srodoniowa, 1966) but this is apparently the first report of the genus from the Neogene of Arctic North America.

Each new piece of information on the DHB flora seems to reaffirm its distinctive character vis-à-vis other Beaufort floras. The present-day distributions of a number of the taxa are similar to the pattern displayed by *Liriodendron* and *Phyllanthus* (Fig. 3). Such distributional changes should not be interpreted in climatic terms (Wolfe and Tanai, 1980) because many of the fossils probably represent extinct species. Nevertheless, these records of plant genera now growing in temperate or even tropical forests do reveal the "archaic" character of the DHB flora and confirm Hills' (1975) assertion that the flora of Duck Hawk Bluffs is late Early to early Middle Miocene in age (i.e., Seldovian — Wolfe, 1981). The DHB flora contains many fossils which have not yet been identified, but do not represent plants typical of northern Canada. If they prove to have the same modern distributional patterns as some of those shown in Table 1, then it might be concluded that DHB Beaufort deposits are older than the Early Miocene, possibly even Late Oligocene.

MEIGHEN ISLAND

Meighen Island at 80°N has numerous exposures of the Beaufort Fm., many of them containing detrital organic deposits rich in plant and insect fossils (Hills and Matthews, 1974; Matthews, 1976, 1979, 1987). It is also the only site where the typical sands and gravels of the Beaufort Fm. interfinger with marine clays.

The fossil flora and fauna suggest an open boreal environment verging on forest-tundra (Hills, 1975; Matthews, 1987). It has been assumed that Meighen Island may be of the same age as Kap København since both are at approximately the same latitude and both represent treeline conditions. Presence of the Atlantic pelecypod, *Arctica*, in Meighen Island marine sediments calls for an age older than

3.4 Ma (Brigham-Grette et al., 1987), but the surprisingly low a11e/11e ratios of these same shells has lead some workers to conclude that the marine unit and overlying terrestrial organic deposits are only *slightly* older than 3.4 Ma (Brigham-Grette et al., 1987, 1988). Evidence from foraminifera suggest an Early Pliocene age (D.H. McNeil, personal communication, 1988), that is, *much* older than Kap København! This conclusion is supported by a recent strontium isotope analysis on *Arctica* shell fragments which suggests a Late Miocene age (either 9 ± 1 Ma or 6.5 Ma; K. G. Miller personal communication, 1988). Most of the plant fossils from Meighen Island come from sites stratigraphically above the marine sediments, so they are younger than the *Arctica* shells; however, there is currently no stratigraphic evidence to suggest that the marine and immediately overlying terrestrial deposits are of greatly different age. Therefore, the Meighen Island flora is at least 3 million years older than that from Kap København.

PRINCE PATRICK ISLAND

Fossils and plants and insects have recently been recovered from samples collected by J.G. Fyles and J. Devaney at a number of Beaufort Fm. localities on Prince Patrick Island (Fig. 1) (Matthews et al., in press). The plant macrofossil assemblages are generally more similar to those from Meighen Island and the upper part of the Ballast Brook exposures (northern Banks Island) (Hills, 1975) than to those from DHB and the lower part of the Ballast Brook exposure (Hills and Ogilvie, 1970; Hills, 1975; Matthews, 1987). This suggests that the Beaufort Fm. on Prince Patrick Island is Late Miocene. But there is a danger in referring all Prince Patrick sites to the same narrow time interval because a few of the assemblages contain fossils of taxa such as *Tubela* (cf), *Betula apoda* (cf), *Cleome*, and *Microdiptera* (= *Mneme* of Matthews, 1987) which have not been recorded previously north of Banks Island. One of the other Prince Patrick sites has yielded a fossil flora that appears more modern than those of Meighen Island (Matthews et al., in press).

NUWOK MEMBER OF THE SAGAVANIRTOK FM., ALASKA

The Nuwok Member, which outcrops at several sites near the northern Alaskan coast is sometimes offered as a mainland correlative of the Beaufort Fm.; hence, new information on its age is relevant in a discussion of the Beaufort Fm. One of the best and most studied Nuwok Member localities is at Carter Creek, Alaska (Fig. 1). The pollen flora from the Carter Creek sequence has been referred to the Seldovian (late Early to early Middle Miocene) (Wolfe, 1972; Wolfe and Tanai, 1980). Two types of marine microfossils indicate quite different ages: foraminifera — Late Oligocene (D. H. McNeil, personal communication, 1988); ostracodes — Pliocene (E.M. Brouwers, personal communication, 1987). A recent Sr isotope analysis on an *Arctica* shell from Carter Creek suggests a Late Oligocene age (24.26 Ma — K.G. Miller, personal communication, 1988). Thus the Nuwok Member at Carter Creek and the Beaufort marine unit on Meighen Island are *not* correlative.

Table 1. Plant macrofossils from the Beaufort Formation at Duck Hawk Bluffs¹

Taxon	1985 ²	88-3 ³	88-1,2 ⁴	88-4 ⁵	Taxon	1985 ²	88-3 ³	88-1,2 ⁴	88-4 ⁵
Characeae					Magnoliaceae				
<i>Chara/Nitella</i> type	+				<i>Liriodendron</i> sp.	?	+	+	
Bryophytes					Capparidaceae				
Pinaceae					<i>Cleome</i> sp.	+			
<i>Abies grandis</i> (Dougl.) Lindl.	cf.	cf.	cf.		<i>Polanisia</i> sp.		+	+	
<i>Larix</i> sp.	+				Crassulaceae				
<i>Pinus</i> 5-needle type	+		+		<i>Sedum</i> sp.	+			
<i>Pinus</i> sp.			+		Saxifragaceae				
<i>Picea</i> sp. (needles)	+	+	+	+	Genus?		+		
<i>P. banksii</i> Hills & Ogilvie	cones				Rosaceae				
<i>Tsuga</i> sp.	+	+			<i>Potentilla</i> sp.	+			+
Taxodiaceae					<i>Rubus</i> sp.	+			+
<i>Metasequoia</i> sp.	+	+	+		Euphorbiaceae				
<i>Glyptostrobus</i> sp.	?	+	?		<i>Phyllanthus</i> sp.			+	
<i>Taxodium</i> sp.	+				Vitaceae				
Cupressaceae					Genus?			+	
<i>Thuja occidentalis</i> L.	cf.	cf.			Rhamnaceae				
Sparganiaceae					<i>Paliurus</i> type			+	
<i>Sparganium</i> sp.				+	Actinidiaceae				
Potamogetonaceae					<i>Actinidia</i> spp.	+	+		
<i>Potamogeton</i> sp.	+	+		+	Hypericaceae				
<i>P. Richardsonii</i> (B.) R.	cf.				<i>Hypericum</i> sp.		+	+	
Alismaceae					Violaceae				
<i>Sagisma</i> sp.		cf.			<i>Viola</i> sp.		+	+	
Cyperaceae					Lythraceae				
<i>Carex</i> spp.	+	+	+		<i>Decodon</i> sp.	+	+	+	+
<i>Dulichium</i>					<i>Microdiptera</i> sp.	+	+	+	
<i>vespiforme</i> C.E.Reid	cf.		cf.		Onagraceae				
<i>Rhynchospora</i> sp.	cf.				<i>Ludwigia</i> sp.			cf.	
<i>Scirpus</i> spp.	+	+			Haloragaceae				
Araceae					<i>Hippuris</i> sp.	+			+
<i>Epipremnum</i>					Araliaceae				
<i>crassum</i> C&E.M.Reid ⁶	+		+		<i>Aralia</i> sp.	+	+	+	+
<i>Aracites</i>					Ericaceae				
<i>Johnstrupii</i> (Hartz.) Nikit.	+				<i>Chamaedaphne</i> sp.	+			
Myricaceae					<i>Arctostaphylos</i>				
<i>Myrica</i> sp.			+		<i>alpina/rubra</i> type	+			
<i>Comptonia</i> spp.	+		+		<i>Andromeda polifolia</i> L.				+
Juglandaceae					Gentianaceae				
<i>Juglans eocineria</i> H,K&S	+				<i>Menyanthes trifoliata</i> L.	+			
Betulaceae					<i>Menyanthes</i> sp. (small type)	+			
<i>Alnus (Alnobetula)</i> sp.	+				Verbenaceae				
<i>Alnus incana</i> (L.) Moench	cf.				<i>Verbena</i> sp.	+			
<i>Betula</i> dwarf shrub type	+				Labiatae				
<i>Betula</i> arboreal type	+		+		<i>Teucrium</i> sp.	+		+	
<i>Betula apoda</i> Nikit.	cf.	cf.			Solanaceae				
Moraceae					<i>Solanum/Physalis</i> type		+	+	
<i>Morus</i> sp.	+	+	+		Caprifoliaceae				
Polygonaceae					<i>Diervilla</i> sp.	+		+	
<i>Rumex</i> sp.	+				<i>Wiegela</i> sp.	+		+	
Chenopodiaceae					<i>Sambucus</i> sp.	+	+	+	+
<i>Chenopodium</i> sp.	+		+						
Aizoaceae									
<i>Sesuvium</i> sp.			cf.						
Ranunculaceae									
<i>Ranunculus</i>									
<i>hyperboreus</i> Rottb.	cf.								
<i>R. (Batrachium)</i> sp.	+			+					

1. Current as of October 1988

2. "1985" signifies taxa from samples collected in 1985 at section C-C' (see Fig. 2)

3. 88-3= sample MRA 7-7-88-3 from organic detritus in sand near the base of section G.

4. 88-1,2= samples MRA 7-7-88-1 and MRA 7-7-88-2 from base of unit Tb₂ in Matthews et al. (1986) and Fig. 2. This level is thought to be equivalent to sample 3H in Fig. 2B and Table 2 of Matthews et al. (1986) and the fossils found in that sample are included in the list (shown by asterisk)

5. 88-4= sample MRA 7-7-88-4 from the upper part of what was formerly ranked as Tb₂ in Matthews et al. (1986). The sample level is thought to be equivalent to that of sample 3E of Figure 2B and Table 2 of Matthews et al. (1986), but few of the taxa listed in the 1986 table (asterisk in Table 1) were seen in this sample.

6. *Epipremnum crassum* has been placed in the organ genus *Scindapsites* by Gregor and Bogner (1984). The original name is used here to facilitate comparison with other floral lists.

CONCLUSIONS

1. Based on Sr isotope analyses, deposits of the Nuwok Member of the Sagavanirtoq Fm. on the Alaskan mainland are more than 19 million years older than Beaufort Fm. marine sediments on Meighen Island. Obviously the two marine units do not represent the same high stand of sea level!
2. A Late Miocene Sr isotope date on Meighen Island *Arctica* fossils supports an Early Pliocene age estimate based on foraminifera. This date casts doubt on the reliability of an age estimate based on amino acid racemization values of the *Arctica* shells (Brigham Grette et al., 1987, 1988).
3. Although both the Worth Point Fm. and the 2 Ma Kap København deposits represent treeline vegetation, the Kap København flora is taxonomically richer and contains at least one extinct plant, *Aracites Johnstrupii*, not yet found in Worth Point sediments. If floral diversity is an index of age, then the Worth Point Fm. may post-date the Kap København Fm.
4. The discovery of fossils of plants such as *Liriodendron* and *Phyllanthus* in sediments of the Beaufort Fm. at Duck Hawk Bluffs emphasizes the distinct character of that flora. They reinforce the impression that DHB Beaufort deposits are among the oldest exposed in the Arctic. Furthermore, plant fossils from the 1988 sample series at DHB show that the site does not contain two Beaufort units of significantly different age.
5. Preliminary work on fossil samples from the Beaufort Fm. on Prince Patrick Island suggests a Late Miocene age because the combined flora is much more similar to that from Meighen Island than to the DHB Beaufort flora.

ACKNOWLEDGMENTS

J. G. Fyles, J.-S. Vincent, and B. R. Pelletier contributed valuable comments on an earlier draft of this report. Alice Telka is thanked for her continuing help in the study of the Beaufort plant and insect fossils. Logistical support was provided by the Polar Continental Shelf Project.

REFERENCES

- Aalto, M.M. and Hirvas, H.
1987: *Aracites interglacialis*, a peat forming extinct plant from Finnish Lapland (abstract); Abstracts, XII INQUA Congress, Ottawa, July 1987; p. 116.
- Bennike, O. and Böcher, J.
— Forest-tundra neighboring the North Pole: plant and insect remains from the Plio-Pleistocene Kap København Fm., North Greenland; Arctic (in press).
- Brigham-Grette, J.
1988: Stratigraphy and paleoenvironments of the high Arctic throughout the late Tertiary and early Pleistocene; Geotimes, June 1988, p. 37.
- Brigham-Grette, J., Matthews, J.V., Jr., and Marincovich, L., Jr.
1987: Age and paleoenvironmental significance of *Arctica* in the Neogene Beaufort Fm. on Meighen Island, Queen Elizabeth Islands, Canada (abstract); in Abstracts of the 16th Arctic Workshop (Research on the roof of the world), Edmonton, Alberta, April 30-May 2, 1987; Boreal Institute for Northern Studies, University of Alberta, Edmonton; p. 12-14.
- Brigham-Grette, J., Matthews, J.V., Jr. and Schweger, C.E.
1988: Nearshore and terrestrial evidence for pre-glacial arctic environments across North America and Greenland (abstract); in Abstracts of the Advanced Research Workshop on the Geologic History of the Polar Oceans: Arctic versus Antarctic, 10-14 October, 1988, Bremen Federal Republic of Germany.
- Dickinson, R.E. and Cicerone, R.J.
1986: Future global warming from atmospheric trace gases; Nature, v. 319, p. 109-115.
- Dorofeev, P.I.
1963: Tertiary Floras of Western Siberia; Academy of Sciences of the U.S.S.R., Komarov Botanical Institute. 345 p. (in Russian).
- Friis, E.M.
1985: Angiosperm fruits and seeds from the Middle Miocene of Jutland (Denmark); Det Kongelige Danske Videnskaberne Selskab Biologiske Skrifter, v. 24, no. 3, 165 p.
- Funder, S., Abrahamsen, N., Bennike, O., and Feyling-Hanssen, R.W.
1985: Forested arctic: evidence from North Greenland. Geology; v. 13, p. 542-546.
- Funder, S., Bennike, O., and Böcher, J.
1988: Kap København-et geologisk Pompeji; Naturens Verden, p. 241-256.
- Fyles, J.G.
1989: High terrace sediments, probably of Neogene age, west-central Ellesmere Island, Northwest Territories; in Current Research, Part D, Geological Survey of Canada, Paper 89-1D.
- Gregor, H.J. and Bogner, J.
1984: Fossile Araceen Mitteleuropas und ihre rezenten Vergleichsformen; Documenta Naturae, v. 19, p. 1-12.
- Hills, L.V.
1975: Late Tertiary floras Arctic Canada: an interpretation; Proceedings of Circumpolar Conference on Northern Ecology, National Research Council of Canada, p. I(65)-I(71).
- Hills, L.V. and Ogilvie, R.T.
1970: *Picea banksii* n. sp., Beaufort Formation (Tertiary), northwestern Banks Island, Arctic Canada; Canadian Journal of Botany, v. 48, p. 457-464.
- Hills, L.V. and Matthews, J.V., Jr.
1974: A preliminary list of fossil plants from the Beaufort Formation Meighen Island; in Report of Activities, Part B, Geological Survey of Canada, Paper 74-1B, p. 224-226.
- Hills, L.V., and J.E., and Sweet, A.R.
1974: *Juglans eocinerea* n. sp., Beaufort Formation (Tertiary) southwestern Banks Island, Arctic Canada; Canadian Journal of Botany, v. 52, p. 65-90.
- Hosie, R.C.
1969: Native Trees of Canada; Canadian Forestry Service, Department of Fisheries and Forestry, Queen's Printer, Ottawa, 380 p.
- Klassen, R.A., Mott, R.J., Matthews, J.V., Jr., and Thompson, F.J.
1988: The stratigraphic and paleobotanical record of interglaciation in the Wabush region of western Labrador (abstract); Climatic Fluctuations and Man III, Annual meeting of the Canadian Committee on Climatic Fluctuations and Man, Ottawa, 28-29 January, 1988, p. 24-26.
- Kuc, M.
1974: The interglacial flora of Worth Point, western Banks Island; in Report of Activities, Part B, Geological Survey of Canada Paper 74-1B, p. 227-231.
- Lancucka-Srodoniowa, M.
1966: Tortonian flora from the "Gdow Bay" in the south of Poland; ACTA Paleobotanica, v. 7, no. 1, 135 p.
- Lindroth, C.H.
1961: The ground-beetles of Canada and Alaska, Part 2. Opuscula Entomologica, Supplementum 20, p. 1-200.
- Matthews, J.V., Jr.
1976: Insect fossils from the Beaufort Formation: geological and biological significance; in Report of Activities, Part B, Geological Survey of Canada, Paper 74-1B, p. 217-227.
- 1979: Late Tertiary Carabid fossils from Alaska and the Canadian Arctic Archipelago, in Carabid Beetles: their Evolution, Natural History, and Classification, G.E. Ball, T.E. Irwin, and D.R. Whitehead, ed.; W. Junk bv., The Hague (Netherlands), p. 425-445.
- 1987: Plant macrofossils from the Neogene Beaufort Formation on Banks and Meighen Islands, District of Franklin; in Current Research, Part A, Geological Survey of Canada, Paper 87-1A, p. 73-87.

- Matthews, J.V., Jr., Mott, R.J., and Vincent, J.-S.**
 1986: Preglacial and interglacial environments of Banks Island: pollen and macrofossils from Duck Hawk Bluffs and related sites, *Géographie physique et Quaternaire*, v. XL, p. 279-298.
- Matthews, J.V., Jr. Oviden, L., and Fyles, J.G.**
 — New data on the late Tertiary Beaufort Formation: Plant and insect fossils from Prince Patrick Island, N.W.T.; *Syllogeus* (in press).
- Ruddiman, W.F. and Raymo, M.E.**
 1988: Northern Hemisphere climate regimes during the past 3 Ma: possible tectonic connections; *Philosophical Transactions of the Royal Society of London*, v. B318, p. 411-430.
- Shackleton, N.J., Imbrie, J. and Pisias, N.G.**
 1988: The evolution of oceanic oxygen isotope variability in the North Atlantic over the past three million years; *Philosophical Transactions of the Royal Society of London*, v. B318, p. 679-688.
- Vincent, J.-S.**
 1983: La géologie du Quaternaire et la géomorphologie de l'île Banks, Arctique canadien, Commission géologique du Canada, Mémoire 405, 118 p.
- Vincent, J.-S. Morris, W.A., and Occhietti, S.**
 1984: Glacial and nonglacial sediments of Matuyama paleomagnetic age on Banks Island, Canadian Arctic Archipelago, *Geology*, v. 12, p. 139-142.
- Vincent, J.-S., Occhietti, S., Rutter, N.W., Lortie, G., Guilbault, J.-P., and de Boutray, B.**
 1983: The late Tertiary-Quaternary stratigraphic record of the Duck Hawk Bluffs, Banks Island, Canadian Arctic Archipelago, *Canadian Journal of Earth Sciences*, v. 20, no. 11, p. 1694-1712.
- Webster, G.L.**
 1967: The genera of Euphorbiaceae in the southeastern United States; *Journal of the Arnold Arboretum*, v. 48, p. 303-361; p. 363-430.
 1970: A revision of *Phyllanthus*(Euphorbiaceae) in the Continental United States; *Brittonia*, v. 22, p. 44-76.
- Wolfe, J.A.**
 1972: An interpretation of Alaskan Tertiary floras; in *Floristics and Paleofloristics of Asia Eastern North America*, A. Graham (ed.); Elsevier, Amsterdam, p. 201-233.
 1981: A chronologic framework for Cenozoic megafossil floras of northwestern North America and its relation to marine geochronology; *Geological Society of America, Special Paper 184*, p. 39-47.
- Wolfe, J.A. and Tanai, T.**
 1980: The Miocene Seldovia Point flora from the Kenai Group, Alaska; *United States Geological Survey, Professional Paper 1105*, 52 p.

Drumlin fields of the Bernard Harbour area, Northwest Territories

Marion B. Potschin¹
Terrain Sciences Division

Potschin, M.B., Drumlin fields of the Bernard Harbour area, Northwest Territories; in Current Research, Part D, Geological Survey of Canada, Paper 89-1D, p. 113-117, 1989.

Abstract

Some of the most spectacular swarms of drumlins in Arctic Canada occur on the dolomite plateau west of Coronation Gulf, Northwest Territories. Based principally on morphometric data, six groups of drumlins are recognized, each occupying a different zone in the region. The description of differences and similarities between drumlins in these zones makes it possible to formulate more fundamental questions concerning the genesis of drumlins.

Résumé

Quelques-uns des groupes les plus spectaculaires de drumlins de l'Arctique canadien occupent le plateau dolomitique situé à l'ouest du golfe Coronation, dans les Territoires du Nord-Ouest. En se basant principalement sur les données morphométriques, on a identifié six groupes différents de drumlins, qui dans la région occupent chacun une zone différente. À partir de la description des différences et similarités des drumlins présents dans ces zones, on peut formuler des questions plus fondamentales sur la genèse des drumlins en général.

¹ Department of Geography, Carleton University, Ottawa, Ontario K1S 5B6

INTRODUCTION

This report describes the distribution and morphology of the drumlins within the Cape Krusenstern map area (87 A); it reports on the composition, orientation, and morphology of drumlins and discusses the intensity of modification by the sea. The Bernard Harbour area as used in this report comprises the land between Basil Bay to the south and Dolphin and Union Strait to the north and between longitude 116° to the west and Coronation Gulf to the east (Fig. 1).

Flat-lying, Lower Paleozoic dolomites underlie this area (Fraser et al., 1960). Glacial till and erratics, sandy gravel, outwash, and glaciomarine sand, silt, and clay form a discontinuous cover so that bedrock outcrops are extensive.

THE MORPHOLOGICAL ZONES OF THE BERNARD HARBOUR DRUMLIN FIELD

Based on size, shape, orientation, and degree of modification by the sea, drumlin fields in the Bernard Harbour area can be divided into six zones (Fig. 1). The length and width of the drumlins were taken from air photographs. The height and slope were measured in the field; height refers to the maximum elevation of a drumlin crest above an adjoining lake or interdrumlin trough. Table 1 lists the measurements related to the drumlins studied.

Zone A

In the vicinity of Bernard Harbour there is a dense concentration of drumlins which is particularly striking because of drumlin heights up to 27 m, steep slopes of up to 23.5°, and sharp crests. The ratio of length to width averages 4.07:1. Based on Kupsch's (1955) classification, these drumlins

Table 1. Summary of drumlin measurements in the Bernard Harbour area*

Zone	n	Orientation (°)	Length, L (m)	Width, W L, W ratio :1	Height (m)	Slope (°)
A	247	262	950	233	4.07	9.0
		242-315	243-3406	104-556	1.3-16.8	3.4-27
B	464	238	575	210	2.74	3.6
		193-271	209-1703	104-487	1.0-12.3	1.7-5.0
C	174	216.5	1200	233	5.14	8.5
		200-241	350-16100	104-420	1.5-17.8	3.4-13.5
D	722	266	731	214	3.42	6.0
		212-310	243-1772	104-521	1.0-7.5	3.4-10.0
E	197	307/1200	325	3.68	12.2	4.9
		253-341	313-2641	70-835	1.3-16.3	4.8-17.8
F	341	227	751	213	3.52	12.0
		195-272	272-2502	104-382	1.4-14.4	5.0-20.0

*The first line represents mean values, the second line represents the range of measured values.

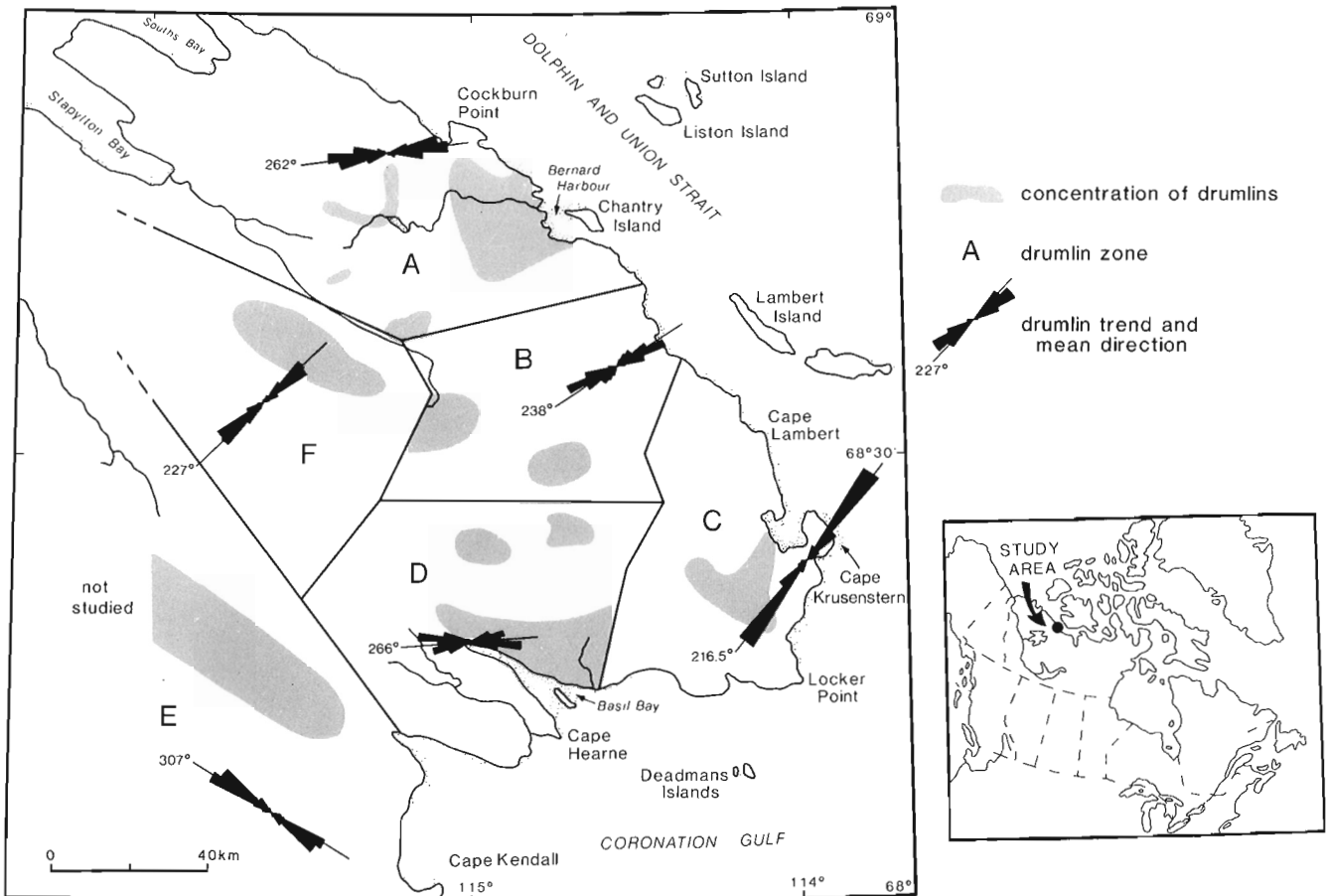


Figure 1. Drumlin fields of the Bernard Harbour area, Northwest Territories.

belong to the group of “lenticular” drumlins; in Muller’s (1963) system they are “long ovoid”; while Shaw (1983) would call them “parabolic”.

Although the orientation of the drumlins in zone A varies around 72° , the majority are concentrated between 235° - 265° with a mean trend of 262° (Fig. 1). The highest concentration of the drumlins in zone A occurs below 70 m a.s.l., well below marine limit; consequently these drumlins have been extensively modified by wave action (Fig. 2).

Zone B

Contrary to the pronounced grouping of drumlins characteristic of zone A, the drumlins of zone B are widely dispersed. With a mean trend of 238° they have the same general orientation as those in zone A. Measurements of 464 drumlins give an average length of 575 m, mean width 210 m, and crest height 3.6. The drumlins in zone B are the smallest in the Bernard Harbour drumlin field.

Furthermore, the average ratio between length and width is 2.74:1, thus they are typical “broad ovoid” (Muller, 1963) or “oval” (Embleton and King, 1975).

Zone C

Drumlins in zone C are concentrated in a belt southwest of Cape Krusenstern (Fig. 1). The main trend of this field is



Figure 2. Wave modified drumlin in zone A, view west; ice flow was towards the top of the photo. 204720-A

towards 216° with variations from 200° to 241° . The dominant characteristic of the drumlins in zone C is their obvious “spindle form” (Shaw, 1983).

The ratio of length to width of 174 drumlins in this field varies from 1.5:1 to 17.8:1, with a mean value of 5.14:1; both the mean and the absolute values are the highest in the Bernard Harbour drumlin field. Kupsch (1955) would classify them “elongated” while Muller (1963) would define them as “ridges”. The average length lies around 1200 m, but individual drumlins can be more than 16 000 m. These drumlins occur below marine limit and show extensive modification by wave action such as large ridges of beach shingles (Fig. 3). The average height of 8.5 m reflects a subdued not an original landform.

Zone D

The drumlins north of Basil Bay are grouped in a spectacular swarm which trends east to west with a pronounced curvature to the south (Fig. 4).

Measurements on 722 drumlins in this zone yield an average length to width ration of 3.42:1 which would classify them as “ovoid” or “lenticular”. There is no doubt,



Figure 3. Shingle beach on the side of a drumlin in zone C; view northeast. 204720-C



Figure 4. Basil Bay drumlin swarm; view west, ice flow was towards the top of the photo. 204720-B

however, that the general appearance of these drumlins on airphotos is best described as “parabolic” (Shaw, 1983). They are smaller and more streamlined than those in zone B to the north.

Zone E

The southwest corner of the map area is part of the Inman River drumlin field, a belt 5-45 km wide which extends northwest ward to the shores of Amundsen Gulf north of Bluenose Lake (St-Onge and McMartin, 1987).

The 198 drumlins in zone E show a mean trend of 307° (Fig. 1). The average drumlin length is 1200 m, the average width 325 m, and an average length to width ratio of 3.68:1. The average height is 12.2 m and the maximum slope averages 4.9°.

Surface exposures and shallow sections indicate that the drumlins are composed of a diamicton with generally well rounded clasts of various lithology in a silty sand matrix. The erratics are dominantly of gabbro and granites (St-Onge and McMartin, 1987).

Zone F

Drumlins in zone F form a complex field, in part because of range in elevation of occurrence from 30 m a.s.l. to near marine limit at 150 m a.s.l. The drumlins at higher elevations have been much less modified by wave action and are higher and have steeper slopes. Figure 5 shows a typical view of the drumlins in zone F. They are slightly higher at the stoss end and have a symmetrical transverse profile. The longest of this set is 2500 m long; it is 12 m high at the northeast stoss end, falls to 8 m in height throughout most of its length, and tapers down to only 5 m at the southwest or lee end. This particular feature has a length to width ratio of 14.4:1, but generally in this zone drumlins are 750 m long and 210 m wide. The average length to width ratio is 3.5:1, which characterizes these drumlins as “lenticular” (Kupsch, 1955), “long-ovoid” (Muller, 1963), or “parabolic” (Shaw, 1983).

DISCUSSION

The morphological zones described in the Bernard Harbour study area result from the activity of the last glacier ice region during the Late Wisconsinan. The two major trends of the drumlins, NE-SW and NW-SE, strongly suggest that they were constructed by two different ice flows which may have originated from the same ice mass to the east.

Because most drumlins occur below marine limit, they display increasing degree of modification by wave action with decreasing elevation. A 6 m high section in a drumlin in the Bernard Harbour (zone A) shows a coarsening upward gravelly sequence overlying till. The marine influence is commonly indicated by marine shells and by marine silty clay sediments covering the surface of the drumlins. In some cases raised beaches cover parts or all of the drumlin (Fig. 2, 3).



Figure 5. Typical drumlins in zone F, view northwest, ice flow was from right to left of photo. 204720-D

In spite of surface appearance and varying morphometry, all sections dug in drumlins show a silty sand diamicton with clasts from gravel to boulders, mostly subangular to rounded with dolomite being by far the dominant rock type (average 85%). Most of the pebbles and cobbles are striated.

CONCLUSION

Based on dominant morphometric characteristics, the drumlins in the Bernard Harbour study area have been grouped into six distinct zones. These preliminary results make it possible to formulate questions which will be addressed during the course of the ongoing study:

1. What is the fundamental reason(s) for the pronounced morphological differences between drumlins in relatively contiguous areas; is it nature of the ice mass; the nature of the material; or a combination of these and other factors?
2. Do the ice flow patterns which the drumlins reflect represent separate events or do they result from different flow patterns within the same ice mass?
3. What is the relationship between drumlin-forming ice mass(es) and the encroaching postglacial sea? What are the influences of one on the other?
4. All evidence gathered indicate that drumlins in the Bernard Harbour area are composed of a clast-rich diamicton. How does this fact fit current theories on the origin of drumlins?

Field work during the summer of 1988 has made it possible to frame the questions, ongoing analyses of data should help to elucidate them.

ACKNOWLEDGMENTS

This study is part of a continuing Master's research project investigating the origin of drumlins in the Bernard Harbour area.

I thank Denis A. St-Onge for providing logistical support. The "Drumlin City" field group (Denis A. St-Onge, Ron W. Avery, Daniel E. Kerr, and Isabelle McMartin) were generous with their support in the field and were stimulating in their discussions with the author. Additional special thanks to Ron W. Avery, who did some of the morphometric analyses on air photographs and without whose continuous dedication and strength, the digging of sections in drumlins would have been a considerably more daunting task.

REFERENCES

- Embleton, C.R. and King, C.A.**
1975: *Glacial and Periglacial Geomorphology*; Edward Arnold, London, 203 p.
- Fraser, J.A., Craig, B.G., Davison, W.L., Fulton, R.J., Heywood, W.W., and Irvine, T.N.**
1960: *Geology, north-central District of Mackenzie, Northwest Territories*; Geological Survey of Canada, Map 18-1960.
- Kupsch, W.O.**
1955: *Drumlins with jointed boulders near Dollard, Saskatchewan*; Geological Society of America, *Bulletin*, v. 66, p. 327-338.
- Muller, E.H.**
1963: *Geology of Grantauqua Country, New York - Part II*; New York State Museum and Sciences, *Bulletin*, no. 392.
- Shaw, J.**
1983: *Drumlin Formation related to inverted melt-water erosional marks*; *Journal of Glaciology*, v. 29, no. 103, p. 461-479.
- St-Onge, D.A. and McMartin, I.**
1987: *Morphosedimentary zones in the Bluenose Lake region, District of Mackenzie*; in *Current Research, Part A*, Geological Survey of Canada, Paper 87-1A, p. 89-100.

Recovery of precise offshore permafrost temperatures from a deep geotechnical hole, Canadian Beaufort Sea

Alan Taylor, Alan Judge, and Vic Allen
Terrain Sciences Division

Taylor, A., Judge, A., and Allen, V., Recovery of precise offshore permafrost temperatures from a deep geotechnical hole, Canadian Beaufort Sea; in Current Research, Part D, Geological Survey of Canada, Paper 89-1D, p. 119-123, 1989.

Abstract

A 440 m multithermistor cable was installed in early September, 1988 in a geotechnical hole drilled through the offshore permafrost of the continental shelf of the Beaufort Sea. An automatic data logger was attached, and hourly temperatures were recorded for 23 days. The data show the thermal recovery of the well from effects of drilling and abandonment, and the approach to equilibrium conditions. Such a modest installation may make a significant contribution to reconstructions of the Pleistocene history of the Beaufort Shelf and to geotechnical engineering models required for offshore development.

Résumé

Au début de septembre 1988, on a installé un câble à multithermistors de 440 m dans un sondage géotechnique effectué dans le pergélisol de la plate-forme continentale de la mer de Beaufort au large des côtes. On y a fixé un système de diagraphie automatique, et enregistré toutes les heures les températures pendant 23 jours. Les données documentent la récupération thermique du puits après les opérations de forage et d'abandon de ce puits, ainsi que le retour à des conditions proches de l'équilibre. Cette modeste installation pourrait jouer un rôle important dans la reconstruction de l'évolution de la plate-forme de la mer de Beaufort au Pléistocène, et à l'élaboration de modèles géotechniques pratiques indispensables à la mise en valeur des zones du large.

INTRODUCTION

A large portion of the continental shelf of the Beaufort Sea is underlain by hundreds of metres of ice-bonded permafrost that is relict from periods during the late Pleistocene when lower sea levels exposed the seabed to subaerial arctic conditions (Fig. 1). Most of the offshore permafrost is presently degrading in response to the recent marine transgression (Mackay, 1972).

A long-standing challenge in permafrost science has been the acquisition of deep ground temperatures through the ice-bonded permafrost of the Beaufort Shelf comparable to those measurements more readily obtained on land. In the Mackenzie Delta and other onshore areas, for example, precision temperature logs have been run in abandoned petroleum exploratory wells, giving a direct measure of the permafrost thickness and the thermal regime (e.g., Judge et al., 1981). For the Beaufort Shelf, the nature of the permafrost and the deep temperature regime have been predicted on theoretical grounds (e.g., Mackay, 1972; Judge, 1974; Lachenbruch et al., 1982; Outcalt, 1985; Nixon, 1986; Allen et al., 1988), some deep temperature measurements have been reported by industry (Weaver and Stewart, 1982), and some regional thermal information has been extracted from geophysical well logs (Judge and Bawden, 1987; Judge et al., 1987). However, no temperature profiles or estimates of undisturbed formation temperatures have been recovered with documented precision within the offshore permafrost body to depths greater than few tens of metres.

An opportunity arose in 1988 to instrument an offshore hole with a precision multithermistor cable and an automatic data logger. In August and early September, Gulf Canada Resources and partners drilled a 500 m geotechnical corehole at the Amaulikak offshore wellsite, Beaufort Sea; the hole was drilled from a caisson-retained island, the Molikpaq (Fig. 2). The site ($70^{\circ}03.3'N$, $133^{\circ}37.8'W$) lies some 80 km northwest of Tuktoyaktuk in 32 m of water (Fig. 1). The purpose of the hole was to obtain core for geotechnical measurements and to study permafrost and the biostratigraphy. The company afforded the authors and other government scientists the opportunity to participate in the corehole

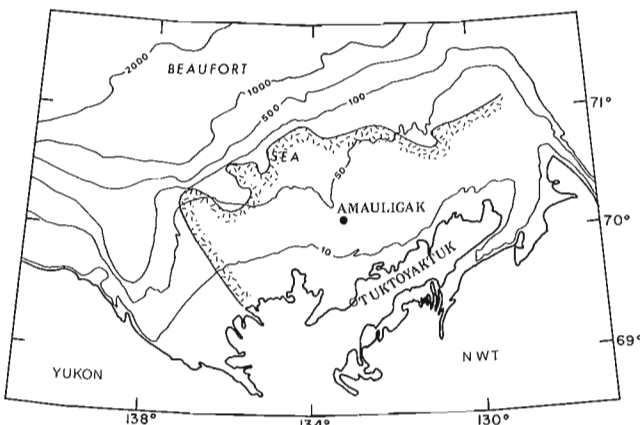


Figure 1. Location of the Gulf et al. Amaulikak corehole #1 within the Mackenzie Delta-Beaufort Sea region. The approximate outer limit of the area underlain by ice-bonded permafrost is shown by the hachured pattern (after Pullan et al., 1987). Bathymetry is in metres.

with an add-on science program. At the end of the drilling, a suite of geophysical logs was run, and a 440 m precision multithermistor cable was left in the hole with an automatic data logger attached at the wellhead. The logger was removed three weeks later, when the Molikpaq was being prepared to move from the location.

This report describes the deployment of the cable in the hole and presents an example of the temperature data acquired. Analysis of the data and interpretation will be undertaken later when measurements on the core and other data are available.

INSTALLATION OF THE TEMPERATURE CABLE

Chilled, oil-based drilling fluids were used in the drilling of the corehole to prevent saline contamination and degradation of the core samples and hole wall. The majority of the hole was cored continuously with a wireline PQ coring system, and subsequent downhole logs indicated that a gauge hole had been achieved. The final program activity at the hole prior to its regulatory abandonment was the installation of the multithermistor cable.

Abandoning a hole containing a relatively delicate electronic cable is not a standard procedure, and special techniques were used to ensure its survival. The upper approximately 100 m of casing had been removed, and the drilling mud displaced by a seawater-based fluid of sufficient density to hold open the hole. The multithermistor cable was run into the hole early on September 7, and an initial set of thermistor resistances were read manually to confirm operation. Next, the cable was monitored while a regulatory cement plug was set around the cable just below the seabed, a further set of resistances were read, and finally the data logger was attached. Figure 3 is a diagrammatic



Figure 2. The Molikpaq, the mobile arctic caisson of Gulf Canada Resources from which the geotechnical corehole was drilled.

representation of the installation. Except for a period of several hours when the logger was disconnected to facilitate work around the hole (September 15), a continuous set of readings was obtained until the system was disconnected on September 30.

The temperature cable consist of 19 YSI-type 44033 thermistors at 22.5 m spacing. These sensors have a nominal resistance of 7355 ohms at 0°C and a manufacturer-specified interchangeability of ± 0.1 K. After manufacture, the thermistor pods on the cable were immersed in an ice bath (0°C) to check integrity (Murray Mitchell, personal communication, 1988); individual thermistors varied from +0.07° to -0.04°C, that is generally adhering to the manufacturer's specifications. Hence, an imprecision in absolute temperature of ± 0.07 K is assumed. Temperatures were recorded automatically with a Sea Data model 1250 data logger that had a resolution of 0.01 K. Thus, small variations (0.01 K) in temperature could be observed at each depth, but a larger uncertainty (± 0.07 K) exists between depths. The logger was set for a 64 minute reading interval.

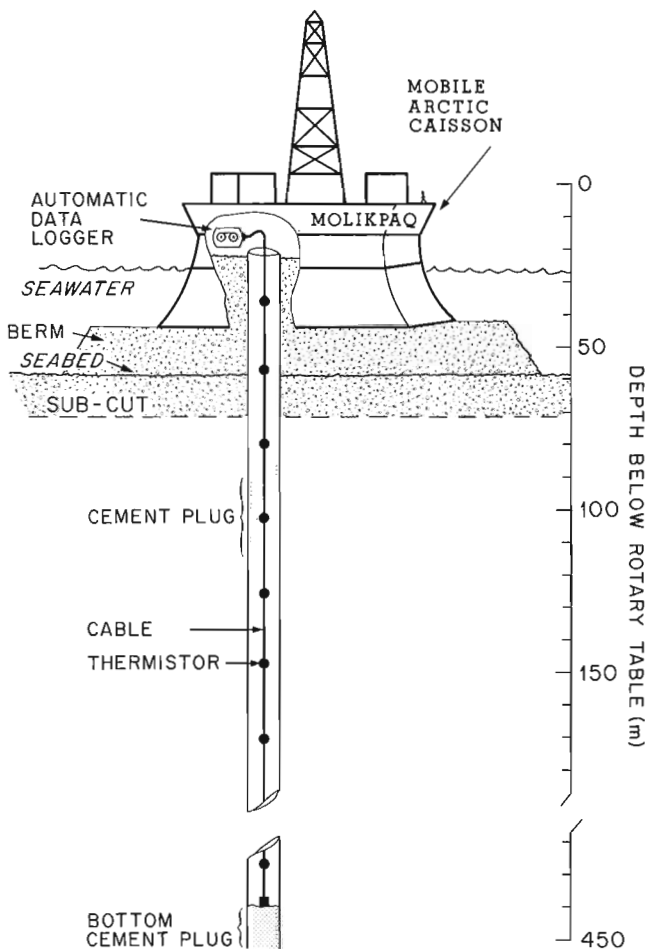


Figure 3. Diagrammatic sketch of the Molikpaq and the instrumentation in the geotechnical hole. The diameter of the hole has been exaggerated; the vertical scale relates the position of the thermistors to the caisson, berm, and seabed.

TEMPERATURE DATA

The complete temperature time series (Fig. 4) illustrates the dynamic recovery of the well from drilling, circulation, and cementing effects. Figure 5 shows temperature profiles versus depth on four dates. All depths are referenced to the rotary table (m RT) on the main rig of the Molikpaq (Fig. 3), some 58 m above the original seabed. The following is a brief discussion of the principal features of the data; detailed analysis will be undertaken later.

1. The time series of temperatures (Fig. 4) reflects a complex history of thermal changes in the wellbore and formation. For the first couple of days following deployment, temperatures between 35 m RT and 125 m RT show a rapid cooling of several degrees (from positive values), while temperatures at greater depth show a cooling of only one or two tenths of a degree. This response arises largely from the temperatures of fluids used to displace the drilling mud, prior to installation of the cable; the upper portion of the hole had been displaced with relatively warm seawater, while the deeper portion had been displaced with a gelled brine that had been pre-chilled.

After this initial cooling from the temperature of the displacement fluids, temperatures within the undisturbed seabed (below 70 m RT) approach an apparent equilibrium temperature over the following twenty-odd days (Fig. 4). With the exception of temperatures at 102 m RT, the maximum temperature change over this longer term is less than 0.1 K; temperatures warm towards equilibrium at 170 m RT and above, and cool to equilibrium at 192 m RT and below. These changes reflect the dynamic thermal response to the preceding approximately three weeks of drilling, when chilled mud was input generally at 8°C, and output at -2°C (Paul Ruffell, personal communication, 1988).

2. The thermistor sensor at 102 m RT is within the regulatory cement plug that was placed September 7 (Fig. 3). The prominent peak in temperatures recorded a day later, and the associated cooling curve (Fig. 4), arise from the heat of hydration of the cement, which acts as a slowly decaying line source of heat. Thermistors at 80 m RT and 125 m RT appear to lie outside the plug, although small shoulders on the cooling curves on September 7 may reflect some heat of hydration being convected above and below the plug.

3. Thermistors at 35 m RT and 57 m RT lie within the sand-filled caisson and sand berm, approximately 20 m and 1 m, respectively, above the seafloor (Fig. 3). The small temperature variations at these positions may arise from thermal transients within the caisson and berm. The variations at the two sensors appear to be correlated, especially on September 19, when a sudden temperature increase (0.3 K) at 35 m RT appears about 2 hours before a sharp, smaller decrease at 57 m RT. At 35 m RT, temperatures rise gradually on September 24, increase sharply early on September 26 and continue to rise to +3.3°C; the high temperatures suggest that this disturbance may arise from preparations to move the Molikpaq. Disturbances correlatable with features of the 35 m trace are seen at 57 m and 80 m, all above the cement plug.

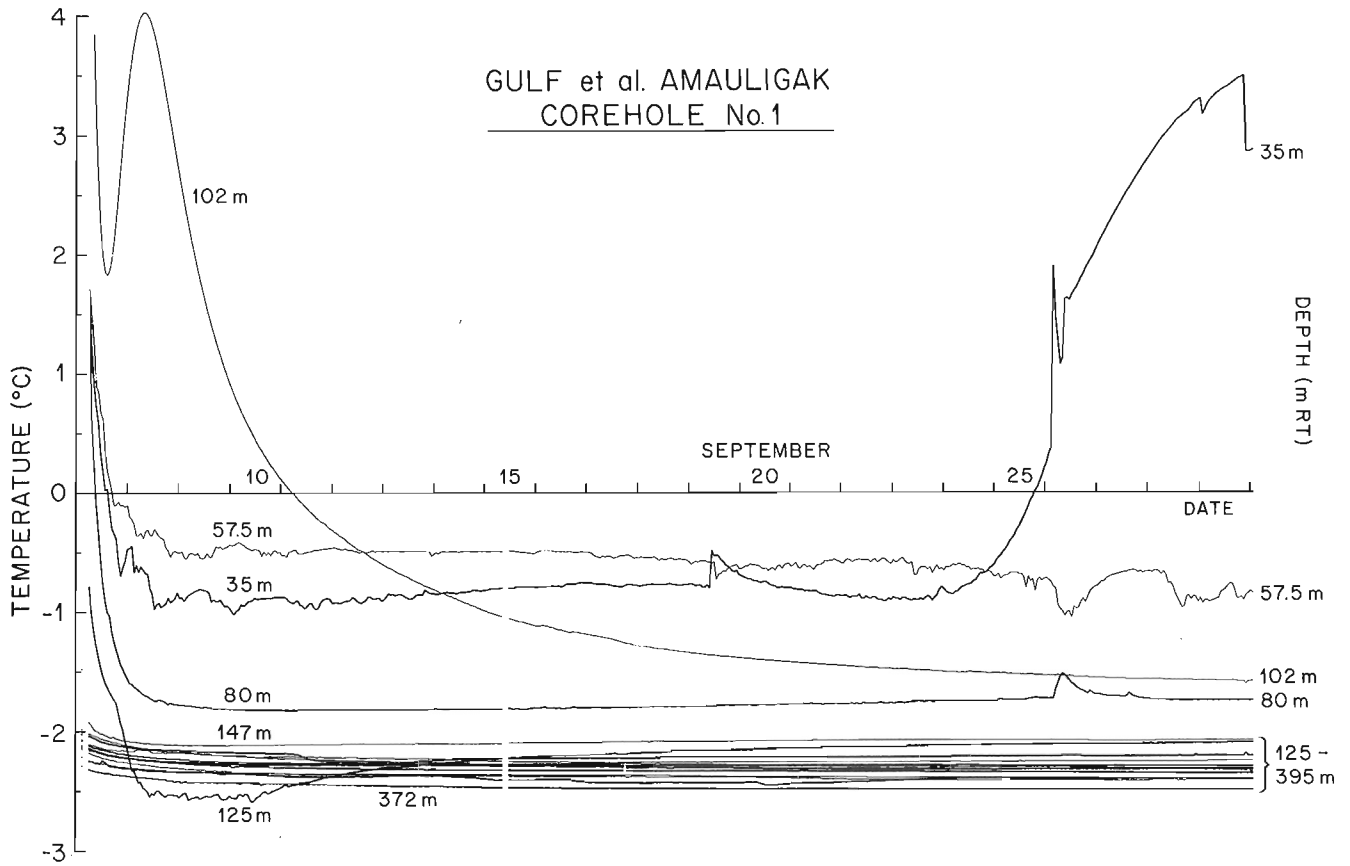
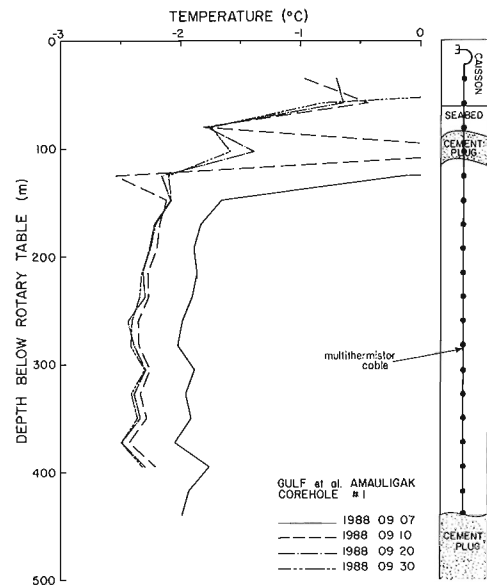


Figure 4. Time series of temperatures recovered from the data logger attached to the cable, for depths indicated. The time axis is scaled from 1988 September 7 to 30.

Figure 5. Temperature-depth profiles for various dates. The approximate positions of the natural seabed, cement plugs, and thermistor pods on the cable are shown. The first log (solid curve) was obtained manually immediately following placement of the cement plug and subsequent logs were obtained by the automatic logger; an unforeseen wiring problem prevented the recording of temperatures below 395 m RT.



4. Many of these features are visible also on the temperature-depth plot (Fig. 5). Temperatures generally decrease with depth, with a minimum of -2.5°C at 372 m RT. This negative temperature gradient in the upper section and an approximately isothermal section below are consistent in a qualitative way with predictions of temperatures in degradational permafrost (e.g. Mackay, 1972; Lachenbruch et al., 1982). Some of the temperature variability between sensors lies within the uncertainty in calibration; however, it may also reflect changes in the downhole lithology. Hence, it is important that thermal conductivity measurements be made on the core before a mathematical analysis is undertaken. Equilibrium, undisturbed temperatures may be calculated from the time series at each depth (method of Lachenbruch and Brewer, 1959).

DISCUSSION

This preliminary examination of the data illustrates the variety of phenomena that are reflected in wellbore temperatures, and suggests that further information may be derived through modelling or detailed analysis of the temperatures in relation to the analysis of the core and well logs.

Permafrost is a thermal phenomenon and, as such, temperature has played a major role in the development of the principal physiographic elements and bathymetric features of the Beaufort Shelf. As the first precision temperature measurements to penetrate a major section of the permafrost body, these data will assist the reconstruction of the Pleistocene history, for which a regional cryogeological model is critical aspect. These temperatures provide a much needed constraint that was unavailable to previous theoretical thermal models for the Beaufort Shelf (e.g., Mackay, 1972; Judge, 1974; Outcalt, 1985; Nixon, 1986).

Similarly, these permafrost temperatures will provide boundary conditions for independent geotechnical engineering analyses. When considered with core lithology and laboratory measurements of physical properties, these temperatures may be used to estimate the unfrozen water content of the natural formations, an important component in their mechanical and thermal properties (e.g., Graham, 1986).

Quantitative analysis of the temperature changes within the well following drilling and abandonment, as discussed briefly above, will provide valuable information on the thermal response of the formations to transient thermal disturbance. If the magnitude of the heat sources can be estimated, the in situ thermal conductivity of the formation may be calculated (Lachenbruch and Brewer, 1959). In particular, the exothermic reaction in the cement plug and the thermistor within it are a field-scale equivalent of the needle probe apparatus used to measure thermal conductivity of soils in the laboratory or in situ (Lachenbruch, 1957). Such calculations may be instructive in comparison with laboratory thermal conductivity measurements to be undertaken on core from the hole.

CONCLUSIONS

1. A 440 m precision multithermistor cable and an automatic data logger have been installed at Gulf et al. Amauligak corehole #1, an offshore geotechnical hole in the Canadian Beaufort Sea. Data were recorded at approximately hourly intervals with a resolution of 0.01 K for over three weeks. These data represent the first precise temperatures obtained through a major section of the permafrost body.
2. The time series of temperatures shows the thermal response of the seabed to the drilling and abandonment process and the gradual return to undisturbed conditions. Temperatures decrease with depth to a minimum of -2.5°C around 314 m below the seabed (372 m RT).
3. At this preliminary stage, the data illustrate the variety of phenomena that are reflected in wellbore temperatures and suggest their key position in the reconstruction of the cryogeological history of the region and in constraining the geotechnical environment.

ACKNOWLEDGMENTS

The geotechnical hole was drilled by Gulf Canada Resources and partners; we sincerely appreciate the efforts of Chris Graham and Bill Livingstone, both of Gulf Canada, for making provision in their program for the installation of the temperature cable. Brian Stacey of Gulf Canada, and Paul Ruffell of EBA Engineering, integrated the deployment of the cable into the abandonment program at the drill site. Len Edelman and Al Shaw of Gulf, and Dave Otto and team from Foundex were of invaluable technical assistance at the drill site. The multithermistor cable was manufactured by Hardy BBT Ltd.; we thank Murray Mitchell for his assistance. Steve Blasco of the Atlantic Geoscience Centre coordinated the science program on the corehole. The Polar Continental Shelf Project, EMR Canada provided logistical support. Funding for the temperature measurement was provided by the Panel on Energy Research and Development (Tasks 6.1 and 6.3), EMR Canada. The authors thank Margo Burgess for valuable comments on the manuscript.

REFERENCES

- Allen, D., Michel, F., and Judge, A.
1988: The permafrost regime in the Mackenzie Delta, Beaufort Sea region, N.W.T. and its significance to the reconstruction of the palaeoclimatic history; *Journal of Quaternary Science*, v. 3, p. 3-13.
- Graham, C.A.
1986: Impact of offshore permafrost on oil and gas production; in *Proceedings of the workshops on subsea permafrost and pipelines in permafrost*, G.H. Johnston and V.R. Parameswaran, (ed.); National Research Council of Canada, Technical memorandum no. 139, p. 35-47.
- Judge, A.S.
1974: Occurrence of offshore permafrost in Northern Canada; in *The coast and shelf of the Beaufort Sea*, J.C. Reed and J.E. Sater, (ed.); Arctic Institute of North America, p. 427-437.

- Judge, A. and Bawden, W.**
1987: Geothermal contours, geothermal gradients; in Marine Science Atlas of the Beaufort Sea: Geology and Geophysics, B.R. Pelletier (ed.); Geological Survey of Canada, Miscellaneous Report 40, p. 6-7.
- Judge, A.S., Pelletier, B.R., and Norquay, I.**
1987: Permafrost base and distribution of gas hydrates; in Marine Science Atlas of the Beaufort Sea: Geology and Geophysics, B.R. Pelletier (ed.); Geological Survey of Canada, Miscellaneous Report 40, p. 39.
- Judge, A.S., Taylor, A.E., Burgess, M., and Allen, V.S.**
1981: Canadian geothermal data collection- northern wells 1978-80; Earth Physics Branch, EMR Canada, Geothermal Series #12, 190 p.
- Lachenbruch, A.H.**
1957: A probe for measurement of thermal conductivity of frozen soils in place; Transactions of the American Geophysical Union, v. 38, p. 691-697.
- Lachenbruch, A.H. and Brewer, M.C.**
1959: Dissipation of the temperature effect in drilling a well in arctic Alaska; United States Geological Survey, Bulletin 1083-C, p. 73-109.
- Lachenbruch, A.H., Sass, J.H., Marshall, B.V., and Moses, T.H., Jr.**
1982: Permafrost, heat flow, and the geothermal regime at Prudhoe Bay, Alaska; Journal of Geophysical Research, v. 87, p. 9301-9316.
- Mackay, J.R.**
1972: Offshore permafrost and ground ice, southern Beaufort Sea, Canada; Canadian Journal of Earth Sciences, v. 9, p. 1550-1561.
- Nixon, J.F.**
1986: Thermal simulation of subsea saline permafrost; Canadian Journal of Earth Sciences, v. 23, p. 2039-2046.
- Outcalt, S.**
1985: A numerical model of subsea permafrost; in Freezing and thawing of soil-water systems, D.M. Anderson and P.J. Williams (ed); American Society of Civil Engineers, New York, p. 58-65.
- Pullan, S., MacAulay, H.A., Hunter, J.A.M., Good, R.L., Gagné, R.M., and Burns, R.A.**
1987: Permafrost distribution determined from seismic refraction; in Marine Science Atlas of the Beaufort Sea: Geology and Geophysics, B.R. Pelletier (ed.); Geological Survey of Canada, Miscellaneous Report 40, p. 37.
- Weaver, J.S. and Stewart, J.M.**
1982: In-situ hydrates under the Beaufort Sea shelf; in Proceedings of the Fourth Canadian Permafrost Conference, H.M. French, (ed); National Research Council of Canada, p. 312-319.

Interaction of climate, vegetation, and soil hydrology at Hot Weather Creek, Fosheim Peninsula, Ellesmere Island, Northwest Territories

Sylvia A. Edlund, Bea Taylor Alt, and Kathy L. Young¹
Terrain Sciences Division

Edlund, S.A., Alt, B.T., and Young, K.L., Interaction of climate, vegetation, and soil hydrology at Hot Weather Creek, Fosheim Peninsula, Ellesmere Island, Northwest Territories; in Current Research, Part D, Geological Survey of Canada, Paper 89-1D, p. 125-133, 1989.

Abstract

Summer 1988 was unusually warm in the region of Fosheim Peninsula (80°N), Ellesmere Island — an area noted for warm summer temperatures. Mean July temperature at Eureka (normally 5.4°C) was 7.2°C and at Hot Weather Creek, 25 km east of Eureka, was 12.7°C. This warmth led to significant ground ice melting as manifested by the recharge of creeks and thaw ponds, surface seepage, accelerated recession of ground ice slumps, and the initiation of numerous active layer detachment slides. Some unusual vegetation patterns indicate that the melting of ground ice in late summer regularly recurs, but the magnitude of response in 1988 was greater than normal.

Our ongoing studies suggest scenarios for possible “greenhouse effects” in the Arctic. This extremely warm summer is an example of the degree of change that such temperatures can trigger and gives an idea of possible immediate effects of global change on the evolution of arctic landscapes.

Résumé

L'été 1988 a été inhabituellement chaud dans la région de la péninsule de Fosheim (80°N), dans l'île d'Ellesmere, une région d'ailleurs bien connue pour ses températures estivales élevées. La température moyenne de juillet à Eureka (normalement de 5,4°C) a été de 7,2°C et au ruisseau Hot Weather, à 25 km, à l'est d'Eureka, de 12,7°C. Ce réchauffement a provoqué une importante fonte de la glace dans le sol, comme en témoignent la réalimentation des ruisseaux et des mares thermokarstiques, les suintements, le recul accéléré des éboulis causé par l'effondrement de la glace dans le sol, et l'amorce de nombreux glissements provoqués par le décollement du mollisol. Quelques schémas inhabituels de répartition de la végétation indiquent que la fonte de la glace dans le sol se produit habituellement vers la fin de l'été, mais que le degré de réponse au réchauffement a été supérieur à la normale en 1988.

Les études en cours présentent aux auteurs des scénarios possibles pour l'« effet de serre » dans l'Arctique. L'été dernier, qui a été extrêmement chaud, est un exemple de l'importance des changements que peut provoquer une telle montée de la température, et nous donne une idée des conséquences immédiates que pourraient avoir les changements globaux pour l'évolution des paysages arctiques.

¹ McMaster University, Hamilton, Ontario L8S 4M1

INTRODUCTION

Fosheim Peninsula (NTS 49 G,H, 340 B), one of the largest lowlands in the High Arctic, is almost completely surrounded by fiords, beyond which mountains rise to more than 500 m. Summer temperatures at the Eureka weather station are anomalously high (5.4°C; Atmospheric Environment Service, 1982) for latitude 80°N. This warmth and the area's remarkable diversity of vegetation, partially documented around Eureka (Bruggemann and Calder, 1953; Porsild and Cody, 1980), are reflected in the official motto of the weather station "Garden Spot of the Arctic". But the reasons for intensity of summer warmth and the regional distribution of the diverse vegetation are poorly understood.

A number of short term, nonstandard weather observations made by scientists supported by the Polar Continental Shelf Project (PCSP) at other sites in the area, and some detailed climate studies north of the Fosheim Peninsula (Jackson, 1959; Barry and Jackson, 1969; King, 1981; Edlund and Alt, in press; Alt and Maxwell, in press), suggest that Eureka temperature records are in fact lower than might be expected for this intermontane zone. A regional congruence between summer climate and vegetation types in the Queen Elizabeth Islands (Edlund and Alt, in press) suggests that the mapping of vegetation patterns may help us understand the regional extent of anomalously warm summer temperatures. To document further the High Arctic summer temperature anomaly in the intermontane zone, we established another weather station inland from Eureka and began to describe the distributions of plant communities in the warmest part of the region, to document phenological responses of vegetation and materials to daily and weekly

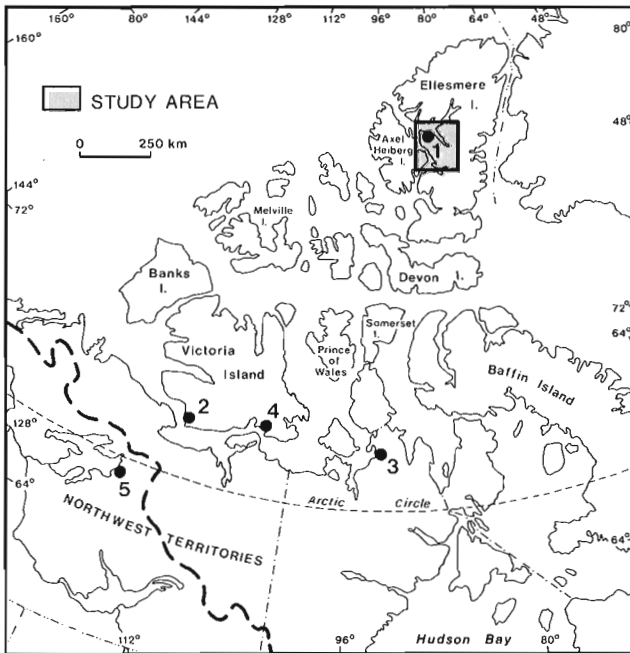


Figure 1. Location map of Fosheim Peninsula study area on Ellesmere Island Northwest Territories. Weather stations: 1. Eureka, 2. Lady Franklin, 3. Shepherd Bay, 4. Cambridge Bay, 5. Port Radium. A dashed line indicates treeline.

changes in summer temperatures, and to map the regional extent of anomalously warm conditions through the use of vegetation patterns as proxy-climate indicators.

Site location

The site selected for long-term monitoring was located along Hot Weather Creek (79°58'N, 84° 28'W), in the midst of a broad, rolling, well vegetated lowland on Fosheim Peninsula between Black Top Ridge and the Sawtooth Range, about 25 km east of Eureka (Fig. 1 and 2). Hot Weather Creek, which has a watershed of about 50 km², is a 15 km long tributary of Slidre River. This site is 16 km from any ocean channel, mountain or major ridge, or large lake.

The watershed, and much of western and central Fosheim Peninsula, is underlain by poorly consolidated clastic rocks of the Eureka Sound Group (Thorsteinsson, 1969, 1971; Thorsteinsson and Tozer, 1970; Ricketts, 1986). In some places younger bedded sand and silt deposits, some of which are probably of Neogene age (Fyles, 1989), overlie the Eureka Sound Group. The peninsula has undergone more than 140 m of emergence since 9 ka; the emergence may be due to glacial isostatic rebound, although no evidence of Late Wisconsinan ice cover has been found in the area (Hodgson, 1985).

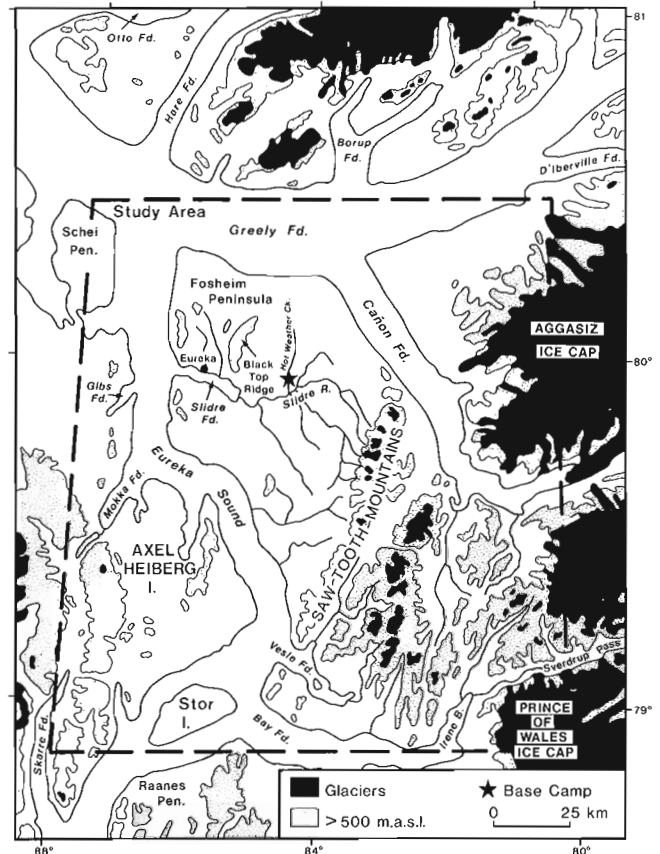


Figure 2. Location of base camp at Hot Weather Creek and study area on Fosheim Peninsula, west-central Ellesmere Island and adjacent Axel Heiberg Island.

The broad lowland plain is dissected by networks of high-centre, frost-fissure polygons more than 30 m in diameter, within which are fields of densely packed hummocks 10 to 50 cm high. In some places junctions of polygon troughs contain small thaw ponds, and the interconnected trough patterns serve as drainage courses for spring meltwater. Many of the local tributaries feeding into Hot Weather Creek follow zig-zag courses which suggest that they resulted from the erosion of ice-wedge troughs.

Instrumentation

On June 21 an automatic weather station, which monitors wind direction and speed, humidity, solar radiation, and both air and soil temperatures throughout the year, was installed by Atmospheric Environment Service (AES) on an interfluvium near Hot Weather Creek 115 m a.s.l. In addition, several other temperature loggers were deployed nearby, including sensors monitoring air, soil, and water temperatures at a nearby thaw pond. In mid July another temperature logger was placed in a wetland at a lower elevation north of base camp. Maximum and minimum temperatures were also manually monitored twice a day in a standard Stevenson screen, in a PCSP "mini-screen" (a more portable type of Stevenson screen) near the automatic weather station, and in a miniscreen at base camp in the valley. The comparisons of these various measurements will be reported elsewhere. Only the base camp data set is used for comparisons in this report.

SUMMER CLIMATE OBSERVATIONS

Preliminary observations stressed the great importance of the timing of snowmelt and the intensity and duration of summer temperatures and precipitation to botanical, hydrological, and geomorphological patterns of this region.

Timing of snowmelt

Snowmelt started in May, and by early June most of the snow cover below 150 m elevation had disappeared. There was no snow in the camp area at the start of the field season (14 June), except for a small snow patch by the headwall of a small detachment slide near camp; only a few snow drifts at higher elevations remained in the watershed. Depth of thaw had already reached 15 to 25 cm on silty materials and 30 to 50 cm on well drained sand. Snow on the upper eastfacing slope of Black Top Ridge persisted until mid July.

Summer temperatures

Eureka experienced a warmer summer than its 30 year norm (Table 1). No temperatures below 0°C were recorded at either Hot Weather Creek or Eureka during the study period. Maximum and minimum daily temperatures at Hot Weather Creek, 25 km inland, almost consistently exceeded those at Eureka (Fig. 3). The difference in means between Hot Weather Creek and Eureka was 4.1°C for the latter half of June, 5.5°C for July, and 3.4°C for early to mid August. The greatest difference in mean daily temperatures between

Table 1. Mean monthly spring and summer temperatures from Eureka and Hot Weather Creek

	Eureka 30 year means*			1988 Temperatures			
	Snow mm	Rain mm	Temp. °C	Eureka °C	diff ¹	HWC °C	Diff ²
May	3.5	tr	-10.7	-7.0	3.7	-	-
June	2.4	3.2	1.8	2.0	0.2	-	-
June 15-30	-	-	-	3.1	-	7.2	4.1
July	1.1	11.0	5.4	7.2	1.8	12.7	5.5
August	2.7	9.0	3.3	-	-	-	-
August 1-18	-	-	-	7.2	-	10.6	3.4
September	10.3	0.2	-8.3	-	-	-	-

* 1951-1980
¹ Difference between temperatures at Eureka 1988 and the Eureka 30 year mean
² Difference between mean temperatures at Hot Weather Creek and Eureka 1988

the two stations, was 12.0°C on 15 July (Fig. 4). From 1 July to 15 August only 3 consecutive days had maximum temperatures less than 10°C.

A comparison of thawing degree days (Table 2) shows that Hot Weather Creek station was 1.5 to 2 times higher than Eureka for June, July, and August. The contrast in growing degree days (GGD) (temperatures above 10°C) is even more striking 6 GGD at Eureka and 129 at Hot Weather Creek.

Precipitation

Rainfall in Fosheim Peninsula and the intermontane area in general is extremely low. The mean annual precipitation at Eureka is 64 mm (Atmospheric Environment Service, 1982). Rainfall was not recorded to AES standards at our camp. Precipitation, generally very light rain, was recorded on 15 days at camp; only 3 days were estimated to have more than 0.5 mm of rain. Snow flurries were observed only a few times, in mid June and on 8-9 July, but without accumulation. Summer precipitation never infiltrated more than 2-5 cm on silty materials, and 5-8 cm on sandy materials. Soil surfaces dried quickly after each rain.

VEGETATION OBSERVATIONS

Hot Weather Creek area

Salix-Dryas hummocky tundra is the most common plant community in the Hot Weather Creek area and is found on almost all moderately drained, neutral to moderately alkaline soils of the silty lowland surfaces. In many places sprawling branches of *Salix arctica* extend horizontally more than 1 m. At slightly drier knolls and on well drained sandy and gravelly deposits, *Dryas* and *Salix* are still dominant, but occur as barrens communities (generally less than 20% total cover).

Major wetlands are rare on Fosheim Peninsula; they are generally locally restricted to clusters of thaw ponds on fluvial terraces near Slidre River and some of its tributaries and

around a few of the large lakes. In wetlands Cyperaceae are dense (in some places >50% cover) with *Carex aquatilis* var. *stans*, *Eriophorum scheuchzeri*, *E. triste*, and occasionally *Carex membranacea* dominating. A number of other Carices and grasses are present as well. Aquatic and emergent species, such as *Pleuropogon sabinei*, *Hippuris vulgaris*, and several species of *Ranunculus*, occur in ponds and around the edges of lakes.

Most slopes and valley bottoms have pockets of sedge wet meadow and sedge-willow communities, particularly in ice-wedge troughs and around small lakes and thaw ponds, and along runnels and some ephemeral creeks. In mid July it was difficult to explain the existence of many of these pocket-sized wetland communities, because the underlying soils had no detectable water to depths of at least 6-10 cm. Later in the season, however, these surfaces contained surface water and in some places water seeped downslope from them; the reappearance of this water will be discussed later.

Table 2. Comparisons of thawing degree days and growing degree days at Eureka and Hot Weather Creek

	June	July	August	Total
Thawing Degree Days				
Eureka (from 30 yr means)	54.0	167.4	102.3	323.7
Eureka 1988	50.8 ¹	224.6	130.8 ²	407.2
Hot Weather Creek 1988	97.6 ¹	392.6	190.8 ²	681.0
Growing Degree Days				
Eureka 1988	0.0 ¹	4.9	1.1 ²	6.0
Hot Weather Creek 1988	0.0 ¹	100.9	28.4 ²	129.3

¹ period of 15 June to 30 June 1988
² period of 1 August to 18 August 1988

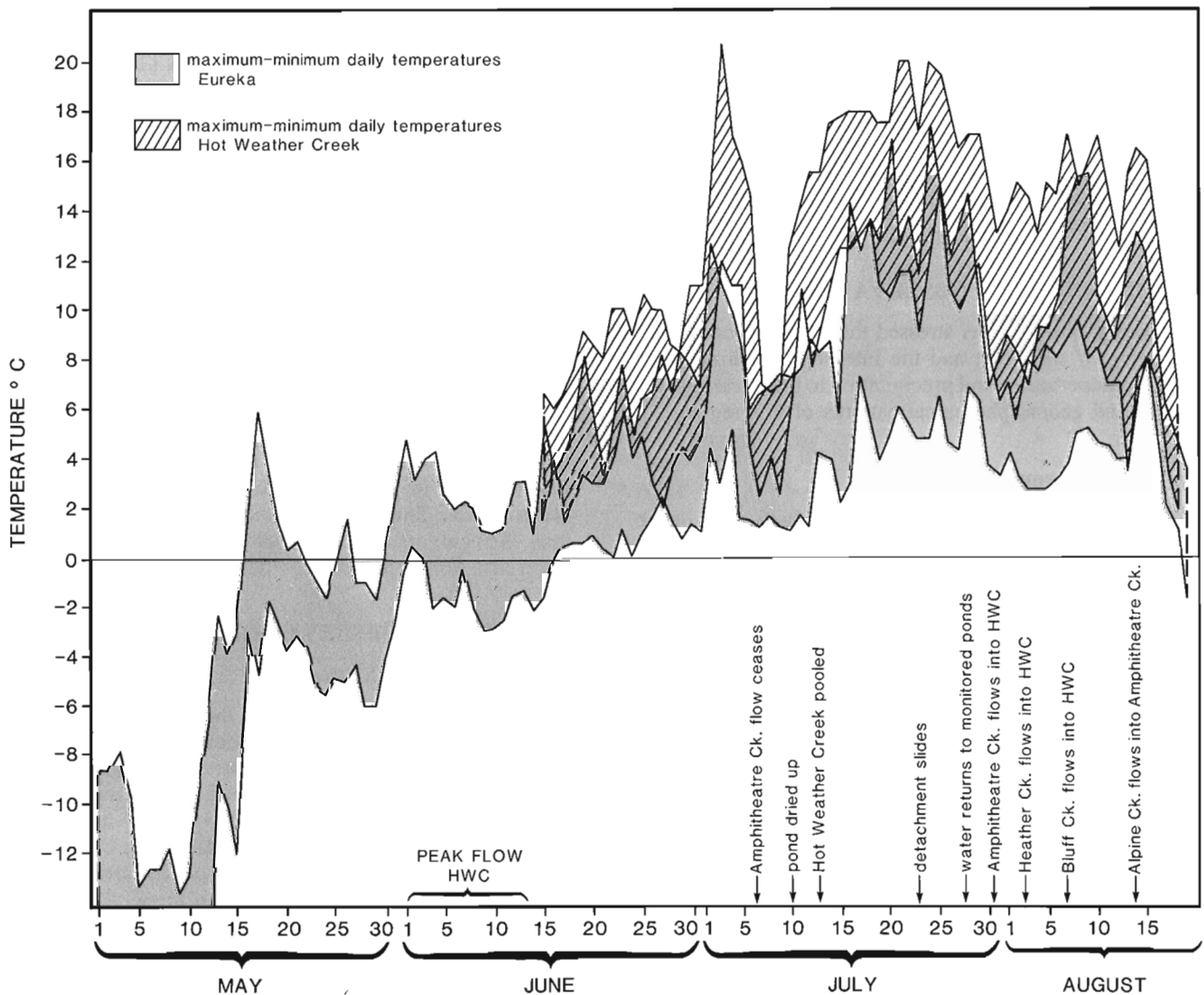


Figure 3. Daily temperature ranges at Eureka and Hot Weather Creek and the timing of hydrologically controlled events at Hot Weather Creek.

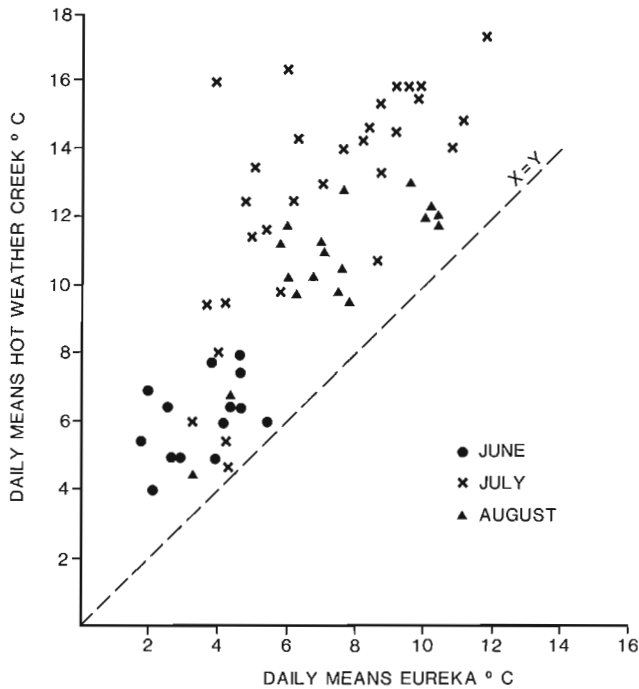


Figure 4. Relationship mean daily temperatures at Eureka and at Hot Weather Creek (modified Stevenson screen at base camp) 14 June to 18 August 1988.

The vascular plant flora of Fosheim Peninsula totals approximately 130 species (Porsild and Cody, 1980) and 144 for northern and central Ellesmere Island (Bruggemann and Calder, 1953; Brassard and Beschel, 1968; Brassard and Longton, 1970; Mausbacher, 1981; Soper and Powell, 1983; Bridgland and Gillett, 1984). Most of these are found on the relatively uniform, weakly alkaline to neutral soils of the Hot Weather Creek area. A few species reported from Fosheim Peninsula that do not occur in the Hot Weather Creek area can be found abundantly at higher elevations or on more acidic soils. Numerous species new to the Fosheim Peninsula were identified, several of which are new to central and northern Ellesmere as well. These new additions, all of which are more typical of Low Arctic environment, will be documented elsewhere.

Fosheim Peninsula area and adjacent Axel Heiberg Island

Fosheim Peninsula supports a dense and diverse vegetation cover as well as some highland and mountain slopes that are virtually unvegetated. Below 240-300 m a.s.l. the vascular plant diversity and plant community structures in other parts of the Fosheim Peninsula are similar to those at Hot Weather Creek. This is particularly so in regions underlain by Eureka Sound Group, although plant diversity decreased above elevations of about 180 m. Large areas of southern and south-western Fosheim Peninsula are more sparsely vegetated, with the typical prostrate shrub communities dominated by *Dryas* and *Salix*. Where water is abundant, both density and diversity of wetland vegetation are comparable to the Hot Weather Creek area.

Few acidic soils (pH of less than 6.8) occur in the area. Where these are present, *Salix* is the dominant vascular plant, with *Cassiope tetragona* present in some abundance. *Cassiope* also occurs locally on weakly alkaline deposits, particularly at the bottom of steep slopes. Above 300 m elevation in the mountainous region between Sawtooth Range and Agassiz and Prince of Wales ice caps and other east-central ice caps, woody species diminish in abundance. Individual plants are smaller and more compact, with branches sprawling for no more than 30 cm. Many individual *Salix* plants failed to flower this summer, and showed no signs of flowering in the previous year. Growth was limited to production of leaves and an extension of the branch by a few millimetres. A few individual plants with catkins were found in early August, but seeds were not mature at that time; however, at lower elevations seeds were being shed.

At these higher elevations herbaceous species such as *Luzula confusa* and *Potentilla hyparctica*, are abundant on more acidic soils, and Saxifrages such as *Saxifraga oppositifolia* and *S. caespitosa* dominate the alkaline soils. Several species that are rare at lower elevations, are common to abundant at higher elevations on both weakly acidic and moderately alkaline soils. These include *Saxifraga nivalis*, *S. foliolosa*, *S. flagellaris*, *S. tenuis*, *S. rivularis*, *Cardamine bellidifolia*, and *Phippsia algida*. *Papaver radicum* is also common on all but the wettest soils. In some areas, only a few herbaceous species such as *Papaver*, *Phippsia algida*, and *Saxifraga caespitosa* occur (cover less than 1%). These changes with elevation are reminiscent of the latitudinal changes of the western and central Queen Elizabeth Islands. Communities on the highlands of Fosheim Peninsula are similar, although often denser, than those at sea level on northern Melville Island, the Ringnes islands, and southern Loughheed Island (Edlund, 1980, 1983a,b,c, 1986; Edlund and Alt, in press).

HYDROLOGICAL AND GEOMORPHICAL PROCESSES

Attention was paid to aspects of soil hydrology because the distribution of plant communities is so greatly dependent on the soil moisture regime. At the time of establishment of the base camp, snowmelt was complete, the top few centimetres of the ground surface were generally dry, and Hot Weather Creek and its tributaries were flowing.

Stream flow and thaw ponds

Peak flow of Hot Weather Creek probably occurred in early June, and upon our arrival Hot Weather Creek was 6-10 cm below the recent high water trash line. The high flow was assumed to be due to snow melt. By 5 to 14 July flow in Hot Weather Creek and its tributaries had ceased. Small isolated pools remained in the stream beds, but by 20 July some had disappeared. These observations suggest that Hot Weather Creek experiences a nival regime typical of many High Arctic streams (Woo, 1986).

During the latter part of the summer, flow returned to many tributaries. This renewed flow generally consisted of

clear water, which, in the absence of significant precipitation inputs, was assumed to come from ground ice melt. On July 29, the southernmost major tributary of Hot Weather Creek began flow again and pools in Hot Weather Creek began to expand. All other major tributaries also eventually flowed into Hot Weather Creek in the first and second weeks of August, the most northerly connected the latest.

Five stage markers recorded slightly increased levels, from 8 to 18 August, in pools in the bed of Hot Weather Creek and one in the southernmost tributary (Fig.5). Eventually many small pools coalesced and, in a few areas, surface flow between pools was noticeable; however, Hot Weather Creek never became a continuously flowing stream again. Daily stream discharge in the southernmost major tributary increased from 0.61 L/s to 1.10 L/s ($\pm 10\%$).

After snowmelt numerous small ponds also occurred in the junctions of frost-fissure troughs on the broad interfluvies. One such pond (Fig. 6), instrumented with thermistors, initially had a maximum water depth of 10-20 cm. By the end of the first week of July, many of the ponds had dried, although in some places the water table was at 10 to 15 cm depth. By the end of the first week in August the monitored pond, and many other ephemeral ponds, again contained water, reaching a depth of 9 cm by 18 August.

Damp spots

Most of the ground surface dried quickly in June, although silty soil still had detectable moisture at 15-20 cm throughout most of late June and mid July. By 18 July damp spots began to appear randomly on silty slopes and on the plain surfaces and slowly increased in size throughout the rest of the summer. Similar damp spots on silty soils were seen in other parts of Fosheim Peninsula and eastern Axel Heiberg Island during reconnaissance studies by helicopter after July 31.

Water ejection features

After 23 July we observed several local areas where water flowed intermittently to the surface as if under pressure. Such areas were generally on silty materials at or near the crest of hills. Silty water flowed through small (1-3 mm diameter) holes or cracks in the surface. In some places the flow left concentric rings of wet silt no more than 1 m in diameter and in other areas downslope flow resulted in tongues of fresh silt, up to 2-3 m long and 50 cm to more than 100 cm wide.

Active layer detachment slides

The silty soils of Fosheim Peninsula are prone to active layer detachment slides (Hodgson and Edlund, 1977). A scar recording one such event was found on the slope behind base camp upon our arrival. The lack of any colonizing vegetation on the face of the slip surface and the presence of a small snowbank against the head wall suggested that this slide occurred in 1987. A few smaller slide scars were found south of camp on the steep slopes of Hot Weather Creek.

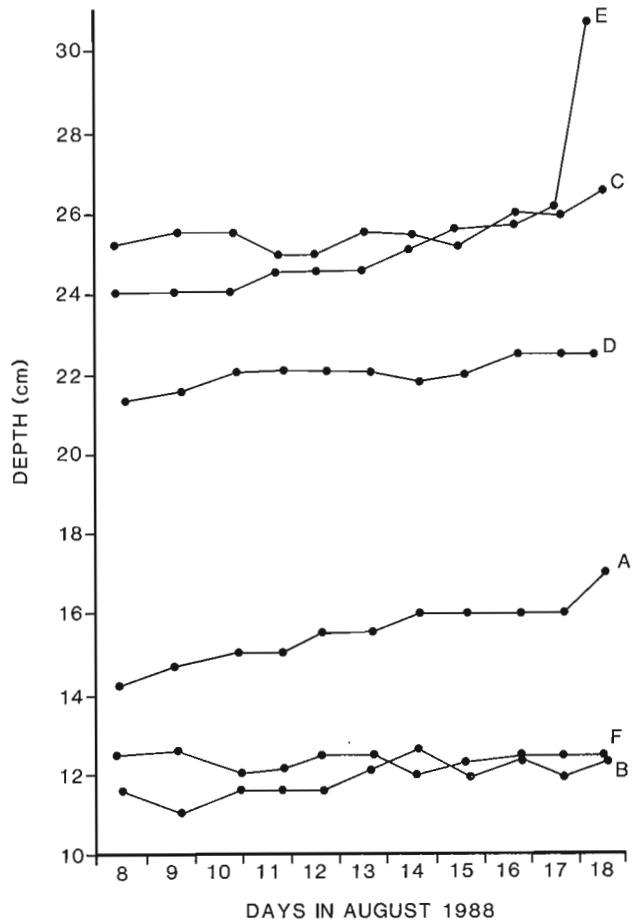


Figure 5. Stage levels of 5 pools in Hot Weather Creek (A-E) and one in southernmost major tributary (F), 8 August to 18 August 1988.



Figure 6. Instrumented thaw pond on the interfluvial above Hot Weather Creek. (photo 204746-B)

Twenty-two major active layer detachment slides occurred along a 3 km stretch of the steep-walled valley of Hot Weather Creek south of camp (Fig. 7) starting on 22 July and occurring intermittently thereafter; most took place between 23 July and 8 August. Five slides occurred on the more gentle slopes north of base camp, three of these after 8 August. At the same time many similar slides were seen all over Fosheim Peninsula and eastern Axel Heiberg Island, generally in silty soils derived from the shale of Eureka Sound Group, and in raised marine sediments.

The failure planes occurred at 50-80 cm depth, which was at or near the depth of thaw. Freshly exposed slip surfaces were initially frozen a few millimetres below the surface. Water pooled on the lower slide scar and then flowed into already established drainage patterns. Water from these features soon flowed into the dry Hot Weather Creek bed, where new pools formed. Several of these slides flowed into the creek bed and a few caused water to pool upstream. In several places the vegetation of large sections of hillsides was completely disrupted.

Ground ice slumps

Three large actively eroding, ground ice slumps, with headwalls two to five times greater than the thickness of the active layer, were located close to camp and scars of a few inactive ones were found in the watershed of Hot Weather Creek and numerous places on Fosheim Peninsula. Massive ice was found in the headwalls at the active sites. Following the visit of our colleagues D.G. Harry and B.H. Luckman (7-9 July) who had noted similar ground ice features elsewhere on the peninsula, a series of markers was placed around the perimeters of two adjacent slumps to document headwall retreat on a weekly basis. Both slumps showed progressive retreat up to 1 m a week through 21 July. By 4 August noticeable subsurface water was seeping along the base of the active layer at both slumps. In addition, in late July subsurface water from a thaw pond at slightly higher elevation flowed along the top of an ice wedge and poured into the one of the slumps, causing accelerated headwall retreat of 25 m in 38 days.

DISCUSSION

Physical implications

During the summer of 1988, Fosheim Peninsula experienced a period of unusually prolonged warm temperature and negligible precipitation. After a typical nival regime of stream water flow, which peaked in early June, flow ceased in Hot Weather Creek and its tributaries in mid July. In late July and August, however, tributaries of Hot Weather Creek were recharged, dry thaw ponds were refilled, damp spots appeared, large numbers of active layer detachment slides developed, and headwall retreat of several ground ice slumps increased. The only possible source of water given the lack of precipitation is from the melt of subsurface ground ice by downward penetration of the active layer.



Figure 7. Numerous active layer detachment slides on the west facing slope of Hot Weather Creek, 2 km from Slidre River; relief is approximately 100 m. (photo 204746-A)

Extensive ice-rich sediments below the active layer were observed in the headwalls of ground ice slumps. Limited direct evidence suggests that fine grained sediments of Fosheim Peninsula contain large quantities of ground ice. Excavation in the centre of one high centre ice-wedge polygon in early June, showed 30 cm of damp silt underlain by silt containing massive, pure ice lenses and layers, and pore ice to a depth of more than 1 m. A number of cores drilled in the early 1970s in areas underlain by Eureka Sound Group rocks contained massive amounts of segregated ice (D.A. Hodgson, personal communication 1988).

Active layer detachment slides occurred at Hot Weather Creek and around Eureka on 23 July 1988. A critical threshold seems to have been reached in the region, even though Hot Weather Creek had surpassed the Eureka area in thawing degree days by 1.5 to 2 times. The number of such slides and slumps at Hot Weather Creek is unusually large when compared with the few, small scars seen earlier in the season and recorded on airphotos dating to 1949. This suggests that formerly an equilibrium between climate and ground ice, and related geomorphic processes had been reached.

Unusual distribution patterns of small wetlands suggest that mid to late summer subsurface ground ice melt may occur with enough regularity to support water-requiring plant communities rather than just during unusually warm summers. The randomly distributed damp spots found on silty surfaces and water ejection features, however, can not be linked to any vegetation patterns. Their occurrence suggests that the magnitude of ground ice thaw may have been much greater than usual this year.

Presently there are no data to assess the magnitude of the contribution that ground ice melt makes in the total summer soil-moisture budget at these sites, nor is there information regarding the movement of subsurface water in this region. Upwelling of silty water on hill crests, sporadic appearance of damp spots, and the mid to late summer replenishment

of water to small wetlands suggest that piping and subsurface percolation are important means of water movement in this region. The hydrological implications of piping and its significance with respect to arctic hydrology and geomorphology have yet to be examined in the High Arctic (A.G. Lewkowicz, University of Toronto, personal communication, 1988), and may be particularly important on Fosheim Peninsula.

The surface vegetation in these areas may provide useful clues to the distribution of subsurface water flow. The conventional wisdom would have plant distribution reflecting soil moisture due to precipitation and spring runoff. Our data suggest that mid to late summer moisture availability from melting of ground ice is also a significant factor in determining patterns of plant communities.

The long-term frequency of such accelerated events is unknown but would seem to be a relatively rare event. However a large amphitheatre-like feature to the north of the base camp, and another major bowl-like depression in which two of the currently active ground ice slumps are found, demonstrate that such events have occurred in the past. The amount of vegetation suggests that these surfaces were active 25-50 years ago and possibly longer. It is interesting to note that other surfaces in large amphitheatres were not reactivated this year.

Botanical implications

The regional distribution of dense and diverse woody plant and sedge communities indicates that the anomalously warm zone covers most of Fosheim Peninsula and adjacent Axel Heiberg Island below 150 to 180 m elevation. Similar vegetation occurs locally at higher elevations and can be considered to indicate pockets of exceptional warmth at such elevations. The herbaceous plant communities more commonly found at high elevations are similar to those seen near sea level in the northwestern Queen Elizabeth Islands (Edlund, 1983a; Edlund and Alt, in press) and reflect much shorter and much cooler summer conditions.

Catastrophic events such as high numbers of detachment slides and activation of ground ice slumps were restricted, almost without exception, to the vegetation zone dominated by the floristically richest woody plant and sedge communities. Such communities are also coincident with areas of warmest temperature. Therefore the regional vegetation broadly indicates zones that may be prone to slumping.

The widespread presence of small wetlands on interflues may serve as the only surface manifestation of massive amounts of subsurface ground ice. Their presence may provide a new tool by which such thaw-sensitive terrain can be detected.

The vegetation and general geomorphology of the Hot Weather Creek area prior to mid July 1988 represent an adjustment to conditions over a number of years which reflect the consistently warm summer temperatures of this intermontane zone. This can serve as a model for what may happen when similar materials elsewhere in the Queen Elizabeth Islands are warmed by a rise in mean summer

temperature of several degrees Celsius for prolonged periods. Although 1988 appears to have been exceptionally warm, the geomorphological and hydrological observations may indicate a possible scenario for this area should the predictions of a summer warming of 4-6°C the magnitude predicted for the "greenhouse effect" due to CO₂ doubling be realized.

The long term effects of prolonged periods of summer warmth of the magnitude experienced in July and August 1988 are less easily predicted. Slope instability would continue until a new equilibrium is reached. This could radically change the appearance of the landscape, both from a geomorphological and biological view and would offer abundant fresh habitats for colonizing plant species.

The summer temperatures experienced in 1988 have their analogs in the southern Arctic. Temperatures recorded at Eureka in summer 1988 are similar to the 30 year mean July temperatures in Low Arctic stations (Fig.1) such as Lady Franklin (6.9°C), Shepherd Bay (7.5°C), Spence Bay (7.4°C), and Cambridge Bay (7.9°C; Atmospheric Environment Service, 1982). Comparisons of temperatures at Hot Weather Creek and stations at similar latitudes are even more startling. Mean July temperatures at Hot Weather Creek exceeded all means for weather stations in the Arctic Islands and came close to those at Port Radium (12.4°C), and the mainland south of treeline (Fig. 1; roughly coincident with the 10°C mean July isotherm), and near the northern forest limit (roughly coincident with the 13°C mean July isotherm; (Hare, 1970).

Continued studies of the botanical and geomorphological responses to events of the summer of 1988 should help provide insight into the possible immediate effects of global warming on landscape evolution in the Arctic. A multidisciplinary approach to such monitoring is needed to decipher the complexity of problems in this region.

ACKNOWLEDGMENTS

We greatly appreciate the logistical support provided by PCSP during 1988. The study benefited from phenological observations and vascular plant collections of B.T. Aniskowicz and E. Robinson, and excellent field assistance of C. Roncato-Spencer (University of Toronto). We also appreciate the contribution of B.H. Luckman University of Western Ontario and GSC) and D.A. Hodgson (GSC) with helpful comments on earlier drafts of this report.

REFERENCES

- Alt, B.T. and Maxwell, J.B.
—: The Queen Elizabeth Island: A case study for arctic climate data availability and regional climate analysis; in *Symposium on the Canadian Arctic Islands, Canada's Missing Dimension*, C.R. Harrington, (ed.); National Museum of Natural Sciences; Syllogus (in press).
- Atmospheric Environment Service
1982: Canadian Climate Normals 1951-1980, The North: Y.T. and N.W.T., Temperature and Precipitation; Atmospheric Environment Service, Environment Canada, Downsview, Ontario, 55 p.
- Barry, R.G. and Jackson, C.I.
1969: Summer weather conditions at Tanquary Fiord, N.W.T. 1963-1967; *Arctic and Alpine Research*, v. 1, no. 3, p.169-180.

- Brassard, G.R. and Beschel, R.E.**
1968: The vascular flora of Tanquary Fiord, northern Ellesmere Island, N.W.T.; Canadian Field-Naturalist, v. 82, no. 2, p. 103-113.
- Brassard, G.R. and Longton, R.G.**
1970: The flora and vegetation of Van Hauen Pass, northwestern Ellesmere Island; Canadian Field-Naturalist, v. 84, p. 357-364.
- Bridgland, J. and Gillett, J.M.**
1984: Vascular plants of the Hayes Sound region, Ellesmere Island, Northwest Territories; Canadian Field-Naturalist, v. 97, p. 279-292.
- Bruggemann, P.F. and Calder, J.A.**
1953: Botanical investigations in northeast Ellesmere Island, 1951; Canadian Field-Naturalist, v. 67, no. 4, p. 157-174.
- Edlund, S.A.**
1980: Vegetation of Loughed Island, District of Franklin; in Current Research, Part A, Geological Survey of Canada, Paper 80-1A, p. 329-333.
1983a: Bioclimatic zonation in a High Arctic region: central Queen Elizabeth Islands; in Current Research, Part A, Geological Survey of Canada, Paper 83-1A, p. 381-390.
1983b: Vegetation of Bathurst Island area Northwest Territories; Geological Survey of Canada, Open File 888.
1983c: Vegetation of the north-central Queen Elizabeth Islands, District of Franklin, N.W.T.; Geological Survey of Canada, Open File 887.
1986: Modern arctic vegetation distribution and its congruence with summer climate patterns; in Proceedings, Impact of Climatic Change on the Canadian Arctic, H.M. French (ed.); Atmospheric Environment Service, Environment Canada, Downsview, Ontario, p. 84-99.
- Edlund, S.A. and Alt, B.T.**
—: Regional congruence of vegetation and summer climate patterns in the Queen Elizabeth Islands, Northwest Territories, Canada; Arctic, v. 42, no. 1 (in press).
- Fyles, J.G.**
1989: High terrace sediments, probably of Neogene age, west-central Ellesmere Island, Northwest Territories; in Current Research, Part D, Geological Survey of Canada, Paper 89-1D.
- Hare, F.K.**
1970: The tundra climate; Royal Society of Canada, Transactions, 4th Series, v. 8, p. 393-399.
- Hodgson, D.A.**
1985: The last glaciation of west-central Ellesmere Island, Arctic Archipelago, Canada; Canadian Journal of Earth Sciences, v. 22, no.3, p. 347368.
- Hodgson, D.A. and Edlund, S.A.**
1977: Biophysical regions, western Fosheim Peninsula and eastern Axel Heiberg Island; Geological Survey of Canada, Open File 501.
- Jackson, C.I.**
1959: Coastal and inland weather contrasts in the Canadian Arctic; Journal of Geophysical Research, v. 64, no. 10, p. 1451-1455.
- King, R. L.**
1981: Das Sommerklima von N-Ellesmere Island, N.W.T., Kanada Eine Beurteilung von Stationswerten unter besonderer Berücksichtigung des Sommers 1978; in Ergebnisse der Heidelberg Ellesmere Island Expedition, D. Barsch and L. King (ed.); Heidelberger Geographische Arbeiten, Heft 69, p. 77-107.
- Mausbacher, R.**
1981: Gefäßpflanzen von Oobloyah Bay, N-Ellesmere Island, N.W.T., Kanada; eine kommentierte Pflanzenliste und phänologische Beobachtungen; in Ergebnisse der Heidelberg Ellesmere Island Expedition, D. Barsch and L. King (ed.); Heidelberger Geographische Arbeiten, Heft 69, p. 541-553.
- Porsild, A.E.**
1964: Illustrated Flora of the Canadian Arctic Archipelago; National Museums of Canada, Bulletin 146, 218 p.
- Porsild, A.E. and Cody, W.J.**
1980: Vascular plants of the Northwest Territories, Canada; National Museums of Canada, 667 p.
- Ricketts, B.D.**
1986: New formations in the Eureka Sound Group, Canadian Arctic Islands; in Current Research, Part B, Geological Survey of Canada, Paper 86-1B, p. 363-374.
- Soper, J.H. and Powell, J.M.**
1983: Botanical studies in the Lake Hazen Region, northern Ellesmere Island, Northwest Territories, Canada; National Museums of Canada, Publications in Natural Sciences, no. 5, 67 p.
- Thorsteinsson, R.**
1969: Geology, Greely Fiord West, District of Franklin; Geological Survey of Canada, Map 1311A.
1971: Geology, Eureka Sound North, District of Franklin; Geological Survey of Canada, Map 1302A.
- Thorsteinsson R. and Tozer, E.T.**
1970: Geology, Slidre Fiord, District of Franklin; Geological Survey of Canada, Map 1298A.
- Woo, M-K.**
1986: Permafrost hydrology in North America; Atmosphere-Ocean, v. 24, no. 3, p. 201-134.

AUTHOR INDEX

Allen, V.	119	Macqueen, R.W.	19
Alt, B.T.	125	Majid, A.H.	25
Avery, R.	95	Matthews, J.V., Jr.	105
Banerjee, I.	9	McMartin, I.	95
Bell, J.S.	49	Mwenifumbo, C.J.	1
Brooks, P.W.	19	Osadetz, K.G.	35
Burgess, M.M.	69	Potschin, M.B.	113
Burn, C.R.	85	Riseborough, D.W.	69
Edlund, S.A.	125	Simony, P.S.	55
Fowler, M.G.	19	Snowdon, L.R.	35
Fyles, J.G.	101	St-Onge, D.A.	95
Gal, L.P.	55	Stasiuk, L.D.	35
Ghent, E.D.	55	Stewart, W.D.	61
Judge, A.	119	Taylor, A.	119
Kerr, D.E.	77	Young, K.L.	125
Lloyd, P.F.	49		

Geological Survey of Canada, Paper 89-1, Current Research is published as eight parts, listed below, that can be purchased separately.

Recherches en cours, une publication de la Commission géologique du Canada, Étude 89-1, est publiée en huit parties, énumérées ci-dessous; chaque partie est vendue séparément.

Part A, Abstracts

Partie A, Résumés

Part B, Eastern and Atlantic Canada

Partie B, Est et région atlantique du Canada

Part C, Canadian Shield

Partie C, Bouclier canadien

Part D, Interior Plains and Arctic Canada

Partie D, Plaines intérieures et région arctique du Canada

Part E, Cordillera and Pacific Margin

Partie E, Cordillère et marge du Pacifique

Part F, National and general programs

Partie F, Programmes nationaux et généraux

Part G, Frontier Geoscience Program, Arctic Canada

Partie G, Programme géoscientifique des régions pionnières, région arctique du Canada

Part H, Frontier Geoscience Program, Queen Charlotte Islands, British Columbia

Partie H, Programme géoscientifique des régions pionnières, îles de la Reine-Charlotte, Colombie-Britannique

